Dynamique intra-annuelle de la formation du bois de trois espèces de conifères (sapin pectiné, épicéa commun et pin sylvestre) dans les Vosges : De la description des patrons saisonniers de la croissance à l'étude de l'influence de l'environnement sur la cinétique du développement cellulaire et les caractéristiques anatomiques du xylène

Henri Cuny

École doctorale RP2E

Thèse de doctorat

Biologie Végétale et Forestière

Soutenue le 28 mai 2013 par

Henri CUNY

DYNAMIQUE INTRA-ANNUELLE DE LA FORMATION DU BOIS DE TROIS ESPÈCES DE CONIFÈRES (SAPIN PECTINÉ, ÉPICÉA COMMUN, PIN SYLVESTRE) DANS LES VOSGES

–

De la description des patrons saisonniers de la croissance à l'étude de l'influence de l'environnement sur la cinétique du développement cellulaire et les caractéristiques anatomiques du xylème

---

Devant le jury composé de :

Sergio ROSSI	Directeur de recherche, Université du Québec, Chicoutimi (Canada)	Rapporteur
Luc PÂQUES	Directeur de recherche, INRA, Orléans	Rapporteur
Daniel EPRON	Professeur, Université de Lorraine, Nancy	Examinateur
Claire DAMESIN	Directeur de recherche, INRA, Orsay	Examinateur
Patrick FONTI	Chargé de recherche, WSL, Birmensdorf (Suisse)	Examinateur
Cyrille RATHGEBER	Chargé de recherche, INRA, Nancy	Co-directeur de thèse
Meriem FOURNIER	Professeur, AgroParisTech, Nancy	Directeur de thèse

Laboratoire d'Étude des Ressources Forêt-Bois (LERFoB)
UMR 1092 INRA-AgroParisTech, route d'Amance, 54280 Champenoux, France

DYNAMIQUE INTRA-ANNUELLE DE LA FORMATION DU BOIS DE TROIS ESPÈCES DE CONIFÈRES (SAPIN PECTINÉ, ÉPICÉA COMMUN, PIN SYLVESTRE) DANS LES VOSGES

–

De la description des patrons saisonniers de la croissance à l'étude de l'influence de l'environnement sur la cinétique du développement cellulaire et les caractéristiques anatomiques du xylème

Henri CUNY

Dessin d'une trachéide en coupe transversale

Remerciements

Au terme de ces trois années et demie de travail, je tiens en premier lieu à remercier mes encadrants, Meriem FOURNIER et Cyrille RATHGEBER. Merci à eux de m'avoir accordé leur confiance en me sélectionnant pour cette thèse et de m'avoir encadré tout au long de sa réalisation. Cyrille notamment, en plus d'être le principal concepteur du projet, a été mon interlocuteur privilégié tout au long de ce travail et il m'a énormément appris. Parfois dur sur l'homme (lui-même avoue avoir occasionnellement recours au « tacle par derrière », les amateurs de foot comprendront l'image), Cyrille m'a constamment aidé et a fait progresser le travail. Par sa disponibilité, sa clairvoyance, ses excellentes idées, ses critiques et ses conseils avisés, je suis conscient qu'il est un acteur majeur du succès de cette thèse et je lui en suis extrêmement reconnaissant.

Cette thèse impliquait un travail de terrain important et sa réussite est donc redevable aux personnes qui ont effectué ce travail. Un grand merci donc à Emmanuel CORNU, qui a été présent du début à la fin de l'expérimentation et a pris en charge une grande diversité de tâches (entre autres le prélèvement des échantillons, les observations phénologiques, le relevé des dendromètres, la mesure de la croissance en hauteur). Merci également à Pierre GELHAYE, Alain MERCANTI et Charline FREYBURGER qui ont accompagné et aidé Emmanuel sur le terrain. Pierre s'est en outre chargé des mesures de densité au laboratoire. Merci à Etienne FARRÉ, qui a veillé au bon fonctionnement des différents capteurs automatiques utilisés sur le terrain et s'est occupé de les relever.

En plus du travail de terrain, cette thèse demandait un important travail de préparation et d'élaboration des échantillons au laboratoire. J'exprime donc toute ma reconnaissance à Maryline HARROUÉ pour le travail considérable qu'elle a réalisé, puisque c'est elle qui s'est chargée intégralement de cette tâche (réalisation de plus de 5000 coupes anatomiques de bois au total !).

Enfin, une thèse implique de nombreuses procédures administratives, certaines n'étant compréhensibles que par des initiés. Je remercie donc les personnes qui m'ont grandement facilité la vie en m'assistant dans ces diverses procédures : Nathalie MOREL, Hélène HURPEAU et Virginie FRILEY du LERFoB ; Christine FIVET de l'école doctorale RP2E ; Vanessa BINET du bureau des études doctorales de l'université de Lorraine. Je tiens également à remercier François NINGRE, qui s'est inquiété de ma situation en fin de thèse et s'est investi pour obtenir le financement des derniers mois, ce que j'ai beaucoup apprécié.

J'exprime ma gratitude aux membres du Jury, qui ont bien voulu évaluer cette thèse et dont les nombreuses critiques constructives m'ont permis de prendre plus de recul sur le travail réalisé. Merci donc à mes rapporteurs, Sergio ROSSI et Luc PÂQUES, ainsi qu'à mes examinateurs, Claire DAMESIN, Patrick FONTI et Daniel EPRON.

La rencontre de Tristan SENGA KIESSÉ fut de celles qui changent le cours des choses. En effet, c'est Tristan qui, le premier, a eu l'idée de tester les modèles additifs généralisés sur

les données de la dynamique de la formation du bois. Tristan est ainsi à l'origine d'un tournant décisif de la thèse, car c'est sur la base de cette idée que nous avons ensuite pu développer une méthode à partir de laquelle la majorité des résultats ont été obtenus. En plus de cela, Tristan, l'un des deux supporters de l'AS Monaco, est une personne avec laquelle j'ai pris beaucoup de plaisir à travailler. Pour tout ça je le remercie.

Merci à mon collègue thésard Mathieu DASSOT, « l'auvergnat », pour cette cohabitation très appréciable, les centaines de litres de tisane ingurgités (3 tisanes de 25 cl par jour chacun pendant 3 ans, je vous laisse faire le calcul !) et les parties de ping-pong régulières (c'est-à-dire quotidiennes). Il faudra vraiment que je vienne visiter l'Auvergne en profondeur, vu les éloges que Mathieu en a dressés pendant 3 ans ça doit être quelque chose. D'après ses dires, le climat y est des plus agréables (il faut dire que relativement à la Lorraine beaucoup de régions ont un climat agréable…), à tel point qu'un maillot de bain dans la valise serait suffisant pour y séjourner ! Merci également à lui pour son aide sur le logiciel R, ainsi que pour l'édition de nombreuses images.

Je souhaite remercier Philippe SANTENOISE, qui n'a jamais rechigné (du moins ne l'a-t-il pas montré…) à m'aider lors de nombreuses prises de tête sur le logiciel R. Je remercie les autres thésards du laboratoire qui m'ont accompagné durant cette thèse : Félix HARTMANN, de la « race supérieure » des physiciens, Nicolas BILOT et sa gouaille légendaire, Vivien BONNESOEUR et son coup droit perfectible, Jean-Baptiste MORRISSET du peuple des chasseurs-cueilleurs, Pierre MÉRIAN de l'ordre vénérable des dendrochronologistes. Merci également aux scientifiques Thiéry CONSTANT, Gérard NEPVEU, Jana DLOUHA, Ignacio BARBEITO et Francis COLIN, toujours disponibles et qui, avec Natasha CLAIRET et Jean-Baptiste MORRISSET, m'ont aidé à finaliser ma présentation de soutenance.

Je remercie mes parents, François et Geneviève, pour leur éducation, leur infinie patience à mon égard, ainsi que pour m'avoir certainement transmis les « gènes du bois » depuis longtemps présents dans la famille. Merci enfin à ma compagne, Amélie PIERREL, bien sûr pour tout ce qu'elle m'apporte tous les jours mais aussi pour m'avoir facilité la vie durant ces années (c'est toujours agréable de n'avoir plus qu'à mettre les pieds sous la table après une dure journée de fin de thèse) et ainsi contribué elle-aussi au succès de cette thèse.

Avant-propos

Ce mémoire de doctorat présente le travail réalisé pendant 3 années et demie, entre le 1er octobre 2009 et le 31 mars 2013, au Laboratoire d'Étude des Ressources Forêts Bois (LERFoB) de l'Institut National de la Recherche Agronomique (INRA) de Nancy.

A travers une revue bibliographique, l'introduction générale (partie I) pose le contexte général et l'objectif de cette thèse, tandis que la partie II expose les bases de la biologie de la formation du bois. La partie III propose ensuite une description exhaustive du dispositif expérimental mis en place pour cette thèse. Les 5 parties de résultats suivantes (partie IV à VIII) présentent les découvertes majeures réalisées. Enfin, la discussion générale (partie IX) propose une synthèse du travail, puis des conclusions sont tirées dans la partie X.

Le mémoire se présente sous la forme d'une thèse sur publications. L'introduction générale, la revue des connaissances sur la biologie de la formation du bois, la description du dispositif expérimental, la discussion générale et la conclusion sont rédigées en français. En revanche, les 5 parties de résultats sont rédigées en anglais, car chacune est constituée d'un article scientifique publié ou en préparation pour publication dans une revue scientifique internationale à comité de lecture. Les références bibliographiques sont listées à la fin de chaque partie. Une liste complète des publications et communications de la thèse est disponible en annexe (annexe 1).

Cette thèse a été financée d'octobre 2009 à septembre 2012 par une bourse du ministère de l'enseignement supérieure et de la recherche reversée par l'Université de Lorraine. À partir d'octobre 2012, la thèse a été financée par le Laboratoire d'Étude des Ressources Forêt-Bois (LERFoB).

Table des matières

Table des articles

NB : Les articles insérés dans ce mémoire suivent les règles des droits d'auteur et sont donc présentés dans un format différent du format de publication adopté par le journal. Le lecteur se reportera aux références ci-dessus pour obtenir les articles dans leur forme publiée.

I INTRODUCTION

I.1 Importance du bois et de la dynamique de sa formation

I.1.1 Le bois est un composant crucial du fonctionnement des écosystèmes

Avec une masse sèche globale estimée à près de 1000 gigatonnes, le bois (xylème secondaire) est, de très loin, le composé biologique le plus abondant de la planète (Groombridge & Jenkins, 2002). En comparaison, la biomasse animale ou celle contenue par les océans apparaissent négligeables (plus de 100 fois inférieures). La majorité du bois (80%) se trouve dans les forêts qui couvrent le tiers des terres émergées (FAO, 2010). Ces forêts jouent un rôle fondamental dans le fonctionnement de la planète. Vis-à-vis de la biodiversité tout d'abord, en procurant un habitat à plus de la moitié des espèces du monde (Groombridge & Jenkins, 2002). Vis-à-vis des grands cycles biogéochimiques ensuite, notamment celui du carbone, un contributeur majeur aux changements climatiques. En prenant en compte leur sol, les forêts stockent les ¾ du carbone de la biosphère et participent à la moitié de la production primaire nette de la planète (Zhao & Running, 2010). La séquestration de carbone par les forêts, en particulier dans le bois, contribue à un puits de carbone qui compense le tiers des émissions liées aux activités humaines, mitigeant ainsi le changement climatique (Canadell & Raupach, 2008). Les forêts participent également à la régulation des cycles de l'eau et des nutriments, stabilisent les sols et protègent leurs ressources.

I.1.2 Le bois est une ressource essentielle pour l'homme

Pour l'Homme, les forêts jouent également un rôle culturel important à travers leur esthétisme, leur usage récréatif, ou encore leur place dans la vie spirituelle de nombreuses communautés dans le monde. En outre, le bois des forêts constitue une ressource essentielle à la vie humaine, utilisée dès la préhistoire, au paléolithique pour la construction de refuges, d'accessoires, d'outils et d'armes, puis comme source d'énergie avec la domestication du feu. Au cours de l'histoire, la disponibilité en bois a ainsi été étroitement liée au succès ou au déclin des civilisations (Perlin, 1997). Aujourd'hui, le bois joue encore un rôle crucial dans nos sociétés en étant un matériau privilégié dans de nombreux domaines comme la construction de bâtiments, la fabrication de meubles ou l'énergie. Sa consommation n'a d'ailleurs jamais été aussi forte, ce qui en fait l'un des produits majeurs du marché mondial (FAO, 2007). Ainsi, 3,5 milliards de m^3 de bois sont utilisés chaque année. Le marché du bois a atteint 257 milliards de dollars US en 2006. Il est en augmentation de 6,6% par an depuis 20 ans. Ce marché va continuer de se développer dans le futur car le bois, en tant que matériau naturel renouvelable, est appelé à devenir une alternative aux combustibles fossiles et composés pétrochimiques à fort coût environnemental (FAO, 2007).

I.1.3 Le bois est généré par la xylogénèse

C'est l'activité de formation du bois, la xylogénèse, qui, en permettant aux plantes de développer des formes larges et variées, est directement à l'origine des nombreux services écologiques, économiques, sociaux, culturels et spirituels rendus par les forêts aux systèmes naturels et à l'humanité. La xylogénèse résulte de l'activité du cambium vasculaire, une couche large de une à quelques cellules capables de se diviser entre le bois et l'écorce des arbres (Larson, 1994). Les nouvelles cellules de bois sont produites par la division des cellules cambiales puis suivent un programme de différenciation pour atteindre leur forme mature et fonctionnelle : elles s'élargissent puis forment une paroi rigide lignifiée et meurent (Wilson, 1984). La partie II de ce manuscrit est dédiée à la description des processus biologiques qui caractérisent la production et la différenciation des cellules du xylème.

I.1.4 La dynamique est un aspect clé de la xylogénèse

Au cours d'une année, la production et la différenciation des cellules du xylème ne prennent place qu'à certaines dates, durent un certain laps de temps et vont à une certaine vitesse qui sont fonction de l'environnement et de l'état physiologique de l'arbre. Ces « quand », « combien de temps » et « à quelle vitesse » caractérisent la dynamique intra-annuelle de la formation du bois. En zone tempérée par exemple, le cambium n'est actif que du printemps à l'automne, lorsque les conditions sont favorables, et s'arrête pendant l'hiver (Wilson, 1984). Cette activité cyclique de la production des cellules se matérialise par l'empilement d'anneaux concentriques de bois autour du tronc, les cernes annuels de croissance. De plus, chaque cellule qui compose un cerne se développe dans la saison selon un timing, des durées et des vitesses spécifiques et possède donc sa propre dynamique de développement. La dynamique est un aspect clé de la xylogénèse car c'est elle qui détermine la quantité et la qualité du bois produit : nombre et morphologie des cellules et densité du bois. Dans ce manuscrit, nous allons explorer la dynamique intra-annuelle de la formation du bois pour trois espèces de conifères – le sapin pectiné (*Abies alba* Mill.), l'épicéa commun (*Picea abies* (L.) Karst.) et le pin sylvestre (*Pinus sylvestris* L.) – en zone tempérée (nord-est de la France).

I.2 Structure et fonction du bois dans l'arbre

I.2.1 Le bois assure des fonctions essentielles pour la plante

Le bois est un tissu biologique végétal produit par les plantes dites ligneuses, dont les arbres sont l'exemple le plus connu. Cependant, il existe d'autres plantes ligneuses telles que les lianes ou les arbustes (par exemple le genévrier). Le bois assure des fonctions essentielles pour la plante, dont les trois principales sont : (1) le support mécanique aux axes qui soutiennent les tissus photosynthétiques au-dessus du sol (Fournier *et al.*, 2006), (2) la conduction de la sève brute (eau et éléments minéraux) des racines vers les feuilles le long du

continuum sol-plante-atmosphère (Sperry *et al.*, 2008) et (3) la mise en réserve de nutriments, carbohydrates, composés de défense, lipides et eau (Kozlowski & Pallardy, 1997). Le bois est composé de plusieurs types de cellules dont les proportions varient selon les espèces. Nous ne décrivons ici que la structure du bois des conifères, qui est plus simple que celle des feuillus.

I.2.2 Les trachéides verticales sont les éléments majeurs du bois des conifères

Le bois des conifères est qualifié d'homoxylé car les trachéides, qui représentent jusqu'à 95% de son volume (Jacquiot, 1955), sont les seuls éléments à assurer la conduction de la sève brute (Figure I.1). Elles sont arrangées en files radiales, c'est-à-dire des files larges d'une cellule orientées dans le sens des rayons. Une trachéide fonctionnelle est une cellule morte, vide, entourée d'une paroi secondaire et à la forme très effilée puisque environ 100 fois plus longue (2,5 à 5 mm) que large (30 µm en moyenne) (Figure I.2). Cependant, la largeur des trachéides ainsi que l'épaisseur de leur paroi varient largement selon le moment auquel elles sont formées dans la saison. Les trachéides formées au début de la saison de végétation sont caractérisées par un diamètre large (30-50 µm) et des parois fines (2-3 µm) et forment le bois initial, aussi appelé bois de printemps. Les trachéides formées en fin de saison de végétation ont un diamètre deux à trois fois plus étroit (15-25 µm) et des parois deux à trois fois plus épaisses (4-8 µm) et forment le bois final, aussi appelé bois d'été. Cette hétérogénéité morphologique amène à des différences fonctionnelles : avec leurs larges lumens (espaces intracellulaires), les trachéides du bois initial sont importantes pour la conduction de la sève brute tandis qu'avec leurs parois épaisses, les trachéides du bois final assurent plutôt la fonction de soutien mécanique du bois (Wilson, 1984).

La sève brute se déplace dans le lumen des trachéides au cours de la transpiration en suivant une trajectoire en hélice depuis l'extrémité d'une trachéide vers l'extrémité de la trachéide adjacente qui la chevauche (Beck, 2010). Le transport est facilité par l'absence de contenu cellulaire, par la perméabilité des parois cellulaires cellulosiques et par la présence abondante de petites ouvertures dans la paroi cellulaire secondaire, appelées ponctuations, au niveau des extrémités contiguës des trachéides qui se chevauchent. Plusieurs années après avoir été formées, les trachéides s'obstruent tandis que les cellules du parenchyme (voir ci-dessous) meurent. Ceci marque le passage d'un bois fonctionnel, le bois d'aubier, à un bois inerte qui ne conduit plus la sève brute, le bois de cœur (car situé plus au centre de la tige).

I.2.3 Autres éléments du bois des conifères

Avec les trachéides verticales, les cellules horizontales du parenchyme sont les éléments que l'on retrouve dans le bois de tous les conifères (Jacquiot, 1955). Les cellules parenchymateuses s'organisent en rayons ligneux (Figure I.1) qui jouent un rôle physiologique important dans le stockage des carbohydrates et des minéraux et dans la translocation radiale de l'eau, des minéraux et de composés organiques (Kozlowski & Pallardy, 1997). Les rayons peuvent également contenir des trachéides disposées

horizontalement. C'est toujours le cas chez les pins et les épicéas, plus rarement chez les sapins (Jacquiot, 1955). Chez certaines espèces, on trouve également des cellules verticales du parenchyme (absentes chez les pins) et des canaux résinifères orientés verticalement ou horizontalement. Les canaux résinifères sont des cavités recouvertes de cellules épithéliales qui sécrètent la résine. Ils sont normalement absents dans le bois des sapins mais peuvent apparaître en réponse à une blessure (canaux résinifères traumatiques), donnant ainsi une fonction protectrice au bois.

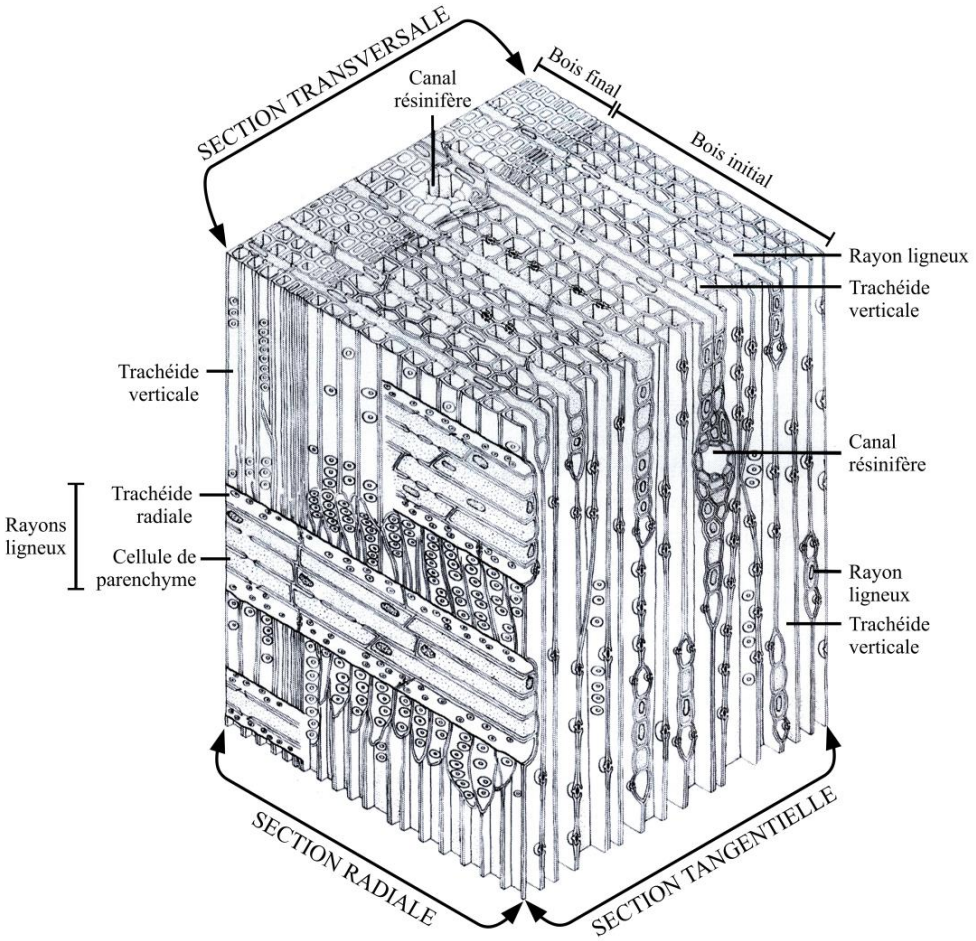

Figure I.1 : structure du bois des conifères. Modifié depuis Raven *et al.* (2007).

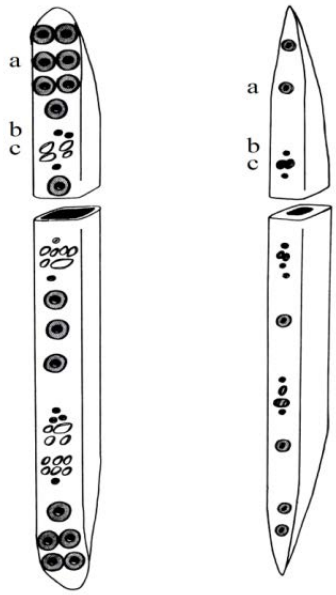

Figure I.2 : trachéides du bois initial (gauche) et du bois final (droite). a. Larges ponctuations inter-trachéide ; b, petites ponctuations vers les trachéides radiales ; c, ponctuations de taille moyenne vers les cellules du parenchyme. Modifié depuis Kozlowski & Pallardy (1997). Notez ici que les proportions ne sont pas respectées puisque une trachéide est environ 100 fois plus haute que large.

I.3 La formation du bois : un processus intégré à la croissance des arbres

Chez les végétaux, la production de nouvelles cellules n'a lieu que dans des zones spécialisées constituées de cellules indifférenciées appelées méristèmes (Evert, 2006; Beck, 2010). L'activité de production cellulaire des méristèmes résulte en une augmentation en longueur et en diamètre des axes avec, en fonction de la différenciation des cellules produites, la formation de tissus variés (histogénèse) et d'organes (organogénèse) tels que les feuilles ou les fleurs. Deux grands types de méristèmes peuvent être distingués selon le type de croissance qu'ils induisent. Les premiers sont les méristèmes primaires, principalement situés à l'apex des racines et des rameaux (dans les bourgeons pour les plantes vasculaires) de toutes les plantes, dont l'activité de production cellulaire résulte plutôt en l'allongement des axes (croissance primaire). Les méristèmes primaires produisent les nouveaux organes et donnent la forme de base de la plante. Chez les ligneux (plantes qui produisent du bois, en opposition aux herbacées), ces méristèmes primaires donnent rapidement naissance aux méristèmes secondaires (ou méristèmes latéraux), situés à la périphérie et sur toute la longueur de la tige, des rameaux et des racines, dont l'activité de production cellulaire permet la croissance en diamètre des axes (croissance secondaire).

Certains méristèmes primaires, comme ceux qui contribuent à la formation des feuilles et des fleurs, cessent de fonctionner lorsque ces organes atteignent leur taille et leur forme génétiquement prédéterminées (croissance déterminée). Mais la plupart des méristèmes primaires et tous les méristèmes secondaires sont capables de s'auto-entretenir et sont des méristèmes dits permanents : leur activité est maintenue durant toute la vie de la plante dont la croissance est alors indéterminée.

L'un des deux méristèmes secondaires, le plus externe dans les axes, est le phellogène. Il produit deux tissus protecteurs : le phelloderme vers l'intérieur et le suber (liège) vers l'extérieur. L'association phelloderme-phellogène-suber constitue le périderme. Le cambium vasculaire est l'autre méristème secondaire que l'on trouve dans les axes des ligneux. Il se trouve entre le xylème secondaire (bois), tissu qu'il produit vers l'intérieur, et le phloème secondaire (liber), tissu conducteur de la sève élaborée (eau, éléments minéraux et produits de la photosynthèse) qu'il produit vers l'extérieur (Figure I.3). L'ensemble des tissus extérieurs au cambium forme l'écorce. Pour les arbres en conditions de croissance favorables, le recrutement du bois est responsable de la majeure partie de la croissance radiale, avec un ratio phloème/xylème entre 1/3 et 1/10 (Evert, 2006; Gričar *et al.*, 2009; Beck, 2010). En zone tempérée, la cyclicité de l'activité du cambium, couplée à la croissance en longueur, se traduit par l'empilement de cônes de bois dans les axes des arbres qui, en section transversale, forment les cernes annuels de croissance (Figure I.4).

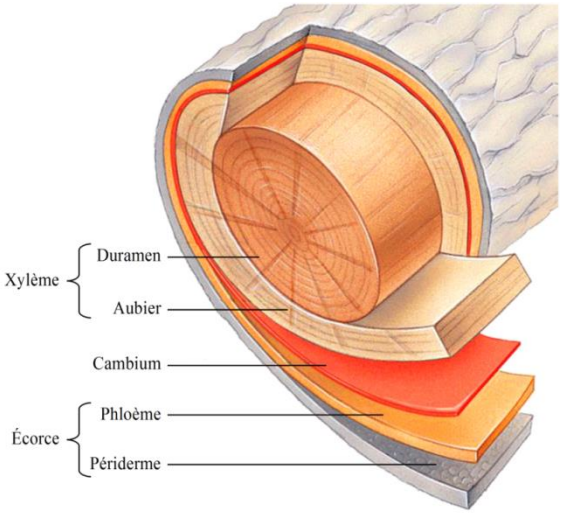

Figure I.3 : Structure des axes des arbres.

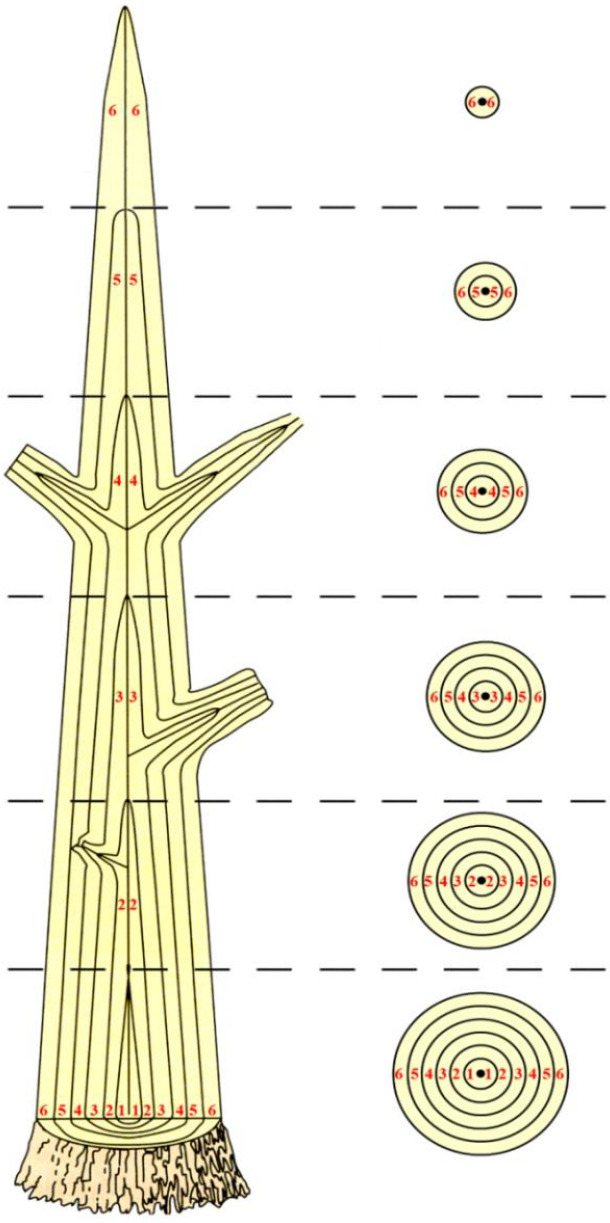

Figure I.4 : Empilement des pousses annuelles dans un arbre. Schéma montrant l'empilement des incréments annuels de xylème dans le tronc et les branches (coupe longitudinale), ainsi que l'empilement des cernes de croissance (coupe transversale). Modifié depuis Raven *et al.* (2007).

I.4 Cambium et activité cambiale

I.4.1 L'apparition du cambium a été une innovation majeure de l'histoire des végétaux

L'apparition du cambium au Dévonien moyen, il y a 360 millions d'années, a été l'un des évènements les plus importants de l'histoire des végétaux (Rowe & Speck, 2005). L'activité cambiale assure la longévité des arbres à travers le renouvellement régulier du xylème et du phloème. Ce potentiel de croissance illimitée, couplé à l'invention préalable de la lignine (Weng & Chapple, 2010), a permis aux arbres de devenir les plus gros organismes vivants, avec le développement des couronnes larges et ramifiées pouvant exposer plusieurs centaines de m² de feuilles à la lumière. Cependant, l'aspect clé de cette innovation concerne sa plasticité, c'est-à-dire sa capacité à générer des variations architecturales et mécaniques en réponse à des changements environnementaux. C'est cette plasticité qui permet aux plantes de s'adapter à des conditions variées et changeantes dans le temps, assurant leur pérennité et leur donnant la possibilité de coloniser des milieux variés (Rowe & Speck, 2005).

I.4.2 Structure du cambium

En plus d'être un méristème histogène, le cambium constitue un pont de communication entre le xylème et le phloème (Catesson & Lachaud, 1993). Le cambium est constitué d'une couche large de une à quelques cellules vivantes, hautement vacuolées, à parois primaires fines (0,1-1 µm) et diamètres étroits (5-8 µm), appelées initiales (Larson, 1994; Lachaud *et al.*, 1999). Deux types de cellules initiales peuvent être trouvées dans le cambium : (1) les initiales radiales courtes isodiamétriques (environ 40 µm de longueur et de diamètre), minoritaires (10-40%), à l'origine des éléments horizontaux du xylème (parenchyme des rayons) et du phloème (Figure I.5A) ; (2) les initiales fusiformes longues, de formes effilées (200 µm à plusieurs mm de longueur, 5-10 µm de diamètre), majoritaires (60-90%) et à l'origine des éléments conducteurs du xylème (trachéides) et du phloème (Figure I.5B).

I.4.3 L'activité cambiale produit le xylème et le phloème

Les initiales peuvent se diviser selon plusieurs directions pour différents objectifs. Les divisions anticlinales (= radiales) permettent de maintenir l'intégrité du cambium, à travers son augmentation en circonférence lors de la croissance du tronc par le maintien de l'équilibre entre les deux types d'initiales Les cellules fusiformes peuvent également se diviser transversalement pour donner deux initiales radiales. Enfin, les divisions périclinales (= longitudinales), qui représentent 90% des divisions cambiales (Lachaud *et al.*, 1999), sont à l'origine de l'activité histogène du cambium en produisant les cellules du bois dans la direction centripète (du côté de la moelle) et du phloème dans la direction centrifuge (du côté de l'écorce). Une initiale cambiale qui se divise dans l'orientation périclinale produit une cellule mère du xylème ou du phloème capable de se diviser à son tour avant de se

différencier en cellule du xylème ou du phloème, l'autre cellule fille gardant les caractéristiques et la fonction d'une initiale cambiale. En général, les cellules mères du xylème se divisent plus souvent que celles du phloème (Larson, 1994), ce qui aboutit à l'incrément supérieur du xylème par rapport au phloème.

I.4.4 Terminologie

Les initiales cambiales qui constituent le cambium au sens strict ne sont pas reconnaissables anatomiquement des cellules mères indifférenciées. Dans cette thèse, les termes « zone cambiale » et « cambium » sont utilisés indifféremment pour désigner la couche de cellules capables de se diviser composée des initiales cambiales et des cellules mères (Figure I.5C). De même, le terme « cellule cambiale » englobe à la fois les initiales cambiales et les cellules mères. Le terme « activité cambiale » est utilisé pour désigner l'activité de production cellulaire par le cambium, alors que le terme « formation du bois » désigne à la fois la production des nouvelles cellules du xylème par l'activité cambiale et la différenciation de ces cellules en cellules fonctionnelles matures.

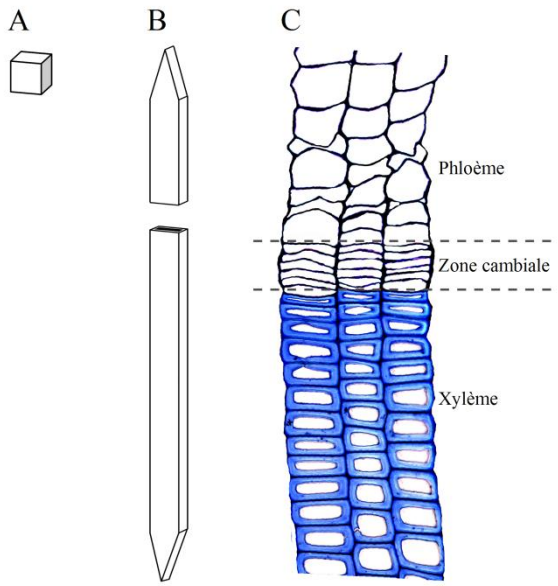

Figure I.5 : initiales cambiales et zone cambiale. Schéma en 3 dimensions d'initiales cambiales radiales (A) et fusiformes (B), et image d'une zone cambiale de pin sylvestre en coupe transversale observée en microscopie optique (×400) et contenant uniquement des cellules fusiformes à l'origine des trachéides (C).

I.5 Caractéristiques des espèces étudiées

Nous avons travaillé sur 3 espèces de conifères : le sapin pectiné (*Abies alba* Mill.), l'épicéa commun (*Picea abies* (L.) Karst.) et le pin sylvestre (*Pinus sylvestris* L.). Une première raison du choix de ces trois espèces est pratique, ces espèces pouvant être trouvées à proximité du lieu du travail. En plus, les arbres des trois espèces poussent naturellement en mélange et peuvent donc être trouvés dans les mêmes conditions de croissance. Une autre raison tient en la nature du bois produit par les conifères, qui est beaucoup plus homogène que celui des feuillus car constitué de 90 à 95% de trachéides. Ceci facilite grandement le suivi de la formation du bois, qui n'est étudiée qu'à travers la production et la différenciation de ce

type cellulaire. Enfin, ces trois espèces sont d'importance majeure en Europe, que ce soit à travers leur large distribution ou leur place prépondérante dans l'industrie.

I.5.1 Caractéristiques générales

Les arbres des trois espèces atteignent généralement entre 25 et 40 m à l'âge adulte, même si des hauteurs de 50 à 60 m sont exceptionnellement atteintes par les sapins et les épicéas. Leur durée de vie est généralement comprise entre 100 et 300 ans, mais il n'est pas rare pour les sapins d'atteindre des âges entre 500 et 600 ans. Les trois espèces sont sempervirentes, avec des durées de vie des feuilles différentes : 2-3 ans pour les pins, 6-7 ans pour les sapins et épicéas (Becker *et al.*, 1995; Reich *et al.*, 1996). Sapins et pins ont un système racinaire plutôt pivotant (pivots et racines horizontales), alors que l'épicéa a un système racinaire plutôt traçant (racines horizontales et pivots secondaires) (Drexhage et al., 2001). La reproduction des trois espèces se fait à partir des cônes, les cônes mâles contenant le pollen qui fertilise les graines contenues par les cônes femelles.

I.5.2 Distribution

Des trois espèces étudiées, le sapin est le moins répandu, avec une distribution limitée aux régions montagneuses de l'est, de l'ouest, du sud et du centre de l'Europe (Wolf, 2003) (Figure I.6). L'aire de présence principale s'étend de la Pologne à la frontière nord de la Grèce en latitude, et de l'ouest des Alpes à la Roumanie et la Bulgarie en longitude. Des aires plus isolées, formant des îlots, sont observées en France (Vosges, Jura, Massif Central, Pyrénées, Corse et Normandie), en Espagne (Pyrénées) et sur toute la longueur de l'Italie (jusqu'à la Calabre, qui constitue l'extrémité sud de sa distribution). Le sapin pectiné peut être trouvé à des altitudes entre 150 m (Pologne et République Tchèque) et 1300 m (Roumanie), exceptionnellement jusqu'à plus de 2100 m dans les Alpes de l'ouest.

L'épicéa présente une distribution beaucoup plus large, du nord de la Sibérie à la péninsule des Balkans en latitude, des Alpes Françaises à l'Est de la Sibérie en longitude (Skrøppa, 2003). Sa distribution verticale s'étend du niveau de la mer à plus de 2300 m d'altitude dans les Alpes du nord.

Le pin sylvestre est le conifère le plus répandu du monde, avec une aire naturelle de distribution qui s'étend du nord de la Norvège au sud de l'Espagne en latitude et de l'ouest de l'Europe (Ecosse) à l'est de la Sibérie en longitude (Mátyás *et al.*, 2004). Sa distribution verticale s'étend du niveau de la mer à plus de 2400 m en montagne.

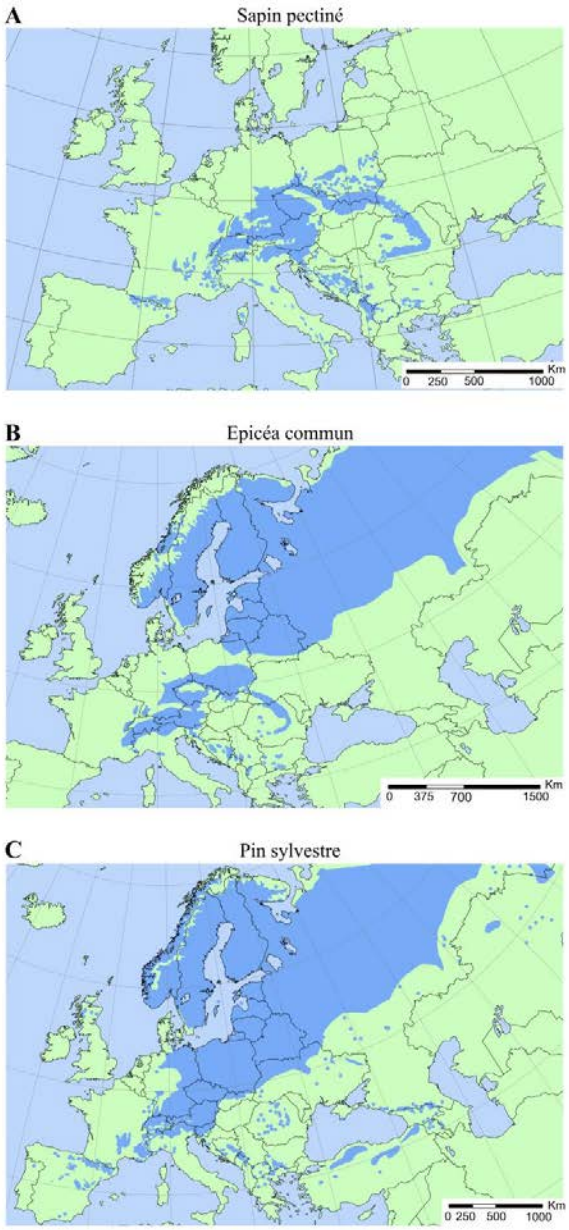

Figure I.6 : Aires de répartition naturelle du sapin pectiné, de l'épicéa commun et du pin sylvestre en Europe. Cartes téléchargées depuis www.euforgen.org.

I.5.3 Croissance

Les trois espèces diffèrent dans leur dynamique de croissance à long terme (Bouriaud & Popa, 2009). Le pin sylvestre a son optimum de croissance aux jeunes âges, puis sa productivité diminue rapidement pour devenir la plus faible des trois espèces. Par contre, la croissance du sapin pectiné est faible aux jeunes âges, mais elle augmente progressivement et reste élevée même pour des arbres âgés. L'épicéa commun présente un comportement intermédiaire : sa croissance optimale est observée plus tard que chez le pin sylvestre, puis sa productivité diminue mais reste la plus forte des trois espèces jusqu'à un âge intermédiaire.

I.5.4 Autécologie

Le pin sylvestre est une espèce de pleine lumière (intolérante à l'ombre) qui ne survit pas à quelques années d'ombrage (Mason *et al.*, 2004). A l'inverse, le sapin est une espèce extrêmement tolérante à l'ombre, capable de supporter des intensités lumineuses réduites (seulement 5 à 20% de la lumière ambiante par exemple) pendant des décennies (Robakowski *et al.*, 2004). L'épicéa commun a un comportement intermédiaire : c'est une espèce de demi-ombre, capable de s'acclimater à de larges variations d'intensités lumineuses (Grassi & Bagnaresi, 2001). Le sapin pectiné est plus sensible au gel et à la sécheresse que l'épicéa commun, alors que le pin sylvestre est la plus résistante à la sécheresse et au froid des trois espèces (Lebourgeois *et al.*, 2010). Le sapin est aussi plus thermophile et à de plus grandes exigences en nutriments que l'épicéa et le pin (Pinto & Gegout, 2005). Ces caractéristiques font du pin sylvestre une espèce pionnière, alors que l'épicéa commun est une espèce intermédiaire et le sapin pectiné une espèce de fin de succession.

I.5.5 Importance pour l'industrie

En Europe, les résineux occupent une place prépondérante dans l'industrie du bois (largement devant les feuillus) et en constante augmentation (Ekström, 2012). Ainsi, l'épicéa commun est l'espèce la plus importante économiquement en Europe, par l'utilisation privilégiée de son bois pour la construction, la pâte à papier, les meubles et les instruments de musique. Cependant, les bois du pin sylvestre et du sapin pectiné ont également une importance majeure pour l'industrie à travers de nombreux usages, surtout pour la construction et la pâte à papier.

I.6 La xylogénèse est étroitement liée à l'environnement

La xylogénèse est un processus étroitement lié à l'environnement. La conséquence la plus directement visible de ce lien étroit avec l'environnement est l'empilement des cernes annuels, résultat de l'activité cyclique du cambium avec l'alternance des saisons favorables et défavorables à la croissance. Au cours de la saison, les facteurs environnementaux influencent la dynamique des processus de la xylogénèse (division, élargissement cellulaire et formation de la paroi secondaire) pour laisser des empreintes permanentes dans la structure du bois formé (Schweingruber, 1996; Vaganov *et al.*, 1999; Wodzicki, 2001; Fonti *et al.*, 2010). Un arbre vivant pendant des siècles, son bois représente une archive naturelle des changements environnementaux. Ainsi, la largeur de cerne (équivalente au nombre de cellules), la densité du bois et la morphologie des cellules (diamètre et épaisseur de la paroi) sont des bio-indicateurs de choix utilisés pour reconstruire et étudier les changements climatiques du dernier millénaire (Hughes *et al.*, 1984; Treydte *et al.*, 2006; IPCC, 2007; Jones *et al.*, 2009; Trouet *et al.*, 2009; Fonti *et al.*, 2010).

Aujourd'hui pourtant, les mécanismes fins par lesquels les facteurs environnementaux influencent la formation du bois sont encore peu connus (Vaganov *et al.*, 2011). Les raisons de

cette méconnaissance sont exposées dans la section I.8 de cette introduction, mais la principale est qu'évaluer l'influence des facteurs environnementaux sur la formation du bois est extrêmement complexe. Comme le processus dépend d'autres processus physiologiques de l'arbre (par exemple la photosynthèse et la respiration) eux-mêmes sujets à l'influence des facteurs environnementaux (Denne & Dodd, 1981), il est classiquement admis que l'influence des facteurs environnementaux peut être directe, par stimulation ou inhibition physique des processus de la xylogénèse, ou indirecte, à travers la disponibilité en carbohydrates et/ou les régulateurs de croissance (Figure I.7).

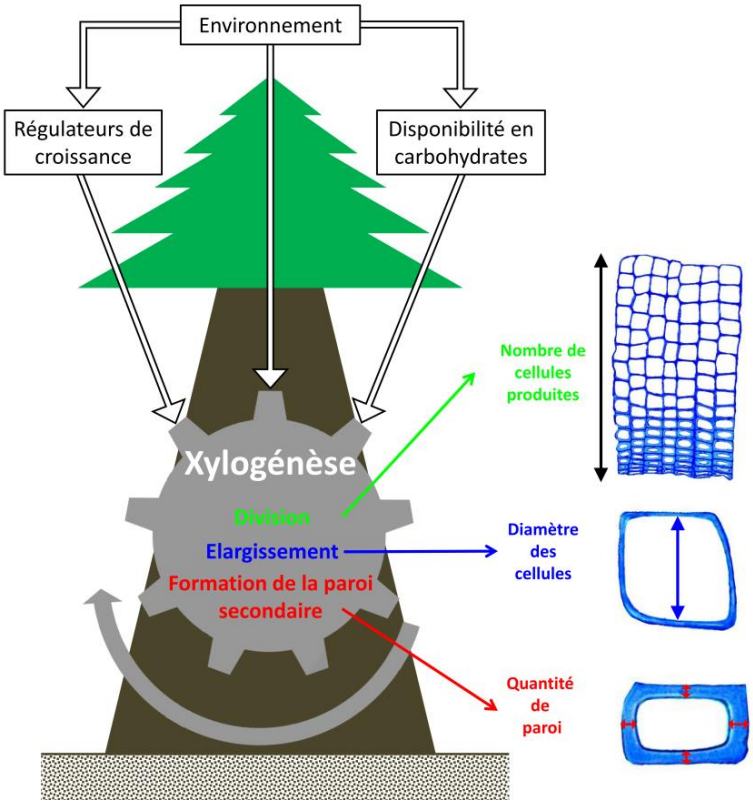

Figure I.7 : Influence de l'environnement sur la formation du bois. Schéma simplifié de l'influence de l'environnement sur la formation du bois. L'influence des facteurs environnementaux sur les processus se fait directement ou via les régulateurs de croissance et/ou la disponibilité en carbohydrates.

I.7 La xylogénèse joue un rôle crucial dans le cycle du carbone

Le bois est constitué pour moitié environ de carbone (≈ 50% de la masse sèche) (Lamlom & Savidge, 2003). Il représente donc un réservoir important de carbone, autour de 400 à 500 gigatonnes (GtC) (Lal, 2008; Chave *et al.*, 2009), soit l'immense majorité du stock de carbone contenu par les plantes (450 – 650 GtC) (Figure I.8). Si le réservoir « bois » apparait faible en comparaison des quantités de carbone trouvées dans le sol ou les océans, il représente tout de même plus de la moitié du total de carbone atmosphérique (estimé entre 730 et 800 GtC), l'un des principaux contributeurs aux changements climatiques. En outre, le rôle de ce réservoir apparait fondamental lorsque l'on considère l'ampleur des échanges entretenus avec l'atmosphère, qui sont les plus importants du cycle. Chaque année, les plantes fixent par la photosynthèse approximativement 120 GtC de carbone atmosphérique. Environ la moitié est libérée par respiration, tandis que l'autre moitié est accumulée sous forme de biomasse (Zhao & Running, 2010), principalement grâce à la xylogénèse qui permet

l'accumulation pérenne du carbone dans les parois des cellules produites par le cambium. Donc, la xylogénèse est le processus qui incorpore les plus larges quantités de carbone qui se retrouvent séquestrées chaque année dans la biomasse terrestre. Aujourd'hui, la séquestration de carbone est même légèrement supérieure au rejet par respiration, ce qui constitue un puits de carbone qui mitige les changements climatiques (Canadell & Raupach, 2008).

Dans ce contexte de changements climatiques, un enjeu crucial est de comprendre ce qui pilote les échanges de carbone entre les écosystèmes et l'atmosphère. Depuis la fin des années 1990, la méthode « Eddy Covariance » a été de plus en plus utilisée pour mesurer les flux nets de carbone dans les écosystèmes forestiers (Baldocchi, 2003). La méthode permet de mesurer les échanges de carbone à l'interface canopée-atmosphère et procure donc des informations très intéressantes sur le cycle du carbone dans les forêts. Cependant, elle ne permet pas de discriminer les différentes composantes du flux. Par exemple, elle ne donne pas d'information directe sur l'accumulation du carbone dans le bois en formation, qui constitue le puits de carbone dominant de l'écosystème (Barford *et al.*, 2001). Le suivi de la dynamique intra-annuelle de la xylogénèse pourrait donc apporter des informations complémentaires, basées sur le suivi des processus et qui renseignent directement sur la dynamique de l'accumulation du carbone dans le bois en formation au cours de la saison. De telles informations permettraient de mieux comprendre les mécanismes qui pilotent les flux de carbone dans les écosystèmes forestiers.

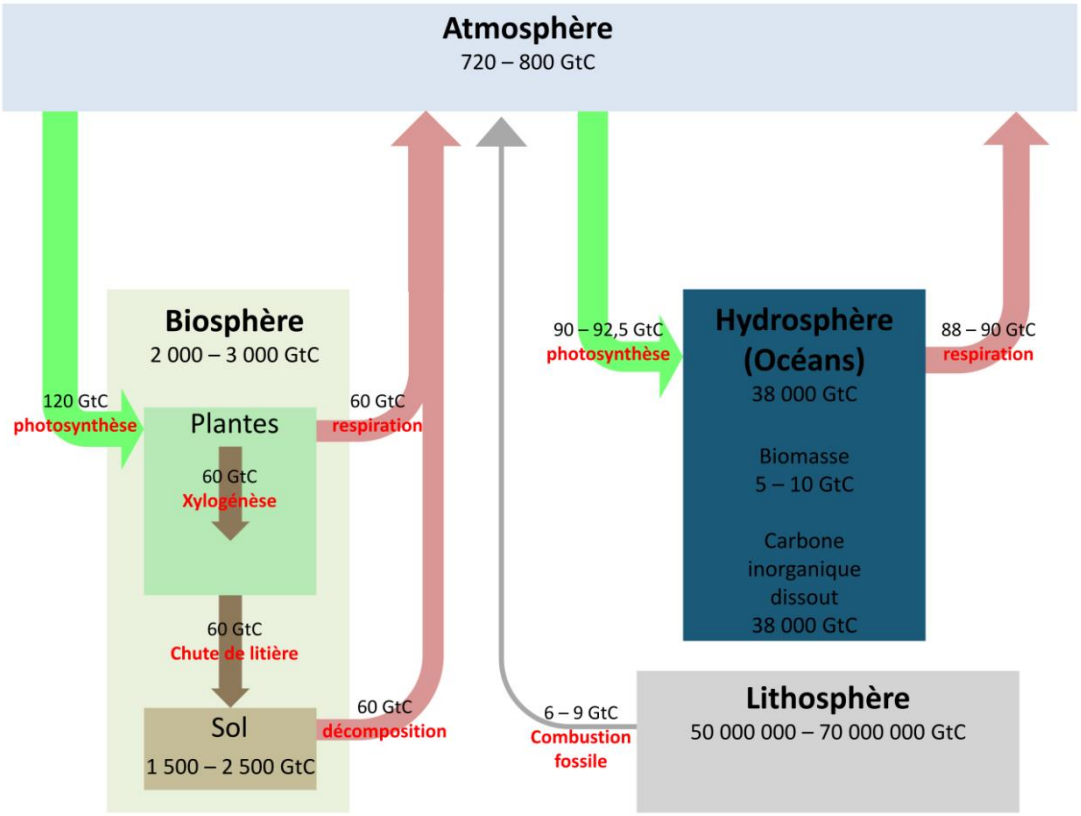

Figure I.8 : Le cycle du carbone. Schéma extrêmement simplifié des grands réservoirs de carbone de la planète, des flux entre ces réservoirs et des mécanismes à l'origine de ces flux. Les chiffres, donnés en gigatonnes de carbone (GtC) ont été compilés à partir de ceux donnés par Falkowski *et al.* (2000), Lal (2008), Zhao & Running (2010) et Groombridge & Jenkins (2002).

I.8 Notre connaissance du fonctionnement de la xylogénèse est fragmentaire

Aujourd'hui, un enjeu crucial de la recherche scientifique est d'évaluer l'influence des changements climatiques en cours et à venir sur les organismes, les populations et les écosystèmes. Les arbres produisent le bois, un tissu important de leur fonctionnement, qui a une incidence majeure sur le fonctionnement des écosystèmes et fournit une ressource essentielle pour l'Homme. Il est donc important de comprendre l'impact des changements environnementaux sur le processus de la formation du bois dans les arbres. Dans cet enjeu, notre degré de compréhension dépendra de notre connaissance du fonctionnement de la xylogénèse (Plomion *et al.*, 2001).

La xylogénèse est particulièrement bien documentée à échelle fine (voir, par exemple, Roberts & McCann, 2000; Savidge *et al.*, 2000; Plomion *et al.*, 2001; Mellerowicz & Sundberg, 2008), par exemple à travers l'étude de l'ultrastructure des cellule au cours du processus (Chaffey *et al.*, 2002; Oda & Hasezawa, 2006), l'exploration des voies de biosynthèse de la cellulose (Somerville, 2006; Blomqvist *et al.*, 2007) ou de la lignine (Whetten & Sederoff, 1995; Boerjan *et al.*, 2003; Vanholme *et al.*, 2008; Vanholme *et al.*, 2010), l'étude des mécanismes moléculaires de régulation au niveau génétique (Hertzberg *et al.*, 2001; Ranik, 2005; Zhong & Ye, 2007; Du & Groover, 2010) ou hormonal (Little & Wareing, 1981; Savidge, 1983; Aloni, 1987; Savidge, 1988; Uggla *et al.*, 1996; Tuominen *et al.*, 1997; Sundberg *et al.*, 2000; Nilsson *et al.*, 2008). Il est d'ailleurs frappant de voir avec quelle intensité la formation du bois est étudiée dans le détail, alors qu'une compréhension globale du processus manque largement (Vaganov *et al.*, 2011). Chaffey (2002) a ainsi parlé de « molécularisation » de la recherche sur la formation du bois. Pourtant, une compréhension complète de la formation du bois nécessite d'intégrer les résultats obtenus à échelle fine avec une connaissance plus globale du fonctionnement du processus. L'étude de la dynamique s'inscrit pleinement dans cette volonté d'une compréhension plus générale du fonctionnement de la xylogénèse.

Bien qu'encore peu explorée, la dynamique de la xylogénèse a fait l'objet d'un intérêt nouveau et fort en même temps que la conscience accrue d'un changement climatique. En effet, une connaissance détaillée du timing, de la durée et de la vitesse des processus est une étape préalable indispensable vers une compréhension mécaniste de l'influence de l'environnement sur la xylogénèse (Gričar *et al.*, 2011). Récemment, un nombre croissant d'études ont ainsi été consacrées au suivi de la dynamique de la xylogénèse et ont procuré d'excellents jeux de données (voir, par exemple, Rossi *et al.*, 2006; Rossi *et al.*, 2008b). Ce suivi a été effectué sur des arbres matures en conditions naturelles de croissance (par exemple de Luis *et al.*, 2007; Rossi *et al.*, 2008a), sur des arbres instrumentés (par exemple Oribe *et al.*, 2001; Gričar *et al.*, 2006; Gričar *et al.*, 2007; de Luis *et al.*, 2011), sur des arbres soumis à des conditions expérimentales sur le terrain (par exemple Gričar & Čufar, 2008; Jyske et al., 2010) ou encore des jeunes arbres en conditions contrôlées sous serres (par exemple Rossi *et al.*, 2009).

La grande majorité de ces études a recherché l'influence des facteurs internes (par exemple l'âge et la taille des arbres) et externes (facteurs climatiques tels la température, le rayonnement et la disponibilité en eau) sur la dynamique de la formation du bois, en se focalisant sur des aspects particuliers du procesus comme la phénologie cambiale (Seo *et al.*, 2008; Moser *et al.*, 2010; Rossi *et al.*, 2011; Swidrak *et al.*, 2011) et de la xylogénèse (Rossi *et al.*, 2007; Deslauriers *et al.*, 2008; Lupi *et al.*, 2012), le taux maximal de production des cellules (Rossi *et al.*, 2006), ou les patrons généraux (phénologie de l'activité cambiale et de la xylogénèse et vitesse de production des cellules) du processus (Mäkinen *et al.*, 2003; Gruber *et al.*, 2009; Linares *et al.*, 2009; Camarero *et al.*, 2010; Gruber *et al.*, 2010; Rathgeber *et al.*, 2011; Zhai *et al.*, 2012).

Ces aspects de la dynamique, en particulier le début, la fin, la durée et la vitesse de production des cellules, sont importants car ils déterminent le nombre total de cellules produites, équivalent à la largeur du cerne. Cependant, un cerne n'est pas qu'un nombre de cellules, c'est aussi la morphologie de chacune de ces cellules, qui en retour influence la densité du bois, un trait fonctionnel crucial et un déterminant majeur des propriétés du bois pour l'industrie (Bowyer *et al.*, 2007). Il semble donc également important de considérer les aspects de la dynamique qui déterminent la morphologie des cellules et la densité du bois, à savoir quand, combien de temps et à quelle vitesse chaque cellule s'est élargie et a formé sa paroi secondaire durant l'année. Ces aspects de la dynamique du développement cellulaire ont été considérés dans les années 1960 – 1970 (voir, par exemple, Whitmore & Zahner, 1966; Skene, 1969; Wodzicki, 1971; Skene, 1972), mais restent toutefois très peu documentés et largement négligés dans la littérature récente.

En plus du manque d'informations sur les aspects du développement cellulaires, on ne connait encore pas bien les mécanismes fins par lesquels la dynamique intra-annuelle de la xylogénèse donne naissance à un cerne. Par exemple, on sait que le diamètre des cellules et la quantité de paroi déposée dépendent respectivement de la cinétique d'élargissement et de formation de la paroi secondaire (Skene, 1969; Skene, 1972), mais sans être capable de dire qui de la durée ou de la vitesse des processus détermine les variations des dimensions entre les cellules du cerne. Au final, le manque d'une caractérisation précise et exhaustive de la dynamique, ainsi que d'une compréhension des mécanismes qui relient cette dynamique à la structure du cerne annuel, limitent notre compréhension des mécanismes par lesquels les facteurs de l'environnement influencent la dynamique de la xylogénèse et la structure du cerne qui en résulte (Vaganov *et al.*, 2011).

I.9 Objectif et plan de la thèse

Cette thèse s'inscrit dans la volonté de comprendre l'influence des facteurs environnementaux sur la formation du bois. À travers une exploration approfondie de l'aspect "dynamique", l'objectif global est d'améliorer notre compréhension du fonctionnement général de la xylogénèse. Le travail repose sur un jeu de données large et original, composé de 45 arbres de 3 espèces de conifères (sapin pectiné, épicéa commun et pin sylvestre) suivis

pendant 3 ans (2007 – 2009) et répartis dans 3 peuplements mélangés le long d'un gradient altitudinal (350 – 650 m) dans le nord-est de la France. Après les parties II et III, qui présentent respectivement les bases biologiques de la formation du bois et le dispositif expérimental mis en place pour cette thèse, les résultats de la thèse sont exposés dans 5 parties successives (parties III à VIII), chacune constituée d'un article scientifique publié ou en préparation pour une revue scientifique internationale. Chacune de ces parties apporte une contribution originale à l'étude du fonctionnement de la dynamique intra-annuelle de la xylogénèse :

- La partie IV (article 1) vise à caractériser les patrons saisonniers de la xylogénèse, c'est-à-dire à un « niveau arbre », la phénologie (début, fin et durée) de l'activité cambiale et de la xylogénèse et la vitesse de production des cellules. Cette partie propose également d'étudier les relations entre la durée, la vitesse de production cellulaire et l'incrément annuel de bois.
- La partie V (article 2) s'intéresse aux aspects moins connus du développement cellulaire et propose ainsi de caractériser la cinétique (timing, durée et vitesse) des processus de différenciation (élargissement et formation de la paroi) pour chaque cellule le long du cerne.
- Sur la base de ce travail, la partie VI (article 3) cherche à établir les mécanismes fins par lesquels la dynamique de la xylogénèse forme la structure du cerne. Ainsi, nous chercherons à savoir si ce sont des changements dans la durée ou dans la vitesse des processus de différenciation qui expliquent les changements dans la morphologie des cellules (taille et épaisseur de la paroi) et la densité du bois le long du cerne.
- La partie VII (article 4) utilise la connaissance de la cinétique des processus de différenciation cellulaire pour caractériser la dynamique saisonnière de l'accumulation de la biomasse dans le bois. La cinétique des processus de différenciation cellulaire est intégrée à l'échelle de l'arbre et le taux journalier de l'accumulation du carbone dans le bois en formation est déterminé et associé aux variables climatiques (température, photopériode, radiation lumineuse et disponibilité en eau).
- La partie VIII (article 5) se base sur les connaissances acquises dans les parties V et VI pour développer une approche mécaniste de l'influence du climat sur le développement cellulaire et la structure du cerne. Pour cela, le travail présenté recherche l'influence des variables climatiques sur les changements dans la cinétique des processus de différenciation cellulaire et dans la morphologie des cellules formée au cours de la saison.

Enfin, la partie IX fait la synthèse des différents résultats établis dans ces 5 parties et des conclusions sont fournies dans la partie X.

I.10 Références

Aloni R. 1987. *The induction of vascular tissues by auxin*.

Baldocchi DD. 2003. Assessing the eddy covariance technique for evaluating carbon dioxide exchange rates of ecosystems: past, present and future. *Global Change Biology* ***9***(4): 479-492.

Barford CC, Wofsy SC, Goulden ML, Munger JW, Pyle EH, Urbanski SP, Hutyra L, Saleska SR, Fitzjarrald D, Moore K. 2001. Factors controlling long-and short-term sequestration of atmospheric CO2 in a mid-latitude forest. *Science* **294**(5547): 1688-1691.

Beck CB. 2010. *An Introduction to Plant Structure and Development*: Cambridge University Press.

Becker M, Bert D, Landmann G, Lévy G, Rameau JC, Ulrich E 1995. Growth and decline symptoms of silver fir and Norway spruce in northeastern France: relation to climate, nutrition and silviculture. In: Landmann G, Bonneau M eds. *Forest decline and air pollution effects in the French mountains*. Berlin: Springer, 120-142.

Blomqvist K, Djerbi S, Aspeborg H, Teeri T 2007. Cellulose biosynthesis in forest trees. In: Malcolm Brown Jr. R, Saxena IM eds. *Cellulose: Molecular and Structural Biology*. Dordrecht, The Netherlands. : Springer, 85-106.

Boerjan W, Ralph J, Baucher M. 2003. Lignin biosynthesis. *Annual Review of Plant Biology* **54**: 519-546.

Bouriaud O, Popa I. 2009. Comparative dendroclimatic study of Scots pine, Norway spruce, and silver fir in the Vrancea Range, Eastern Carpathian Mountains. *Trees-Structure and Function* **23**(1): 95-106.

Bowyer JL, Shmulsky R, Haygreen JG. 2007. *Forest products and wood science*: Wiley-Blackwell.

Camarero JJ, Olano JM, Parras A. 2010. Plastic bimodal xylogenesis in conifers from continental Mediterranean climates. *New Phytologist* **185**(2): 471-480.

Canadell JG, Raupach MR. 2008. Managing forests for climate change mitigation. *Science* **320**(5882): 1456-1457.

Catesson AM, Lachaud S. 1993. The cambium, structure, function and control of its seasonal activity. *Acta Botanica Gallica* **140**(4): 337-350.

Chaffey N. 2002. Why is there so little research into the cell biology of the secondary vascular system of trees? *New Phytologist* **153**(2): 213-223.

Chaffey N, Barlow P, Sundberg B. 2002. Understanding the role of the cytoskeleton in wood formation in angiosperm trees: hybrid aspen (Populus tremula x P-tremuloides) as the model species. *Tree Physiology* **22**(4): 239-249.

Chave J, Coomes D, Jansen S, Lewis SL, Swenson NG, Zanne AE. 2009. Towards a worldwide wood economics spectrum. *Ecology Letters* **12**(4): 351-366.

de Luis M, Gričar J, Čufar K, Raventós J. 2007. Seasonal dynamics of wood formation in *Pinus halepensis* from dry and semi-arid ecosystems in Spain. *Iawa Journal* **28**(4): 389-404.

de Luis M, Novak K, Raventós J, Gričar J, Prislan P, Čufar K. 2011. Cambial activity, wood formation and sapling survival of Pinus halepensis exposed to different irrigation regimes. *Forest Ecology and Management* **262**(8): 1630-1638.

Denne M, Dodd R 1981. The environmental control of xylem differentiation. *Xylem cell development*. Tunbridge Wells: Castle House Publications 236-255.

Deslauriers A, Rossi S, Anfodillo T, Saracino A. 2008. Cambial phenology, wood formation and temperature thresholds in two contrasting years at high altitude in southern Italy. *Tree Physiology* **28**(6): 863-871.

Drexhage M, Lebourgeois F, Jabiol B, Bruciamacchie M. 2001. Tempête et racines. *Forêt-Entreprise* **139**(3): 46-49.

Du J, Groover A. 2010. Transcriptional Regulation of Secondary Growth and Wood Formation. *Journal of Integrative Plant Biology* **52**(1): 17-27.

Ekström H 2012. Wood raw material markets, 2011-2012 *UNECE/FAO Forest products annual market review, 2011-2012*. Geneva, Switzerland: UNECE/FAO, 37-46.

Evert RF. 2006. *ESAU'S PLANT ANATOMY - Meristems, Cells, and Tissues of the Plant Body: Their Structure, Function, and Development*. Hoboken: John Wiley & Sons, Inc.

Falkowski P, Scholes RJ, Boyle E, Canadell J, Canfield D, Elser J, Gruber N, Hibbard K, Hogberg P, Linder S, Mackenzie FT, Moore B, Pedersen T, Rosenthal Y, Seitzinger S, Smetacek V, Steffen W. 2000. The global carbon cycle: A test of our knowledge of earth as a system. *Science* **290**(5490): 291-296.

FAO 2007. Global wood and wood products flow - trends and perspectives. Shanghai, China: FAO Advisory Committe on Paper and Wood Products.

FAO. 2010. *Global Forest Resources Assessment 2010: main report*. Rome: Food and Agriculture Organization of the United Nations.

Fonti P, von Arx G, Garcia-Gonzalez I, Eilmann B, Sass-Klaassen U, Gaertner H, Eckstein D. 2010. Studying global change through investigation of the plastic responses of xylem anatomy in tree rings. *New Phytologist* **185**(1): 42-53.

Fournier M, Stokes A, Coutand C, Fourcaud T, Moulia B. 2006. *Tree biomechanics and growth strategies in the context of forest functional ecology*.

Grassi G, Bagnaresi U. 2001. Foliar morphological and physiological plasticity in Picea abies and Abies alba saplings along a natural light gradient. *Tree Physiology* **21**(12-13): 959-967.

Gričar J, Čufar K. 2008. Seasonal dynamics of phloem and xylem formation in silver fir and Norway spruce as affected by drought. *Russian Journal of Plant Physiology* **55**(4): 538-543.

Gričar J, Krze L, Čufar K. 2009. Number of cells in xylem, phloem and dormant cambium in silver fir (*Abies alba*), in trees of different vitality. *Iawa Journal* **30**(2): 121-133.

Gričar J, Rathgeber CBK, Fonti P. 2011. Monitoring seasonal dynamics of wood formation. *Dendrochronologia* **29**(3): 123-125.

Gričar J, Zupančič M, Čufar K, Koch G, Schmitt U, Oven P. 2006. Effect of local heating and cooling on cambial activity and cell differentiation in the stem of Norway spruce (*Picea abies*). *Annals of Botany* **97**(6): 943-951.

Gričar J, Zupančič M, Čufar K, Oven P. 2007. Regular cambial activity and xylem and phloem formation in locally heated and cooled stem portions of Norway spruce. *Wood Science and Technology* **41**(6): 463-475.

Groombridge B, Jenkins MD. 2002. *World atlas of biodiversity: earth's living resources in the 21st century*.

Gruber A, Baumgartner D, Zimmermann J, Oberhuber W. 2009. Temporal dynamic of wood formation in *Pinus cembra* along the alpine treeline ecotone and the effect of climate variables. *Trees-Structure and Function* **23**(3): 623-635.

Gruber A, Strobl S, Veit B, Oberhuber W. 2010. Impact of drought on the temporal dynamics of wood formation in *Pinus sylvestris*. *Tree Physiology* **30**(4): 490-501.

Hertzberg M, Aspeborg H, Schrader J, Andersson A, Erlandsson R, Blomqvist K, Bhalerao R, Uhlen M, Teeri TT, Lundeberg J, Sundberg B, Nilsson P, Sandberg G. 2001. A transcriptional roadmap to wood formation. *Proceedings of the National Academy of Sciences of the United States of America* **98**(25): 14732-14737.

Hughes MK, Schweingruber FH, Cartwright D, Kelly PM. 1984. July-August temperature at Edinburgh between 1721 and 1975 from tree-ring density and width data. *Nature* **308**(5957): 341-344.

IPCC 2007. Climate change 2007: the physical science basis.Contribution of Working Group I to the fourth assessment report of the Intergovernmental Panel on Climate Change. Cambridge, UK.

Jacquiot C. 1955. *Atlas d'anatomie du bois des conifères*. Paris.

Jones PD, Briffa KR, Osborn TJ, Lough JM, van Ommen TD, Vinther BM, Luterbacher J, Wahl ER, Zwiers FW, Mann ME, Schmidt GA, Ammann CM, Buckley BM, Cobb KM, Esper J, Goosse H, Graham N, Jansen E, Kiefer T, Kull C, Kuettel M, Mosley-Thompson E, Overpeck JT, Riedwyl N, Schulz M, Tudhope AW, Villalba R, Wanner H, Wolff E, Xoplaki E. 2009. High-resolution palaeoclimatology of the last millennium: a review of current status and future prospects. *Holocene* **19**(1): 3-49.

Jyske T, Hölttä T, Mäkinen H, Nöjd P, Lumme I, Spiecker H. 2010. The effect of artificially induced drought on radial increment and wood properties of Norway spruce. *Tree Physiology* **30**(1): 103-115.

Kozlowski TT, Pallardy SG. 1997. *Physiology of woody plants (second edition)*: Academic Press.

Lachaud S, Catesson AM, Bonnemain JL. 1999. Structure and functions of the vascular cambium. *Comptes Rendus de l'Académie des Sciences - Series III - Sciences de la Vie* **322**(8): 633-650.

Lal R. 2008. Sequestration of atmospheric CO2 in global carbon pools. *Energy & Environmental Science* **1**(1): 86-100.

Lamlom SH, Savidge RA. 2003. A reassessment of carbon content in wood: variation within and between 41 North American species. *Biomass & Bioenergy* **25**(4): 381-388.

Larson PR. 1994. *The vascular cambium: development and structure*. Berlin Heidelberg: Springer-Verlag.

Lebourgeois F, Rathgeber CBK, Ulrich E. 2010. Sensitivity of French temperate coniferous forests to climate variability and extreme events (*Abies alba*, *Picea abies* and *Pinus sylvestris*). *Journal of Vegetation Science* **21**(2): 364-376.

Linares JC, Camarero JJ, Carreira JA. 2009. Plastic responses of *Abies pinsapo* xylogenesis to drought and competition. *Tree Physiology* **29**(12): 1525-1536.

Little CHA, Wareing PF. 1981. Control of cambial activity and dormancy in *Picea sitchensis* by indol-3-ylacetic and abscisic acids. *Canadian Journal of Botany-Revue Canadienne De Botanique* **59**(8): 1480-1493.

Lupi C, Morin H, Deslauriers A, Rossi S. 2012. Xylogenesis in black spruce: does soil temperature matter? *Tree Physiology* **32**(1): 74-82.

Mäkinen H, Nöjd P, Saranpää P. 2003. Seasonal changes in stem radius and production of new tracheids in Norway spruce. *Tree Physiology* **23**(14): 959-968.

Mason WL, Edwards C, Hale SE. 2004. Survival and early seedling growth of conifers with different shade tolerance in a Sitka spruce spacing trial and relationship to understorey light climate. *Silva Fennica* **38**(4): 357-370.

Mátyás C, Ackzell L, Samuel CJA 2004. EUFORGEN Technical Guidelines for genetic conservation and use for Scots pine (*Pinus sylvestris*). Rome, Italy: International Plant Genetic Resources Institute.

Mellerowicz EJ, Sundberg B. 2008. Wood cell walls: biosynthesis, developmental dynamics and their implications for wood properties. *Current Opinion in Plant Biology* **11**(3): 293-300.

Moser L, Fonti P, Büntgen U, Esper J, Luterbacher J, Franzen J, Frank D. 2010. Timing and duration of European larch growing season along altitudinal gradients in the Swiss Alps. *Tree Physiology* **30**(2): 225-233.

Nilsson J, Karlberg A, Antti H, Lopez-Vernaza M, Mellerowicz E, Perrot-Rechenmann C, Sandberg G, Bhalerao RP. 2008. Dissecting the molecular basis of the regulation of wood formation by auxin in hybrid aspen. *Plant Cell* **20**(4): 843-855.

Oda Y, Hasezawa S. 2006. Cytoskeletal organization during xylem cell differentiation. *Journal of Plant Research* **119**(3): 167-177.

Oribe Y, Funada R, Shibagaki M, Kubo T. 2001. Cambial reactivation in locally heated stems of the evergreen conifer *Abies sachalinensis* (Schmidt) Masters. *Planta* **212**(5-6): 684-691.

Perlin J. 1997. *Forest journey : the role of wood in the development of civilization*.

Pinto PE, Gegout JC. 2005. Assessing the nutritional and climatic response of temperate tree species in the Vosges Mountains. *Annals of Forest Science* **62**(7): 761-770.

Plomion C, Leprovost G, Stokes A. 2001. Wood formation in trees. *Plant Physiology* **127**(4): 1513-1523.

Ranik M. 2005. *Expression profiling and characterization of wood formation genes in Eucalyptus.* University of Pretoria Pretoria.

Rathgeber CBK, Rossi S, Bontemps J-D. 2011. Cambial activity related to tree size in a mature silver-fir plantation. *Annals of Botany* **108**(3): 429-438.

Raven PH, Evert RF, Eichhorn SE. 2007. *Biologie végétale*.

Reich PB, Oleksyn J, Modrzynski J, Tjoelker MG. 1996. Evidence that longer needle retention of spruce and pine populations at high elevations and high latitudes is largely a phenotypic response. *Tree Physiology* **16**(7): 643-647.

Robakowski P, Wyka T, Samardakiewicz S, Kierzkowski D. 2004. Growth, photosynthesis, and needle structure of silver fir (Abies alba Mill.) seedlings under different canopies. *Forest Ecology and Management* **201**(2-3): 211-227.

Roberts K, McCann MC. 2000. Xylogenesis: the birth of a corpse. *Current Opinion in Plant Biology* **3**(6): 517-522.

Rossi S, Deslauriers A, Anfodillo T, Carraro V. 2007. Evidence of threshold temperatures for xylogenesis in conifers at high altitudes. *Oecologia* **152**(1): 1-12.

Rossi S, Deslauriers A, Anfodillo T, Carrer M. 2008a. Age-dependent xylogenesis in timberline conifers. *New Phytologist* **177**(1): 199-208.

Rossi S, Deslauriers A, Anfodillo T, Morin H, Saracino A, Motta R, Borghetti M. 2006. Conifers in cold environments synchronize maximum growth rate of tree-ring formation with day length. *New Phytologist* **170**(2): 301-310.

Rossi S, Deslauriers A, Gričar J, Seo J-W, Rathgeber CBK, Anfodillo T, Morin H, Levanic T, Oven P, Jalkanen R. 2008b. Critical temperatures for xylogenesis in conifers of cold climates. *Global Ecology and Biogeography* **17**(6): 696-707.

Rossi S, Morin H, Deslauriers A, Plourde P-Y. 2011. Predicting xylem phenology in black spruce under climate warming. *Global Change Biology* **17**(1): 614-625.

Rossi S, Simard S, Rathgeber CBK, Deslauriers A, De Zan C. 2009. Effects of a 20-day-long dry period on cambial and apical meristem growth in *Abies balsamea* seedlings. *Trees-Structure and Function* **23**(1): 85-93.

Rowe N, Speck T. 2005. Plant growth forms: an ecological and evolutionary perspective. *New Phytologist* **166**(1): 61-72.

Savidge RA. 1983. The role of plant hormones in higher plant cellular differentiation. II. Experiments with the vascular cambium, and sclereid and tracheid differentiation in the pine, *Pinus contorta*. *Histochemical Journal* **15**(5): 447-466.

Savidge RA. 1988. Auxin and ethylene regulation of diameter growth in trees. *Tree Physiology* **4**(4): 401-414.

Savidge RA, Barnett JR, Napier R. 2000. *Cell and molecular biology of wood formation*. Oxford, UK: BIOS Scientific Publishers Ltd.

Schweingruber FH. 1996. *Tree rings and environment: dendroecology*.

Seo JW, Eckstein D, Jalkanen R, Rickebusch S, Schmitt U. 2008. Estimating the onset of cambial activity in Scots pine in northern Finland by means of the heat-sum approach. *Tree Physiology* **28**(1): 105-112.

Skene DS. 1969. The period of time taken by cambial derivatives to grow and differentiate into tracheids in *Pinus radiata* D. Don. *Annals of Botany* **33**(2): 253-262.

Skene DS. 1972. The kinetics of tracheid development in *Tsuga canadensis* Carr. and its relation to tree vigour. *Annals of Botany* **36**(1): 179-187.

Skrøppa T 2003. EUFORGEN Technical Guidelines for genetic conservation and use for Norway spruce (*Picea abies*). Rome, Italy: International Plant Genetic Resources Institute.

Somerville C 2006. Cellulose synthesis in higher plants. *Annual Review of Cell and Developmental Biology*, 53-78.

Sperry JS, Meinzer FC, McCulloh KA. 2008. Safety and efficiency conflicts in hydraulic architecture: scaling from tissues to trees. *Plant Cell and Environment* **31**(5): 632-645.

Sundberg B, Uggla C, Tuominen H. 2000. *Cambial growth and auxin gradients*.

Swidrak I, Gruber A, Kofler W, Oberhuber W. 2011. Effects of environmental conditions on onset of xylem growth in Pinus sylvestris under drought. *Tree Physiology* **31**: 483–493.

Treydte KS, Schleser GH, Helle G, Frank DC, Winiger M, Haug GH, Esper J. 2006. The twentieth century was the wettest period in northern Pakistan over the past millennium. *Nature* **440**(7088): 1179-1182.

Trouet V, Esper J, Graham NE, Baker A, Scourse JD, Frank DC. 2009. Persistent Positive North Atlantic Oscillation Mode Dominated the Medieval Climate Anomaly. *Science* **324**(5923): 78-80.

Tuominen H, Puech L, Fink S, Sundberg B. 1997. A radial concentration gradient of indole-3-acetic acid is related to secondary xylem development in hybrid aspen. *Plant Physiology* **115**(2): 577-585.

Uggla C, Moritz T, Sandberg G, Sundberg B. 1996. Auxin as a positional signal in pattern formation in plants. *Proceedings of the National Academy of Sciences of the United States of America* **93**(17): 9282-9286.

Vaganov EA, Anchukaitis KJ, Evans MN 2011. How well understood are the processes that create dendroclimatic records? A mechanistic model of the climatic control on conifer tree-ring growth dynamics. In: Hughes MK, Swetnam TW, Diaz HF eds. *Dendroclimatology*. London: Springer-Verlag, 37-75.

Vaganov EA, Hughes MK, Kirdyanov AV, Schweingruber FH, Silkin PP. 1999. Influence of snowfall and melt timing on tree growth in subarctic Eurasia. *Nature* **400**(6740): 149-151.

Vanholme R, Demedts B, Morreel K, Ralph J, Boerjan W. 2010. Lignin Biosynthesis and Structure. *Plant Physiology* **153**(3): 895-905.

Vanholme R, Morreel K, Ralph J, Boerjan W. 2008. Lignin engineering. *Current Opinion in Plant Biology* **11**(3): 278-285.

Weng J-K, Chapple C. 2010. The origin and evolution of lignin biosynthesis. *New Phytologist* **187**(2): 273-285.

Whetten R, Sederoff R. 1995. Lignin biosynthesis. *Plant Cell* **7**(7): 1001-1013.

Whitmore FW, Zahner R. 1966. Development of the xylem ring in stems of young red pine trees. *Forest Science* **12**: 198-210.

Wilson BF. 1984. *The growing tree*. Amherst: The university of Massachusetts press.

Wilson BF, Wodzicki TJ, Zahner R. 1966. Differentiation of cambial derivatives: proposed terminology. *Forest Science* **12**(4): 438-440.

Wodzicki TJ. 1971. Mechanism of xylem differentiation in *Pinus sylvestris* L. *Journal of Experimental Botany* **22**(72): 670-687.

Wodzicki TJ. 2001. Natural factors affecting wood structure. *Wood Science and Technology* **35**(1-2): 5-26.

Wolf H 2003. EUFORGEN Technical Guidelines for genetic conservation and use for silver fir (*Abies alba*). Rome, Italy: International Plant Genetic Resources Institute.

Zhai L, Bergeron Y, Huang J-G, Berninger F. 2012. Variation in intra-annual wood formation, and foliage and shoot development of three major Canadian boreal tree species. *American Journal of Botany* **99**(5): 827-837.

Zhao M, Running S. 2010. Drought-Induced Reduction in Global Terrestrial Net Primary Production from 2000 Through 2009. *Science* **329**(5994): 940-943.

Zhao M, Running SW. 2010. Drought-induced reduction in global terrestrial net primary production from 2000 through 2009. *Science* **329**(5994): 940-943.

Zhong R, Ye Z-H. 2007. Regulation of cell wall biosynthesis. *Current Opinion in Plant Biology* **10**(6): 564-572.

II BIOLOGIE DE LA FORMATION DU BOIS

II.1 Un processus biologique complexe

Les plantes, les animaux et les champignons suivent des processus de spécialisation cellulaire de façon à former des groupes spécifiques de cellules adaptées à la prise en charge de fonctions particulières. L'un des exemples les plus remarquables de spécialisation cellulaire chez les plantes est la formation du xylème (= xylogénèse). En effet, ce processus représente un exemple de différenciation cellulaire dans une forme exceptionnellement complexe (Plomion *et al.*, 2001). La xylogénèse nécessite l'ajustement des processus biologiques clés du fonctionnement des végétaux tels que la photosynthèse et la respiration (Gordon & Larson, 1968), le prélèvement d'eau (Abe *et al.*, 2003) et la nutrition (Lautner *et al.*, 2007). La xylogénèse implique également de nombreux processus fondamentaux du développement des végétaux, incluant la division cellulaire, la signalisation cellulaire (communication entre cellules qui régit leur développement, leur organisation et coordonne leur activité), l'élargissement cellulaire, la spécification cellulaire, la synthèse et le dépôt de paroi cellulaire, la lignification et la mort cellulaire programmée (Roberts & McCann, 2000). Le fonctionnement coordonné de ces processus est contrôlé par une large variété de facteurs exogènes (environnement) et endogènes (gènes, phytohormones), ainsi que par des interactions entre ces facteurs (Plomion *et al.*, 2001; Savidge, 2001).

En général, la xylogénèse n'est décrite qu'à travers la formation des éléments conducteurs et de soutien, c'est-à-dire les trachéides (conifères) et les fibres et les vaisseaux (feuillus), qui constituent l'immense majorité du bois. La différenciation de ces cellules implique 5 processus fondamentaux : (1) la division, (2) l'élargissement cellulaire, (3) la formation de la paroi secondaire, (4) la lignification et (5) la mort cellulaire programmée.

II.2 La division

II.2.1 Mécanisme de la division

La production des nouvelles cellules du xylème se fait par division périclinale des cellules cambiales. Chez les eucaryotes (animaux, végétaux et champignons), les cellules en division poursuivent une séquence régulière d'évènements appelée cycle cellulaire. Le cycle cellulaire est un processus hautement ordonné qui résulte en la formation de deux cellules filles identiques à la suite de plusieurs phases : G1, S, G2 et M (Taiz & Zeiger, 1998; Evert, 2006). La phase G1 correspond à une période d'intense activité biochimique, durant laquelle la cellule grossit légèrement et les différentes organelles, les enzymes et d'autres molécules du cytoplasme augmentent en nombre. En phase S, l'ADN est répliqué par duplication des chromosomes, puis la cellule entre en phase G2 lors de laquelle les structures requises pour la division commencent à s'assembler et les chromosomes commencent à se condenser. Enfin, lors de la phase M, la cellule se divise par mitose (division du noyau, aussi appelée caryocinèse) et cytocinèse (division du cytoplasme). La mitose est elle-même constituée de plusieurs phases qui aboutissent à la séparation du matériel génétique contenu par le noyau en deux jeux identiques (Figure II.1).

Contrairement aux cellules animales, les cellules végétales sont entourées d'une paroi primaire fine (0.1-1 µm), souple mais résistante qui assure un soutien mécanique, régule le volume et le contenu cellulaire, définit et maintient la forme de la cellule, « colle » les cellules ensemble, stocke des réserves de nourriture et constitue une barrière de protection (Taiz & Zeiger, 1998; Rose, 2003). La paroi primaire est principalement composée de polysaccharides, avec des microfibrilles de cellulose (15-40% du poids sec) intégrées dans une matrice très hydratée (75-80% d'eau dans la paroi primaire) d'hémicelluloses (20-30%) et de pectines (30-50%), en association avec quelques protéines structurales (1-10%) (Taiz & Zeiger, 1998; Cosgrove & Jarvis, 2012). La cytocinèse nécessite donc la formation d'une nouvelle paroi primaire pecto-cellulosique entre les deux noyaux séparés. À la fin de la télophase, une structure composée de microtubules, de microfilaments d'actine et de réticulum endoplasmique, appelée phragmoplaste, se forme au niveau équatorial de la cellule, entre les deux ensembles de chromosomes, à partir de sous-unités dissociées du fuseau mitotique (structure composé de microtubules et protéines associées qui sépare les chromosomes lors de la mitose). Le phragmoplaste sert de charpente à la formation de la nouvelle paroi. Des vésicules provenant de l'appareil de Golgi contenant des précurseurs des composants de la paroi, viennent s'y associer et fusionnent pour former la plaque cellulaire, une cloison qui aboutit à la séparation définitive de deux cellules filles. Par la suite, les vésicules continuent de fusionner : les membranes des vésicules fusionnent ensemble et avec la membrane plasmique de la cellule en division pour former les nouvelles membranes plasmiques des deux cellules filles, tandis que le contenu des vésicules fournit les précurseurs à partir desquels la lamelle moyenne (membrane primitive composée de pectine qui joue un rôle dans l'adhérence entre les cellules et sur laquelle ira se déposer la paroi primaire) et la paroi primaire sont assemblées.

La cytocinèse lors de la division périclinale des cellules cambiales fusiformes est très particulière, car elle implique de former de la paroi primaire en grande quantité (Lachaud *et al.*, 1999). En effet, une cellule fusiforme pouvant être plusieurs centaines de fois plus longue que large, elle doit former une nouvelle paroi sur toute sa longueur lorsqu'elle se divise périclinalement, alors que pour les autres types cellulaires, la paroi est générée dans la partition la plus petite possible de la cellule. Par exemple, la surface de paroi qui doit être déposée est plusieurs centaines de fois supérieure à celle déposée dans les méristèmes primaires (Lachaud *et al.*, 1999). En conséquence, la déposition de la plaque cellulaire périclinale puis de la paroi primaire limitent probablement la fréquence des divisions cambiales : lorsqu'il faut de grandes vitesses de production cellulaire, l'arbre doit augmenter la taille de la population de cellules cambiales (Mellerowicz *et al.*, 2001), d'où les très bonnes relations obtenues entre le nombre de cellules cambiales et le taux de production (Gregory & Wilson, 1968; Gričar *et al.*, 2009).

Une autre particularité des cellules cambiales est qu'elles contiennent une large vacuole centrale qui contient de l'eau et des solutés. Une telle vacuole serait un moyen économique de se diviser pour les très grandes cellules cambiales fusiformes, car elle réduit la dépense d'énergie nécessaire à la biosynthèse de cytoplasme à chaque mitose (Lachaud *et al.*, 1999; Cosgrove, 2000b).

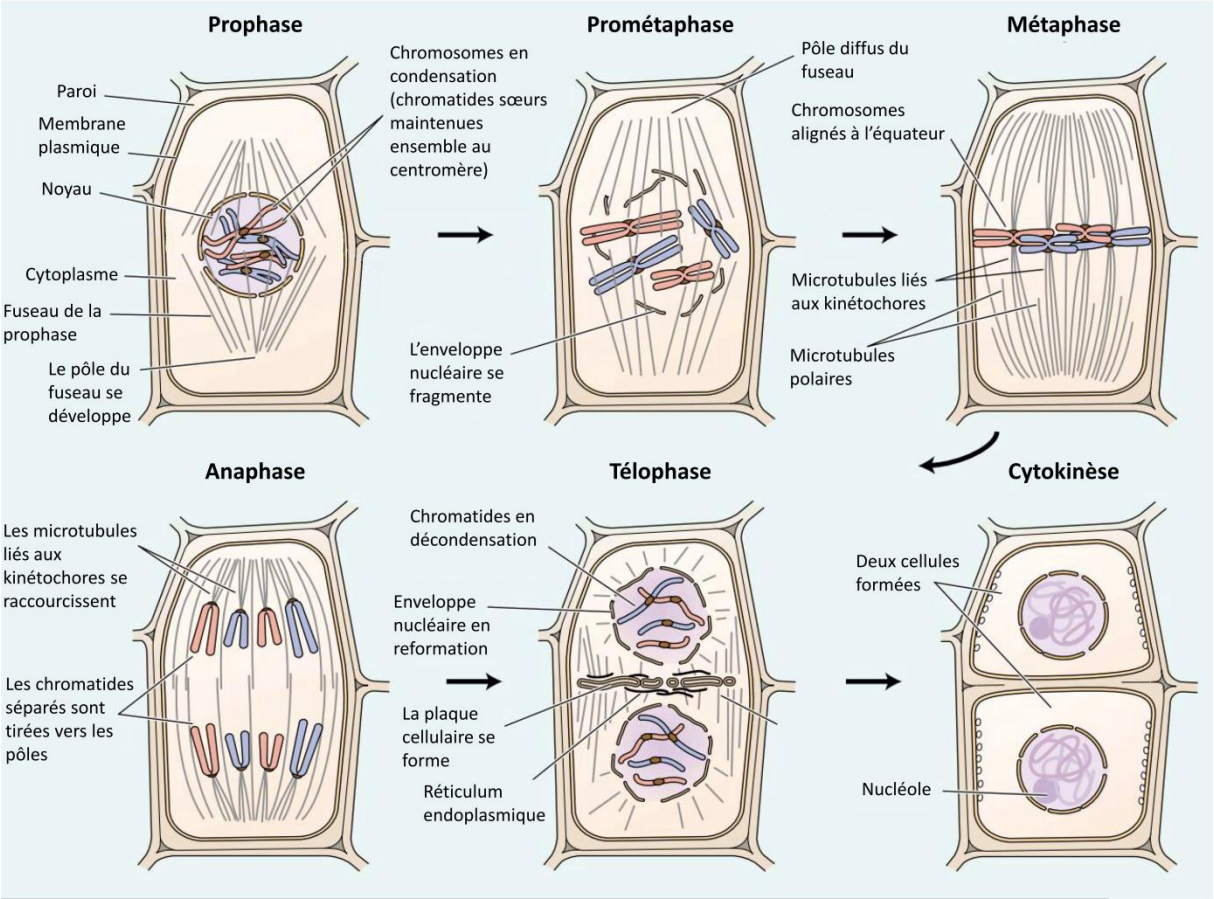

Figure II.1 : mitose d'une cellule végétale telle que subie par une cellule cambiale. En prophase, le matériel génétique dupliqué se condense en chromosomes, c'est-à-dire des paires de molécules d'ADN identiques (chromatides) reliées au centromère, et les microtubules du cytosquelette s'organisent pour former le fuseau mitotique. En prométaphase, l'enveloppe nucléaire se désagrège, certains microtubules s'accrochent à des complexes protéiques spécialisés (kinétochores) qui se forment au niveau des centromères des chromosomes. En métaphase, les microtubules liés aux kinétochores guident les chromosomes condensés à l'équateur de la cellule. En anaphase, les chromatides sœurs se séparent et migrent vers les pôles opposés de la cellule. En télophase, les chromatides se décondensent et l'enveloppe nucléaire se reforme pour individualiser les deux jeux identiques de matériel génétique en deux noyaux. La plaque cellulaire se forme, ce qui aboutira à la séparation définitive des deux cellules filles lors de la cytocinèse, pendant laquelle la membrane plasmique et la paroi primaire sont déposées. Modifié depuis (Taiz & Zeiger, 1998).

II.2.2 Régulation intrinsèque de la division

Le processus de division est contrôlé par des hormones végétales dont les plus connues sont les auxines, des hormones qui ont été impliquées dans la régulation de tous les aspects du développement des végétaux (Taiz & Zeiger, 1998). L'auxine joue un rôle fondamental dans l'induction et la progression du cycle cellulaire (Perrot-Rechenmann, 2010). Au niveau du cambium, il a été montré que l'auxine initie et maintient l'activité de division cellulaire (Little & Wareing, 1981; Savidge, 1983; Sundberg & Little, 1990), influence le taux de division cambiale (Little & Sundberg, 1991; Uggla *et al.*, 1998), ainsi que les proportions relatives de xylème et de phloème formé (Aloni, 1987). Cependant, l'auxine est nécessaire mais non suffisante pour stimuler les divisions cellulaires dans les tissus végétaux et la présence de cytokinine est également indispensable (Matsumoto-Kitano *et al.*, 2008). Enfin, les

gibbérellines sont également connues pour promouvoir la division cellulaire (Taiz & Zeiger, 1998). Auxines, cytokinines et gibbérellines agissent en stimulant la synthèse de protéines kinases cycline-dépendantes (CDKs), qui sont les enzymes clés de la régulation du processus de division (Taiz & Zeiger, 1998; Stals & Inze, 2001; Perrot-Rechenmann, 2010) : l'activité de régulation des CDKs est essentielle pour l'entrée des cellules qui ne se divisent pas dans le cycle cellulaire et pour le bon déroulement de celui-ci (contrôle de la transition de G1 à S et de G2 à M) (Stals & Inze, 2001).

II.3 L'élargissement cellulaire

Les nouvelles cellules produites dans la zone cambiale ressemblent au départ aux cellules cambiales, c'est-à-dire des cellules très allongées, avec un diamètre étroit, entourées d'une paroi primaire fine et élastique qui sont encore anatomiquement très éloignées des cellules matures et fonctionnelles du xylème. Une cellule produite dans la zone cambiale destinée à devenir un élément du xylème doit donc passer par un processus de différenciation qui lui permettra d'atteindre les caractéristiques morphologiques et physiologiques propres à ce type cellulaire. L'élargissement cellulaire, qui consiste en une augmentation irréversible du volume cellulaire, est la première phase de cette différenciation.

II.3.1 Mécanisme de l'élargissement cellulaire

L'élargissement cellulaire est un processus commun à tout type de cellules végétales. L'élargissement des cellules végétales et très différent de celui des cellules animales du fait de la présence de la paroi végétale qui définit la forme de la cellule. La paroi des cellules végétales, qui agit comme une barrière sélective, maintient une différence de pression osmotique ($\Delta\pi$) importante entre le protoplasme (espace intracellulaire) et l'apoplasme (espace extracellulaire) (Schopfer, 2006). Dans l'état de pleine turgescence, ce $\Delta\pi$ est compensé par une pression hydrostatique (turgescence, P) d'égale magnitude. Le potentiel hydrique de la cellule ($\Psi = P - \Delta\pi$) est alors nul. L'élargissement cellulaire se fait par relâchement de la paroi primaire et entrée d'eau dans la cellule (Cosgrove, 2000b; Cosgrove, 2000a; Schopfer, 2006).

Ce processus mécano-hydraulique peut être divisé en trois étapes: (1) à l'état de pleine turgescence, le contenu cellulaire exerce une contrainte sur la paroi, qui est étirée élastiquement (réversiblement) et est alors dans un état de tension dû à P (Figure II.2A). (2) Cette contrainte est libérée par un relâchement non élastique (irréversible) de la paroi (Figure II.2B), ce qui diminue P et (3) en retour entraîne l'absorption d'eau qui restaure P à son niveau précédent et produit un élargissement irréversible de la cellule (Schopfer, 2006). Comme pour la division, l'élargissement des cellules du xylème est fait de façon économique en remplissant la cellule d'une large vacuole centrale qui contient de l'eau et des solutés (Cosgrove, 2000b). Le relâchement de la paroi se fait sous l'action coordonnée de plusieurs enzymes qui rompent les liaisons entre les polysaccharides de la paroi (Rose & Bennett, 1999). En théorie, l'élargissement devrait rapidement s'arrêter car l'absorption d'eau entraîne

une dilution des solutés et donc de $\Delta\pi$, ce qui diminue le potentiel d'absorption d'eau par la cellule. Pour pallier ce problème, les cellules en élargissement maintiennent un $\Delta\pi$ constant par l'absorption active de solutés en parallèle du prélèvement d'eau. Un élargissement cellulaire régulier peut ainsi être maintenu pendant plusieurs heures ou plusieurs jours (Schopfer, 2006).

L'élargissement cellulaire est rendu possible par la combinaison remarquable d'élasticité et de rigidité de la paroi primaire, qui lui permet de supporter une distension tout en résistant aux importantes forces mécaniques imposées par la pression de turgescence (Cosgrove, 2000b). En outre, l'amincissement de la paroi durant l'extension est empêché par la déposition de paroi nouvellement synthétisée au cours du processus (Taiz & Zeiger, 1998; Cosgrove, 2000a) (Figure II.2C). La cellulose est synthétisée au niveau de la membrane plasmique par de grands complexes ordonnés de protéines appelés rosettes. Ces complexes sont formés de 6 sous-unités, contenant elles-mêmes de nombreuses unités (supposément 6) de cellulose synthase qui synthétisent les chaines linéaires de glucose qui composent les microfibrilles (Mutwil *et al.*, 2008). Les hémicelluloses et pectines sont synthétisées par des enzymes dans l'appareil de Golgi puis délivrées à la paroi par exocytose de minuscules vésicules (Taiz & Zeiger, 1998).

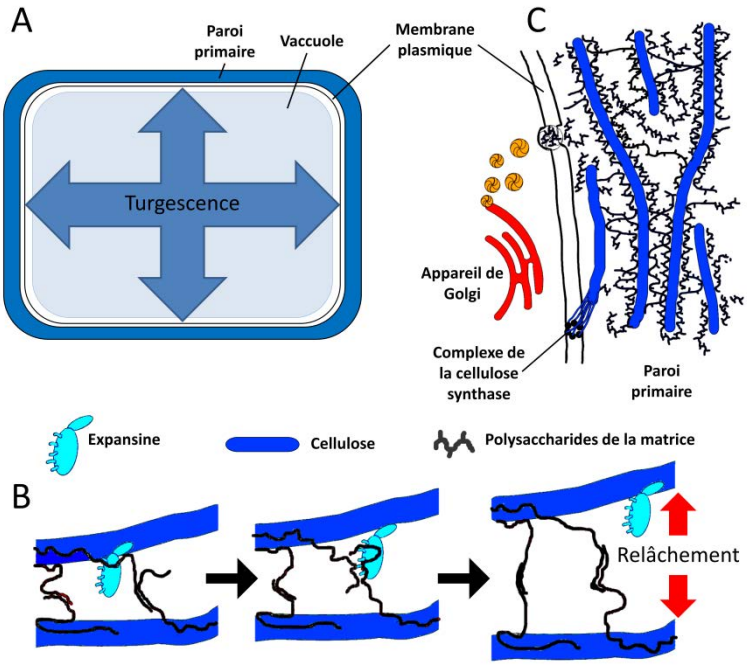

Figure II.2 : mécanismes de l'élargissement cellulaire. En A, la cellule est à l'état de pleine turgescence, avec une large vacuole centrale remplie d'eau qui exerce une pression sur la paroi qui est en tension. En B, la paroi est relâchée par affaiblissement des liaisons entre les polymères sous l'action d'enzymes (ici l'expansine), ce qui permet son élongation et l'entrée d'eau. En C, de la nouvelle paroi est déposée pour empêcher la rupture lors d'un élargissement prolongé. Modifié depuis Crosgrove (2000b).

II.3.2 Régulation intrinsèque de l'élargissement

Au même titre que la division cellulaire, le processus d'élargissement est régulé par des phytohormones, avec en premier lieu l'auxine mais aussi la cytokinine et les gibbérellines (Taiz & Zeiger, 1998). Ces phytohormones agiraient en augmentant l'extensibilité de la paroi, mais en empruntant des mécanismes moléculaires différents. L'action de l'auxine serait étroitement liée à des protéines clés du relâchement de la paroi appelées expansines

(Cosgrove, 2000b; Cosgrove *et al.*, 2002). Les expansines sont des protéines pH-dépendantes et sont activées à valeurs de pH acides. Or, l'auxine stimule l'activité et/ou le nombre des pompes à protons H+-ATPase de la membrane plasmique, induisant ainsi une extrusion de protons H+ et une acidification du milieu extracellulaire (Perrot-Rechenmann, 2010). Cette acidification active en retour les expansines qui provoquent alors le relâchement de la paroi en affaiblissant les liaisons entre les polysaccharides qui la constituent. Au contraire, le mode d'action des gibbérélines et cytokinines n'a pas été associé à une acidification (Taiz & Zeiger, 1998). Le mécanisme moléculaire de leur action est encore peu connu mais pourrait être en rapport avec l'enzyme xyloglucan-endotransglycosylase (XET) (Taiz & Zeiger, 1998), qui intervient également dans le processus de relâchement et d'extension de la paroi primaire lors de l'élargissement cellulaire (Rose & Bennett, 1999; Cosgrove, 2000a).

II.4 La formation de la paroi secondaire et la lignification

Après s'être élargie, une cellule du xylème (trachéide, fibre ou vaisseau) commence la construction d'une paroi secondaire épaisse, rigide et multicouche entre la paroi primaire et la membrane plasmique (Figure II.3). C'est le début de la déposition de cette paroi qui mettrait un terme à l'élargissement cellulaire (Abe *et al.*, 1997; Mellerowicz et al., 2001). La paroi secondaire n'est présente que dans certaines cellules spécialisées dont les trachéides, les vaisseaux et les fibres alors que toutes les cellules végétales, excepté certaines cellules reproductrices, sont entourées d'une paroi primaire. Suivant la formation de la paroi secondaire, la lignification – de la lamelle moyenne et des parois primaires et secondaires – est l'une des étapes finales à la différenciation des cellules du xylème. La paroi secondaire lignifiée donne force et rigidité aux tissus végétaux (Cosgrove & Jarvis, 2012). Ainsi, l'évolution des parois secondaires lignifiées a apporté aux plantes la force mécanique pour faire face aux pressions négatives générées dans les conduits du xylème par la transpiration, ainsi que le renforcement structurel nécessaire pour croitre verticalement au-dessus du sol et coloniser les terres (Weng & Chapple, 2010). Parce qu'elle est beaucoup plus épaisse que la paroi primaire, la paroi secondaire constitue le plus gros stock de biomasse des plantes terrestres (Zhong & Zheng-Hua, 2009).

La paroi secondaire diffère en structure et composition de la paroi primaire. Elle est composée d'un réseau de microfibrilles de cellulose (40-80%) et hémicellulose (10-40%) imperméabilisé, rigidifié et rendu plus résistant aux pathogènes par l'imprégnation de la lignine (5-30%) (Bidlack *et al.*, 1992; Zhong & Zheng-Hua, 2009). Elle est également moins hydratée que la paroi primaire, contenant environ 30% d'eau (Cosgrove & Jarvis, 2012). Elle est divisée en trois couches – S1 (externe), S2 (moyenne) et S3 (interne) – qui diffèrent principalement par l'orientation des microfibrilles de cellulose et leur épaisseur. L'orientation des microfibrilles de cellulose dans ces trois couches est plus ordonnée que dans la paroi primaire (Abe *et al.*, 1997). La couche S1 présente un angle presque transversal des microfibrilles qui change progressivement dans le sens horaire vers le lumen de la cellule, jusqu'à la disposition longitudinale qui caractérise la couche S2 qui est la plus épaisse. Enfin, la couche S3 est caractérisée par une brusque réorientation des microfibrilles qui retourne à

une hélice transversale. Les changements d'orientation des microfibrilles lors de la formation des couches successives de la paroi cellulaire vont toujours de pair avec la réorientation des microtubules corticaux (Abe *et al.*, 1995; Prodhan *et al.*, 1995; Chaffey *et al.*, 1999), ce qui supporte l'hypothèse que les microtubules contrôlent l'orientation des microfibrilles de cellulose dans la paroi.

II.4.1 Mécanisme de la formation de la paroi secondaire et de la lignification

La formation de la paroi secondaire commence par la déposition contre la paroi primaire d'une matrice dense de microfibrilles de cellulose et hémicellulose qui forme la couche S1. Comme pour la formation de la paroi primaire (Figure II.2C), la cellulose est synthétisée au niveau des rosettes de la membrane plasmique, tandis que les hémicelluloses sont synthétisées dans l'appareil de Golgi puis délivrées à la paroi par exocytose de vésicules. Alors que l'angle des microfibrilles est presque transversal dans la couche S1, les microfibrilles sont ensuite déposées selon l'arrangement longitudinal qui caractérise la couche S2. La couche S3 est enfin formée contre la couche S2 avec la brusque réorientation des microfibrilles dans l'hélice transversale. La paroi secondaire des trachéides n'est pas déposée de façon uniforme sur toute la surface cellulaire et est absente au niveau de surfaces bien définies, les ponctuations, qui permettent à l'eau de passer de trachéides à trachéides lors de son transport des racines vers les feuilles (Beck, 2010).

La lignification de la paroi primaire et de la lamelle moyenne commence après le début de la formation de la paroi secondaire, alors que la lignification de la paroi secondaire commence généralement une fois que sa formation est achevée (Donaldson, 2001). Après avoir été synthétisés dans le cytosol à partir de la phénylalanine, les composants de base de la lignine (appelés monolignols) sont transportés au niveau de la paroi par un mécanisme encore inconnu (Boerjan *et al.*, 2003; Vanholme *et al.*, 2010). Ils sont alors oxydés et polymérisés pour former une chaîne linéaire (13 à 20 unités monolignols) de lignine qui est incorporée à la paroi. La lignine est déposée dans les couches intercellulaires et dans les espaces entre microfibrilles. Elle forme alors des liaisons chimiques avec les hémicelluloses, agissant ainsi comme un ciment (Donaldson, 1991, Donaldson, 2001).

II.4.2 Régulation intrinsèque de la formation de la paroi secondaire et de la lignification

Il existe un nombre important de gènes impliqués dans la biosynthèse, le transport, la déposition et l'assemblage des constituants de la paroi secondaire (Mellerowicz *et al.*, 2001; Reiter, 2002; Brown *et al.*, 2005; Mellerowicz & Sundberg, 2008; Vanholme *et al.*, 2010; Zhong *et al.*, 2011). La construction de la paroi secondaire doit être un processus hautement régulé car les cellules ont besoin d'une expression coordonnée de tous ces gènes. C'est pourquoi les facteurs de transcription, des protéines qui se fixent à des séquences spécifiques d'ADN et régulent ainsi l'expression des gènes, joueraient un rôle crucial dans la régulation

de la formation de la paroi secondaire (Zhong & Ye, 2007; Mellerowicz & Sundberg, 2008; Vanholme *et al.*, 2010; Zhong *et al.*, 2011).

Par contre, il existe beaucoup moins de connaissance sur la régulation hormonale de la formation de la paroi secondaire et de la lignification par rapport à la division ou l'expansion cellulaire (Mellerowicz *et al.*, 2001). L'auxine jouerait un rôle sur la formation de la paroi secondaire mais de façon indirecte. En effet, cette hormone est distribuée selon un gradient entre les différentes zones du xylème : la concentration en auxines est maximale dans la zone cambiale, diminue dans la zone d'élargissement et atteint un niveau très faible voire nul dans la zone de formation de la paroi secondaire (Uggla *et al.*, 1996; Tuominen *et al.*, 1997; Uggla *et al.*, 1998; Stals & Inze, 2001). Ce gradient a été interprété comme servant de signal de positionnement qui délimiterait les différentes zones de différenciation. L'auxine agirait comme un morphogène, c'est à dire une molécule de signal qui provoque des réponses cellulaires spécifiques selon sa concentration. Une concentration faible ou nulle favoriserait le début de la formation de la paroi secondaire. Un effet hormonal direct pourrait tout de même exister sur la lignification car il a été montré que l'auxine augmentait la lignification du xylème secondaire de tabac (Sitbon *et al.*, 1999). Cependant, cette stimulation de l'auxine était associée à une augmentation de la production d'éthylène qui est connu pour induire plusieurs enzymes impliquées dans la biosynthèse de la lignine (Sitbon *et al.*, 1999). Enfin, il a été montré pour des cellules du xylème en culture que les brassinostéroides, une classe de phytohormones, sont nécessaires à l'induction du développement d'une paroi secondaire (Yamamoto *et al.*, 2001).

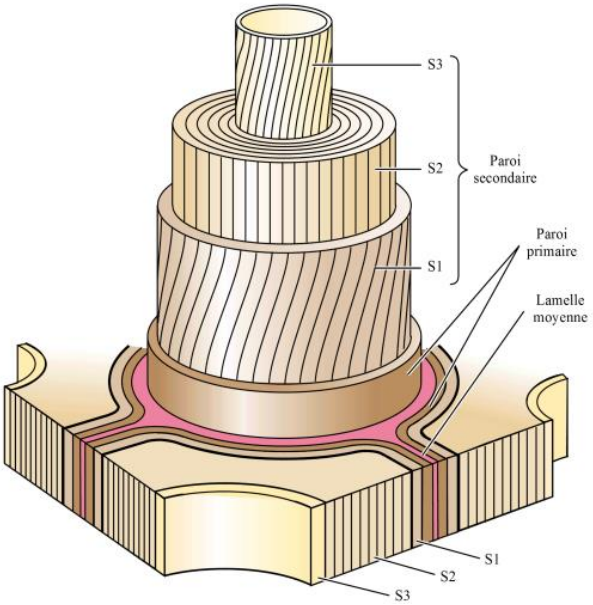

Figure II.3 : Structure de la paroi secondaire.
Diagramme d'une paroi secondaire épaisse telle que l'on peut en trouver chez les trachéides du bois final. Modifié depuis Taiz & Zeiger (1998).

II.5 La mort cellulaire programmée

La mort cellulaire programmée marque la fin de la différenciation des cellules du xylème et leur entrée dans leur forme mature et fonctionnelle. Cependant, ce processus actif et hautement ordonné (programmé) de « suicide » est suivi par de nombreuses cellules des

organismes multicellulaires (champignons, animaux ou végétaux) (Ellis *et al.*, 1991). Il est essentiel dans la suppression ou la formation de cellules et tissus spécifiques (Ellis *et al.*, 1991). Par exemple chez les plantes, le processus joue un rôle central dans le développement et la défense contre les pathogènes (Greenberg, 1996; Jones, 2001). Bien qu'ayant des similitudes, les mécanismes moléculaires de la mort cellulaire programmée diffèrent selon les organismes et les types cellulaires considérés. Celle des éléments du xylème constitue peut-être le plus remarquable exemple de mort cellulaire programmée chez les végétaux (Greenberg, 1996). En effet, la plupart des cellules différenciées matures exécutent des fonctions spécialisées jusqu'à leur mort, alors que les cellules conductrices du xylème meurent avant d'assurer leur fonction.

II.5.1 Mécanisme de la mort cellulaire programmée

La mort cellulaire programmée des éléments du xylème est un mécanisme spécifique dans lequel la vacuole joue un rôle central (Fukuda, 2000). Le déclencheur principal de la mort cellulaire programmée est un influx régulé d'ions Ca^{2+}, probablement à travers les canaux de la membrane plasmique (Groover & Jones, 1999; Jones, 2001). La mort se manifeste alors rapidement par un éclatement soudain (3 minutes) de la vacuole et la cessation immédiate des mouvements cytoplasmiques (Groover & Jones, 1999; Fukuda, 2000). L'éclatement de la vacuole libère des hydrolases qui attaquent et dégradent les organelles, vidant ainsi la cellule de son contenu cellulaire.

II.5.2 Régulation intrinsèque de la mort cellulaire programmée

Kuriyama & Fukuda (2002) prétendent que la régulation de la mort cellulaire programmée des cellules végétales est principalement hormonale. Cependant, les mécanismes de régulation de la mort cellulaire programmée et de la formation de la paroi seraient indissociables, car la plupart des agents qui régulent le premier processus régulent également le second (Bollhöner *et al.*, 2012). Par exemple, les brassinostéroides, qui initient la formation de la paroi secondaire, initient également la mort cellulaire programmée (Fukuda, 2000; Yamamoto *et al.*, 2001). De la même façon, Groover & Jones (1999) proposent un mécanisme qui met en étroite relation la mort cellulaire programmée des cellules du xylème avec la formation de la paroi secondaire. Dans ce mécanisme, la déposition du matériel pariétal est accompagnée de la sécrétion d'une protéase qui s'accumule dans la matrice extracellulaire. Lorsque l'activité de la protéase atteint un seuil critique, elle déclenche l'influx d'ions calcium et la mort qui met un terme à la formation de la paroi.

II.6 Exemple des trachéides

Chez les conifères, les trachéides, qui représentent entre 90 et 95% du volume du xylème (Jacquiot, 1955), suivent leur programme de différenciation constitué des processus décrits ci-dessus (Figure II.4). Elles forment alors des tubes vides entourés d'une paroi (primaire et secondaire) lignifiée perforée par de nombreuses petites ouvertures

(ponctuations) qui connectent les cellules adjacentes. Les trachéides du bois initial formées au début de la saison développent un diamètre large (30-50 µm) durant leur phase d'élargissement et des parois fines (2-3 µm) durant la phase de formation de la paroi secondaire. Au contraire, les trachéides du bois final formées vers la fin de la saison de croissance développent un diamètre étroit (15-25 µm) et des parois épaisses (4-6 µm). Une particularité de l'élargissement des trachéides est qu'il se fait exclusivement dans la direction radiale.

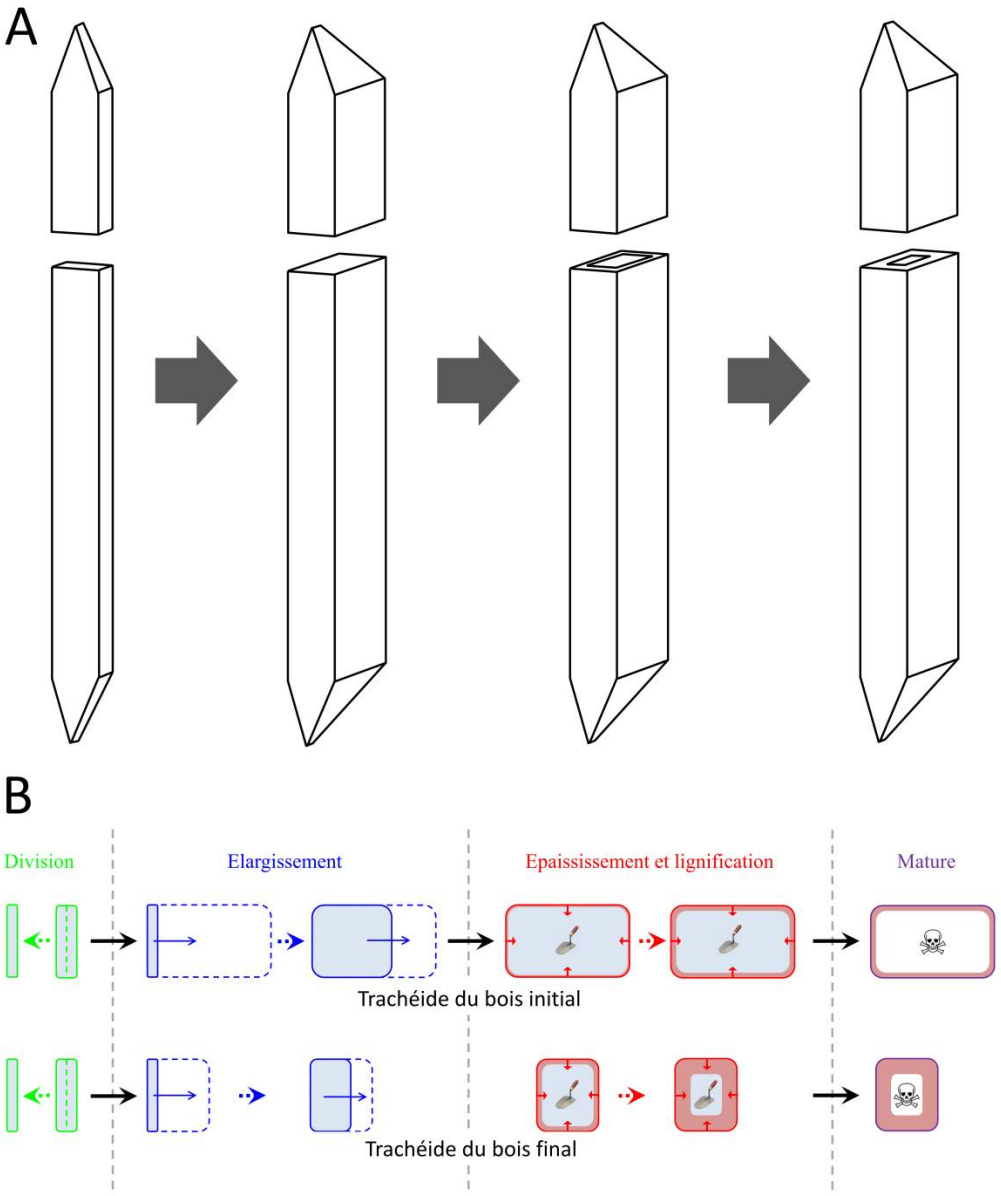

Figure II.4 : La formation des trachéides. A. Développement d'une trachéide en 3 dimensions. La représentation est très schématique et ne respecte pas les proportions car une trachéide est environ 100 fois plus longue que large. En outre, elle ne tient pas compte d'un éventuel allongement des cellules. B. Diagramme présentant la production et la différenciation d'une trachéide du bois initial et d'une trachéide du bois final en vue transversale. Dans les deux cas, une nouvelle cellule est générée par la division d'une cellule cambiale, puis s'élargit, forme une paroi secondaire qui se lignifie et meurt. Il résulte de ce programme de différenciation une trachéide mature fonctionnelle, avec un large diamètre et une paroi fine pour une trachéide du bois initial, un diamètre étroit et une paroi épaisse pour une trachéide du bois final.

II.7 Références

Abe H, Funada R. 2005. Review - The orientation of cellulose microfibrils in the cell walls of tracheids in conifers. *Iawa Journal* **26**(2): 161-174.

Abe H, Funada R, Ohtani J, Fukazawa K. 1995. Changes in the arrangement of microtubules and microfibrils in differentiating conifer tracheids during the expansion of cells. *Annals of Botany* **75**(3): 305-310.

Abe H, Funada R, Ohtani J, Fukazawa K. 1997. Changes in the arrangement of cellulose microfibrils associated with the cessation of cell expansion in tracheids. *Trees-Structure and Function* **11**(6): 328-332.

Abe H, Nakai T, Utsumi Y, Kagawa A. 2003. Temporal water deficit and wood formation in Cryptomeria japonica. *Tree Physiology* **23**(12): 859-863.

Aloni R. 1987. *The induction of vascular tissues by auxin*.

Beck CB. 2010. *An Introduction to Plant Structure and Development*: Cambridge University Press.

Bidlack J, Malone M, Benson R. 1992. Molecular structure and component integration of secondary cell walls in plants. *Proceedings of the Oklahoma Academy of Science* **72**: 51-56.

Boerjan W, Ralph J, Baucher M. 2003. Lignin biosynthesis. *Annual Review of Plant Biology* **54**: 519-546.

Bollhöner B, Prestele J, Tuominen H. 2012. Xylem cell death: emerging understanding of regulation and function. *Journal of Experimental Botany* **63**(3): 1081-1094.

Brown DM, Zeef LAH, Ellis J, Goodacre R, Turner SR. 2005. Identification of novel genes in Arabidopsis involved in secondary cell wall formation using expression profiling and reverse genetics. *Plant Cell* **17**(8): 2281-2295.

Chaffey N, Barnett J, Barlow P. 1999. A cytoskeletal basis for wood formation in angiosperm trees: the involvement of cortical microtubules. *Planta* **208**(1): 19-30.

Cosgrove DJ. 2000a. Expansive growth of plant cell walls. *Plant Physiology and Biochemistry* **38**(1-2): 109-124.

Cosgrove DJ. 2000b. Loosening of plant cell walls by expansins. *Nature* **407**(6802): 321-326.

Cosgrove DJ, Jarvis MC. 2012. Comparative structure and biomechanics of plant primary and secondary cell walls. *Frontiers in plant science* **3**: 204-204.

Cosgrove DJ, Li LC, Cho HT, Hoffmann-Benning S, Moore RC, Blecker D. 2002. The growing world of expansins. *Plant and Cell Physiology* **43**(12): 1436-1444.

Donaldson LA. 1991. Seasonal changes in lignin distribution during tracheid development in *Pinus radiata* D. Don. *Wood Science and Technology* **25**(1): 15-24.

Donaldson LA. 2001. Lignification and lignin topochemistry—an ultrastructural view. *Phytochemistry* **57**(6): 859-873.

Ellis RE, Yuan JY, Horvitz HR. 1991. Mechanisms and functions of cell death. *Annual Review of Cell Biology* **7**: 663-698.

Evert RF. 2006. *ESAU'S PLANT ANATOMY - Meristems, Cells, and Tissues of the Plant Body: Their Structure, Function, and Development*. Hoboken: John Wiley & Sons, Inc.

Fukuda H. 2000. Programmed cell death of tracheary elements as a paradigm in plants. *Plant Molecular Biology* **44**(3): 245-253.

Gordon JC, Larson PR. 1968. Seasonal Course of Photosynthesis, Respiration, and Distribution of ^{14}C in Young Pinus resinosa Trees as Related to Wood Formation. *Plant physiology* **43**(10): 1617-1624.

Greenberg JT. 1996. Programmed cell death: A way of life for plants. *Proceedings of the National Academy of Sciences of the United States of America* **93**(22): 12094-12097.

Gregory R, Wilson BF. 1968. A comparison of cambial activity of white spruce in Alaska and New England. *Canadian Journal of Botany - Revue Canadienne de Botanique* **46**(6): 733-734.

Gričar J, Krze L, Čufar K. 2009. Number of cells in xylem, phloem and dormant cambium in silver fir (*Abies alba*), in trees of different vitality. *Iawa Journal* **30**(2): 121-133.

Groover A, Jones AM. 1999. Tracheary element differentiation uses a novel mechanism coordinating programmed cell death and secondary cell wall synthesis. *Plant physiology* **119**(2): 375-384.

Jacquiot C. 1955. *Atlas d'anatomie du bois des conifères*. Paris.

Jones AM. 2001. Programmed cell death in development and defense. *Plant Physiology* **125**(1): 94-97.

Kataoka Y, Kondo T. 1998. FT-IR microscopic analysis of changing cellulose crystalline structure during wood cell wall formation. *Macromolecules* **31**(3): 760-764.

Kuriyama H, Fukuda H. 2002. Developmental programmed cell death in plants. *Current Opinion in Plant Biology* **5**(6): 568-573.

Lachaud S, Catesson AM, Bonnemain JL. 1999. Structure and functions of the vascular cambium. *Comptes Rendus de l'Académie des Sciences - Series III - Sciences de la Vie* **322**(8): 633-650.

Lautner S, Ehlting B, Windeisen E, Rennenberg H, Matyssek R, Fromm J. 2007. Calcium nutrition has a significant influence on wood formation in poplar. *New Phytologist* **173**(4): 743-752.

Little CHA, Sundberg B. 1991. Tracheid production in response to indole-3-acetic acid varies with internode age in *Pinus sylvestris* stems. *Trees-Structure and Function* **5**(2): 101-106.

Little CHA, Wareing PF. 1981. Control of cambial activity and dormancy in *Picea sitchensis* by indol-3-ylacetic and abscisic acids. *Canadian Journal of Botany-Revue Canadienne De Botanique* **59**(8): 1480-1493.

Matsumoto-Kitano M, Kusumoto T, Tarkowski P, Kinoshita-Tsujimura K, Vaclavikova K, Miyawaki K, Kakimoto T. 2008. Cytokinins are central regulators of cambial activity. *Proceedings of the National Academy of Sciences of the United States of America* **105**(50): 20027-20031.

Mellerowicz EJ, Baucher M, Sundberg B, Boerjan W. 2001. Unravelling cell wall formation in the woody dicot stem. *Plant Molecular Biology* **47**(1-2): 239-274.

Mellerowicz EJ, Sundberg B. 2008. Wood cell walls: biosynthesis, developmental dynamics and their implications for wood properties. *Current Opinion in Plant Biology* **11**(3): 293-300.

Mutwil M, Debolt S, Persson S. 2008. Cellulose synthesis: a complex complex. *Current Opinion in Plant Biology* **11**(3): 252-257.

Perrot-Rechenmann C. 2010. Cellular responses to auxin: division versus expansion. *Cold Spring Harbor perspectives in biology* **2**(5): a001446-a001446.

Plomion C, Leprovost G, Stokes A. 2001. Wood formation in trees. *Plant Physiology* **127**(4): 1513-1523.

Prodhan A, Funada R, Ohtani J, Abe H, Fukazawa K. 1995. Orientation of microfibrils and microtubules in developing tension-wood fibers of Japanese ash (*Fraxinus mandshurica* var. *japonica*). *Planta* **196**(3): 577-585.

Reiter WD. 2002. Biosynthesis and properties of the plant cell wall. *Current Opinion in Plant Biology* **5**(6): 536-542.

Roberts K, McCann MC. 2000. Xylogenesis: the birth of a corpse. *Current Opinion in Plant Biology* **3**(6): 517-522.

Rose J. 2003. *The plant cell wall*: John Wiley & Sons.

Rose JKC, Bennett AB. 1999. Cooperative disassembly of the cellulose-xyloglucan network of plant cell walls: parallels between cell expansion and fruit ripening. *Trends in Plant Science* **4**(5): 176-183.

Savidge RA. 1983. The role of plant hormones in higher plant cellular differentiation. II. Experiments with the vascular cambium, and sclereid and tracheid differentiation in the pine, *Pinus contorta*. *Histochemical Journal* **15**(5): 447-466.

Savidge RA. 2001. Intrinsic regulation of cambial growth. *Journal of Plant Growth Regulation* **20**(1): 52-77.

Schopfer P. 2006. Biomechanics of plant growth. *American Journal of Botany* **93**(10): 1415-1425.

Sitbon F, Hennion S, Little CHA, Sundberg B. 1999. Enhanced ethylene production and peroxidase activity in IAA-overproducing transgenic tobacco plants is associated with increased lignin content and altered lignin composition. *Plant Science* **141**(2): 165-173.

Stals H, Inze D. 2001. When plant cells decide to divide. *Trends in Plant Science* **6**(8): 359-364.

Sundberg B, Little CHA. 1990. Tracheid production in response to changes in the internal level of indole-3-acetic acid in 1-year-old shoots of Scots pine. *Plant physiology* **94**(4): 1721-1727.

Taiz L, Zeiger E. 1998. *Plant physiology*.

Tuominen H, Puech L, Fink S, Sundberg B. 1997. A radial concentration gradient of indole-3-acetic acid is related to secondary xylem development in hybrid aspen. *Plant Physiology* **115**(2): 577-585.

Uggla C, Mellerowicz EJ, Sundberg B. 1998. Indole-3-acetic acid controls cambial growth in Scots pine by positional signaling. *Plant Physiology* **117**(1): 113-121.

Uggla C, Moritz T, Sandberg G, Sundberg B. 1996. Auxin as a positional signal in pattern formation in plants. *Proceedings of the National Academy of Sciences of the United States of America* **93**(17): 9282-9286.

Vanholme R, Demedts B, Morreel K, Ralph J, Boerjan W. 2010. Lignin Biosynthesis and Structure. *Plant Physiology* **153**(3): 895-905.

Weng J-K, Chapple C. 2010. The origin and evolution of lignin biosynthesis. *New Phytologist* **187**(2): 273-285.

Yamamoto R, Fujioka S, Demura T, Takatsuto S, Yoshida S, Fukuda H. 2001. Brassinosteroid levels increase drastically prior to morphogenesis of tracheary elements. *Plant physiology* **125**(2): 556-563.

Zhong R, McCarthy RL, Lee C, Ye Z-H. 2011. Dissection of the Transcriptional Program Regulating Secondary Wall Biosynthesis during Wood Formation in Poplar. *Plant Physiology* **157**(3): 1452-1468.

Zhong R, Ye Z-H. 2007. Regulation of cell wall biosynthesis. *Current Opinion in Plant Biology* **10**(6): 564-572.

Zhong R, Zheng-Hua Y 2009. Secondary cell walls. *Encyclopedia of Life Sciences*. Chichester, UK: John Wiley & Sons, Ltd., 1-9.

III DISPOSITIF EXPÉRIMENTAL

III.1 Caractéristiques des sites étudiés

III.1.1 Position géographique

Trois sites instrumentés ont été installés début 2007 dans le nord-est de la France, dans les Vosges du nord (massif du Donon) (Figure III.1), le long d'un gradient altitudinal de 300 m environ (Figure III.2). Les trois sites sont répartis sur un axe nord-sud d'environ 15 km. Le site du bas (370 m d'altitude, Moselle, 48°38' N, 7°09' E), le plus au nord, se trouve à proximité de la commune de Walscheid. Le site du milieu (430 m d'altitude, Moselle, 48°36' N, 7°08' E) se trouve à 5 km au sud, proche de la commune d'Abreschviller. Le site du haut (650m d'altitude, Bas-Rhin, 48°28' N, 7°08' E), à 10 km au sud du site du milieu, se trouve à proximité de la commune de Grandfontaine. Les trois sites se trouvent en milieu de versant sur des pentes modérées à fortes (de 10 à 30°). Les sites de Walscheid et Grandfontaine bénéficient d'une exposition respectivement au sud-ouest (227°) et au sud-sud-est (147°), alors que le site d'Abreschviller est exposé à l'ouest (277°).Dans la suite, chaque site est nommé selon la commune à laquelle il se rattache.

III.1.2 Types de sols

Afin de déterminer les caractéristiques des sols, deux fosses pédologiques ont été creusées sur chaque site. L'analyse des fosses pédologiques a mis en évidence des sols de types similaires pour les trois sites, c'est-à-dire des sols plutôt acides avec un alocrisol à Walscheid et des podzols à Abreschviller et Grandfontaine. Un substrat de nature gréseuse, une texture sableuse et un humus de forme dysmoder ont été observés pour chaque site. La profondeur de sol prospectable par les racines était plus grande à Walscheid (105 cm) qu'à Grandfontaine (95 cm) et la plus faible à Abreschviller (70 cm).

III.1.3 Climat

D'une manière générale, le climat sur le massif vosgien est tempéré mais présente des tendances continentales marquées. Les hivers sont longs et rigoureux tandis que les étés peuvent être chauds et orageux. Les Vosges sont caractérisées par des précipitations abondantes car l'orientation nord-sud du massif arrête les nuages venant de l'Ouest.

Les conditions climatiques moyennes sur la période 1961-1990 ont été estimées par la méthode AURELHY (Analyse Utilisant le RElief pour L'HYdrométéorologie), une méthode développée par Météo-France et qui consiste à interpoler les valeurs des paramètres climatiques entre les points disposant des 30 années de mesure, en reliant la variabilité spatiale des paramètres à celle du relief (Benichou & Breton, 1987). Cette méthode est utilisée pour réaliser une climatologie fine, à 1 km de résolution spatiale. Elle montre que le gradient altitudinal s'accompagne d'une augmentation de plus de 30% des précipitations (1159, 1253 et 1532 mm à Walscheid, Abreschviller et Grandfontaine) et d'une diminution de la

température annuelle de 1 °C (8,7 °C à Walscheid, 8,5 °C à Abreschviller et 7,7 °C à Grandfontaine), visible également dans l'augmentation de 20% du nombre de jours de gel (87 jours à Walscheid, 92 jours à Abreschviller et 109 jours à Grandfontaine).

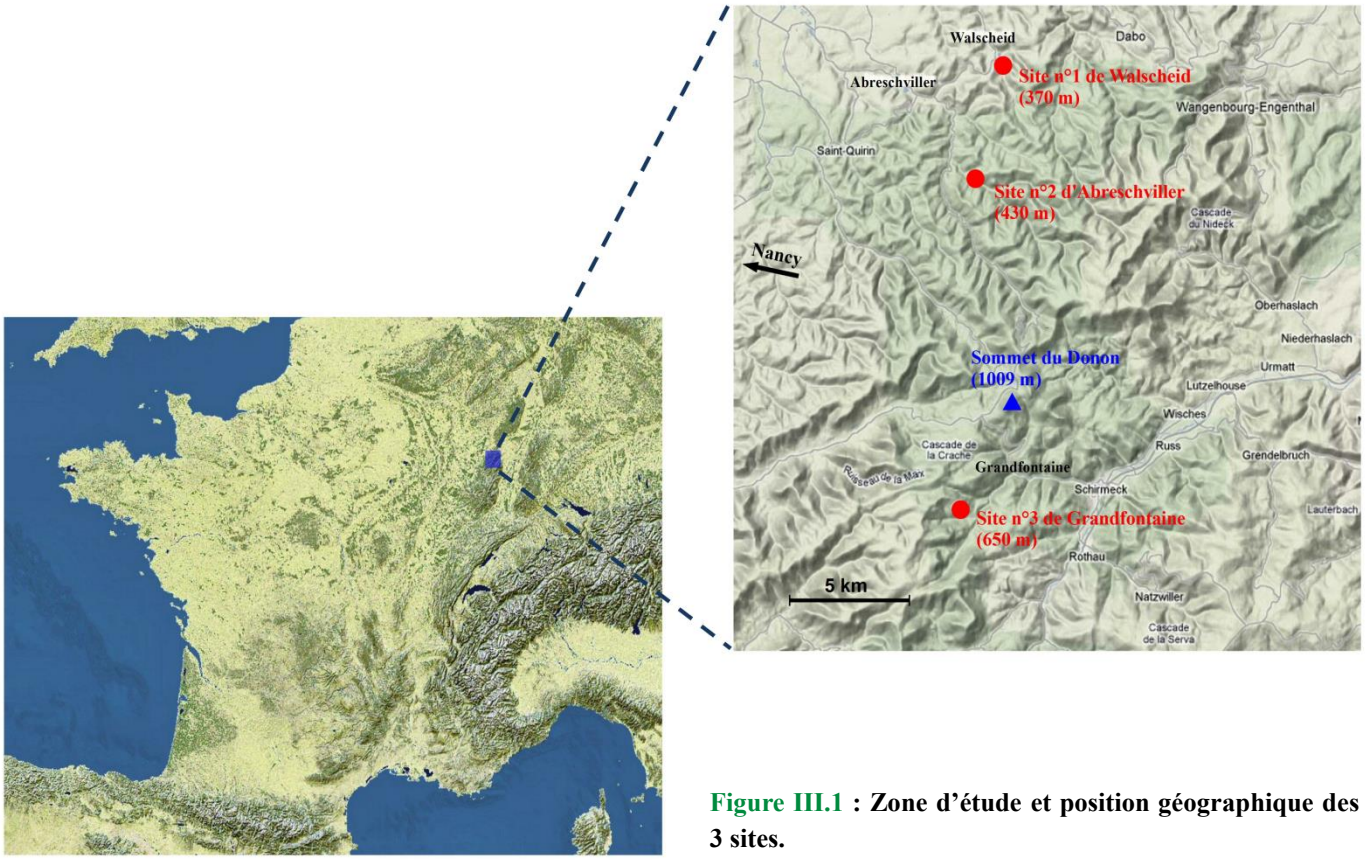

Figure III.1 : Zone d'étude et position géographique des 3 sites.

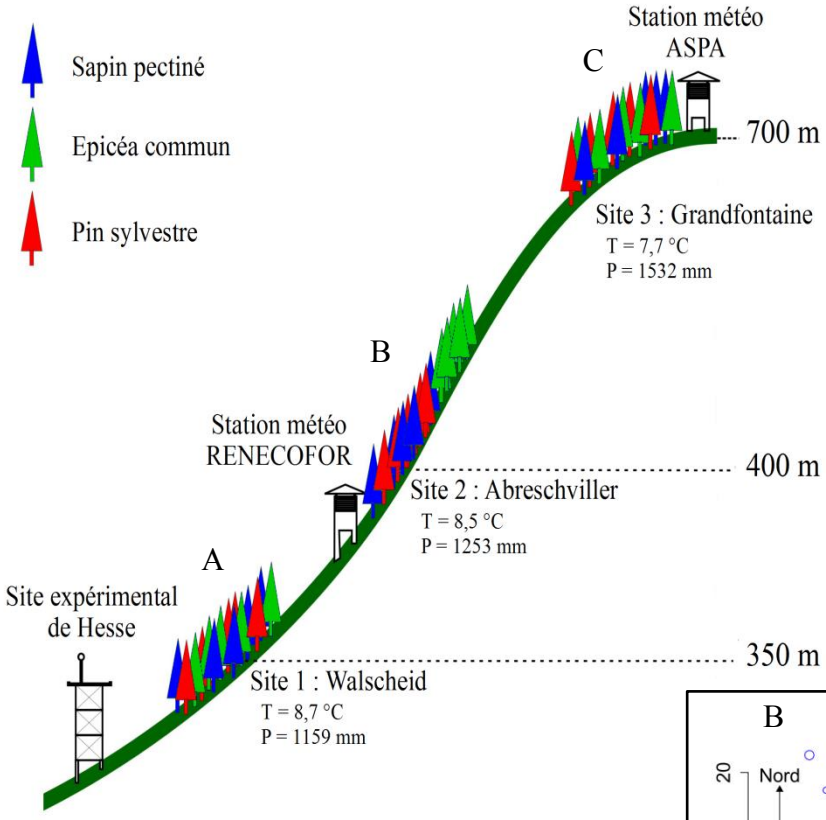

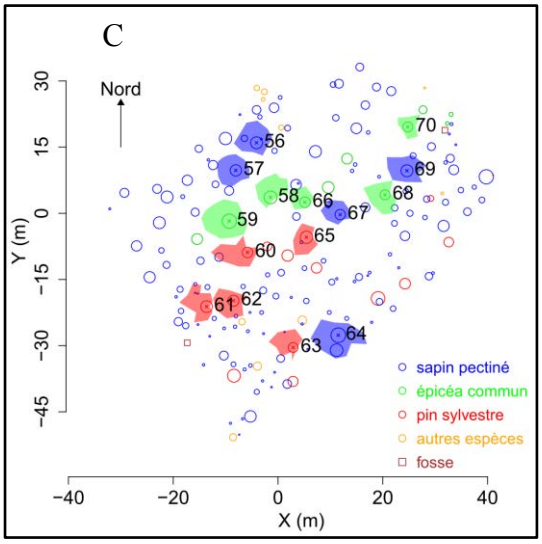

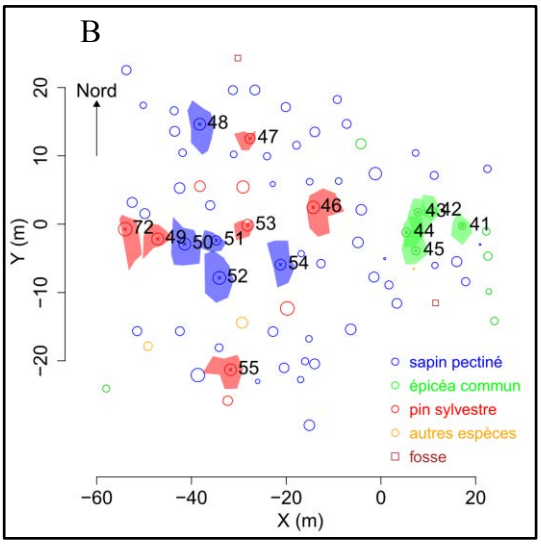

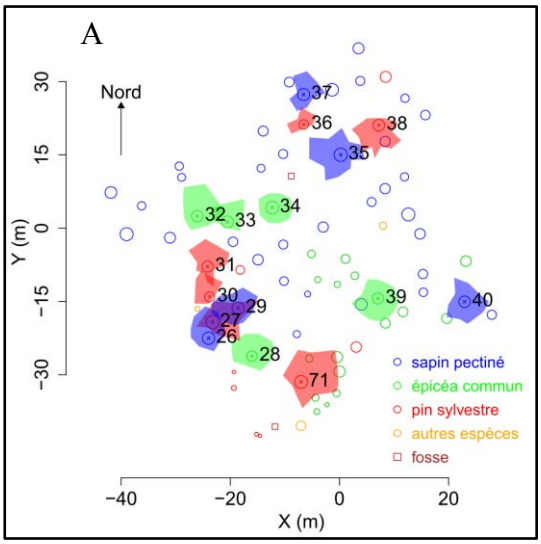

Figure III.2 : Schéma du dispositif expérimental et cartographie des sites de Walscheid (A), Abreschviller (B) et Grandfontaine (C). Les cercles représentent les diamètres à 1m30 (facteur d'élargissement ×4) de tous les arbres du peuplement, les polygones représentent les surfaces projetées du houppier des arbres suivis.

III.1.4 Structure des peuplements

Les sites ont été sélectionnés en collaboration avec l'Office National des Forêts (ONF) afin d'être représentatifs des peuplements mélangés de l'étage collinéen du nord-est de la France. Ainsi, chacun se trouve dans une forêt mélangée de résineux composée majoritairement de sapins pectinés (*Abies alba* Mill.) accompagnés d'épicéas communs (*Picea abies* (L.) Karst.) et de pins sylvestres (*Pinus sylvestris* L.). Quelques essences feuillues comme le bouleau, le chêne et le hêtre sont également disséminées.

III.1.4.1 Le peuplement de Walscheid

Le peuplement de Walscheid présente une densité de 189 tiges/ha, pour une surface terrière de 34 m²/ha. Il est majoritairement constitué de sapins (50%) en mélange avec des épicéas (28%) et des pins (18%), avec quelques chênes (3%) et hêtres (1%). Les arbres présentent un diamètre à 1m30 de 43 ± 11 cm (moyenne ± écart type) et une hauteur de 28 ± 5 m (Figure III.3A et B).

III.1.4.2 Le peuplement d'Abreschviller

Le peuplement d'Abreschviller a une densité (253 tiges/ha) et une surface terrière (45 m²/ha) plus grandes qu'à Walscheid. La proportion de sapins y est également plus importante (74%), avec pour conséquence une diminution du pourcentage d'épicéas (14%) et de pins (5%). Quelques bouleaux (4%) et hêtres (1%) sont également dispersés dans le peuplement. Globalement, les arbres y ont un diamètre plus large (47 ± 13 cm) et sont plus hauts (31 ± 6 m) qu'à Walscheid (Figure III.3C et D).

III.1.4.3 Le peuplement de Grandfontaine

Le peuplement de Grandfontaine présente la plus forte densité (431 tiges/ha), pour une surface terrière équivalente à celle d'Abreschviller (45 m²/ha). La proportion de sapins y est encore plus forte (79%), le reste du peuplement étant principalement constitué d'épicéas (7%) et de pins (8%), ainsi que de quelques bouleaux (2%), hêtres (2%) et chênes (2%). C'est le peuplement où les arbres présentent les diamètres les plus étroits (31 ± 17 cm) et sont les plus petits (20 ± 9 m) (Figure III.3E et F).

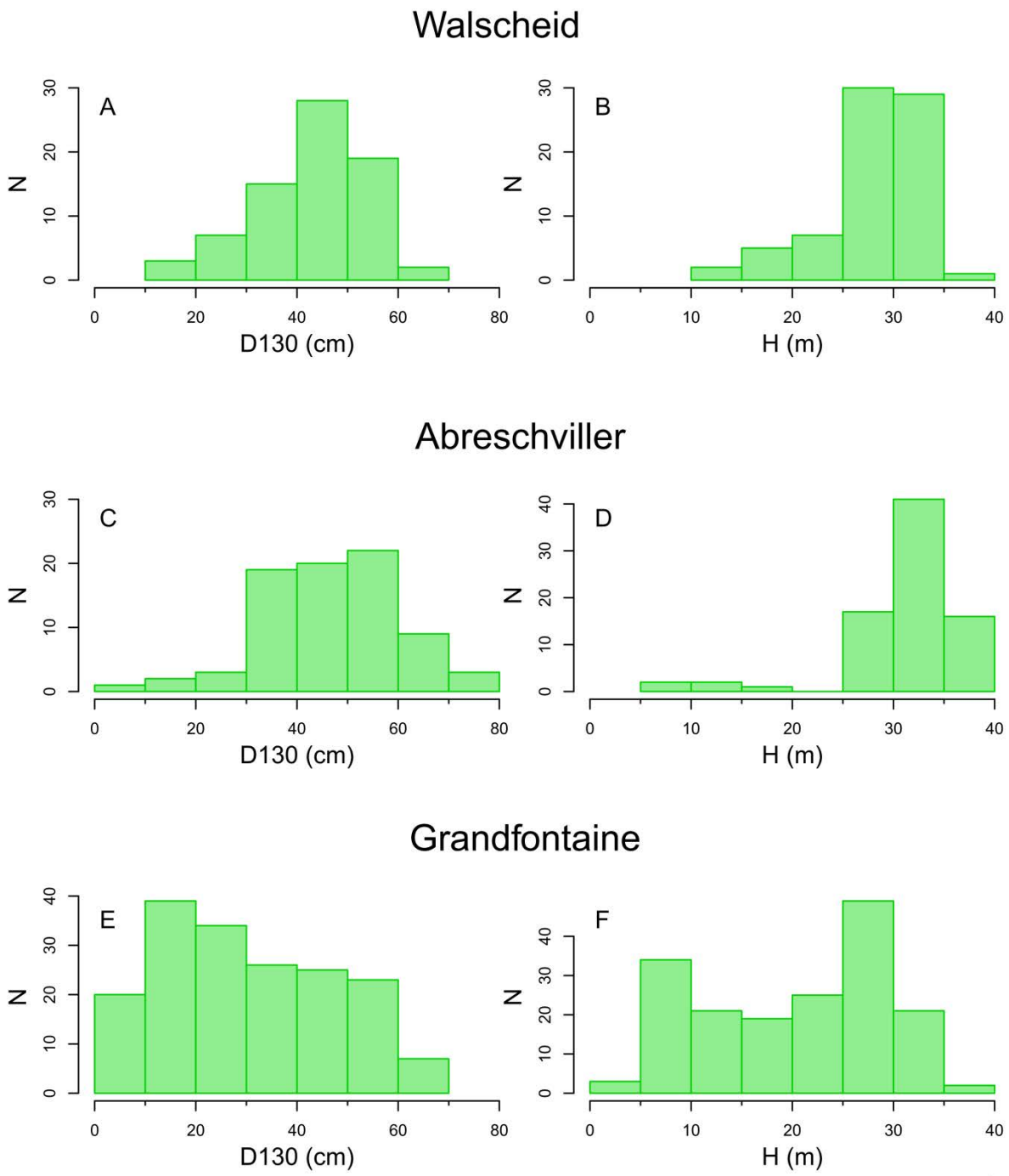

Figure III.3 : Effectifs (N) par classes de diamètre à 1m30 (D130) et de hauteur (H) pour les 3 peuplements étudiés.

III.2 Caractéristiques des arbres sélectionnés

Début 2007, à partir d'un inventaire complet des peuplements, 5 épicéas, 5 pins sylvestres et 5 sapins ont été choisis sur chaque site, soit 15 arbres par site pour un total de 45 arbres (5 arbres × 3 espèces × 3 sites). Début 2009, un pin sylvestre (n°30) de Walscheid a été remplacé (par le n°71) après la découverte d'une grosse blessure dans la partie supérieure du tronc. Un pin (n°47) a également été remplacé (par n° 72) la même année à Abreschviller après avoir remarqué qu'il présentait une croissance quasiment nulle. Seuls des arbres dominants ont été sélectionnés, afin de minimiser l'influence du statut social sur la formation du bois (Rathgeber *et al.*, 2011). Ainsi, en moyenne, les arbres sélectionnés mesuraient 32 ± 3 m et présentaient un diamètre à 1m30 de 55 ± 8 cm.

En dépit de cette première sélection, des différences subsistaient entre les espèces et entre les sites au niveau de l'âge et des caractéristiques dendrométriques des arbres (Table III.1). Ainsi à Abreschviller, les sapins étaient plus gros (60 cm) que les épicéas (41 cm), qui étaient eux-mêmes plus gros que les pins (33 cm), alors que les diamètres étaient similaires entre les espèces et entre les sites de Walscheid et de Grandfontaine (54 cm en moyenne). En outre, excepté à Walscheid où les arbres avaient le même âge (93 ans en moyenne), les pins étaient plus vieux que les sapins et les épicéas. À Abreschviller, les pins (162 ans) avaient 30 ans de plus que les sapins (135 ans) et 80 ans de plus que les épicéas (85 ans). A Grandfontaine, les pins (119 ans) avaient 45 ans de plus que les sapins et les épicéas qui avaient le même âge (74 ans en moyenne). La hauteur moyenne des arbres suivis était similaire entre les 3 trois sites, autour de 32 m. Cependant, les pins étaient plus petits que les sapins et les épicéas de 4 m à Abreschviller (32 contre 36 m) et de 5 m à Grandfontaine (27 contre 32 m). Finalement, les surfaces de houppiers variaient entre espèces à Abreschviller et Grandfontaine, avec des houppiers en moyenne 30% plus étendus pour les sapins que pour les pins et les épicéas. La surface de houppiers variait aussi entre les sites : en moyenne, elle était la plus grande à Walscheid (41m² en moyenne), 50% de plus qu'à Abreschviller (21 m² en moyenne) et 20% de plus qu'à Grandfontaine (32 m² en moyenne).

Cette thèse ne porte que sur les arbres présentés en Table III.1 et suivis de 2007 à 2009. Cependant, le suivi s'est prolongé en 2010 mais a été modifié : les sites de Abreschviller et Grandfontaine ont été respectivement totalement et partiellement désinstallés, alors que le dispositif a été agrandi à Walscheid avec la sélection de 9 arbres supplémentaires (3 de chaque espèce).

Table III.1 : Caractéristiques des arbres suivis. Age, diamètre à 1m30 (D130), hauteur (H) et surface du houppier (CA) (moyenne ± écart-type).

Site	Espèce	Arbre	Age	D130 (cm)	H (m)	CA (m²)
Walscheid	Sapin	26	93	56	27	41
		29	92	55	31	43
		35	99	60	30	61
		37	91	55	34	29
		40	98	53	31	42
		Moyennes	**94 ± 4**	**56 ± 3**	**31 ± 2**	**43 ± 12**
	Epicéa	28	97	48	29	44
		32	101	53	35	50
		33	82	55	33	27
		34	82	59	32	32
		39	85	51	33	49
		Moyennes	**89 ± 9**	**53 ± 4**	**32 ± 2**	**40 ± 11**
	Pin	27	101	61	28	50
		30	104	46	32	23
		31	90	51	30	36
		36	90	43	36	14
		38	85	53	32	43
		71	99	59	28	80
		Moyennes	**95 ± 8**	**52 ± 6**	**31 ± 3**	**41 ± 25**
Abreschviller	Sapin	48	140	62	40	29
		50	136	63	36	32
		51	137	49	37	12
		52	138	68	35	40
		54	127	56	35	25
		Moyennes	**135 ± 5**	**60 ± 7**	**36 ± 2**	**28 ± 10**
	Epicéa	41	70	36	31	13
		42	78	37	31	11
		43	82	39	33	19
		44	81	47	32	17
		45	112	45	32	21
		Moyennes	**85 ± 16**	**41 ± 5**	**32 ± 1**	**16 ± 4**
	Pin	46	163	66	32	34
		47	154	53	40	9
		49	173	64	37	17
		53	164	61	38	9
		55	156	61	35	26
		72	162	71	32	23
		Moyennes	**162 ± 7**	**33 ± 6**	**36 ± 3**	**20 ± 8**
Grandfontaine	Sapin	56	78	57	31	37
		57	81	54	32	34
		64	69	70	34	58
		67	67	49	30	21
		69	69	57	30	35
		Moyennes	**73 ± 6**	**57 ± 8**	**31 ± 2**	**37 ± 13**
	Epicéa	58	68	61	33	30
		59	69	68	37	57
		66	82	51	32	18
		68	69	47	31	30
		70	84	47	30	15
		Moyennes	**74 ± 8**	**55 ± 9**	**33 ± 3**	**30 ± 17**
	Pin	60	122	50	31	34
		61	124	56	27	34
		62	125	53	25	31
		63	113	46	28	25
		65	113	59	26	23
		Moyennes	**119 ± 6**	**53 ± 5**	**27 ± 2**	**29 ± 5**

III.3 Suivi météorologique

III.3.1 Stations hors peuplement

Un des avantages de travailler sur le massif du Donon est de pouvoir s'appuyer sur trois stations météorologiques présentes à proximité de chacun des sites étudiés (Figure III.2). La première station fait partie du site expérimental de Hesse du laboratoire d'Écologie et Écophysiologie forestière (EEF) de l'INRA de Nancy et se trouve à environ 5 km du site de Walscheid. La seconde station fait partie d'une placette permanente du Réseau National de suivi à long terme des ÉCOsystèmes FORestiers (RENECOFOR), située à 300 m environ du site d'Abreschviller. La troisième station appartient à l'Association pour la Surveillance et l'Étude de la Pollution Atmosphérique en Alsace (ASPA) et se trouve à 2 km environ du site de Grandfontaine (Tour ASPA). Chacune de ces stations mesure de nombreuses variables climatiques (température, précipitations, radiation lumineuse, humidité relative de l'air, vent) à une échelle fine (1/2h)

III.3.2 Stations intra-peuplement

A partir de 2008, nous avons disposé de notre propre station météo. La station a été installée le 23 avril 2008 sur le site d'Abreschviller pour suivre les conditions météorologiques directement au sein du peuplement. La station consiste en une centrale d'enregistrement (Campbell Scientific, CR1000) à laquelle ont été reliés plusieurs capteurs :

- Un capteur de mesure de la température et de l'humidité relative de l'air (Campbell Scientific, CS215), installé sur 1 mât d'environ 1m50 de hauteur fixé au milieu de la placette.
- Un pyranomètre (Campbell Scientific, LP02), qui mesure la radiation solaire, également installé sur le mât.
- 3 sondes d'hygrométrie (Campbell Scientific, CS616) et 3 sondes de température (Campbell Scientific, 107) installées dans le sol à différentes profondeurs (le premier couple sonde d'hygrométrie-sonde de température à 5cm de profondeur, le second à 15 cm et le troisième à 40 cm).
- 6 sondes de température, du même type que celles installées dans le sol (Campbell Scientific, 107), réparties autour du tronc de deux arbres (Sapin 61 et Pin 66) selon différentes orientations, l'extrémité de la sonde insérée sous l'écorce pour mesurer la température au niveau du cambium.

Pour chaque capteur, la centrale enregistre une valeur toutes les ½ h. La station météo a été démontée du site d'Abreschviller le 10 décembre 2009. Début 2010, une station météo supplémentaire, avec les mêmes composants, a été acquise. Les deux stations météo ont alors été installées à Walscheid et Grandfontaine le 7 avril 2010, pour être démontées le 16 novembre de la même année.

III.4 Suivi de la formation du bois

III.4.1 Prélèvement des échantillons

L'une des principales difficultés pour étudier la xylogénèse est qu'il est difficile d'y accéder (Chaffey, 2002). Le processus n'est pas directement visible, donc son suivi passe par des prélèvements répétés du xylème en développement au cours de la saison. Afin d'être aussi peu invasif que possible, des petits échantillons appelés microcarottes (1.5 cm de longueur, 0.2 mm de diamètre) ont été prélevés chaque semaine, de avril à novembre, sur le tronc des arbres suivis à l'aide d'un Trephor, un outil spécifiquement conçu pour ce type de prélèvements (Rossi *et al*., 2006a). Le Trephor est un emporte-pièce particulier composé d'un manche sur lequel sont fixés : une tête de perçage en acier inoxydable, et deux bras coplanaires asymétriques (Figure III.4A). La tête de perçage est composée d'un tube coupant relié à une chambre d'extraction ouverte sur le côté. Le tube coupant est inséré perpendiculairement dans le tronc en tapant avec un marteau sur le manche (Figure III.4B). La tête du Trephor est retirée du tronc à la main en se servant des bras asymétriques pour faire tourner l'appareil comme un tire-bouchon (Figure III.4C). L'appareil est accompagné d'une baguette de laiton qui est utilisée comme extracteur. La microcarotte qui se trouve dans le tube coupant est alors poussée à l'aide de l'extracteur dans la chambre d'extraction en passant par le tube coupant (Figure III.4D). Les microcarottes contiennent généralement quelques cernes des années précédentes, le cerne en formation de l'année en cours, le cambium et l'écorce.

Les microcarottes étaient prélevées à hauteur de poitrine sur le tronc. Pour chaque arbre, l'orientation géographique du premier prélèvement de l'année était tirée au sort afin d'assurer la bonne répartition des orientations dans les populations étudiées. Les prélèvements suivants étaient effectués en décrivant une spirale légèrement ascendante autour du tronc, dans le sens des aiguilles d'une montre, afin de ne pas former une ceinture continue de blessures. En outre, un espacement de 1 cm était respecté entre les prélèvements successifs pour éviter les réactions à la blessure tout en limitant l'influence de la variabilité circonférentielle dans le jeu de donnée final (Wodzicki & Zajaczkowski, 1970). Avant prélèvement, l'écorce de l'arbre était nettoyée voire partiellement enlevée, en particulier chez les pins sylvestres qui ont une écorce plus épaisse que les sapins et les épicéas. Les microcarottes collectées étaient placées dans des microtubes Eppendorf contenant une solution d'éthanol diluée à 50% et stockées à 5 °C pour éviter la détérioration des tissus vivants.

III.4.2 Préparation des échantillons

Une seconde difficulté au suivi de la xylogénèse tient en la petite taille des éléments qui composent le xylème. Pour réussir à observer le développement de ces éléments, des sections histologiques doivent donc être préparées à parti des microcarottes pour observer le développement du xylème avec un microscope. La réalisation des sections est délicate car les microcarottes sont constituées de deux parties à la consistance très différente : une partie dure

et résistante qui correspond au bois mature et une partie souple et fragile constituée du xylème en développement, du cambium et de l'écorce. Cependant, le suivi d'un protocole de préparation et de découpe des échantillons permet de surmonter ce problème (Rossi *et al.*, 2006b). Tout d'abord, sous la loupe binoculaire, les microcarottes étaient orientées de façon à ce que les trachéides soient parallèles à un axe vertical. La face supérieure de la microcarotte était alors marquée au crayon graphite HB afin de matérialiser cette orientation qui doit être conservée en vue de réaliser une coupe transversale des échantillons. Les microcarottes étaient successivement déshydratées, nettoyées, et infiltrées par immersion dans des bains d'éthanol, d-limonène et paraffine en utilisant un automate d'imprégnation (STP121, MM France, Francheville, France) (Harroué *et al.*, 2011). Les microcarottes étaient ensuite enrobées dans des blocs de paraffine avec une station d'enrobage (EC 350, MM France) puis des sections transversales de 5-10 µm d'épaisseur étaient coupées avec un microtome à rotation (HM 355S, MM France). Les sections étaient colorées avec de l'acétate de violet de crésyl (0,16% dans l'eau) puis fixées sur des lames en utilisant une laque transparente (Histolaque LMR®).

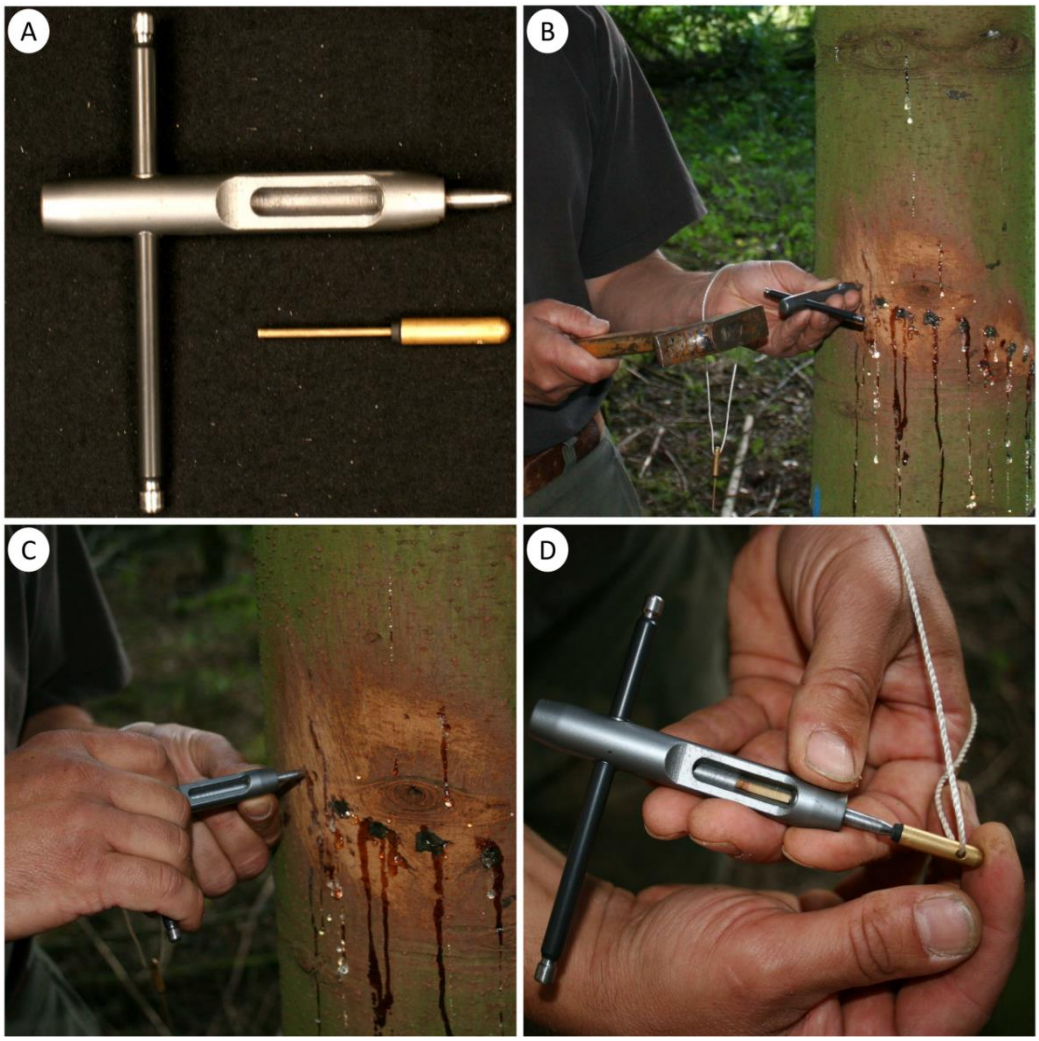

Figure III.4 : Prélèvement des microcarottes avec un Trephor. A. Le Trephor accompagné de sa baguette de laiton utilisée comme extracteur. B. Insertion du Trephor dans le tronc à l'aide d'un marteau. C. Retrait du Trephor en tournant l'appareil comme un tire-bouchon. D. Récupération de la microcarotte dans la chambre d'extraction à l'aide de l'extracteur.

III.4.3 Observations microscopiques

En tout, environ 4300 sections (45 arbres × 3 années × 32 prélèvements annuels par arbre) ont été observées avec un microscope optique (IMAGER M2, Carl Zeiss SAS, France) à des grossissements allant de 100 à 400 (objectifs ×10, ×20, ×40). Chaque section contient une « photographie » du cerne en formation à l'instant du prélèvement. Pour chaque arbre, l'observation des « photographies » successives permet de suivre la mise en place du cerne au cours de la saison (Figure III.5). En outre, sur chaque « photographie », la succession temporelle des phases de différenciations suivies par chaque cellule forme une succession spatiale de zones de développement le long du cerne (Figure III.6A). Les cellules dans la zone cambiale ont une paroi primaire fine et de petits diamètres radiaux (Figure III.6B). Ces cellules se divisent par mitose pour produire les cellules du xylème vers l'intérieur et les cellules du phloème vers l'extérieur. Les cellules produites du côté du xylème entrent ensuite dans la phase d'élargissement, où elles subissent une augmentation marquée de leur diamètre, principalement dans la direction radiale, par relâchement de la paroi sous l'action d'enzymes, prélèvement d'eau pour faire grandir le protoplasme et déposition de nouveau matériel pariétal pour éviter l'amincissement et la rupture de la paroi (Cosgrove, 2000). Les diamètres radiaux augmentent sept à huit fois pour les trachéides du bois initial (30 – 50 µm de diamètre final) et deux à trois fois pour les trachéides du bois final (10 – 25 µm) Ainsi, les cellules en élargissement ont un plus grand diamètre que les cellules cambiales et sont encore entourées de parois primaires fines (Figure III.6C).

Après l'élargissement commence la construction d'une paroi secondaire multicouche, rigide et imperméable composée de cellulose, hémicellulose et lignine (Zhong & Zheng-Hua, 2009). Les parois secondaires sont deux à trois fois plus fines dans le bois initial (2-3µm) que dans le bois final (4-6µm). Leur formation commence par la déposition de microfibrilles de cellulose et hémicellulose, suivie par la déposition de lignine, qui agit comme un ciment en étant déposée dans les espaces entre microfibrilles (Donaldson, 1991). Une particularité de la paroi secondaire est que les microfibrilles de cellulose sont orientées de telle façon qu'elles réfléchissent la lumière polarisée (Abe *et al.*, 1997). Donc contrairement aux cellules en élargissement qui ont des parois primaires sombres en lumière polarisée (Figure III.6D), les cellules en phase de formation de la paroi secondaire ont une paroi biréfringente (Figure III.6E). L'avancement de la lignification est suivi à partir de l'acétate de violet de crésyl, qui colore la cellulose en violet et la lignine en bleu (Kutscha *et al.*, 1975). Ainsi, les cellules en phase de formation de la paroi secondaire démontrent des parois bicolores (bleu et violet), indiquant que la lignification était inachevée (Figure III.6F).

Enfin, les cellules subissent la mort cellulaire programmée. Un flux de calcium provoque l'éclatement de la vacuole qui libère des hydrolases qui dégradent le contenu cellulaire mais pas la paroi secondaire (Jones, 2001). Les trachéides matures ont des parois entièrement lignifiées et donc complètement bleues, avec des diamètres larges et des parois fines pour les trachéides du bois initial (Figure III.6G), et des diamètres étroits et des parois épaisses pour les trachéides du bois final (Figure III.6H). Pour chaque échantillon, le nombre

de cellules dans les phases de division, d'élargissement, d'épaississement et lignification de la paroi et dans l'état mature était compté le long de trois files radiales.

III.4.4 Standardisation des observations

La formation du bois n'est pas homogène dans l'arbre : à un instant donné, le nombre de nouvelles trachéides produites varie en fonction de la hauteur et de l'orientation autour du tronc (Wodzicki & Zajaczkowski, 1970). En conséquence, il est difficile de savoir si les variations du nombre de cellules entre les échantillons sont dues à la croissance (le signal qui nous intéresse) ou à cette variabilité intra-arbre (bruit). Afin de réduire ce bruit, nous avons utilisé la méthode de standardisation des comptages développées dans Rossi *et al.* (2003). La méthode est basée sur l'hypothèse que l'hétérogénéité de croissance dans l'arbre pour une année donnée se répète de façon similaire l'année suivante. Les sections sur lesquelles la formation du cerne est observée contiennent aussi quelques cernes formés les années précédentes. Il est donc possible de corriger les valeurs de l'année en cours à partir des variations de largeur de cerne observées pour l'année précédente. Ainsi, le nombre de cellule (ou la largeur du cerne) de l'année précédente était compté (mesurée) le long de 3 files radiales pour chaque échantillon et utilisé(e) pour standardiser le nombre brut de l'année en cours selon :

$$Xi_{j,s} = Xi_j * \frac{\bar{X}_{j-1}}{Xi_{j-1}}$$

où $Xi_{j,s}$ est le nombre de cellules standardisé pour la section i de l'année j, Xi_j le nombre de cellules brut pour la section i de l'année j, $\bar{X}_{j-1}$ le nombre moyen de cellules (ou la largeur de cerne moyenne) pour l'ensemble des sections de l'année j-1, Xi_{j-1} le nombre de cellules (ou la largeur de cerne) sur la section i de l'année j-1. Une fonction dédiée du package CAVIAR (Rathgeber, 2012) du logiciel R (R Development Core Team, 2011) était utilisée pour appliquer cette standardisation à tous les échantillons de notre jeu de données.

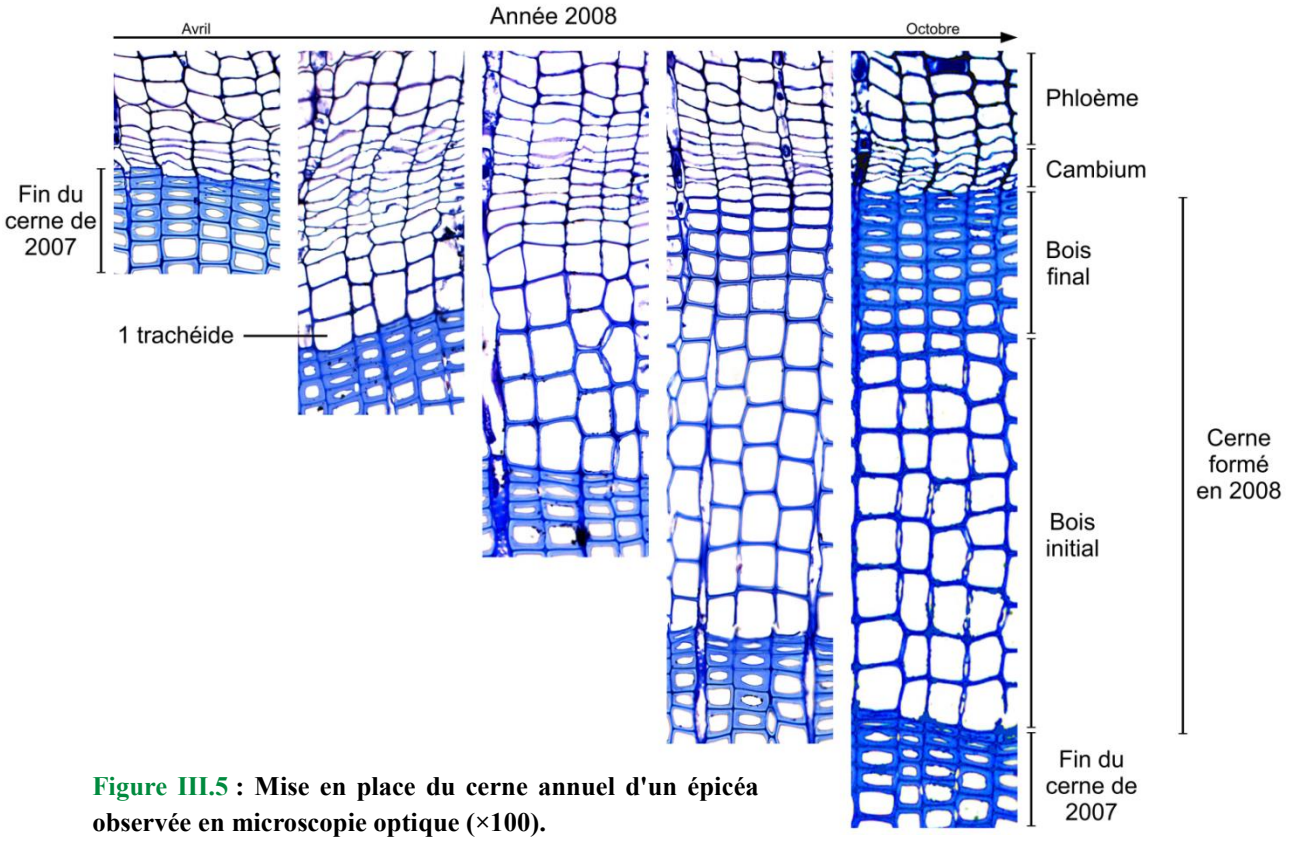

Figure III.5 : Mise en place du cerne annuel d'un épicéa observée en microscopie optique (×100).

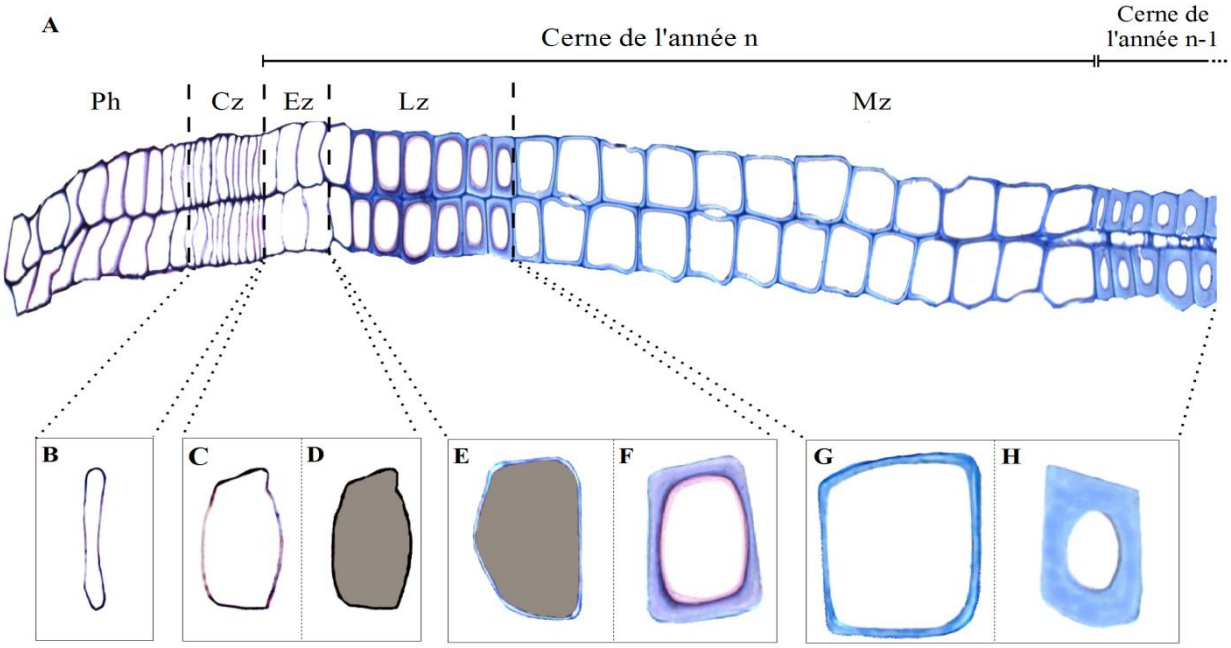

Figure III.6 : Maturation du xylème observée chez le pin sylvestre. La figure III.6A montre deux files radiales isolées d'une section anatomique de bois (6 µm d'épaisseur, coloration à l'actétate de violet de crésyl) coupée transversalement à partir d'un échantillon prélevé le 14 août 2009. Elles contiennent le phloème (Ph), les zones cambiale (Cz), d'élargissement (Ez), d'épaississement et lignification (Lz) et mature (Mz) de différenciation des trachéides. Les figures III.6B à III.6H illustrent des cellules isolées de chaque zone de différentiation avec une cellule cambiale (B), une cellule en élargissement en lumière normale (C) et polarisée (D), une cellule en épaississement en lumière polarisée (E) et normale (F), une cellule mature du bois initial du cerne de l'année en cours (G) et une cellule mature du bois final du cerne de l'année précédente (H).

III.5 Mesure des dimensions des trachéides

Pour chaque arbre à la fin de chaque année, une section bien préservée contenant le cerne entièrement formé était sélectionnée pour mesurer les dimensions des trachéides le long du cerne produit durant l'année (Figure III.7A). La mesure de ces dimensions, de l'ordre du µm, nécessite de travailler sur une image du cerne avec un zoom et une résolution suffisants. Ainsi, une image digitale du cerne était construite à partir de l'observation de la section au microscope (grossissement ×100) équipé d'une caméra digitale (Sony, modèle XCD-U100CR) et connecté à un ordinateur sur lequel est installé le logiciel d'acquisition d'image archimed (Microvision instruments, France). L'image était ensuite analysée avec le logiciel d'analyse d'image WinCell (Regent instruments, Canada) pour mesurer dans la direction radiale le diamètre du lumen et l'épaisseur de la paroi des trachéides le long de 6 files radiales en moyenne (Figure III.7B). Le diamètre du lumen dans la direction tangentielle et la surface transversale du lumen sont également mesurés. A partir des mesures, nous avons estimé l'épaisseur de la paroi tangentielle sur la base d'un rapport de 1,2 entre l'épaisseur de la paroi radiale et l'épaisseur de la paroi tangentielle (Rathgeber *et al.*, 2006). Enfin, le diamètre de la cellule dans les directions radiales et tangentielle était calculé comme la somme du diamètre et de la double épaisseur de la paroi dans la direction correspondante, puis les surfaces transversales de la cellule et de la paroi étaient calculées sur la base d'une forme rectangulaire des trachéides.

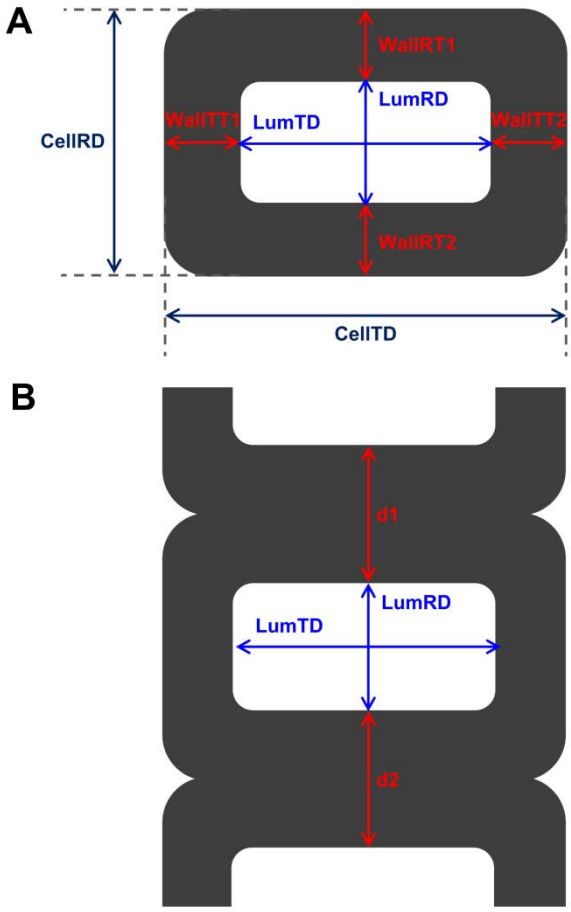

Figure III.7 : Dimensions des trachéides. La figure III.7A présente les différentes dimensions d'une trachéide en coupe transversale, avec le diamètre radial (LumRD) et tangentiel (LumTD) de son lumen, l'épaisseur de ses deux parois radiales (WallRT1 et WallRT2) et tangentielles (WallTT1 et WallTT2) et son diamètre radial (CellRD) et tangentiel (CellTD). La figure III.7B présente le fonctionnement du logiciel WinCell, qui, pour chaque cellule le long d'une file radiale, mesure LumRD et LumTD et la distance entre les lumens des cellules voisines (d1 et d2). WallRT1 et WallRT2 sont alors estimées par d1/2 et d2/2, respectivement, et l'épaisseur de paroi radiale (WallRT) est calculée comme la moyenne de WallRT1 et WallRT2.

III.6 Mesure de la densité du bois

Deux carottes standards ont été prélevées sur chaque arbre à la tarière de Pressler pour analyse microdensitométrique. La microdensitométrie est une technique qui utilise les rayons X pour accéder aux variations de la densité du bois à l'intérieur du cerne (profil de densité) (Polge, 1966). L'absorption des rayons X par le bois dépend de deux choses : l'épaisseur et la densité de l'échantillon traversé. Afin que l'absorption ne dépende que de la densité, les carottes étaient sciées dans le sens longitudinal à une épaisseur constante de 2 mm. Les barrettes obtenues étaient ensuite exposées aux rayons X pendant quatre heures. Les rayons X sont émis par un générateur XRG 3000 INEL en conditions électriques standards (tension = 7,5 kV, intensité = 12mA), avec une distance source/barrettes de 2.50 m. Un détecteur quantifie alors les rayons X qui traversent l'échantillon et fournit une image en niveaux de gris.

Le logiciel CRAD convertit les niveaux de gris en densité du bois. On obtient alors une carte numérique de la densité du bois le long de l'échantillon. A partir de cette carte, le logiciel CERD est ensuite utilisé pour indexer les limites de cerne à partir du contraste de densité entre le bois final d'un cerne et le bois initial du cerne suivant (Mothe *et al.*, 1998). Chaque accroissement annuel est alors divisé en 10 zones de mesure dans sa direction radiale et 20 zones, appelées « vingtiles », dans sa direction tangentielle. Pour chaque cerne, les 200 densités moyennes des 10 x 20 zones sont calculées. Enfin, les moyennes des 10 zones radiales de mesures sont calculées. Le fichier final résultant est un fichier texte qui fournit la description de chaque cerne le long de la carotte correspondante par les variables suivantes : âge, année calendaire, densités moyenne, minimale et maximale, densités et largeurs du bois initial et du bois final, profil de densité simplifié représenté par les vingtiles (dont chacun représente la densité moyenne d'une bande tangentielle de largeur égale à 5% de la largeur du cerne). Les caractéristiques des cernes de l'arbre étaient enfin calculées en faisant la moyenne des variables des deux carottes.

III.7 Suivi de la croissance radiale

III.7.1 Dendromètres manuels à bande

Des dendromètres manuels à bande (EMS Brno, DB 20) ont été installés à hauteur de poitrine sur chacun des arbres étudiés afin de mesurer les variations circonférentielles du tronc (Figure III.8A). Les dendromètres manuels à bande fonctionnent selon le principe du pied à coulisse, ce qui permet une mesure de la circonférence du tronc au dixième de millimètre. Ils sont constitués d'une réglette fixe graduée en millimètres et d'une réglette mobile, appelée vernier, graduée tous les 0,9 millimètres. Un ressort maintient le vernier en position autour du tronc et permet son déplacement lorsque la circonférence du tronc varie. La graduation 0 du vernier donne la valeur en millimètre sur l'échelle fixe, tandis que trait du vernier qui est en correspondance avec un des traits de la partie fixe donne le chiffre des dixièmes de millimètres (Figure III.8B). Les relevés se font manuellement, chaque semaine, en même

temps que sont effectués les prélèvements des microcarottes. Les dendromètres ont été installés le 12 avril 2007 et le premier relevé a été effectué le 17 du même mois.

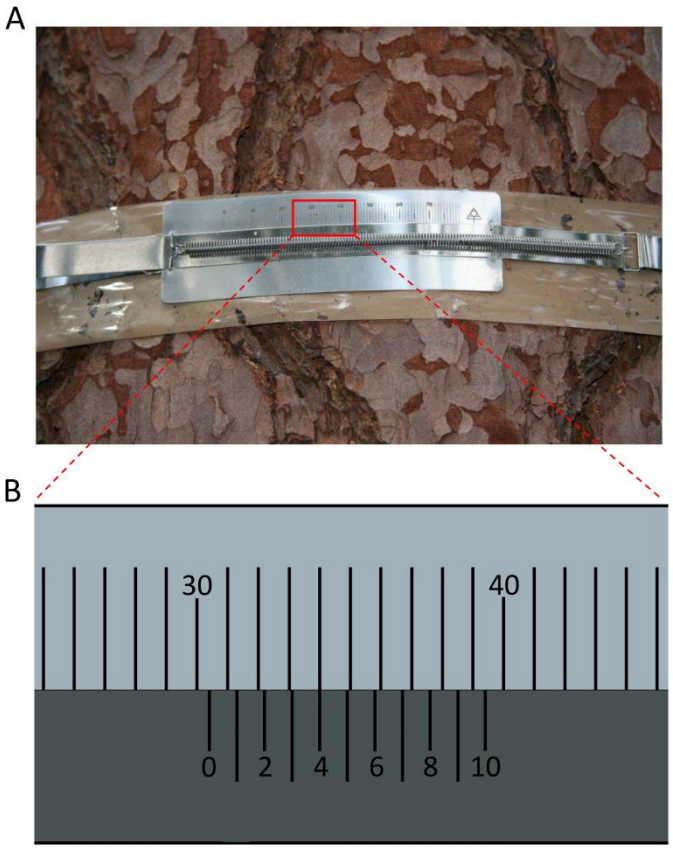

Figure III.8 : Dendromètre manuel à bande. La figure III.8A montre un dendromètre manuel à bande installé sur un pin sylvestre. La figure III.8B montre un agrandissement de la zone de lecture. Le 0 du vernier (gris foncé) donne une valeur de 30 mm sur l'échelle fixe (gris clair), tandis que c'est le trait 4 du vernier qui est en correspondance avec un trait de l'échelle fixe. L'opérateur relève alors une valeur de 30.4 mm.

III.7.2 Dendromètres automatiques à points

Début 2007, deux arbres par espèce et par site ont également été chacun équipés d'un dendromètre automatique ponctuel composé d'un capteur (RS composants, 317-780) et d'un enregistreur (EMS Brno, Minikin TP). En mars 2009, un arbre supplémentaire par espèce et par site a été équipé d'un dendromètre automatique. En 2010, tous les arbres de Walscheid (24 arbres) ont été équipés de dendromètres automatiques.

Au contraire des dendromètres à bande, qui permettent une mesure sur toute la circonférence du tronc, les dendromètres ponctuels ne permettent d'enregistrer les variations radiales du tronc qu'au point mesuré. L'enregistreur des dendromètres correspond à un potentiomètre linéaire, c'est-à-dire un type de résistance variable à trois bornes, dont l'une est reliée au capteur du dendromètre par un curseur. Ce système permet de recueillir une valeur de résistance qui varie proportionnellement à la distance entre ses bornes et le curseur. Au point mesuré, la variation du rayon de l'arbre fera se déplacer la tige du capteur reliée au curseur du potentiomètre qui traduit alors le déplacement en une variation proportionnelle de la tension (Figure III.9). L'enregistreur mesure la tension toutes les minutes puis conserve une valeur moyenne par demi-heure.

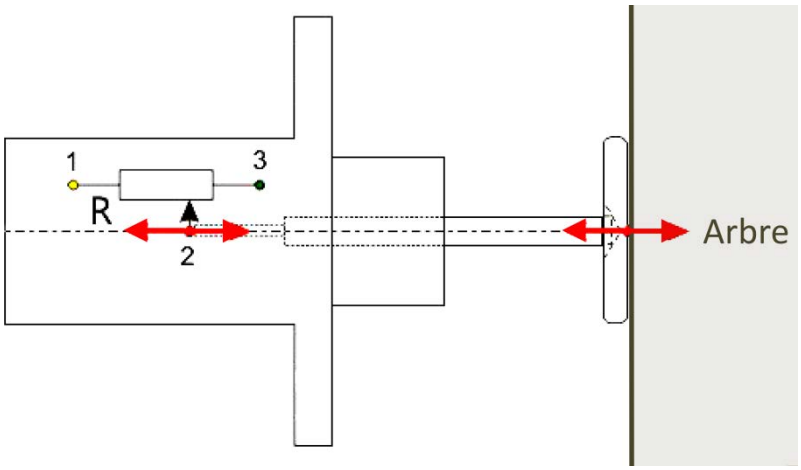

Figure III.9 : Dendromètre automatique ponctuel. Au point mesuré, la variation du rayon de l'arbre fera se déplacer la tige du capteur reliée au curseur lui-même relié à la borne 2 d'un potentiomètre (résistance R). L'enregistreur applique une tension électrique entre les bornes 1 et 3 et mesure la tension entre les bornes 1 et 2 qui sera proportionnelle au déplacement de la tige du capteur.

III.8 Suivi de la phénologie foliaire et de l'élongation des rameaux

L'élongation des rameaux et la phénologie foliaire étaient observées chaque semaine à la jumelle dans le tiers supérieur des houppiers des arbres étudiés. La longueur des nouvelles pousses était visuellement estimée, tandis que le développement des aiguilles était décrit par trois étapes successives se déroulant après la dormance hivernale et aboutissant aux nouvelles aiguilles matures de l'année: (1) le gonflement des bourgeons, (2) le débourrement et (3) la maturation des aiguilles. Pour les trois espèces, les bourgeons dormants étaient entièrement ceints d'écailles et de petite taille (Figure III.10A et E), alors que les bourgeons gonflés étaient reconnaissables par l'augmentation de leur taille (Figure III.10B et F). Le débourrement différait fortement entre le pin et les deux autres espèces et était distingué selon les critères du protocole d'observation phénologique utilisé par le réseau RENECOFOR (Ulrich & Cecchini, 2009). Chez les sapins et les épicéas, le débourrement était enregistré quand les bourgeons étaient entièrement ouverts, les écailles tombées laissant les aiguilles en développement clairement apparentes (Figure III.10C). Chez les pins, le débourrement était enregistré quand les aiguilles en développement étaient clairement apparentes à la base des nouvelles pousses, émergeant des écailles, les bourgeons n'étant encore que partiellement ouverts (Figure III.10G). La maturation des aiguilles était indiquée par leur couleur, qui passait progressivement d'un vert tendre à un vert foncé (Figure III.4D et H). Les aiguilles de l'année en cours étaient considérées matures lorsqu'elles présentaient la même couleur que celles des années précédentes.

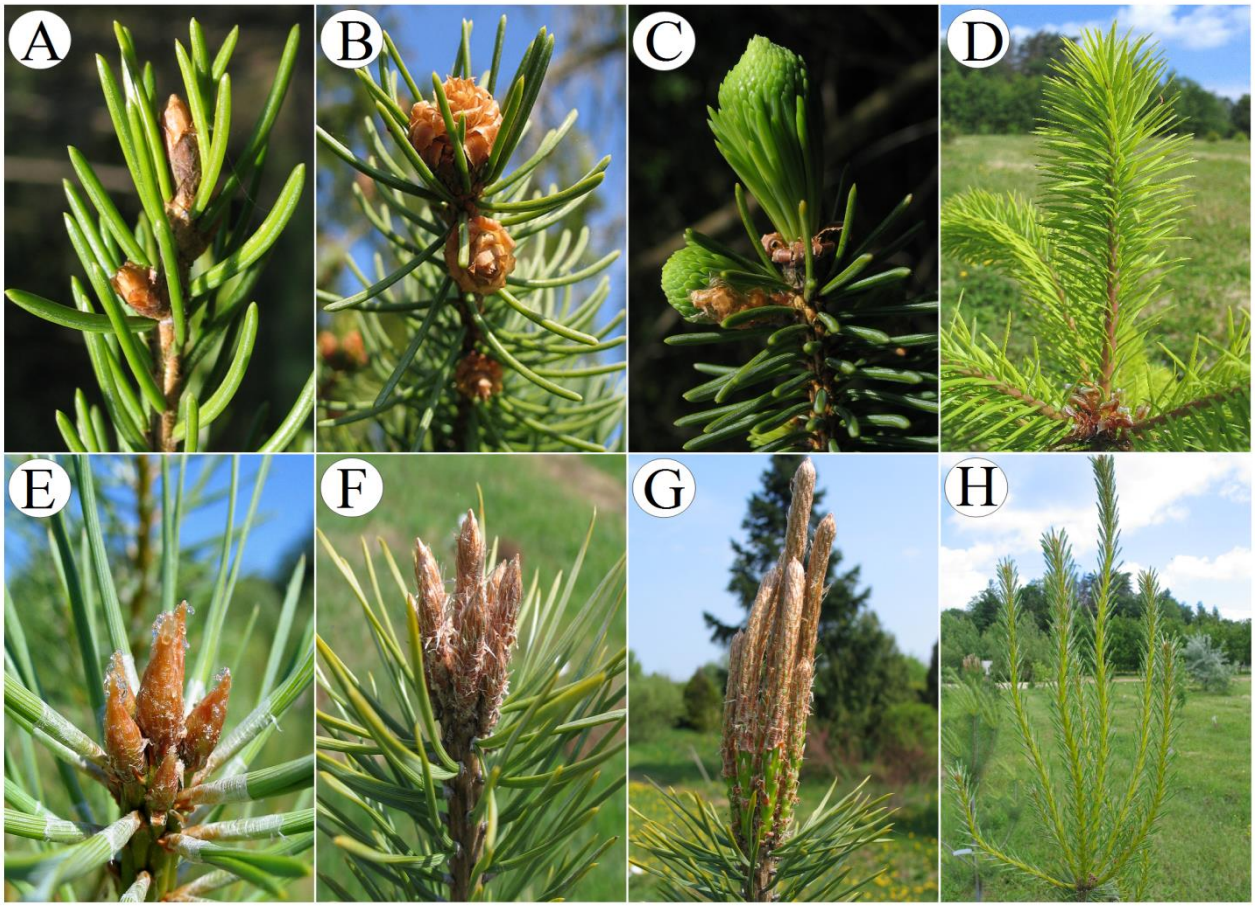

Figure III.10 : Phénologie foliaire observée chez de jeunes épicéas communs et pins sylvestres dans un milieu ouvert à proximité des sites étudiés. Bourgeons dormants (A), bourgeons gonflés (B), bourgeons éclos (C) et aiguilles en maturation (D) observés chez l'épicéa. Bourgeons dormants (E), bourgeons gonflés (F), bourgeons éclos (G) et aiguilles en maturation (H) observés chez le pin (Photos : Fabrice Bonne).

III.9 Suivi de la croissance en hauteur

La croissance en hauteur a été suivie chaque semaine à Walscheid pour 4 épicéas en 2009 et pour les 15 arbres des trois espèces en 2010, en utilisant un tachéomètre appelé station totale (Leica, TPS400). Comme un théodolite, la station totale mesure les angles horizontaux et verticaux pour déterminer une direction de visée, mais permet en plus de mesurer une distance avec un laser. Pour un point visé, les angles et la distance sont automatiquement mesurés et stockés dans la carte mémoire de l'appareil. A partir de ces coordonnées, la distance séparant deux points de mesure peut alors être calculée.

Une cible a été tracée à la base du tronc de chaque arbre suivi et sert de référence à notre mesure (Figure III.11). Après avoir enregistré les coordonnées de ce point, on mesure les coordonnées de l'apex de l'arbre. La distance séparant l'apex de la cible peut alors être calculée. D'une semaine à l'autre, l'évolution de cette distance est due au déplacement de l'apex, ce qui permet d'estimer la croissance en hauteur de l'arbre.

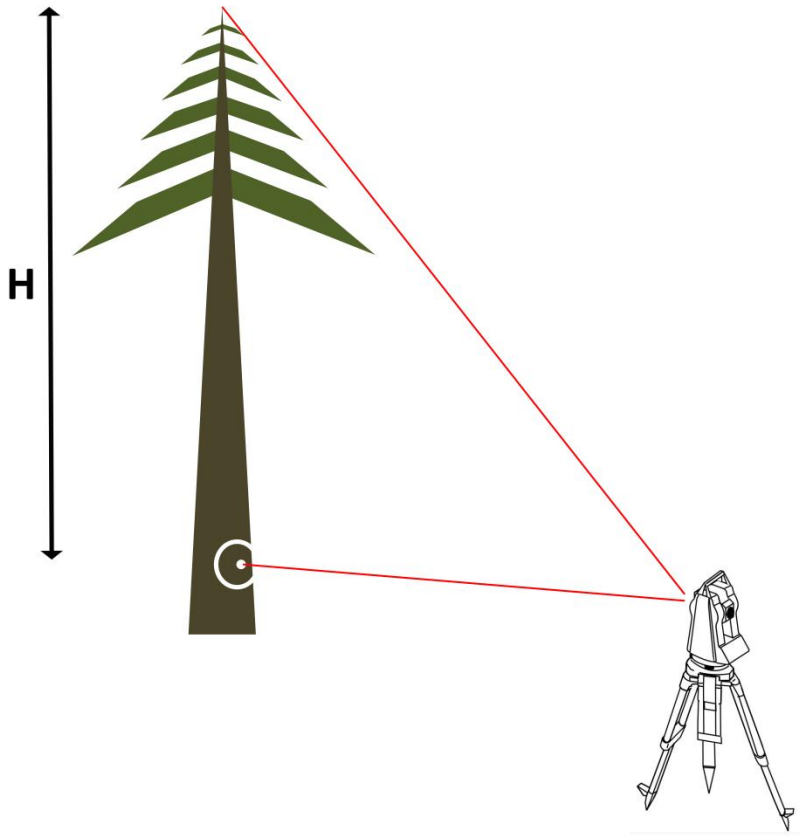

Figure III.11 : Mesure de la hauteur avec une station totale. Une cible a été tracée à la base du tronc. Chaque semaine, elle est visée avec le laser et servira de point de référence à la mesure. Une fois le point « cible » enregistré, l'apex est visé. La distance entre l'apex et la cible (H) peut alors être calculée à partir des coordonnées des deux points.

III.10 Références

Abe H, Funada R, Ohtani J, Fukazawa K. 1997. Changes in the arrangement of cellulose microfibrils associated with the cessation of cell expansion in tracheids. *Trees-Structure and Function* **11**(6): 328-332.

Benichou P, Breton Ol. 1987. Taking account of topography to produce maps of rainfall zones: the Aurelhy method. *Colloques de l'INRA*(39): 51-69.

Chaffey N 2002. An introduction to the problems of working with trees. In: Chaffey N ed. *Wood formation in trees - Cell and molecular biology techniques*. London: Taylor & Francis.

Cosgrove DJ. 2000. Loosening of plant cell walls by expansins. *Nature* **407**(6802): 321-326.

Donaldson LA. 1991. Seasonal changes in lignin distribution during tracheid development in *Pinus radiata* D. Don. *Wood Science and Technology* **25**(1): 15-24.

Harroué M, Cornu E, Rathgeber CBK. 2011. Méthodes de prélèvement et de préparation des échantillons pour l'étude de l'activité cambiale et de la formation du bois *Cahier des techniques de l'INRA* **73**: 45-62.

Jones AM. 2001. Programmed cell death in development and defense. *Plant physiology* **125**(1): 94-97.

Kutscha NP, Hyland F, Schwarzmann JM. 1975. Certain seasonal changes in balsam fir cambium and its derivatives. *Wood Science and Technology* **9**(3): 175-188.

Mothe F, Duchanois G, Zannier B, Leban JM. 1998. Microdensitometric analysis of wood samples: data computation method used at Inra-ERQB (CERD program). *Annales Des Sciences Forestieres* **55**(3): 301-313.

Polge H. 1966. *Etablissement des courbes de variation de la densité du bois par exploration densitométrique de radiographies d'échantillons prélevés à la tarière sur des arbres vivants - Applications dans les domaines technologique et physiologique. Station de Recherches sur la Qualité des Bois, INRA-CRF.*, Université Nancy I Nancy - Champenoux.

R Development Core Team 2011. R: A language and environment for statistical computing. Vienna, Austria: R Foundation for Statistical Computing. http://www.R-project.org/.

Rathgeber CBK 2012. Cambial activity and wood formation: data manipulation, visualisation and analysis using R. R package version 1.4-1. http://CRAN.R-project.org/package=CAVIAR.

Rathgeber CBK, Decoux V, Leban J-M. 2006. Linking intra-tree-ring wood density variations and tracheid anatomical characteristics in Douglas fir (*Pseudotsuga menziesii* (Mirb.) Franco). *Annals of Forest Science* **63**(7): 699-706.

Rathgeber CBK, Rossi S, Bontemps J-D. 2011. Cambial activity related to tree size in a mature silver-fir plantation. *Annals of Botany* **108**(3): 429-438.

Rossi S, Anfodillo T, Menardi R. 2006a. Trephor: a new tool for sampling microcores from tree stems. *Iawa Journal* **27**(1): 89-97.

Rossi S, Deslauriers A, Anfodillo T. 2006b. Assessment of cambial activity and xylogenesis by microsampling tree species: An example at the alpine timberline. *Iawa Journal* **27**(4): 383-394.

Rossi S, Deslauriers A, Morin H. 2003. Application of the Gompertz equation for the study of xylem cell development. *Dendrochronologia* **21**(1): 33-39.

Ulrich E, Cecchini S. 2009. *Manuel de référence n°12 pour les observations phénologiques - Placettes des niveaux A et B (Level II plots within the European Union) - Deuxième version*

Wodzicki TJ, Zajaczkowski S. 1970. Methodical problems in studies on seasonal production of cambial xylem derivatives. *Acta societatis botanicorum poloniae* **39**(3): 509-520.

Zhong R, Zheng-Hua Y 2009. Secondary cell walls. *Encyclopedia of Life Sciences*. Chichester, UK: John Wiley & Sons, Ltd., 1-9.

IV STRATÉGIES DE VIE DANS LA DYNAMIQUE INTRA-ANNUELLE DE LA FORMATION DU BOIS

Cette partie propose une caractérisation des patrons saisonniers généraux de la xylogénèse pour les trois espèces étudiées. C'est-à-dire à un « niveau arbre », la phénologie (début, fin et durée) cambiale et de la xylogénèse et la vitesse de l'activité cambiale au cours de la saison. Ces patrons sont comparés entre les espèces et les différences sont interprétées en termes de stratégie écologique. La partie donne également les patrons généraux de la mise en place des rameaux et des aiguilles. En outre, nous recherchons les relations entre la dynamique de l'activité cambiale et l'incrément annuel de xylème, c'est-à-dire à savoir si ce sont les changements dans la durée ou dans la vitesse de production des cellules qui déterminent la variabilité de l'incrément annuel du xylème entre les arbres. Les données utilisées ne concernent que le site haut du gradient, c'est-à-dire le site de Grandfontaine, avec les 15 arbres des 3 espèces et les 3 années (2007 – 2009) de suivi. La partie est constituée d'un article scientifique (article 1 de ce manuscrit) publié dans la revue Tree Physiology.

Life strategies in intra-annual dynamics of wood formation: example of three conifer species in a temperate forest in north-east France

Henri E. Cuny[1], Cyrille B.K. Rathgeber[1], François Lebourgeois[2], Mathieu Fortin[1] & Meriem Fournier[2]

*Tree Physiology (2012) **32**(5), 612-625*

[1] INRA, UMR1092, Laboratoire d Etude des Ressources Foret Bois (LERFoB), Centre INRA de Nancy, F-54280 Champenoux, France

[2] AgroParisTech, UMR1092, Laboratoire d Etude des Ressources Foret Bois (LERFoB), ENGREF, 14 rue Girardet, F-54000 Nancy, France

Summary

We investigated whether timing and rate of growth are related to the life strategies and fitness of three conifer species. Intra-annual dynamics of wood formation, shoot elongation and needle phenology were monitored over 3 years in five Norway spruces (*Picea abies* (L.) Karst.), five Scots pines (*Pinus sylvestris* L.) and five silver firs (*Abies alba* Mill.) grown intermixed. For the three species, the growing season (delimited by cambial activity onset and cessation) lasted about 4 months, while the whole process of wood formation lasted 5–6 months. Needle unfolding and shoot elongation followed the onset of cambial activity and lasted only one-third of the season. Pines exhibited an 'extensive strategy' of cambial activity, with long durations but low growth rates, while firs and spruces adopted an 'intensive strategy' with shorter durations but higher growth rates. We estimated that about 75% of the annual radial increment variability was attributable to the rate of cell production, and only 25% to its duration. Cambial activity rates culminated at the same time for the three species, whereas shoot elongation reached its maximal rate earlier in pines. Results show that species-specific life strategies are recognizable through functional traits of intra-annual growth dynamics. The opposition between Scots pine extensive strategy and silver fir and Norway spruce intensive strategy supports the theory that pioneer species are greater resource expenders and develop riskier life strategies to capture resources, while shade-tolerant species utilize resources more efficiently and develop safer life strategies. Despite different strategies, synchronicity of the maximal rates of cambial activity suggests a strong functional convergence between co-existing conifer species, resulting in head-on competition for resources.

Keywords: cambial activity, competition, functional trait, mixed stand, phenology, tree growth, wood formation.

Introduction

Living organisms develop different life strategies to access vital resources and cope with intra- and inter-species competition (Grime, 1977). These strategies can be seen in functional traits, which are measurable features that determine individual and species performance (e.g., survival, growth and reproduction) and, ultimately, their fitness in a given environment (Ackerly, 2003). For tree species, growth timing and intensity may provide critical functional traits portraying their life strategies, and the result of these strategies may be evaluated using the annual growth increment recorded in tree rings, which is known to be closely related to individual tree fitness (Baraloto *et al.*, 2005; Poorter *et al.*, 2008; Martinez-Vilalta *et al.*, 2010). Indeed, during an annual cycle, trees must adjust their period of activity to maximize resource exploitation and minimize exposure to harmful events. According to their life strategies, tree species may respond differently to this unavoidable trade-off between growth and survival. Early onset and late termination of growth may involve high risks because they increase exposure to disturbance, such as herbivore damage, and harmful climatic events such as spring or autumn frosts (Lockhart, 1983; Hanninen, 1991). However, a tree that begins growth early in spring can benefit from favorable conditions and avoid competition with its later neighbors (Augspurger *et al.*, 2005). In contrast, a tree that begins

late and ends early but demonstrates a high rate of growth may surpass its neighbors in longer-period growth.

It has been theorized that early-successional species are more prone to take risks, while late-successional species are associated with safer life strategies (Korner, 2006; Korner & Basler, 2010). Pioneer species, for example, are often photoperiod insensitive in spring and become temperature sensitive once their chilling demand has been fulfilled, allowing them to grow as soon as the climate is favorable. Late-successional species, however, can be controlled by photoperiod in spring, with temperature only exerting a limited modulating effect once the critical day length has come, preventing them from beginning too early. Such intertwined influences of environmental factors and life strategies are not documented in boreal and temperate conifer species, for which temperature is known to control spring phenological events (Wielgolaski, 1999; Deslauriers *et al.*, 2008; Rossi *et al.*, 2008b; Lebourgeois, Francois *et al.*, 2010). However, the differences observed between early- and late-successional species in cambial activity resumption (Rossi *et al.*, 2006b; Rossi *et al.*, 2008b) and budburst (Lebourgeois, Francois *et al.*, 2010) seem consistent with the theory of riskier life strategies in pioneer species. The contrasting strategies adopted by early- and late-successional species are also visible in their long-term growth dynamics. At the seedling stage, in an open field, early-successional species generally reach higher growth rates than late-successional species because they have higher capacities to capture resources (Reich *et al.*, 1998; Lusk, 2004; Niinemets, 2006). Late-successional species, however, are more efficient in their resource utilization, which ultimately allows them to grow at higher rates and surpass early-successional species during forest closure (Lusk, 2004; Niinemets, 2006; Boyden *et al.*, 2009).

Over 3 years, from 2007 to 2009, we monitored needle phenology and intra-annual dynamics of shoot elongation, cambial activity and wood formation in five silver firs (*Abies alba* Mill.), five Norway spruces (*Picea abies* (L.) Karst.) and five Scots pines (*Pinus sylvestris* L.). We chose to base our study on silver fir, Norway spruce and Scots pine because they are the three main conifer species in Europe and can be found growing in the same site despite contrasting autecologies. Selecting species of the same plant functional type (i.e., evergreen conifer) allowed us to compare their life strategies according to pioneer or late-successional status, without confusion with the deciduous or evergreen character. Finally, conifers produce wood comprising 90% of tracheids, which facilitates monitoring and comparing their intra-annual wood formation dynamics.

The very shade-tolerant silver fir is more frost- and drought-sensitive than the intermediate shade-tolerant Norway spruce, while the light-demanding Scots pine is the most drought- and cold-resistant of the three species (Lebourgeois, F. *et al.*, 2010). Silver fir is also more thermophilic and has higher nutrient requirements than Norway spruce or Scots pine (Pinto & Gegout, 2005). The three species also differ in their long-term growth dynamics (Bouriaud & Popa, 2009). Scots pine has optimal growth at younger ages, and its productivity then rapidly decreases to become the lowest of the three species. In contrast, silver fir presents a slow growth rate at young age, but its productivity gradually increases and remains high

even for old trees. Norway spruce demonstrated an intermediate behavior: its optimum growth is observed later than for Scots pine, then its productivity decreases but remains the highest of the three species until intermediate age. All these characteristics make Scots pine a pioneer species, while Norway spruce is an intermediate- and silver fir is a late-successional species.

The main objective of this study was to understand how the intra-annual dynamics of wood formation is related to species life strategies. As a pioneer species, we expected Scots pine to present longer growth durations due to earlier onsets and later cessations. As intermediate- and late-successional species, we expected Norway spruce and silver fir to produce greater growth increments due to higher cell production rates. Considering the contrasting life strategies of the investigated species, we expected that the functional diversity of the stand, with respect to the intra-annual dynamics of wood formation, was sufficient to lead to a mutual beneficial sharing of the resources in time, resulting in a 'soft' competition between trees.

Materials and methods

Study site and tree selection

The studied stand (70 × 50 m, see Figure IV.S1 available as Supplementary material) is located in a mixed forest composed of silver firs, Norway spruces and Scots pines in the Vosges Mountains (48°29′N, 7°09′E, and 643 m ASL), in north-east France. It was selected in consultation with the French national long-term monitoring network of forest ecosystems in order to be representative of submontane temperate coniferous forests of north-east France and to present the three studied species well intermixed. The study region is characterized by a mild continental temperate climate, with mean annual precipitation and temperature of 1600 mm and 9.4 °C. The three studied years were close to these mean values, with 1606 mm and 10.3 °C for 2007, 1121 mm and 9.9 °C for 2008 and 1162 mm and 10.1 °C for 2009.

Based on a complete inventory of the stand, five dominant and healthy silver firs, Norway spruces and Scots pines were selected. Their total height and crown area were measured, and two standard cores were taken at breast height to estimate their age. Manual band dendrometers were installed at breast height in March 2007 and read weekly to monitor stem circumference variations. The annual circumferential increment (ACI, see Table IV.S1 available as Supplementary material for the list of variables used along with their notations and units) was computed as the median of the measurements taken after cambial activity cessation.

Needle phenology and shoot elongation monitoring

Shoot elongation and needle phenology were monitored weekly in the upper tier of the crown of each studied tree using binoculars. The length of new shoots was visually assessed, and needle unfolding was described using three successive phenological stages occurring after winter bud dormancy: (i) budburst, (ii) maturing needles and (iii) mature needles. In the three species, dormant buds were totally enclosed by scales and recognizable by their small size

(Figure IV.S2a and IV.S2d). Budburst differed between species and was distinguished according to the criteria of the phonological observations protocol of the French national long-term monitoring network of forest ecosystems (Ulrich & Cecchini, 2009). In firs and spruces, budburst date was recorded when buds were fully open, scales had fallen and developing needles were clearly apparent (Figure IV.S2b). In pines, bud-burst date was recorded when developing needles were clearly visible at the bottom of the new shoots, emerging from the scales, even if buds were still elongating and only partially open (Figure IV.S2e). Maturation of needles was indicated by their color, which progressively changed from light to dark green. Current-year needles, in comparison with those of the previous years, were considered mature when they demonstrated the same color.

For each tree, onset ($t_{i,\ N}$) and cessation ($t_{f,\ N}$) of needle unfolding were defined, respectively, as the date at which 50% of buds were broken and 50% of needles were mature; the duration of needle unfolding (Δ_N) was computed as the time between $t_{f,\ N}$ and $t_{i,\ N}$. Onset ($t_{i,\ S}$) and cessation ($t_{f,\ S}$) of shoot elongation were defined, respectively, as the date at which 50% of shoots began to lengthen and 50% of shoots reached their final length; duration of shoot elongation (Δ_S) was computed as the time between $t_{f,\ S}$ and $t_{i,\ S}$. Daily dates were estimated based on weekly observations using linear interpolations.

To assess shoot elongation dynamics, length of new shoots was fitted with a logistic curve (Karkach, 2006) using the SSlogis function of the R statistical software (R Core Team, 2012):

$$lS(t) = \frac{A}{1 + e^{\frac{t_{p,\ S} - t}{c}}} \quad (1)$$

where *lS(t)* is the length of shoots at time *t*; *A* is the upper horizontal asymptote parameter representing the final shoot length; $t_{p,\ S}$ is the date of the inflection point; and *c* is a numeric scale parameter of the time axis. From this model, the maximal ($r_{x,\ S}$) and mean ($r_{m,\ S}$) shoot elongation rates were estimated.

Overall measure of fit was assessed by the modeling efficiency (r^2), a statistic close to the coefficient of determination that can be used for nonlinear models (Mayer & Butler, 1993).

Tree sampling and sample preparation

Microcores (2 mm diameter, 15–20 mm length) were collected weekly from April to November at breast height on the stems of the selected trees using a Trephor ® (Vitzani, Belluno, Italy) (Rossi *et al.*, 2006a) and following an ascending spiral pattern (Deslauriers *et al.*, 2003). Successive microcores were taken about 1 cm apart from each other to avoid wound reaction without considerably increasing the influence of stem circumferential variability on the final dataset. The collected microcores were placed in Eppendorf microtubes with ethanol solution (50% in water) and stored at 5 °C. Each sample was oriented under a stereomicroscope at ×10–20 magnification, and the transverse side was marked with a pencil. Microcores were successively cleaned, dehydrated and infiltrated by immersion in baths of ethanol, d-limonene and paraffin using an automatic tissue processor (STP121, MM France,

Francheville, France) (Rossi *et al.*, 2006a). Microcores were then embedded in paraffin blocks with an embedding station (EC 350, MM France), and 5–10-µm-thick transverse sections were cut with a rotary microtome (HM 355S, MM France). Sections were stained with cresyl violet acetate (0.16% in water) and permanently mounted on glass slides using Histolaque LMR ®.

Microscopic observations

Overall, 1450 anatomical sections were observed using an optical microscope (Orthoplan, Leitz, Germany) under visible and polarized light at ×125–400 magnification to distinguish the different phases of cell development. For each sample, the radial number of cells in the cambial (n_C), enlargement (n_E), cell-wall thickening and lignification (n_L) and mature zones (n_M) was counted along three radial files according to the criteria described by Rossi *et al.* (2006b). Cambial cells were characterized by thin cell walls and small radial diameters. Cells in the radial enlargement phase were larger than cambial cells and had thin walls that were not birefringent under polarized light. Cells in the cell-wall thickening and lignification phase were birefringent under polarized light and demonstrated violet and blue walls. Tracheids were considered mature when walls were completely blue.

Timing of wood formation

A set of five critical dates and three durations was computed from the cell-counting dataset using logistic regressions (Rathgeber *et al.*, 2011a). The onset of enlarging ($t_{i,\,E}$), cell-wall thickening and lignification ($t_{i,\,L}$) and mature phases ($t_{i,\,M}$), and the cessation of enlarging ($t_{f,\,E}$) and cell-wall thickening and lignification phases ($t_{f,\,L}$) were defined as the dates at which 50% of the radial files were active (onset) or non-active (cessation). The durations of enlarging (Δ_E) and cell-wall thickening and lignification (Δ_L) phases were the time between the onset and cessation of these phases.

As recommended by Rathgeber *et al.* (2011a), our assessment of tracheid production timing was based on the xylem cell enlargement phase rather than the cambial cell dividing phase. Thus, $t_{i,\,E}$, $t_{f,\,E}$ and Δ_E were also used as proxies for the onset, cessation and duration of cambial activity, respectively. $t_{i,\,E}$ and $t_{f,\,L}$ were used as proxies for onset and cessation of xylogenesis ($\Delta_X = t_{i,\,L} - t_{i,\,E}$).

Standardization

The number of cells varied according to the height and the orientation of the sample along the stem and consequently among the different samples within and between the trees (Wodzicki & Zajaczkowski, 1970). According to Rossi *et al.* (2003), the number of cells from the previous year was counted on three radial files per sample and used to standardize the raw number of the current year. A dedicated function of the R package CAVIAR (Rathgeber, 2011) was used to apply this standardization to all the samples in our dataset.

Cell number computation

The total number of tracheids produced at time t during the season was computed as the sum of the standardized number of cells belonging to the xylem ($n_T(t) = n_E(t) + n_L(t) + n_M(t)$).

The final ring cell number was computed as the median of the total number of cells ($n_T(t)$) of all the samples taken after $t_{f,\,E}$. The number of cambial cells before and after the growing season was also computed as the median number of cambial cells in all the samples taken before $t_{i,\,E}$ or after $t_{f,\,E}$, respectively.

Rate of tracheid production

To assess tracheid production dynamics, the number of cells over time was fitted using a Gompertz function (Rossi *et al.*, 2003) defined as

$$n_T(t) = A.e^{-e^{\beta-\kappa.t}} \quad (2)$$

where $n_T(t)$ is the standardized total number of tracheids at time t; A is the upper horizontal asymptote parameter representing the final number of tracheids; β is the x-axis placement parameter that reflects the choice of origin time; and κ is the growth rate parameter that determines the spread of the curve along the time axis. These parameters were estimated for each tree using a dedicated function of the R package CAVIAR (Rathgeber, 2011). Overall measure of fit was assessed by the modeling efficiency (r^2). The date of the inflection point ($t_{p,\,T}$) and the corresponding maximal rate of tracheid production ($r_{x,\,T}$) were computed, as well as the mean rate ($r_{m,\,T}$), accounting for the period during which 90% of the tracheids were produced (Rathgeber *et al.*, 2011b). To test whether the rate of tracheid production depended more on the number of cambial cells or on the division frequency of each cambial cell, the mean cell cycle length (CCL_m) was computed by dividing the mean number of cambial cells observed through the growing season by $r_{m,\,T}$, and the minimal cell cycle length (CCL_n) was calculated by dividing the number of cambial cells at $t_{p,\,T}$ by $r_{x,\,T}$.

Statistical analyses

Linear mixed-effects models were used to test the effect of species on the selected potential functional traits. Mixed-model approach is recommended in the case of repeated measurements because it evaluates the effects of fixed factors (in our case, the species), taking into account the effects of random factors (trees and years), on the response variable (the potential functional traits) (Zuur *et al.*, 2009). The standard deviation of the year random effect allowed us to estimate the year-to-year variability of each potential functional trait. Estimations of the model parameters were performed with the R package lme4 (Bates *et al.*, 2011).

Simple physical model of annual radial growth

The ACI was expressed as a function of the maximal rate ($r_{x,\,T}$), and duration (Δ_E) of tracheid production:

$$ACI = f(r_{x,\,T} \times \Delta_E) \quad (3)$$

The effect of species on this product was also tested using the same linear mixed-effects modeling procedure to check model consistency. Moreover, a sensitivity analysis of the model was performed to compare the contribution of the rate and duration to the annual increment (Cariboni *et al.*, 2007).

Results

Dendrometric characteristics of the monitored trees

The monitored trees presented similar stem diameters but the silver firs and Norway spruces were on average 5 m taller and 45 years younger than the Scots pines (Table IV.1). Moreover, the firs had larger crown areas. The three species demonstrated significant differences concerning their annual production of shoots and wood. Firs exhibited radial increments (either evaluated by number of cells, tree-ring width, or stem circumference variation) more than twice those of spruces and pines ($P < 0.01$). These differences were also visible in the wintering cambium, with firs showing two more dormant cambial cells than spruces and pines ($P < 0.01$), as well as during the growing season, with the firs producing more cells (Figure IV.1). Finally, pines produced shoots 1–2 cm longer than firs and spruces ($P < 0.01$).

Table IV.1: Main characteristics and annual production (mean ± SE) of the monitored trees from the three studied species (silver fir, Norway spruce and Scots pine). Diameter at breast height (DBH), height (H), age, projected crown area (CA), final ring cell number (RCN), tree-ring width (TRW), annual circumferential increment (ACI), number of cambial cells before the onset (ICN) and after the termination (FCN) of the growing season and final shoot length (FSL).

	DBH (cm)	H (m)	Age	CA (m²)	RCN	TRW (mm)	ACI (mm)	ICN	FCN	FSL (cm)
Pines	53 ± 2	27 ± 1	119 ± 3	29 ± 2	29.7 ± 3.0	1.1 ± 0.1	6.8 ± 0.7	5.5 ± 0.2	5.9 ± 0.2	10.5 ± 0.3
Firs	57 ± 3	31 ± 1	73 ± 3	37 ± 6	67.9 ± 7.5	2.5 ± 0.2	15.5 ± 1.2	7.2 ± 0.3	7.8 ± 0.3	8.5 ± 0.3
Spruces	55 ± 4	33 ± 1	74 ± 4	30 ± 7	33.9 ± 4.4	1.3 ± 0.1	7.8 ± 0.8	5.5 ± 0.2	5.7 ± 0.1	8.7 ± 0.2

Needle phenology and intra-annual dynamics of shoot elongation

For firs and spruces, budburst occurred between late April and mid-May and was followed by the onset of shoot elongation the following week (Figure IV.2). In contrast, in pines, shoot elongation began at the end of April or the beginning of May, 3 weeks before the onset of needle unfolding. Mixed-effect models estimated that budburst occurred 2 weeks earlier in firs and spruces when compared with pines ($P < 0.01$), but the onset of shoot elongation began 3 weeks earlier in pines ($P < 0.01$; Figure IV.3a). Overall, the onset of shoot elongation in pines was the first phenological event recorded during the year, occurring 1 week before budburst in firs and spruces ($P < 0.01$); thus, Scots pine was the first species to begin primary growth. A variability of 1 week was observed between years for the dates of budburst and shoot elongation onset.

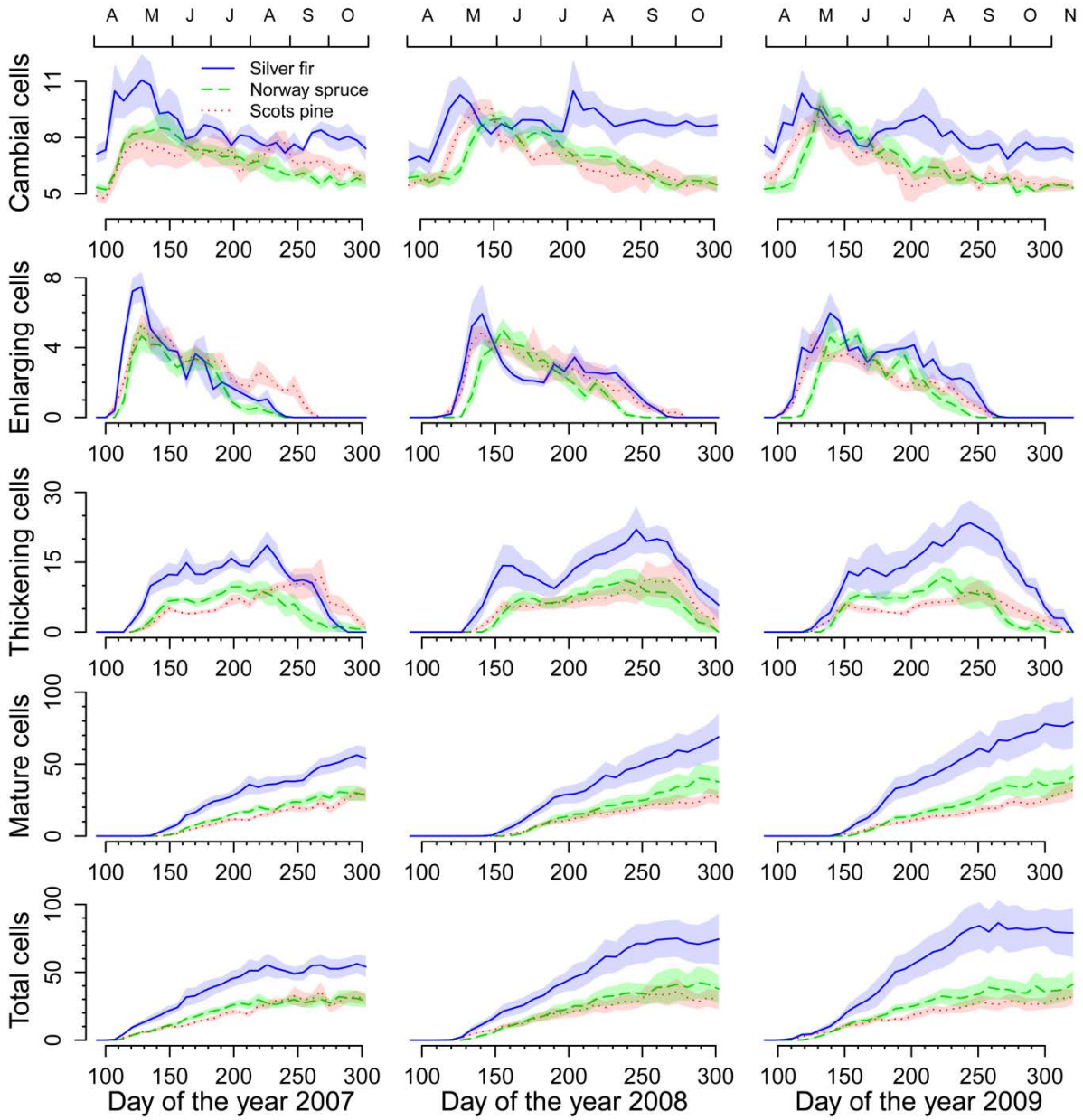

Figure IV.1: Intra-annual wood formation dynamics. For each species, the line represents the mean cell number of the five monitored trees, and the shadowed area delimits the 90% confidence intervals.

On average, shoots reached their final length in June (Figure IV.2). Shoot elongation cessation varied by 4 days from year to year, but occurred 1 week earlier for pines than for firs and spruces ($P < 0.01$; Figure IV.3b). Shoots lengthened over 5–6 weeks, 1 week longer in pines than in firs or spruces ($P < 0.01$; Figure IV.3c), with an estimated year-to-year variability of only 1 day. For the three species, needles were mature 1 week after shoot elongation cessation, between mid-June and the very beginning of July (Figure IV.2). Needles were mature 1 week earlier for pines than for firs and spruces ($P < 0.01$; Figure IV.3d), with year-to-year variability estimated at 3 days.

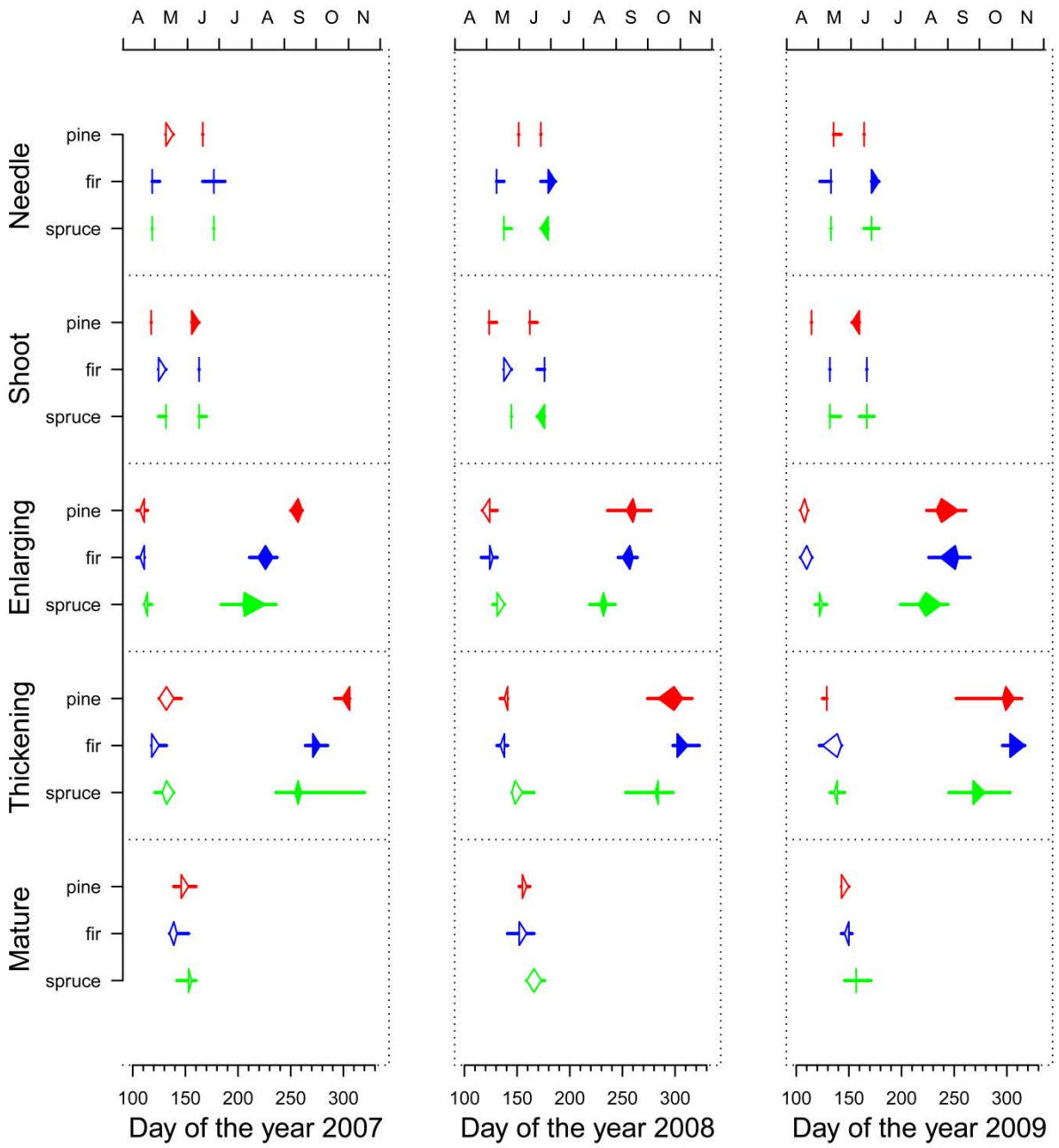

Figure IV.2: Needle unfolding, shoot elongation and wood formation calendar. Onset and cessation of needle unfolding and shoot elongation, along with critical dates of wood formation for pines, firs and spruces. Critical dates of wood formation are the onset and cessation of the enlarging and thickening phases along with the onset of the mature phase. Note: for each date, the five trees are represented by diamond-crossed-by-a-line marks; the left end of the line represents the first tree to begin or finish, the left end of the diamond the second tree, the middle of the diamond the third tree, the right end of the diamond the fourth tree and the right end of the line the fifth tree.

The logistic function yielded good results in fitting shoot elongation dynamics (Table IV.S2, Figures IV.S3, IV.S4 and IV.S5). The shoot elongation rates were similar between the three species, with a maximal rate of 0.39 ± 0.02 (mean ± standard error) and a mean rate of 0.23 ± 0.01 cm/day (Figure IV.3e). Year-to-year variations of the maximal and mean rates were small (16 and 12%, respectively). Despite similar rate shapes and magnitudes across species, the earlier onset observed in pines was also visible in the pattern of shoot elongation

rates through the growing season and resulted in a shift of the pine curve, while spruce and fir curves tended to overlap (Figure IV.4). Thus, the maximal rate of shoot elongation occurred around the middle or end of May, 1 week earlier for pines than for firs and spruces ($P < 0.01$; Figure IV.3f), with year-to-year variability estimated at 6 days.

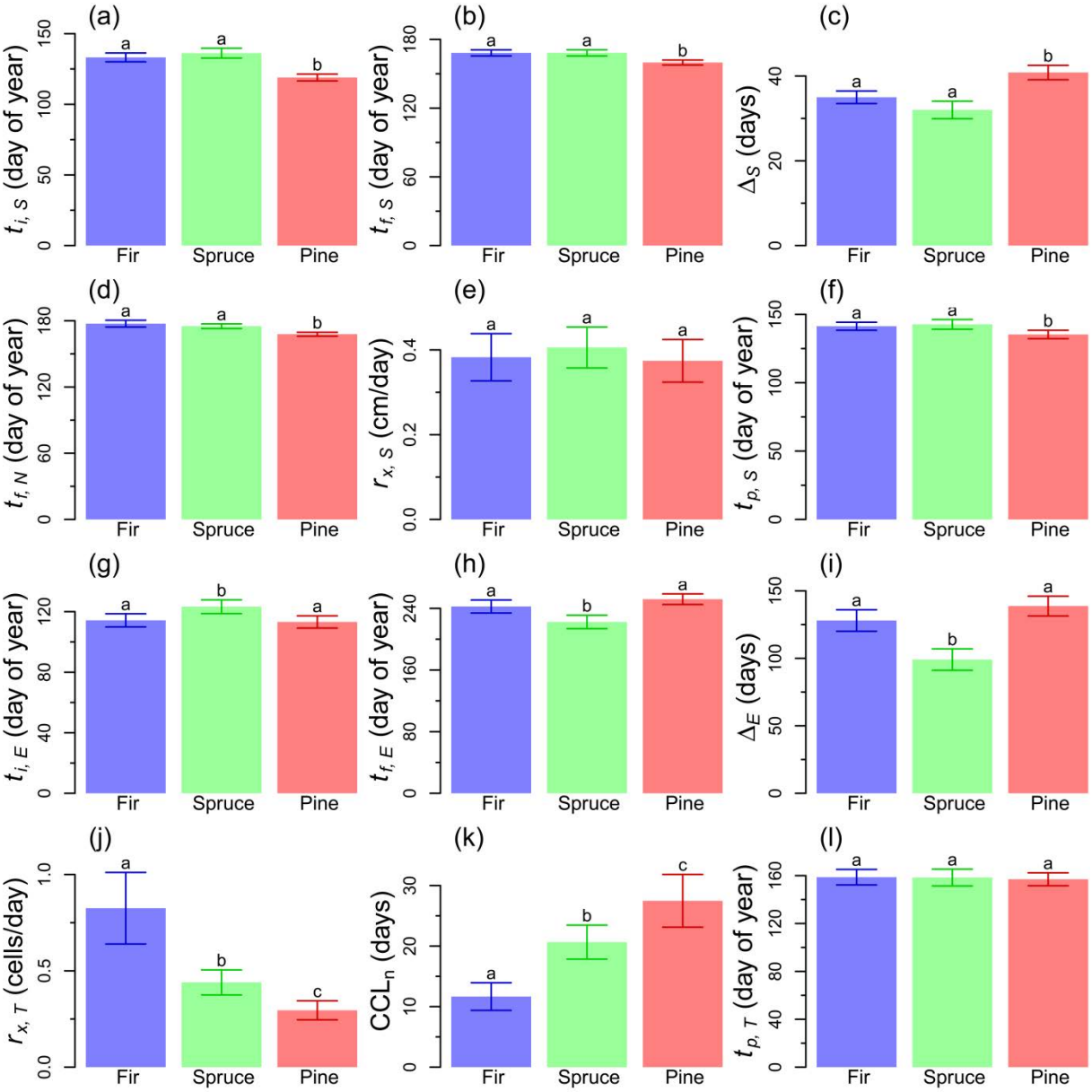

Figure IV.3: Comparison of the intra-annual dynamics of shoot elongation, needle unfolding and wood formation between the three studied species. Onset ($t_{i,S}$), cessation ($t_{f,S}$), duration (Δ_S), maximal rate ($r_{x,S}$), occurrence of the maximal rate ($t_{p,S}$) of shoot elongation and cessation ($t_{f,N}$) of needle unfolding. Onset ($t_{i,E}$), cessation ($t_{f,E}$), duration (Δ_E), maximal rate ($r_{x,T}$), minimal length of the cell cycle (CCL_n) and occurrence of the maximal rate ($t_{p,T}$) of tracheid production. Letters above bars indicate whether differences between species are significant ($P < 0.05$) based on linear mixed-effects models.

Intra-annual dynamics of xylem cell production and maturation

Regardless of species or year, the number of dividing, enlarging, thickening and mature cells followed a general pattern of variation through the vegetation season commonly described as three delayed bell curves followed by a sigmoid curve (Figure IV.1). However,

the bell curves representing the number of dividing cells in the cambial zone were clearly skewed to the left, indicating a quick onset followed by a slow cessation of the process. Between mid-April and early May, the number of cambial cells increased, on average from 5.5 ± 0.2 to 9.0 ± 0.7 cells for the spruces and pines and from 7.2 ± 0.3 to 10.6 ± 1.4 cells for the firs. Then, it gradually decreased through the growing season and finally returned approximately to its initial value, corresponding to the number of cambial cells at rest.

Following the increase in the number of cambial cells by only a few days, xylem cells began to enlarge between mid-April and mid-May, depending on the year and the species (Figure IV.2). Pines and firs entered the enlarging phase 1 week earlier than spruces ($P < 0.01$; Figure IV.3g), even though a year-to-year variation of 1 week was estimated. As for the dividing cells, the number of enlarging cells through the growing period exhibited a bell curve clearly skewed to the left (Figure IV.1). It increased quickly in spring to culminate at 4.8 ± 0.6 cells for the spruces and pines and 6.5 ± 1.2 cells for the firs, and then decreased progressively. Xylem cell enlargement ceased between the second part of July and mid-September, depending on species and year, with a greater variability among trees, both within and between species, than at its onset (Figure IV.2). Despite this greater variability, spruces ceased significantly (by 3 weeks) earlier than firs and pines ($P < 0.01$; Figure IV.3h), while a mean variation of 1 week was estimated between years. Due to their earlier onsets and later cessations, firs and pines had enlarging phase durations significantly longer than spruces (on average 4.5 and 3.5 months, respectively, $P < 0.01$; Figure IV.3i). These durations did not vary from year to year because the variations observed at the onset of the enlarging phase were counterbalanced by the variations observed at its cessation.

Secondary cell-wall formation began in late April or May, depending on year and species, about 2 weeks after enlarging phase onset (Figure IV.2). Pines and firs began 1 week earlier than spruces ($P < 0.01$), even though the year-to-year variability was estimated at 1 week. In contrast to the dynamics observed for the dividing and enlarging cells, the number of thickening cells through the growing season demonstrated a bell curve slightly skewed to the right, indicating a slow onset and rapid cessation (Figure IV.1). The firs accumulated twice as many thickening cells (21.3 ± 4.3) than the pines and spruces (10.9 ± 2.8). Secondary cell-wall formation ended between September and November, depending on the year and the species, about 2 months after enlarging phase cessation, with a greater variability among trees (within as well as between species) than at its onset (Figure IV.2). Nevertheless, spruces ended 3 weeks earlier than firs and pines ($P < 0.01$), with an estimated year-to-year variation of 1 week. The duration of the thickening phase was 1 month longer for pines and firs than for spruces (on average 5.5 and 4.5 months, respectively, $P < 0.01$). The total duration of xylem formation also lasted 1 month longer for pines and firs than for spruces (on average 6 and 5 months, respectively, $P < 0.01$).

The first mature cells appeared at the end of May or the beginning of June, 2 weeks after the onset of the thickening phase and 1 month after the onset of the enlarging phase (Figure IV.2). A mean year-to-year variation of 1 week was estimated, but pines and firs began 1 week earlier than spruces ($P < 0.01$). Mature cells accumulated steadily through the season, making

the expected sigmoid shape difficult to observe on the mean curves (Figure III.1). The sigmoid shape, however, was clearly visible on the curves for the total number of xylem cells.

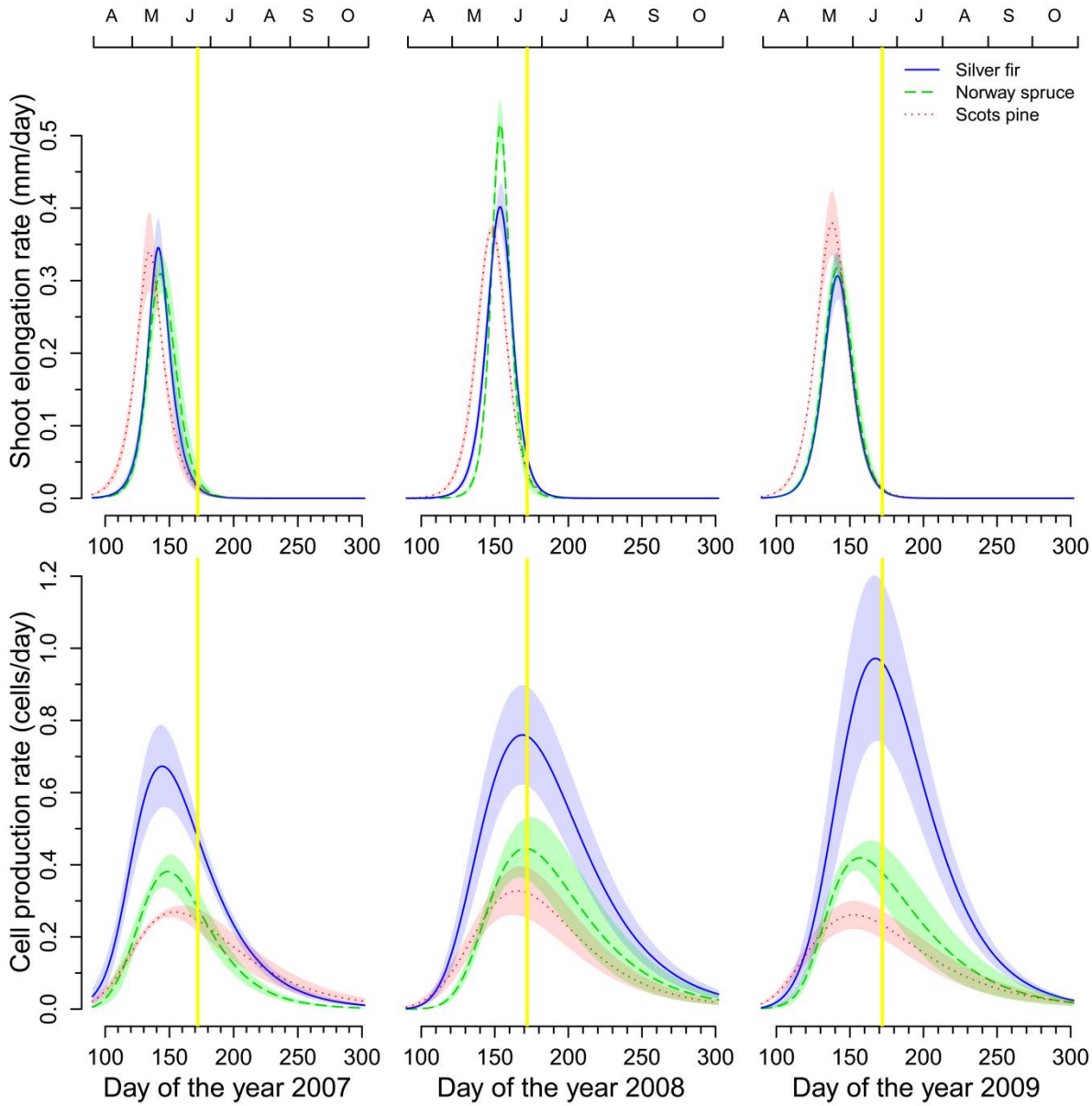

Figure IV.4: Rates of shoot elongation and tracheid production. For each species, the line represents the mean of the five monitored trees, and the shadowed area delimits the 90% confidence interval. The vertical yellow line represents summer solstice.

Regardless of species, Gompertz function yielded good results in fitting the production of xylem cells through the growing period (see Table IV.S3, Figures IV.S6, IV.S7 and IV.S8). However, the tracheid production rates derived from these fittings differed between the three species (Figure IV.3j). Pines presented the lowest rates, with maximal and mean rates around 0.29 ± 0.03 and 0.18 ± 0.02 cells/day, respectively. Spruces demonstrated higher rates than pines, with maximal and mean rates around 0.44 ± 0.03 and 0.26 ± 0.02 cells/day, respectively ($P < 0.01$). Firs exhibited maximal and mean rates two times greater (0.83 ± 0.10 and 0.50 ± 0.06 cells/day, respectively) than those of spruces and pines ($P < 0.01$). These rates were stable from year to year, with mean variations <5%. Significant linear relationships were

found between the maximal rate and the number of cambial cells observed at its occurrence, as well as between the mean rate and the mean number of cambial cells through the growing season ($P < 0.01$).

The mean and minimal cell cycle lengths followed the same pattern of variation as the mean and maximal rates, with fir cell cycle lengths shorter than those of spruces, which were themselves shorter than those of pines ($P < 0.01$, Figure IV.3k). However, the differences between species were smaller when considering the cell cycle length, with minimal and mean lengths of 12 ± 1 and 20 ± 2 days for firs, 21 ± 1 and 31 ± 2 days for spruces and 27 ± 2 and 43 ± 3 days for pines.

Although the cell production rates and cell cycle lengths differed between the three species, their evolutions through the growing season were similar (Figure IV.4). The most impressive feature was that the maximum rates of tracheid production (corresponding also to the minimal cell cycle length) occurred at the same time for the three species ($P > 0.5$), a couple of weeks before the summer solstice (Figure IV.3l). The date itself varied by about 9 days from year to year, but within a particular year trees, whatever their species, synchronized their maximal growth.

Simple physical model of annual radial growth

The onset ($t_{i,\,E}$), cessation ($t_{f,\,E}$) and duration (Δ_E) of cambial activity presented species-specific relationships with the ACI, with significant relationships for firs ($P < 0.01$) and spruces ($P < 0.01$) and no significant relationship for pines (Figure IV.5a). In contrast, a species-independent relationship was established between the maximal rate of cambial activity ($r_{x,\,T}$) and ACI ($P < 0.01$; Figure IV.5b). The relationship between $r_{x,\,T}$ and Δ_E was also species specific with significant and linear relationships for firs ($P < 0.01$) and spruces ($P < 0.1$) and no significant relationship for pines (Figure IV.5c). Three behaviors were identified through the manner in which species occupied the duration vs. rate space: (i) the spruces presented short durations and medium rates, (ii) the firs presented medium durations and high rates and (iii) the pines presented long durations and low rates.

The model ACI = $r_{x,\,T} \times \Delta_E$ yielded good results ($P < 0.01$; Figure IV.5d), with no significant effect of species on the rate–duration product. Sensitivity analysis revealed that when $r_{x,\,T}$ was kept constant to its mean value while Δ_E was made to vary around its mean within a range of twice its standard deviation, the resulting ACI varied from 7.1 to 12.3 mm (i.e., a range of variation of 5.2 mm). However, when Δ_E was kept constant to its mean value while $r_{x,\,T}$ was made to vary around its mean within a range of twice its standard deviation, the resulting ACI varied from 2.1 to 17.3 mm (i.e., a range of variation of 15.2 mm). Therefore, the simulated ACI was three times more sensitive to $r_{x,\,T}$ than to Δ_E, or ACI variability was attributable to ~25% of Δ_E and 75% of $r_{x,\,T}$.

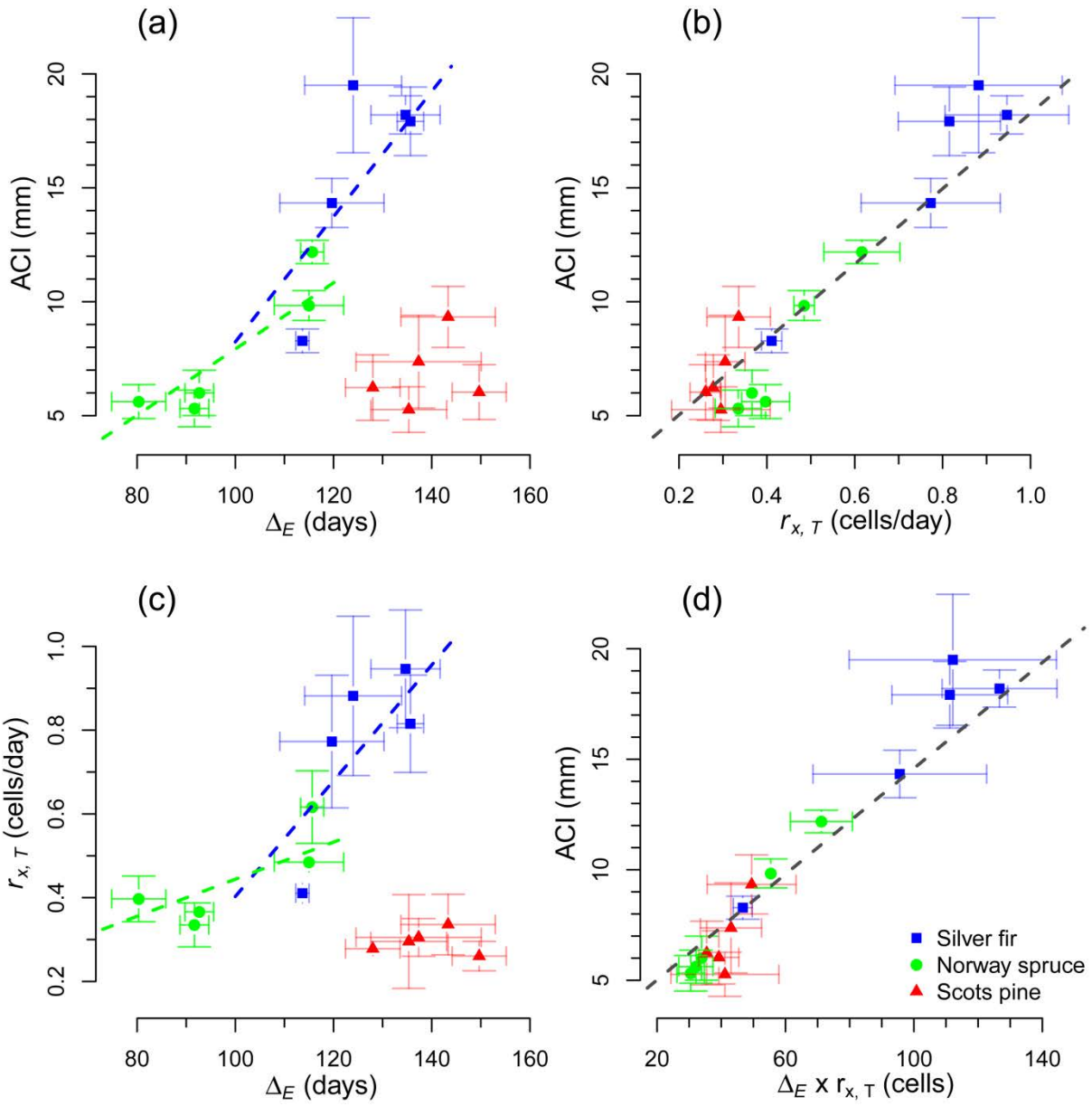

Figure IV.5: Relationships between the duration of the growing period (Δ_E), the rate of tracheid production ($r_{x,T}$) and the annual circumferential increment (ACI).

Discussion

Intra-annual dynamics of wood formation in temperate and cold forest ecosystems

In our study site located at mid-altitude in a temperate coniferous forest, cambial activity began between late April and early May, a few days before the onset of needle unfolding and shoot elongation. While needle unfolding and shoot elongation lasted only 1–1.5 months, tracheids accumulated over 3–4.5 months and matured over 5–6 months, so that the major part of wood formation occurred after the production of needles and shoots (Rossi *et al.*, 2009). During the growth period, the cambium produced cells at an average rate of 0.31 ± 0.03 cells day^{-1}, for a final number of 44 ± 4 cells in the annual tree ring. Very similar timings and rates of tracheid production and differentiation have been described in temperate

forests in central Europe, for Scots pine in Poland (Wodzicki, 1971; Wodzicki, 2001) and for Norway spruce and silver fir in Slovenia (Gričar, 2007). Conifers grown in subalpine and boreal forest ecosystems exhibit similar rates of cambial activity (Deslauriers & Morin, 2005; Rossi *et al.*, 2008a) but are associated with very different timing. In such cold environments, cambial activity begins 2–4 weeks later, finishes 2–4 weeks earlier, and thus lasts 1–2 months less than those in temperate forests, which results in lower annual production, generally <30 tracheids (Rossi *et al.*, 2006b; Rossi *et al.*, 2007; Deslauriers *et al.*, 2008; Lupi *et al.*, 2010; Rossi *et al.*, 2011).

Influence of tree age and size on wood formation traits

Based on the theory that pioneer species adopt riskier life strategies than late-successional species (Korner, 2006; Korner & Basler, 2010), we expected an earlier onset of growth in pines. Primary growth actually began earlier in Scots pine, but surprisingly cambial activity began at the same time for pines and firs. The greater age and the lower height of pines (Table IV.1) may explain this unexpected result. Indeed, Rossi *et al.* (2008a) reported that cambial activity began later as trees aged, while Rathgeber *et al.* (2011b) found that, at the same age, smaller silver firs begin cambial activity later than taller ones. Therefore, because the selected pines were older and smaller than the firs and spruces, we probably overestimated their onset and underestimated their cessation and durations of wood formation. Moreover, by establishing the wood-formation calendar of similar-age (≈40 years old) trees grown in the same stand, Rathgeber *et al.* (2011a) found that cambial activity began 20 days earlier for Scots pine than for silver fir. This body of evidence supports the hypothesis that early- successional species adopt riskier life strategies, as indicated in their wood formation phenology by early onsets and late cessations.

In our study, pines exhibited a lower cell production rate than firs and spruces. However, Rossi *et al.* (2008a) and Rathgeber *et al.* (2011b) found that cambial activity was less intense for older and smaller trees. Therefore, we calculated the rates of cell production in the dataset used by Rathgeber *et al.* (2011a) in order to compare trees of the same age and of comparable size, and we found that the maximum and mean rates of cambial activity were higher ($P < 0.01$) for silver firs (0.82 ± 0.18 and 0.49 ± 0.11 cells/day, respectively) than for Scots pines (0.50 ± 0.12 and 0.30 ± 0.09 cells/day, respectively).

The use of cell cycle length was also a method to minimize the effects of tree age and size by ‘standardizing’ the rate of cell production by the number of dividing cells, amplifying the intrinsic species behavior. The computation of this crucial functional trait slightly reduced the differences in cell production rate observed between species. However, the contrasting behaviors remained strong, with the minimal cell cycle duration being twice as long for Scots pine as for silver fir, Norway spruce being in between. Once again, this body of evidence supports the idea that early-successional species present a lower rate of production than late-successional species because they are less efficient at converting environmental resources into growth.

Life strategies in intra-annual wood formation dynamics

Our results demonstrated that the contrasting life strategies adopted by the three species were clearly apparent in the functional traits depicting the key features of their intra-annual wood formation dynamics. For example, to produce similar radial increment, cambial activity lasted 40% longer in pine than in spruce because its cell production rate was 30% slower. Firs were more difficult to compare with the two other species because they produced radial annual increments twice as large. However, the fir-specific relationships between radial increment and duration of cambial activity (see the slopes of the dashed lines in Figure IV.5a) and the non-specific relationship between radial increment and cell production rate (see Figure IV.5b) indicated that firs used less time than pines to produce similar radial increments because they exhibited higher rates. In summary, we described the Scots pine growth strategy as 'extensive' because it was characterized by long durations and low rates, illustrating the characteristic behavior of early-successional species, which are prone to explore space and time to capture resources but are not very efficient in their utilization. In contrast, we described the growth strategy adopted by fir and spruce as 'intensive' because it was characterized by higher rates and shorter durations, illustrating the behavior of late-successional species, which are more cautious in their exploration of space and time but are more efficient in the utilization of the limited resources they have access to. The high rates of growth associated with the 'intensive' strategy suggest that at the dominant stage, silver fir, and to a lesser extent Norway spruce, are better competitors than Scots pine, while the long growing periods associated with the 'extensive' strategy suggest that Scots pine is closer to the stress top of Grime's C-S-R triangle (Grime, 1977).

Firs reached higher rates of cambial activity than spruces, which themselves reached higher rates than pines because they have more dividing cambial cells during the growing season and, above all, because they have shorter cell cycles. The number of cambial cells is known to depend on tree species (Larson, 1994) and vitality (Gričar *et al.*, 2009), and its influence on the rate of cell production is already well documented (Vaganov *et al.*, 2006). The strong influence of the cell cycle length is consistent with the results obtained by Deslauriers *et al.* (2009). As cell cycle length is closely linked to the quantity of sucrose available around dividing cells (Riou-Khamlichi *et al.*, 2000), the shorter cell cycles observed in firs and spruces suggest that they can produce more assimilates than pines. The results of Deslauriers *et al.* (2009), however, suppose differences in cell cycle length between two poplar genotypes that have similar photosynthetic capacities, indicating that genetic control can also be envisaged.

The suggested ability of fir and spruce to produce more assimilates may be related to their management of foliage turn-over. Indeed, late-successional evergreen conifer species have slower foliage turnover than pioneer species. For example, leaf life span reaches 6–7 years in firs and spruces, compared with only 2–3 years in pines (Becker *et al.*, 1995). A slow foliage turnover allows the accumulation of several leaf cohorts that finally develop larger leaf areas than those of shorter turnover species without spending more energy (Lusk, 2004).

Life strategies, fitness and functional convergence of conifer species

When regrouping the data from the three species, we estimated that about 75% of the annual radial increment variability was attributable to the rate of cell production and only 25% to its duration. Rathgeber *et al.* (2011b) found the same values to explain the tree-ring width variability between trees belonging to different social status in a mature silver fir plantation. These results suggest that the rate of cell production is the main component of the growth process that influences the fitness of a particular tree compared with its neighbors, whether of the same or different species. Mixed stands have been theorized to achieve greater overall productivity than monocultures because of the 'competitive production principle', assuming that the competition acting between trees of different species is inferior to that between trees of the same species (Vandermeer, 1989). This reduction of competition is a consequence of the functional diversity between species, which leads to a complementary resource use in two dimensions: first in space, e.g., by the complementarity of crown and root architectures; second in time, by the occupation of different time windows to carry out different vital processes (Richardson & O'Keefe, 2009; Ishii & Asano, 2010). Indeed, we observed that needle phenology and primary growth critical dates (onset, maximal rate occurrence and cessation) were spread over a few weeks depending on the species. In contrast, we found that the maximal rate of tracheid production culminated at the same time for the three species, indicating that most wood production occurs at the same time for all trees. For conifers, shoot production and wood formation mainly depend on current-year assimilates (Hansen & Beck, 1990; Oribe *et al.*, 2003). Shoots, however, represent <10% of the annual carbon allocation, whereas wood is the strongest carbon sink, representing around 45% of the annual allocation (Grote, 1998). Therefore, even if the spreading observed in shoot production suggests complementary resource use in time, the low quantity of energy needed to produce new shoots indicates that its benefit is limited.

On the contrary, the synchronicity observed in the occurrence of the maximal rate of wood production shows that species allocate great quantities of carbon to their stem simultaneously. Similar results were found by Rathgeber *et al.* (2011b) for silver firs of different social status within a close monospecific stand. Thus, within a close conifer stand, the occurrence of the maximal rate of cell production is controlled by the same environmental factors regardless of tree species or size. Its convergence toward the summer solstice may suggest, as proposed by Rossi *et al.* (2006c), that the maximum day length is this common environmental factor triggering growth decrease, allowing trees to safely finish secondary wall lignification before winter. However, the inter-annual variations we observed concerning this trait are not fully consistent with this hypothesis and suggest that other climatic factors (soil humidity for example) may play a role. Whatever the environmental control behind this synchronization, it demonstrates a strong functional convergence between conifer species, leading to a 'hard' head-on competition for resources, with all the trees fully expressing their needs at the same time. This functional convergence may be heightened by the evergreen character of the studied species, which makes a real 'phenological escape' impossible and thus limits the benefit of a competition-avoidance strategy (Richardson & O'Keefe, 2009). The fact that early-successional species are not able to avoid the head-on competition imposed by this

synchronization with late-successional species may be a clue to explain their elimination during conifer forest maturation.

Conclusions

For the three studied conifer species, the growing season (as delimited by cambial activity onset and cessation) lasted about 4 months, while the whole process of wood formation lasted ~5–6 months. Needle unfolding and shoot elongation followed the onset of cambial activity and lasted about one-third of the season. Species-specific life strategies were recognizable through critical functional traits of intra-annual wood formation dynamics. Pines exhibited an 'extensive strategy' characterized by long duration and low rate of growth, while firs and spruces adopted an 'intensive strategy' with shorter durations and higher rates. The opposition between Scots pine extensive strategy and silver fir and Norway spruce intensive strategy is consistent with the theory that pioneer species are more disposed to take risks for exploring space and time in order to capture new resources, while shade-tolerant species safely favor maximal efficiency in the use of available resources.

Despite the fact that both the timing and rates of wood formation provided pertinent functional traits indicative of contrasting species life strategies, we estimated that about 75% of the annual radial increment variability could be attributed to the rate of cambial activity, and only 25% to its duration. Considering the strong link between secondary growth and fitness of forest trees, this result suggests that, whatever the life strategy, fitness relies mainly on one single crucial functional trait: the rate of cambial activity.

Moreover, this rate of cambial activity culminated at the same time for all the trees of the stand, whereas shoot elongation, for example, reached its maximal rate earlier in pines than in firs and spruces. These results suggest a strong functional convergence between co-existing conifer species concerning key traits that influence fitness. Furthermore, the synchronization of the rates of cambial activity indicates that all the trees express their maximal resource need at the same time, which must result in a hard head-on competition. The fact that early-successional species are not able to avoid this competition may be a clue to explain their elimination during conifer forest maturation.

Acknowledgments

We thank E. Cornu, E. Farré, C. Freyburger, P. Gelhaye and A. Mercanti for fieldwork and monitoring; M. Harroué for sample preparation in the laboratory; F. Bonne for the phenology pictures; T. Franceschini for his help on mixed models and P. Fonti for his comments on an early version of this manuscript; M. Dassot for his help in editing the pictures.

References

Ackerly DD. 2003. Community assembly, niche conservatism, and adaptive evolution in changing environments. *International Journal of Plant Sciences* **164**(3): 165-184.

Augspurger CK, Cheeseman JM, Salk CF. 2005. Light gains and physiological capacity of understorey woody plants during phenological avoidance of canopy shade. *Functional Ecology* **19**(4): 537-546.

Baraloto C, Goldberg DE, Bonal D. 2005. Performance trade-offs among tropical tree seedlings in contrasting microhabitats. *Ecology* **86**(9): 2461-2472.

Bates D, Maechler M, Bolker B 2011. lme4: Linear mixed-effects models using S4 classes. R package version 0.999375-39.

Becker M, Bert D, Landmann G, Lévy G, Rameau JC, Ulrich E 1995. Growth and decline symptoms of silver fir and Norway spruce in northeastern France: relation to climate, nutrition and silviculture. In: Landmann G, Bonneau M eds. *Forest decline and air pollution effects in the French mountains*. Berlin: Springer, 120-142.

Bouriaud O, Popa I. 2009. Comparative dendroclimatic study of Scots pine, Norway spruce, and silver fir in the Vrancea Range, Eastern Carpathian Mountains. *Trees-Structure and Function* **23**(1): 95-106.

Boyden SB, Reich PB, Puettmann KJ, Baker TR. 2009. Effects of density and ontogeny on size and growth ranks of three competing tree species. *Journal of Ecology* **97**(2): 277-288.

Cariboni J, Gatelli D, Liska R, Saltelli A. 2007. The role of sensitivity analysis in ecological modelling. *Ecological Modelling* **203**(1-2): 167-182.

Deslauriers A, Giovannelli A, Rossi S, Castro G, Fragnelli G, Traversi L. 2009. Intra-annual cambial activity and carbon availability in stem of poplar. *Tree Physiology* **29**(10): 1223-1235.

Deslauriers A, Morin H. 2005. Intra-annual tracheid production in balsam fir stems and the effect of meteorological variables. *Trees-Structure and Function* **19**(4): 402-408.

Deslauriers A, Morin H, Begin Y. 2003. Cellular phenology of annual ring formation of *Abies balsamea* in the Quebec boreal forest (Canada). *Canadian Journal of Forest Research - Revue Canadienne De Recherche Forestière* **33**(2): 190-200.

Deslauriers A, Rossi S, Anfodillo T, Saracino A. 2008. Cambial phenology, wood formation and temperature thresholds in two contrasting years at high altitude in southern Italy. *Tree Physiology* **28**(6): 863-871.

Gričar J. 2007. *Xylo- and phloemogenesis in silver fir (Abies alba Mill.) and Norway spruce (Picea abies (L.) Karst.).* University of Ljubljana Ljubljana.

Gričar J, Krze L, Čufar K. 2009. Number of cells in xylem, phloem and dormant cambium in silver fir (*Abies alba*), in trees of different vitality. *Iawa Journal* **30**(2): 121-133.

Grime JP. 1977. Evidence for the existence of three primary strategies in plants and its relevance to ecological and evolutionary theory. *The American naturalist* **111**(982): 1169-1194.

Grote R. 1998. Integrating dynamic morphological properties into forest growth modelling - II Allocation and mortality. *Forest Ecology and Management* **111**(2-3): 193-210.

Hanninen H. 1991. Does climatic warming increase the risk of frost damage in northern trees. *Plant Cell and Environment* **14**(5): 449-454.

Hansen J, Beck E. 1990. The fate and path of assimilation products in the stem of 8-year-old Scots pine (*Pinus sylvestris* L.) trees. *Trees-Structure and Function* **4**(1): 16-21.

Ishii H, Asano S. 2010. The role of crown architecture, leaf phenology and photosynthetic activity in promoting complementary use of light among coexisting species in temperate forests. *Ecological Research* **25**(4): 715-722.

Karkach AS. 2006. Trajectories and models of individual growth. *Demographic Research* **15**: 347-400.

Korner C 2006. Significance of temperature in plant life. In: Morison JIL, Morecroft MD eds. *Plant Growth and Climate Change*. Oxford: Blackwell Publishing Ltd, 48-69.

Korner C, Basler D. 2010. Phenology Under Global Warming. *Science* **327**(5972): 1461-1462.

Larson PR. 1994. *The vascular cambium: development and structure*. Berlin Heidelberg: Springer-Verlag.

Lebourgeois F, Pierrat J-C, Perez V, Piedallu C, Cecchini S, Ulrich E. 2010. Simulating phenological shifts in French temperate forests under two climatic change scenarios and four driving global circulation models. *International Journal of Biometeorology* **54**(5): 563-581.

Lebourgeois F, Rathgeber CBK, Ulrich E. 2010. Sensitivity of French temperate coniferous forests to climate variability and extreme events (*Abies alba*, *Picea abies* and *Pinus sylvestris*). *Journal of Vegetation Science* **21**(2): 364-376.

Lockhart JA. 1983. Optimum growth initiation time for shoot buds of deciduous plants in a temperate climate. *Oecologia* **60**(1): 34-37.

Lupi C, Morin H, Deslauriers A, Rossi S. 2010. Xylem phenology and wood production: resolving the chicken-or-egg dilemma. *Plant Cell and Environment* **33**(10): 1721-1730.

Lusk CH. 2004. Leaf area and growth of juvenile temperate evergreens in low light: species of contrasting shade tolerance change rank during ontogeny. *Functional Ecology* **18**(6): 820-828.

Martinez-Vilalta J, Mencuccini M, Vayreda J, Retana J. 2010. Interspecific variation in functional traits, not climatic differences among species ranges, determines demographic rates across 44 temperate and Mediterranean tree species. *Journal of Ecology* **98**: 1462-1475.

Mayer DG, Butler DG. 1993. Statistical validation. *Ecological Modelling* **68**(1-2): 21-32.

Niinemets U. 2006. The controversy over traits conferring shade-tolerance in trees: ontogenetic changes revisited. *Journal of Ecology* **94**(2): 464-470.

Oribe Y, Funada R, Kubo T. 2003. Relationships between cambial activity, cell differentiation and the localization of starch in storage tissues around the cambium in locally heated stems of *Abies sachalinensis* (Schmidt) Masters. *Trees-Structure and Function* **17**(3): 185-192.

Pinto PE, Gegout JC. 2005. Assessing the nutritional and climatic response of temperate tree species in the Vosges Mountains. *Annals of Forest Science* **62**(7): 761-770.

Poorter L, Wright SJ, Paz H, Ackerly DD, Condit R, Ibarra-Manriques G, Harms KE, Licona JC, Martinez-Ramos M, Mazer SJ, Muller-Landau HC, Pena-Claros M, Webb CO, Wright IJ. 2008. Are functional traits good predictors of demographic rates? Evidence from five Neotropical forests. *Ecology* **89**(7): 1908-1920.

R Core Team 2012. R: A language and environment for statistical computing. R Foundation for Statistical Computing, Vienna, Austria. ISBN 3-900051-07-0, URL http://www.R-project.org/.

Rathgeber CBK 2011. CAVIAR: cambial activity and wood formation—data manipulation, visualisation and analysis using R. R package version 1.0.

Rathgeber CBK, Longuetaud F, Mothe F, Cuny H, Le Moguedec G. 2011a. Phenology of wood formation: Data processing, analysis and visualisation using R (package CAVIAR). *Dendrochronologia* **29**(3): 139-149.

Rathgeber CBK, Rossi S, Bontemps J-D. 2011b. Cambial activity related to tree size in a mature silver-fir plantation. *Annals of Botany* **108**(3): 429-438.

Reich PB, Tjoelker MG, Walters MB, Vanderklein DW, Bushena C. 1998. Close association of RGR, leaf and root morphology, seed mass and shade tolerance in seedlings of nine boreal tree species grown in high and low light. *Functional Ecology* **12**(3): 327-338.

Richardson AD, O'Keefe JF 2009. Phenological differences between understory and overstory: A case study using the long-term Harvard Forest records. In: Noormets A ed. *Phenology of Ecosystem Processes*. New York: Springer, 87-117.

Riou-Khamlichi C, Menges M, Healy JMS, Murray JAH. 2000. Sugar control of the plant cell cycle: Differential regulation of Arabidopsis D-type cyclin gene expression. *Molecular and Cellular Biology* **20**(13): 4513-4521.

Rossi S, Anfodillo T, Menardi R. 2006a. Trephor: a new tool for sampling microcores from tree stems. *Iawa Journal* **27**(1): 89-97.

Rossi S, Deslauriers A, Anfodillo T. 2006b. Assessment of cambial activity and xylogenesis by microsampling tree species: An example at the alpine timberline. *Iawa Journal* **27**(4): 383-394.

Rossi S, Deslauriers A, Anfodillo T, Carraro V. 2007. Evidence of threshold temperatures for xylogenesis in conifers at high altitudes. *Oecologia* **152**(1): 1-12.

Rossi S, Deslauriers A, Anfodillo T, Carrer M. 2008a. Age-dependent xylogenesis in timberline conifers. *New Phytologist* **177**(1): 199-208.

Rossi S, Deslauriers A, Anfodillo T, Morin H, Saracino A, Motta R, Borghetti M. 2006c. Conifers in cold environments synchronize maximum growth rate of tree-ring formation with day length. *New Phytologist* **170**(2): 301-310.

Rossi S, Deslauriers A, Gričar J, Seo J-W, Rathgeber CBK, Anfodillo T, Morin H, Levanic T, Oven P, Jalkanen R. 2008b. Critical temperatures for xylogenesis in conifers of cold climates. *Global Ecology and Biogeography* **17**(6): 696-707.

Rossi S, Deslauriers A, Morin H. 2003. Application of the Gompertz equation for the study of xylem cell development. *Dendrochronologia* **21**(1): 33-39.

Rossi S, Morin H, Deslauriers A, Plourde P-Y. 2011. Predicting xylem phenology in black spruce under climate warming. *Global Change Biology* **17**(1): 614-625.

Rossi S, Rathgeber CBK, Deslauriers A. 2009. Comparing needle and shoot phenology with xylem development on three conifer species in Italy. *Annals of Forest Science* **66**(2).

Ulrich E, Cecchini S. 2009. *Manuel de référence n°12 pour les observations phénologiques - Placettes des niveaux A et B (Level II plots within the European Union) - Deuxième version*

Vaganov EA, Hughes MK, Shashkin AV. 2006. *Growth nynamics of conifer tree rings*. Heidelberg: Springer.

Vandermeer J. 1989. *The ecology of intercropping*. Cambridge: Cambridge University Press.

Wielgolaski FE. 1999. Starting dates and basic temperatures in phenological observations of plants. *International Journal of Biometeorology* **42**(3): 158-168.

Wodzicki TJ. 1971. Mechanism of xylem differentiation in *Pinus sylvestris* L. *Journal of Experimental Botany* **22**(72): 670-687.

Wodzicki TJ. 2001. Natural factors affecting wood structure. *Wood Science and Technology* **35**(1-2): 5-26.

Wodzicki TJ, Zajaczkowski S. 1970. Methodical problems in studies on seasonal production of cambial xylem derivatives. *Acta societatis botanicorum poloniae* **39**(3): 509-520.

Zuur AF, Ieno EN, Walker NJ, Saveliev AA, Smith GM. 2009. *Mixed effects models and extensions in ecology with R*. New York: Springer-Verlag.

Supplementary material

Table IV.S1: List of the variables.

Notation	Variable	Unit
DBH	Diameter at breast height	cm
H	Tree height	m
CA	Crown area	m²
TRW	Tree-ring width	mm
RCN	Number of cells in the tree-ring	number of cells
ICN	Number of cells in the cambium during the resting period before the beginning of cambial activity	number of cells
FCN	Number of cells in the cambium during the resting period after the end of cambial activity	number of cells
ACI	Annual circumferential increment	mm
FSL	Final length of new shoots	cm
n_C	Number of cells in the cambial zone	number of cells
n_E	Number of cells in the radial enlarging zone	number of cells
n_L	Number of cells in the wall thickening and lignification zone	number of cells
n_M	Number of cells in the mature zone	number of cells
$t_{i,S}$	Beginning of shoot elongation	day of year
$t_{f,S}$	End of shoot elongation	day of year
Δ_S	Duration of shoot elongation	days
$r_{m,S}$	Mean rate of shoot elongation	cm/day
$r_{x,S}$	Maximal rate of shoot elongation	cm/day
$t_{p,S}$	Occurrence of the maximal rate of shoot elongation	day of year
$t_{i,N}$	Beginning of needle unfolding	day of year
$t_{f,N}$	End of needle unfolding	day of year
Δ_N	Duration of needle unfolding	days
$t_{i,E}$	Beginning of the enlarging phase	day of year
$t_{f,E}$	End of the enlarging phase	day of year
Δ_E	Duration of the enlarging phase	days
$t_{i,L}$	Beginning of the thickening and lignification phase	day of year
$t_{f,L}$	End of the thickening and lignification phase	day of year
Δ_L	Duration of the thickening and lignification phase	days
$t_{i,M}$	Beginning of the mature phase	day of year
Δ_X	Duration of xylogenesis	days
$r_{m,T}$	Mean rate of tracheid production	cells/day
$r_{x,T}$	Maximal rate of tracheid production	cells/day
$t_{p,T}$	Occurrence of the maximal rate of tracheid production	day of year
CCL_m	Mean cell cycle length	days
CCL_n	Minimal cell cycle length	days

Table IV.S2: Parameters (A, tp, S, c) and goodness of fit (r2) of the logistic functions fitted to the length of new shoots for each studied tree in 2007, 2008 and 2009.

Year	Species	Tree	A	$t_{p,\,S}$	c	r^2
2007	Scots pine	1	10	134	4.6	1.00
		2	10	136	9.2	0.99
		3	10	133	7.6	1.00
		4	10	134	7.8	0.99
		5	10	139	10.3	0.99
	Silver fir	6	6	141	4.5	1.00
		7	8	141	4.0	1.00
		8	10	145	7.7	1.00
		9	10	142	7.6	0.99
		10	8	141	7.5	1.00
	Norway spruce	11	10	148	5.9	1.00
		12	10	152	7.7	1.00
		13	8	139	6.8	1.00
		14	8	141	6.1	0.99
		15	8	140	5.0	1.00
2008	Scots pine	1	10	147	6.4	0.99
		2	10	147	7.0	0.99
		3	10	147	7.0	0.99
		4	10	147	7.0	0.99
		5	10	151	5.8	1.00
	Silver fir	6	10	155	4.7	1.00
		7	8	155	5.4	1.00
		8	10	154	6.2	1.00
		9	10	152	6.7	1.00
		10	9	150	5.5	0.99
	Norway spruce	11	8	154	3.6	1.00
		12	9	155	4.2	1.00
		13	10	156	5.8	1.00
		14	9	152	4.2	1.00
		15	8	153	3.5	1.00
2009	Scots pine	1	12	138	5.8	1.00
		2	11	138	7.8	1.00
		3	11	138	7.8	1.00
		4	12	138	7.2	1.00
		5	8	136	7.9	0.99
	Silver fir	6	7	142	6.9	0.99
		7	8	143	6.6	0.99
		8	9	141	5.2	1.00
		9	7	142	6.9	0.99
		10	8	142	7.0	0.99
	Norway spruce	11	8	141	6.4	1.00
		12	9	147	6.6	1.00
		13	9	144	6.1	0.99
		14	8	138	7.0	0.99
		15	8	139	5.1	1.00

Table IV.S3: Parameters (A, β, κ) and goodness of fit (r^2) of the Gompertz functions fitted to the number of produced tracheids for each studied tree in 2007, 2008 and 2009.

Year	Species	Tree	A	β	$\kappa \times 10^2$	r^2
2007	Scots pine	1	16.3	5.63	3.89	0.82
		2	28.8	3.66	2.44	0.94
		3	43.3	3.75	2.15	0.81
		4	29.1	3.67	2.42	0.72
		5	30.6	4.14	2.69	0.93
	Silver fir	6	35.2	5.24	3.53	0.94
		7	65.6	3.82	2.70	0.97
		8	41.4	5.14	3.51	0.94
		9	56.1	4.48	3.06	0.94
		10	70.4	6.08	4.28	0.96
	Norway spruce	11	28.0	6.25	4.03	0.97
		12	37.5	4.84	3.31	0.94
		13	17.6	5.83	4.57	0.95
		14	31.7	6.08	3.96	0.96
		15	23.8	6.52	4.44	0.92
2008	Scots pine	1	42.6	5.58	3.26	0.87
		2	23.0	5.22	3.15	0.93
		3	21.7	4.22	2.71	0.95
		4	18.2	4.55	2.99	0.96
		5	52.7	4.03	2.44	0.98
	Silver fir	6	31.7	5.29	3.32	0.98
		7	107.1	4.70	2.83	0.98
		8	64.4	5.51	3.02	0.97
		9	99.6	4.75	2.81	0.93
		10	53.2	5.48	3.42	0.98
	Norway spruce	11	14.7	7.16	4.39	0.96
		12	76.9	4.86	2.66	0.97
		13	36.6	5.19	3.08	0.96
		14	45.8	5.40	3.15	0.97
		15	22.6	7.05	4.29	0.97
2009	Scots pine	1	11.3	4.73	3.40	0.85
		2	26.5	4.85	3.17	0.95
		3	30.8	4.53	3.15	0.93
		4	39.3	3.75	2.22	0.90
		5	29.4	3.54	2.14	0.96
	Silver fir	6	33.0	4.78	3.19	0.92
		7	131.0	5.94	3.69	0.99
		8	77.2	6.65	3.77	0.98
		9	71.1	4.70	3.01	0.96
		10	83.5	6.00	3.46	0.96
	Norway spruce	11	18.5	8.00	5.17	0.90
		12	60.7	4.98	2.87	0.99
		13	23.5	8.00	5.57	0.85
		14	49.2	4.27	2.55	0.93
		15	26.8	5.63	3.58	0.93

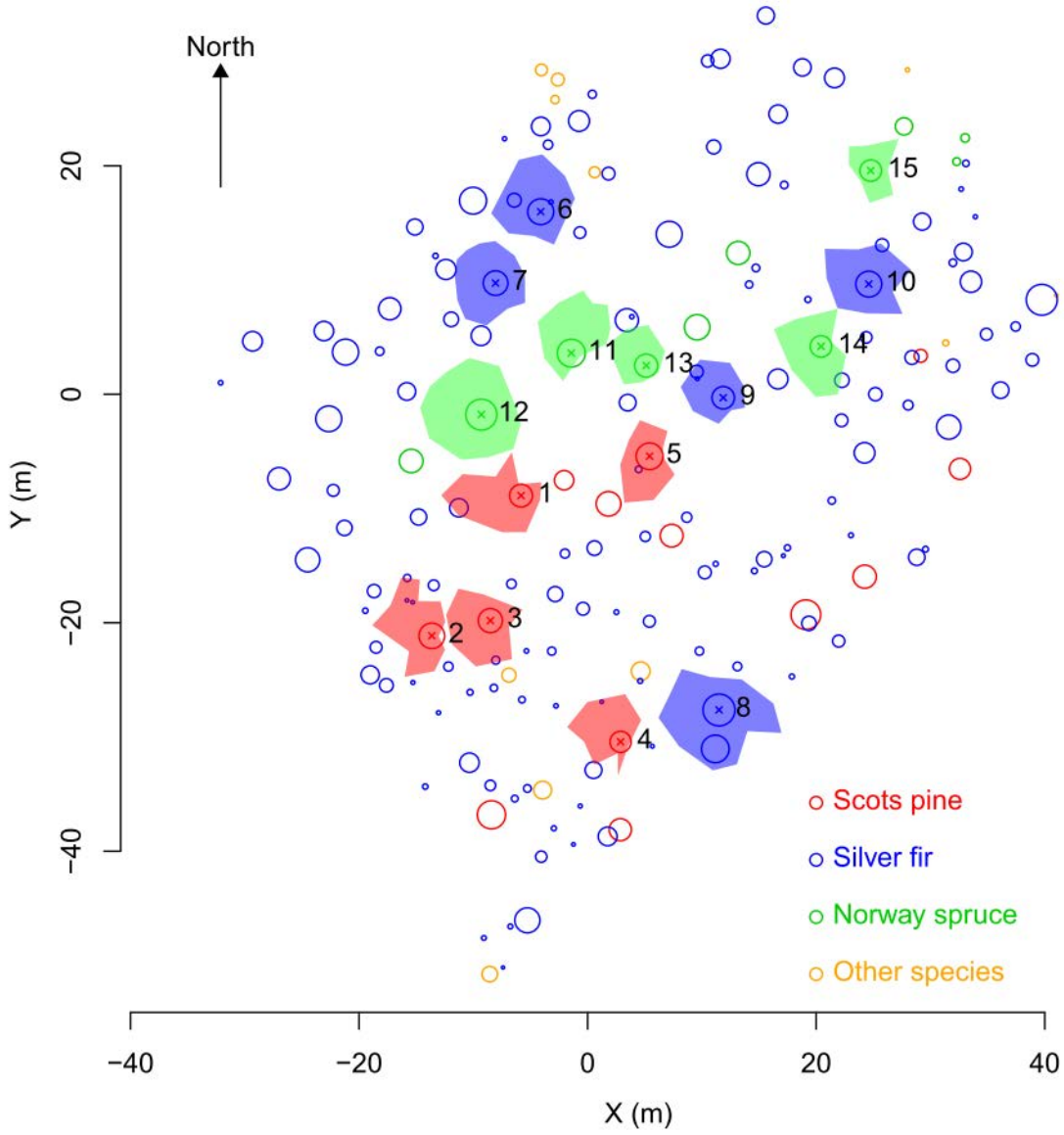

Figure IV.S1: Map of the studied stand. Circles represent the diameters at breast height (DBH; after multiplying the observed DBH by a factor of four) of all the stems in the studied stand. Polygons represent the projected crown area of the 15 monitored trees.

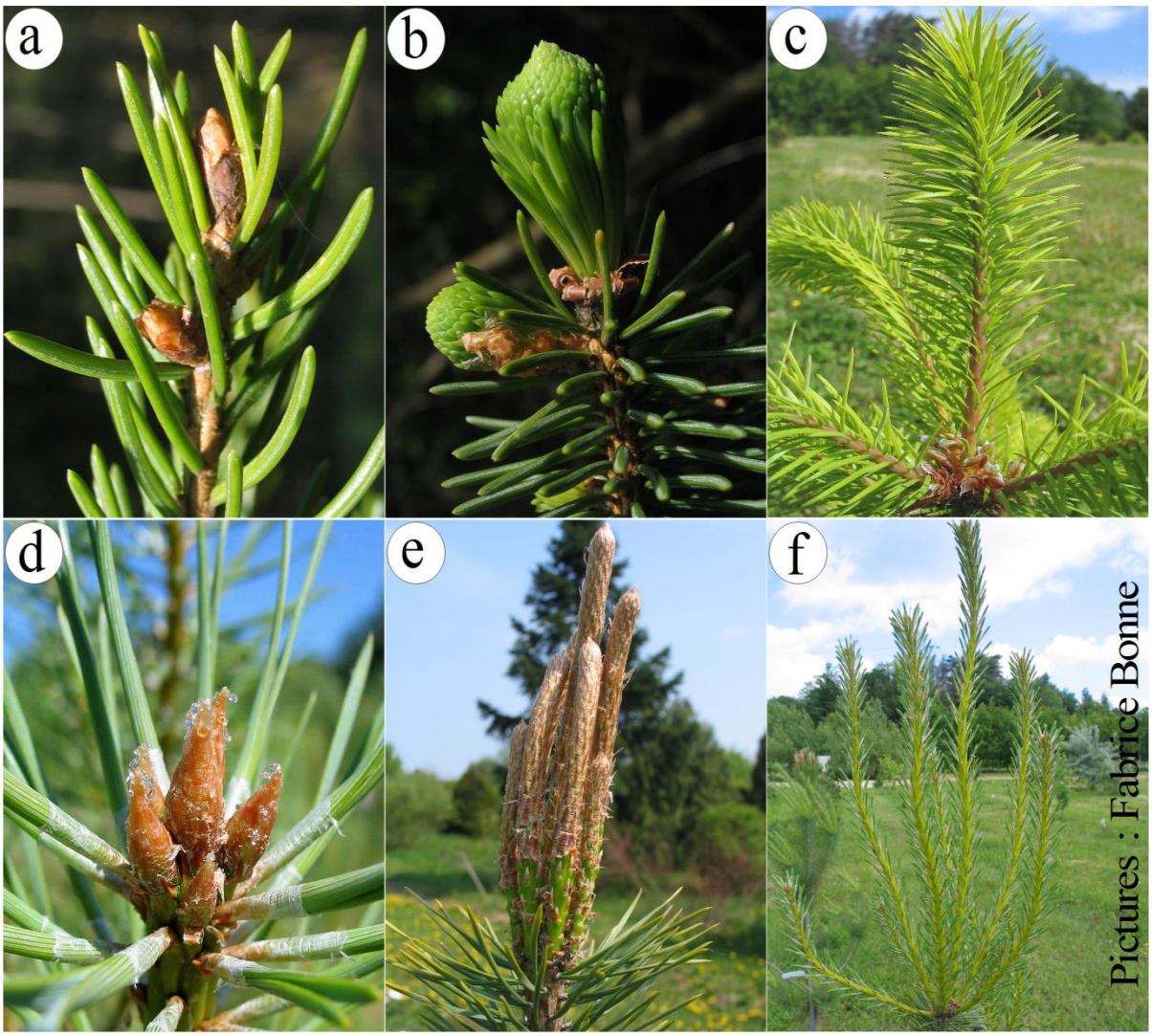

Figure IV.S2: Needle phenology observed in young Norway spruce and Scots pine trees in an open field close to the studied stand. Dormant winter-buds (a), spring broken-buds (b) and maturing needles (c) observed in Norway spruce. Dormant winter-buds (d), spring broken-buds (e) and maturing needles (f) observed in Scots pine.

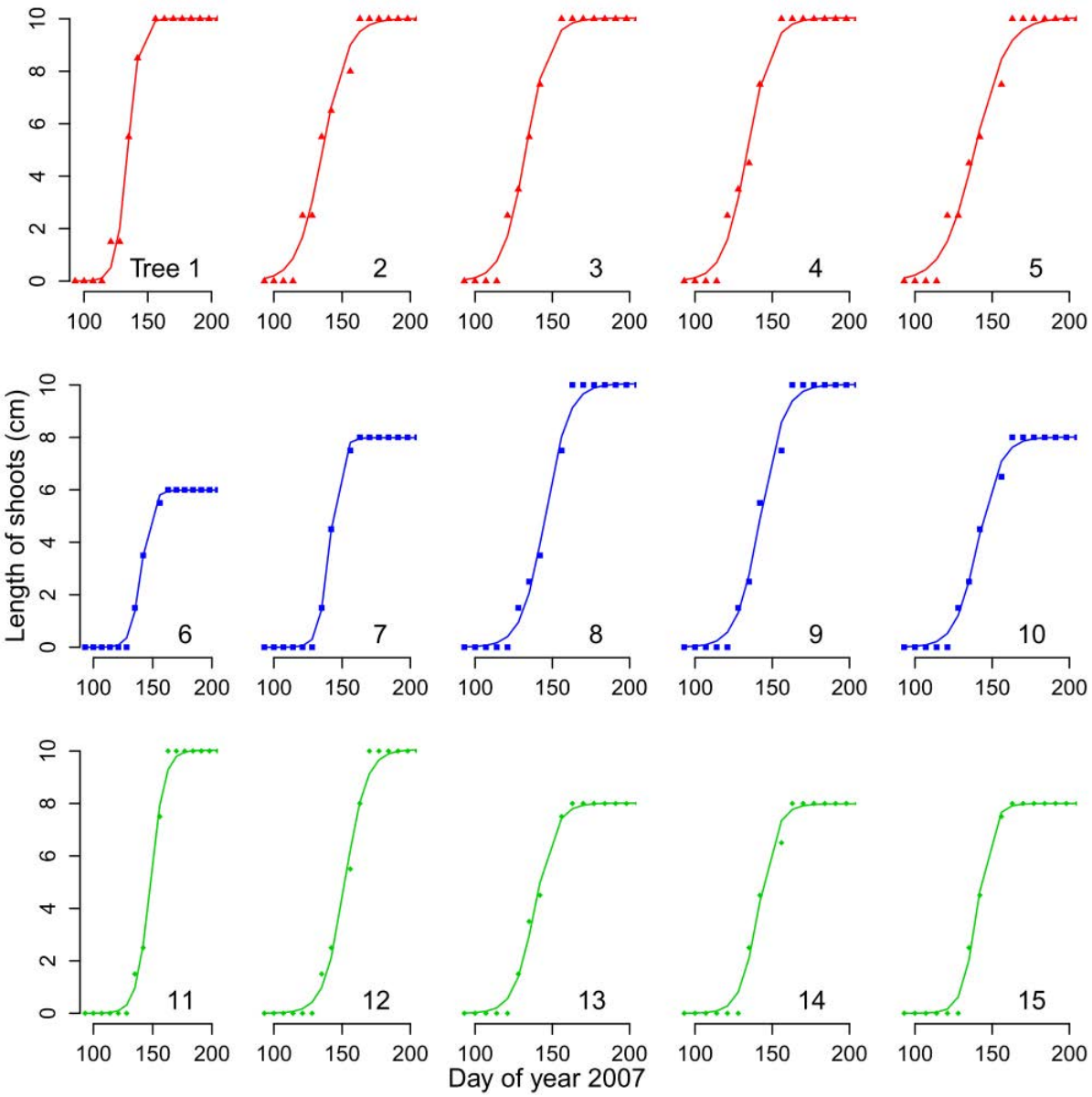

Figure IV.S3: Fittings of the logistic function to the length of shoots for the five Scots pines (tree 1 to 5), five silver firs (trees 6 to 10) and five Norway spruces (trees 11 to 15) in 2007.

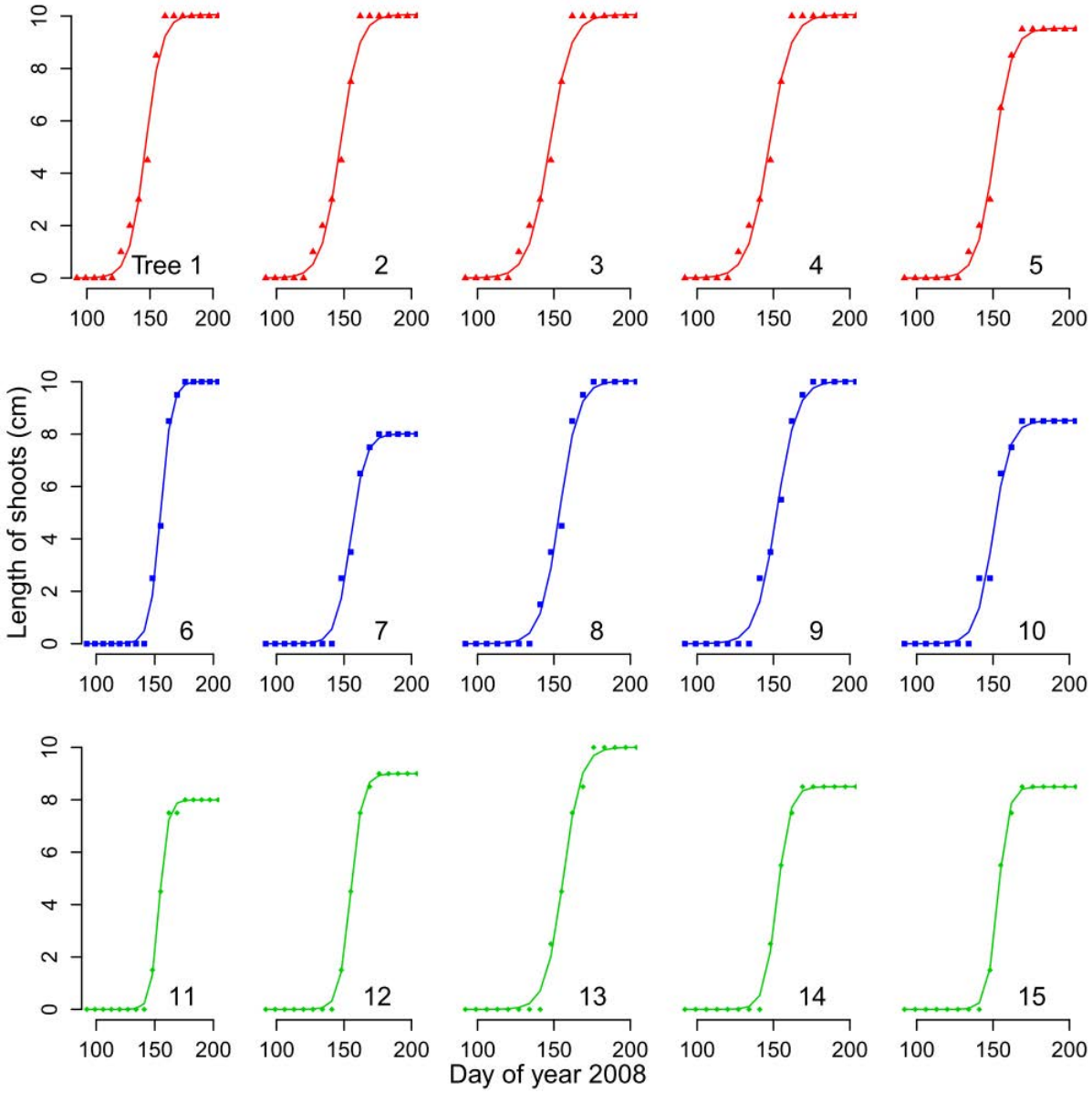

Figure IV.S4: Fittings of the logistic function to the length of the shoots for the five Scots pines (tree 1 to 5), five silver firs (trees 6 to 10) and five Norway spruces (trees 11 to 15) in 2008.

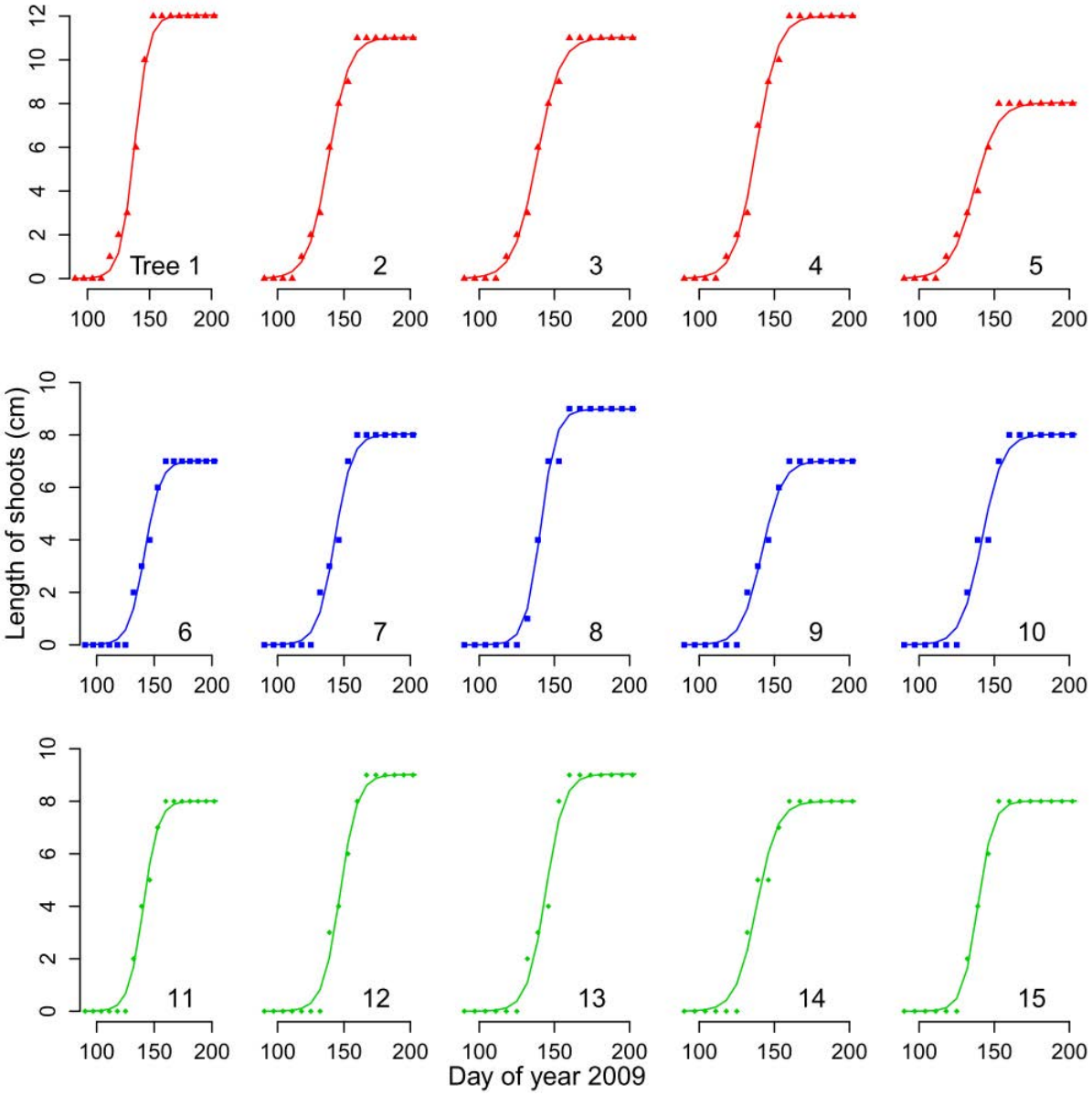

Figure IV.S5: Fittings of the logistic function to the length of the shoots for the five Scots pines (tree 1 to 5), five silver firs (trees 6 to 10) and five Norway spruces (trees 11 to 15) in 2009.

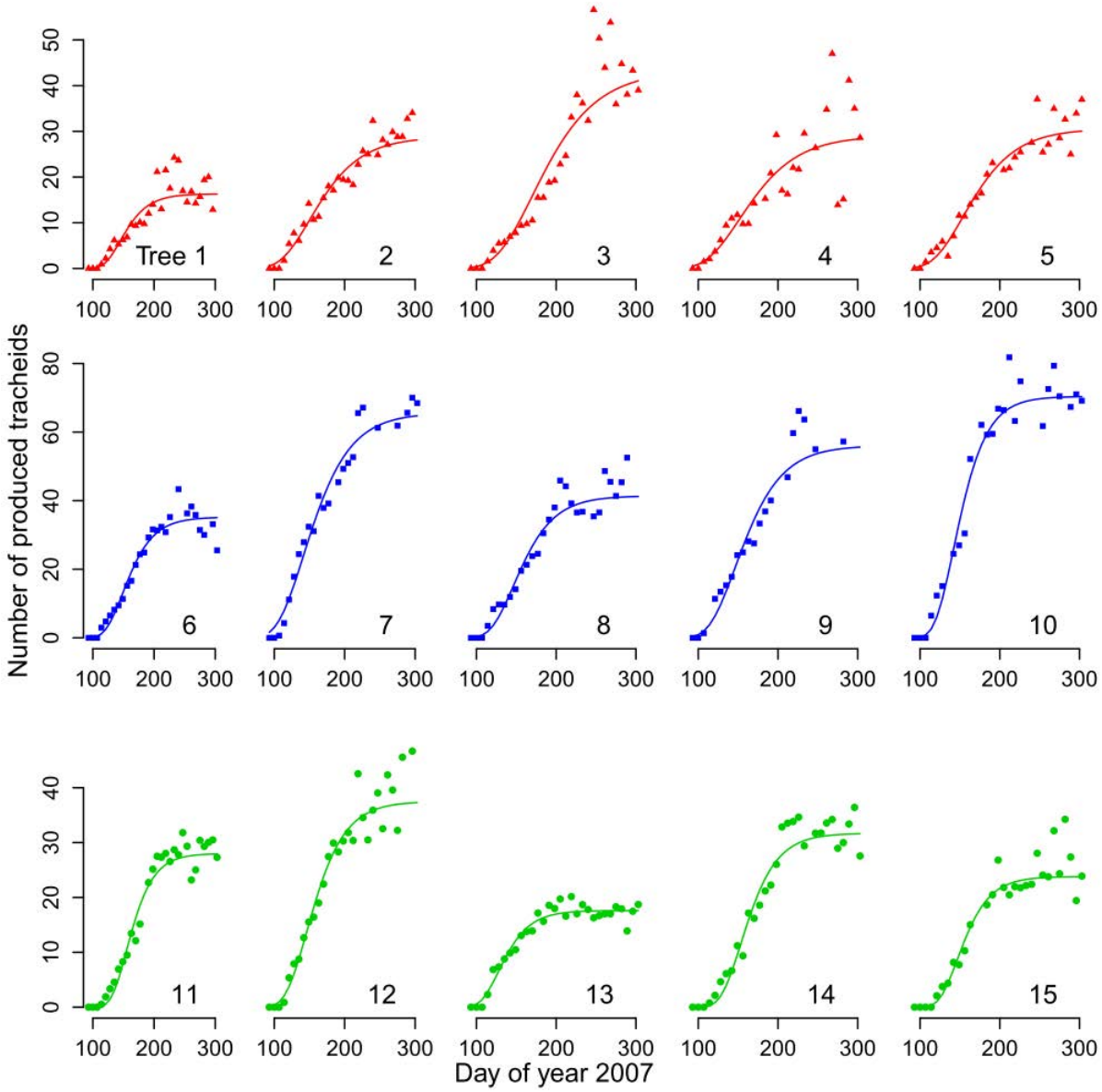

Figure IV.S6: Fittings of the Gompertz function to the number of produced tracheids for the five Scots pines (tree 1 to 5), five silver firs (trees 6 to 10) and five Norway spruces (trees 11 to 15) in 2007.

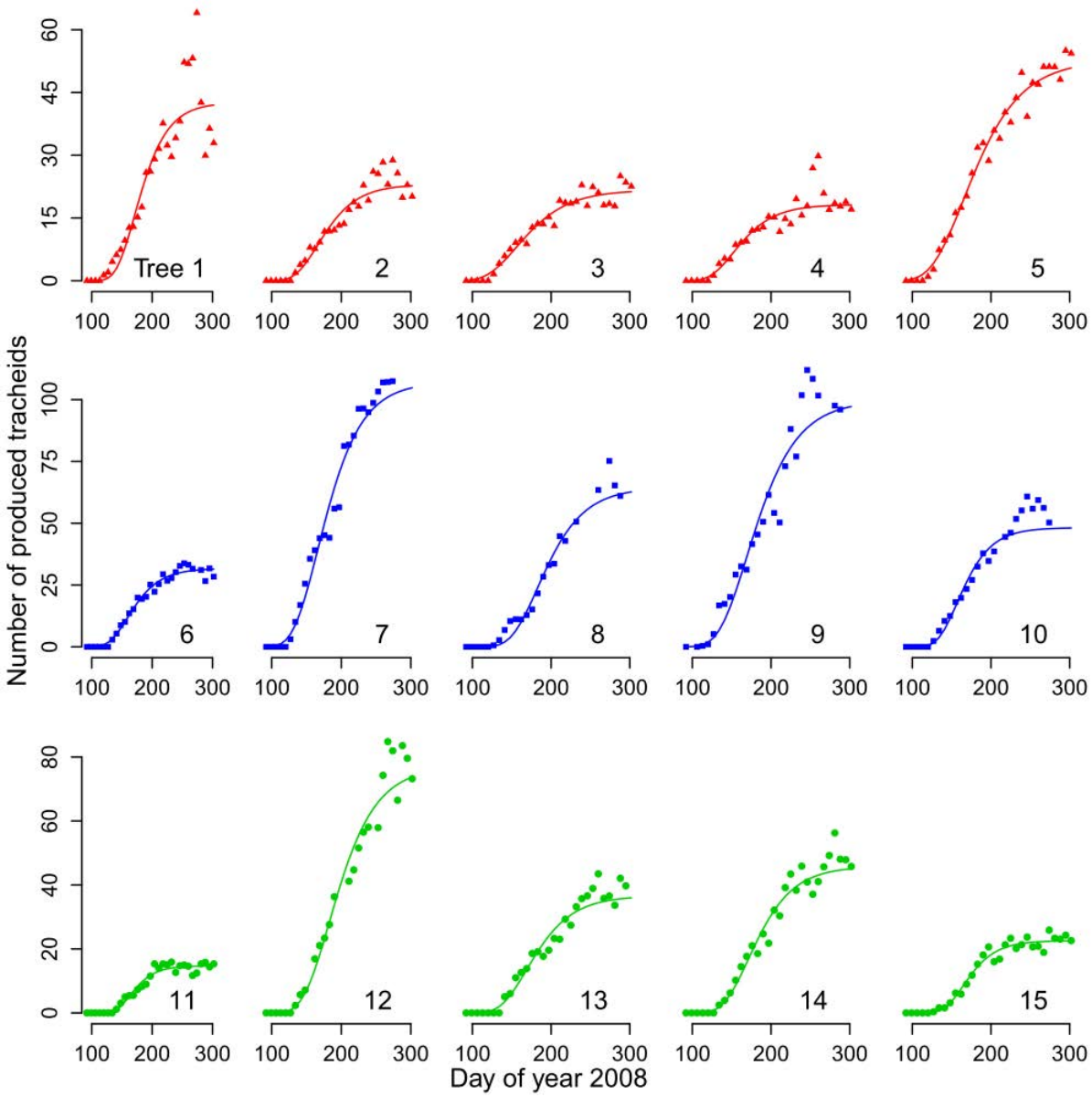

Figure IV.S7: Fittings of the Gompertz function to the number of produced tracheids for the five Scots pines (tree 1 to 5), five silver firs (trees 6 to 10) and five Norway spruces (trees 11 to 15) in 2008.

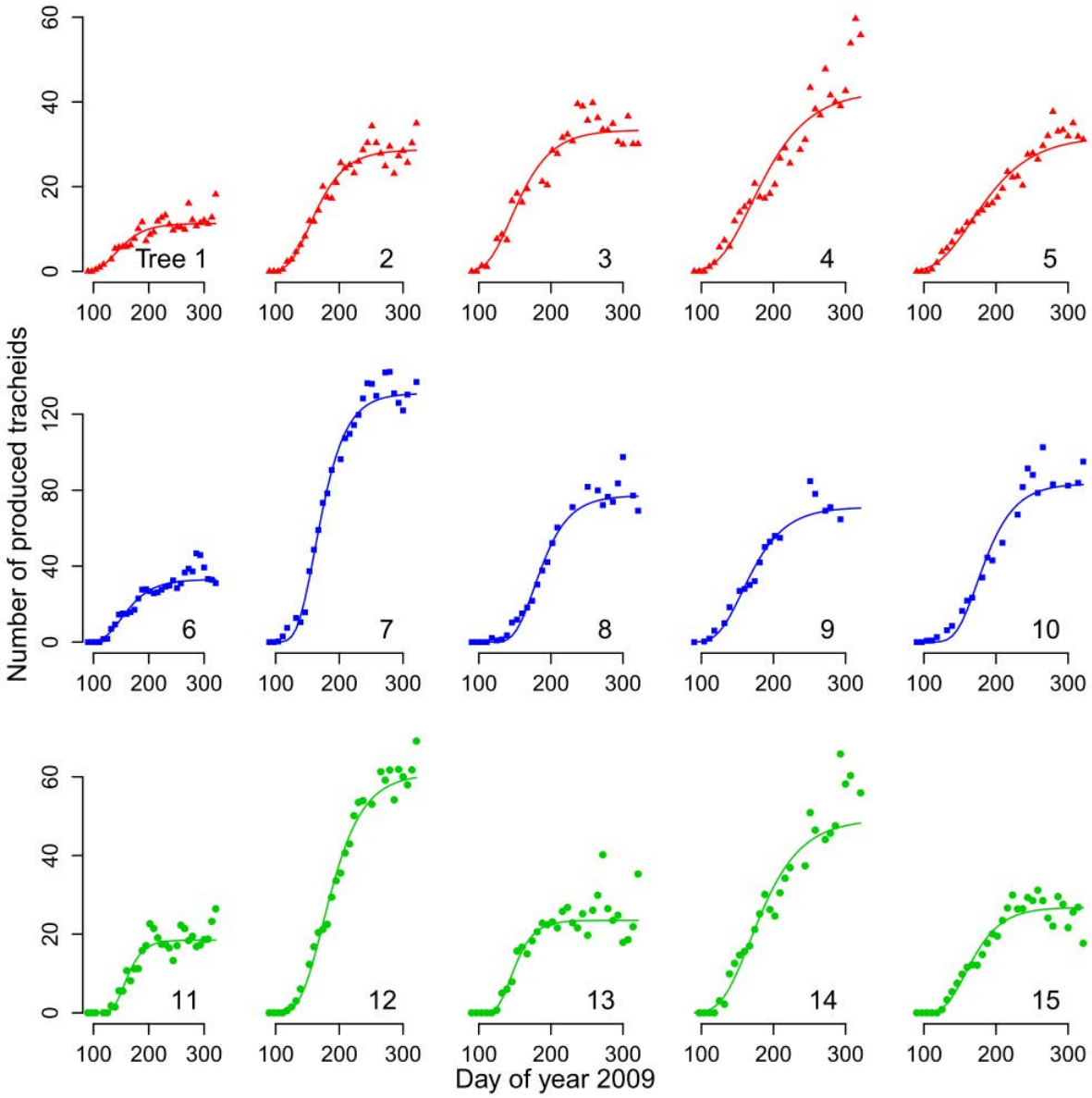

Figure IV.S8: Fittings of the Gompertz function to the number of produced tracheids for the five Scots pines (tree 1 to 5), five silver firs (trees 6 to 10) and five Norway spruces (trees 11 to 15) in 2009.

V COMPLEXITÉ INTRINSÈQUE DE LA DYNAMIQUE INTRA-ANNUELLE DE LA FORMATION DU BOIS

Alors que les patrons saisonniers généraux de la xylogénèse (« niveau arbre ») ont été décrits dans la partie précédente, cette partie propose maintenant de continuer à explorer la dynamique intra-annuelle de la formation du bois mais au niveau de la cellule. Pour cela, une méthode innovante, basée sur les modèles additifs généralisés, est développée afin de calculer quand, combien de temps et à quelle vitesse chaque cellule le long du cerne s'est élargie et a formé sa paroi secondaire durant la saison. En outre, nous regardons comment cette cinétique du développement cellulaire forme les patrons saisonniers de l'évolution du nombre de cellules dans les différentes zones de différenciation le long du cerne, ainsi que le flux de cellules entre ces zones. Comme pour la partie précédente, les données utilisées ne concernent que le site haut du gradient, c'est-à-dire le site de Grandfontaine, avec les 15 arbres des 3 espèces et les 3 années (2007 – 2009) de suivi. Cette partie est constituée d'un article scientifique (article 2) publié dans la revue Journal of Experimental Botany.

Generalized additive models reveal the intrinsic complexity of wood formation dynamics

Henri E. Cuny[1*], Cyrille B.K. Rathgeber[1], Tristan Senga Kiessé[1], Felix P. Hartmann[1], Ignacio Barbeito[1], Meriem Fournier[2]

Journal of Experimental Botany (2013)

[1] INRA, UMR1092, Laboratoire d Etude des Ressources Foret Bois (LERFoB), Centre INRA de Nancy, F-54280 Champenoux, France

[2] AgroParisTech, UMR1092, Laboratoire d Etude des Ressources Foret Bois (LERFoB), ENGREF, 14 rue Girardet, F-54000 Nancy, France

Summary

The intra-annual dynamics of wood formation, which involves the passage of newly produced cells through three successive differentiation phases (division, enlargement, and wall thickening) to reach the final functional mature state, has traditionally been described in conifers as three delayed bell-shaped curves followed by an S-shaped curve. We challenged the classical view represented by the 'Gompertz function approach' (GFs) using two novel approaches based on parametric generalised linear models (GLMs) and 'data driven' generalised additive models (GAMs). These three approaches (GFs, GLMs, and GAMs) were used to describe seasonal changes in cell numbers in each of the xylem differentiation phases and to calculate the timing of cell development in three conifer species [Picea abies (L.), Pinus sylvestris L., and Abies alba Mill.]. GAMs outperformed GFs and GLMs in describing intra-annual wood formation dynamics, showing two left-skewed bell-shaped curves for division and enlargement, and a right-skewed bimodal curve for thickening. Cell residence times progressively decreased through the season for enlargement, whilst increasing late but rapidly for thickening. These patterns match changes in cell anatomical features within a tree ring, which allows the separation of earlywood and latewood into two distinct cell populations. This paper presents a novel statistical approach and renews our understanding of xylogenesis, a dynamic biological process in which the rate of cell production interplays with cell residence times in each developmental phase to create complex seasonal patterns.

Keywords: cambial activity, conifers, generalised linear and additive models (GLMs and GAMs), Gompertz functions (GFs), timing of cell development, tree ring, xylogenesis, wood formation.

Introduction

Despite the key role of wood in terrestrial biosphere and human societies, our understanding of the complex biological processes involved in its formation remains fragmentary (Plomion *et al.*, 2001; Chaffey, 2002). In particular, the dynamics (timing, duration, and rate) of the wood formation phases (cambial division, cell enlargement, and secondary cell-wall formation) remains poorly explored, despite this being of fundamental importance in determining the quantity (number of cells produced) and quality (cell anatomical characteristics) of the wood formed (Vaganov *et al.*, 2011).

In recent years, a growing number of studies have been devoted to wood formation monitoring, and these have provided excellent datasets (see, for example, Rossi *et al.*, 2006b; Rossi *et al.*, 2008). However, most of these studies have only focused on key aspects of the process, such as the onset and cessation of xylem formation (Rossi *et al.*, 2011), the maximal rate of cell production (Rossi *et al.*, 2006b), or more general intra-annual growth patterns (Camarero *et al.*, 2010; Rathgeber *et al.*, 2011; Cuny *et al.*, 2012). Thus, a complete description of wood formation dynamics can only be found in isolated studies (Wodzicki, 1971; Horacek *et al.*, 1999).

During wood formation, cells successively pass through three phases to reach a permanently mature state: (1) division, (2) enlargement, and (3) wall thickening (Wilson *et al.*, 1966). The temporal succession of the differentiation phases undergone by the cells forms a spatial succession of developmental zones along the tree ring. Drawing inspiration from hydrological system modelling, the three developmental zones and the mature zone can be viewed as four interconnected reservoirs, with cells 'flowing' from one reservoir to the next as they differentiate (see Figure V.S1A available as Supplementary material). In conifers, the seasonal dynamics of the number of cells passing through the successive developmental zones has traditionally been described as three delayed bell-shaped curves followed by an S-shaped curve (Figure V.S1B) (Rossi *et al.*, 2006a; Lupi *et al.*, 2010; Cuny *et al.*, 2012). This classical view is based on the assumption that the flow of the source (i.e. the rate of cell production) follows a bell-shaped curve through the season (Larson, 1994) and drives the dynamics of the subsequent reservoirs.

Through the growing season, cells accumulate asymmetrically, with an initial positive exponential phase followed by gradual slowing. Consequently, the Gompertz function (GF) – an asymmetric sigmoid growth function, where the rate is maximal at 1/3 of the asymptote before to slow down progressively – has been used to fit the data and calculate the timing of cell development (Figure V.S1C) (Camarero *et al.*, 1998; Rossi *et al.*, 2003). This method allows variations in cell residence times in the different zones of xylogenesis to be calculated through the season, but only where these are close to linear (Deslauriers *et al.*, 2003; Rossi *et al.*, 2006a).

Some pioneer studies have found that developing tracheids spend less time in enlargement and more time in thickening as the growing season proceeds (Whitmore & Zahner, 1966; Skene, 1969; Wodzicki, 1971; Skene, 1972; Kutscha *et al.*, 1975). Such findings argue against the idea of repeated bell-shaped curves, which implies that cell residence times change in parallel between the successive reservoirs through the season. Instead, they suggest that developing tracheids accumulate in the enlargement reservoir at the beginning of the season, when the increase in cell diameter is greatest, and then accumulate in the thickening reservoir at the end of the season, when the main focus is on building and lignifying their thick cell walls.

This lead us to propose the following hypothesis: the rate of cell transition from one development zone to the next and the cell residence times in these zones are not monotonous through a growing season, so that the resulting changes in the number of cells in the successive zones should be intrinsically more complex than the classical view; additionally, it should be possible to see the footprint of cell anatomical features in the intra-annual dynamics of the process that produced them, so that we can distinguish the transition between earlywood (large, thin-walled cells) and latewood (small, thick-walled cells) in the intra-annual pattern of enlarging and thickening cell numbers.

To test this hypothesis, we applied three statistical modelling approaches to three conifer species (to ensure robustness) over 3 years of monitoring (to ensure generality): (1)

the traditionally used parametric Gompertz function (GF), which fits bell- and S-shaped distributions and represents the classical view; (2) another parametric approach using generalised linear models (GLMs); and (3) a semi-parametric approach using generalised additive models (GAMs), which are more flexible and are thus able to highlight structures in the data distribution that differ from bell- or S-shaped curves, thereby allowing us to challenge the classical view of wood formation dynamics.

Materials and methods

Study site, xylem sampling, and sample preparation

Dominant and healthy Scots pines [Pinus sylvestris L.], silver firs [Abies alba Mill.], and Norway spruces [Picea abies (L.) Karst.] (n = 5 per species) were selected in a mixed stand located in the Vosges Mountains (48° 29′ N, 7° 09′ E, and 643 m ASL), in northeast France (Table V.S1 of Supplementary material). Microcores were collected weekly from the tree stems from April to November 2007–2009 and prepared in the laboratory to obtain transverse sections (5–10 µm thick), which were stained with cresyl violet acetate and permanently mounted on glass slides. For detailed information about the study site, tree characteristics, sampling strategy, and sample preparation, see Cuny *et al.* (2012).

Microscopic observations of xylem cell differentiation

Overall, 1450 anatomical sections were observed using an optical microscope (AxioImager.M2; Carl Zeiss SAS, France) under visible and polarized light at ×100–400 magnification to distinguish the cells in the different developmental zones. Cambial cells had a rectangular shape, were surrounded by a thin primary wall and had small radial diameters, whereas cells in the enlargement zone still had thin primary walls but had larger radial diameters. In contrast to cells in the cambial and enlargement zones, cells in the thickening zone developed a secondary wall that appeared bright under polarized light because of its particular arrangement of cellulose microfibrils (Abe *et al.*, 1997). Cresyl violet acetate staining, whereby cellulose stains purple and lignin stains blue (Kutscha *et al.*, 1975), was used to follow the advancement of lignification, with cells in the thickening phase exhibiting purple and blue walls, indicating that lignification was in progress, whereas mature cells had entirely lignified and thus completely blue walls.

Gompertz function, and generalised linear and additive models

For each sample, the radial number of cells in the cambial (n_C, see Table V.S2 for the list of variables used along with their notations and units), enlargement (n_E), thickening (n_T) and mature (n_M) zones was counted along three radial cell files (see Table V.S3 for a description of the number of cells in each zone and their variation). The number of cells from the previous year was also counted on three radial files per sample and used to standardise the number of cells of the current year to reduce within-tree growth variability (Rossi *et al.*, 2003). A dedicated function of the package CAVIAR (Rathgeber, 2012) was used to apply this standardisation using R statistical software (R Development Core Team, 2011).

Following Rossi *et al.* (2003), Gompertz functions (GFs) were fitted to the standardised number of mature cells, which is cumulative.

Thus, the GF is defined as:

$$N(t) = \mathrm{A}.\,\mathrm{e}^{-\mathrm{e}^{\beta-\kappa.\mathrm{t}}} \quad (1)$$

where N(t) is the number of mature cells at time t; A is the upper asymptote parameter representing the final number of cells; β is the *x*-axis placement parameter that reflects the location of the origin; and κ is the growth rate parameter that determines the spread of the curve along the time axis.

However, contrary to previous studies (Rossi *et al.*, 2003), we considered it a better practice to fit the first derivative of the Gompertz function (GF') directly to the standardised number of cells in the division, enlargement, and thickening zones. Thus, GF' is expressed as:

$$\mathrm{N(t)} = \mathrm{A}.\,\kappa.\,\mathrm{e}^{-\mathrm{e}^{\beta-\kappa.\mathrm{t}}}.\,\mathrm{e}^{\beta-\kappa.\mathrm{t}} \quad (2)$$

GF and GF' parameters were estimated using the nls function in R, which determines the non-linear (weighted) least-squares estimates of the parameters of a nonlinear model (Bates & Chambers, 1992).

Additionally, we used two new approaches to model intra-annual wood formation dynamics based on generalised linear and additive models (GLMs and GAMs, respectively). The advance in regression analysis provided by GLMs and GAMs has been an important statistical development over the last 30 years. GAMs are semi-parametric extensions of GLMs, which are themselves mathematical extensions of classical linear models (Wood, 2006).

The advantages of GLMs are that they define (1) a link function between a non-linear response variable and explanatory variables, and (2) a probability distribution for non-normal errors (McCullagh & Nelder, 1983). This makes them particularly appropriate for modelling count data (in our case cell number variations) by using a log as a link function, and a Poisson distribution for errors.

GAMs are GLMs in which the linear predictor depends, in part, on a sum of smooth functions of the predictors. GAMs are referred to as being data driven rather than model driven, because the data determine the nature of the relationship between the response variable and the set of explanatory variables rather than assuming a certain type of parametric relationship (Hastie & Tibshirani, 1986). The strength of GAMs lies in their ability to deal with highly nonlinear and non-monotonic relationships between the response and the set of explanatory variables, which helps develop ecological models that better represent the underlying data, thereby increasing our understanding of biological systems (Guisan *et al.*, 2002).

In this study, the weekly count of cells in each zone of wood formation was expressed as a function of the day of the year:

$$\log(\mathrm{n}) = \alpha + \mathrm{s(d)} + \varepsilon, \quad (3)$$

where n is the vector of the weekly count of cells in the considered zone, d is the vector of the corresponding day of the year, s is an unspecified smooth function, α is the intercept, and ε is the error term. GAMs were fitted in R using the mgcv package (Wood, 2006).

Gompertz functions (GFs & GFs'), GLMs, and GAMs were fitted for every year on each individual tree. The values of the fitted models were then averaged over the three studied years in order to calculate means representing the general wood formation dynamics of a species.

Goodness-of-fit measurement

We assessed the goodness-of-fit of the GFs, GLMs, and GAMs by computing the mean absolute error (MAE), as this is the most natural and most easily interpretable measure of model accuracy (Willmott & Matsuura, 2005). The MAE gives the mean absolute difference between the model predicted values and the observations in the units of the response:

$$\mathrm{MAE} = \frac{\sum_{i=1}^{n} |y_i - \hat{y}_i|}{n}, \quad (4)$$

where y_i is the i^{th} observed value, and $\hat{y}_i$ is the corresponding model-fitted value.

One problem with the MAE is that it depends on the scale of the response, meaning that it cannot be compared across series. Therefore, to compare the fittings between the different zones, in which the cell numbers differed, the mean absolute percentage error (MAPE) was also computed (Armstrong & Collopy, 1992):

$$\mathrm{MAPE} = \sum_{i=1}^{n} \frac{\left|\frac{y_i - \hat{y}_i}{\bar{y}}\right|}{n} \quad (5)$$

where y_i is the i^{th} observed value, $\hat{y}_i$ is the corresponding fitted value, and $\bar{y}$ is the mean of the n observed values.

In addition, we calculated the modelling efficiency (EF), a relative measure of the goodness-of-fit that gives the proportion of variation in the response captured by the model (Mayer & Butler, 1993).This statistic is similar to the coefficient of determination (r^2), but can be used for nonlinear models:

$$EF = 1 - \frac{\sum_{i=1}^{n} (y_i - \hat{y}_i)^2}{\sum_{i=1}^{n} (y_i - \bar{y})^2} \quad (6)$$

EF is close to 1 when there is a good fit, and is ≤ 0 when the model has equal or lower predictive power than the mean of the observations.

We also calculated the Akaike information criterion (AIC), which penalised the goodness-of-fit of the model by the number of parameters (Akaike, 1973):

$$AIC = -2.\log(L) + 2.k, \quad (7)$$

where L refers to the maximised value of the likelihood function for the fitted model and k is the number of parameters. AIC is a relative measure: it tells nothing about how well a model fits the data in an absolute sense, but is used to compare models. In a set of models, the model that has the lowest AIC is selected because it provides the best compromise between the goodness-of-fit and the number of parameters.

Residence duration

Four numerical functions (S) were defined to represent the cumulative number of cells:

$$S_{CETM}(t) = N_C(t) + N_E(t) + N_T(t) + N_M(t) \quad (8)$$

$$S_{ETM}(t) = N_E(t) + N_T(t) + N_M(t) \quad (9)$$

$$S_{TM}(t) = N_T(t) + N_M(t) \quad (10)$$

$$S_M(t) = N_M(t), \quad (11)$$

where N represents functions (GFs, GLMs, or GAMs) that predict the number of cells in the cambial (N_C), enlargement (N_E), thickening (N_T), and mature (N_M) zones at date t. Because these numerical functions are strictly increasing, their inverse function (S^{-1}) can be used to compute cell timings. For a cell i, the dates of entrance into the enlargement ($t_{E,i}$), thickening ($t_{T,i}$), and mature ($t_{M,i}$) zones were computed as:

$$t_{E,i} = S_{ETM}^{-1}(i) \quad (12)$$

$$t_{T,i} = S_{TM}^{-1}(i) \quad (13)$$

$$t_{M,i} = S_M^{-1}(i) \quad (14)$$

Transition rate

For each approach, the rate of cell production by the cambial zone ($r_{C,t}$) and the entry rate of cells into the enlargement ($e_{E,t}$), thickening ($e_{T,t}$), and mature ($e_{M,t}$) zones at day t were computed as:

$$r_{C,t} = S_{CETM}(t) - S_{CETM}(t-1) \quad (18)$$

$$e_{E,t} = S_{ETM}(t) - S_{ETM}(t-1) \quad (19)$$

$$e_{T,t} = S_{TM}(t) - S_{TM}(t-1) \quad (20)$$

$$e_{M,t} = S_M(t) - S_M(t-1) \quad (21)$$

Results

Comparative performance of models

Generalised additive models (GAMs) gave the best fits to the changes in cell numbers in the different zones of xylogenesis, with errors (MAE and MAPE) being, on average, twice as low as those computed for GLM and GF fittings (Table V.1). Model efficiencies were also, on average, 30% higher for GAMs than for GLMs and GFs, showing that GAMs explained cell number variations better than the other models. Finally, AIC computed from GAMs were 30% lower than those computed from GF and GLM, indicating that GAMs offer the best trade-off between goodness-of-fit and parsimony.

Changes in cell numbers in the zones of xylogenesis

The number of cambial cells increased rapidly and culminated early, at the beginning of June, for all three species (Figure V.1A, B, C). This remarkable pattern was well reproduced by the GAMs, which showed bell-shaped curves skewed to the left (Figure V.2 A, B, C). In contrast, GLMs and GFs were not able to preserve this pattern, delaying the occurrence of maximal cell numbers until later in the season and underestimating them (Table V.2). Later in the season, the number of cambial cells gradually decreased and finally returned to approximately its initial value. Once again, GAMs reproduced this progressive decrease better

than GFs and GLMs.

In the enlargement zone, the number of cells also increased rapidly at the beginning of the growing season, in April. The number culminated at the very beginning of June, before decreasing progressively back to zero in September–October, indicating the end of tree growth (Figure V.1D, E, F). All three approaches were able to capture this pattern, showing bell-shaped curves skewed to the left (Figure V.2D, E, F), with curves obtained using GFs being close to those obtained using GAMs. GLMs, however, were unable to follow the rapid early increase in enlarging cells, again resulting in a shift of the maximum to later in the season (Table V.2).

Table V.1: Mean absolute error (MAE), mean absolute percentage error (MAPE), model efficiency (EF), and Akaike information criterion (AIC) computed from the fittings of the Gompertz functions (GFs), and generalised linear and additive models (GLMs and GAMs) on the number of cells in the cambial (CZ), diameter enlargement (EZ), wall thickening (TZ), and mature (MZ) zones for Scots pine, Norway spruce, and silver fir (n = 5 per species) during 2007, 2008, and 2009 (means).

Zone	Sp	MAE (cell)			MAPE (%)			EF (%)			AIC		
		GF	GLM	GAM	GF	GLM	GAM	GF	GLM	GAM	GF	GLM	GAM
CZ	Pine	0.75	0.74	0.39	11	11	6	43	45	83	246	248	227
	Fir	0.83	0.82	0.55	9	10	7	29	30	61	247	249	232
	Spruce	0.73	0.71	0.39	11	11	6	50	52	82	245	245	228
EZ	Pine	0.61	0.68	0.28	32	35	14	81	73	94	226	256	160
	Fir	0.81	0.88	0.31	44	46	17	68	59	93	254	333	164
	Spruce	0.41	0.46	0.17	35	38	15	83	75	95	227	198	135
TZ	Pine	1.72	1.73	0.71	34	34	14	67	67	92	300	519	236
	Fir	3.02	3.08	1.06	30	30	11	74	74	96	338	805	292
	Spruce	1.48	1.4	0.45	36	33	10	78	78	97	293	456	198
MZ	Pine	1.64	1.25	1.01	14	11	9	94	95	97	302	320	238
	Fir	2.85	2.24	1.44	11	9	5	97	97	99	330	442	271
	Spruce	1.47	1.39	0.84	12	11	7	96	96	98	295	312	217

In the thickening zone, the number of cells rapidly increased and reached an initial peak in the first half of June (Figure V.1G, H, I). The number then plateaued or slightly declined over 2–3 weeks, and then increased again to reach a second peak later in the season, which was greater than the first and thus corresponded to the maximum number of cells observed in this zone. In spruce, this maximum occurred at the beginning of August, which was 2 weeks earlier than in fir (mid-August) and 1 month earlier than in pine (beginning of September). The difference in magnitude between the two peaks differed between species, with the second late peak being 30% greater than the first peak in fir and spruce, but 100% greater in pine. Following this late maximum, the number of cells rapidly decreased until November, when no more cells remained in the thickening zone, indicating the end of biomass allocation to the stem. Only GAMs were able to capture the complex pattern of cell number changes in the thickening zone, clearly showing a bimodal curve skewed to the right (Figure V.2G, H, I). In contrast, the less flexible GFs and GLMs presented bell-shaped curves that exhibited their

unique maximum at the place of the local minimum between the early and late peaks indicated by the raw data and GAMs (Figures V.1G, H, I and V.2G, H, I).

From the beginning of June to November, there was a steady accumulation of cells in the mature zone (Figure V.1J, K, L). Only GAMs were able to detect two periods of faster accumulation separated by a period of slower increase (Figure V.2J, K, L).

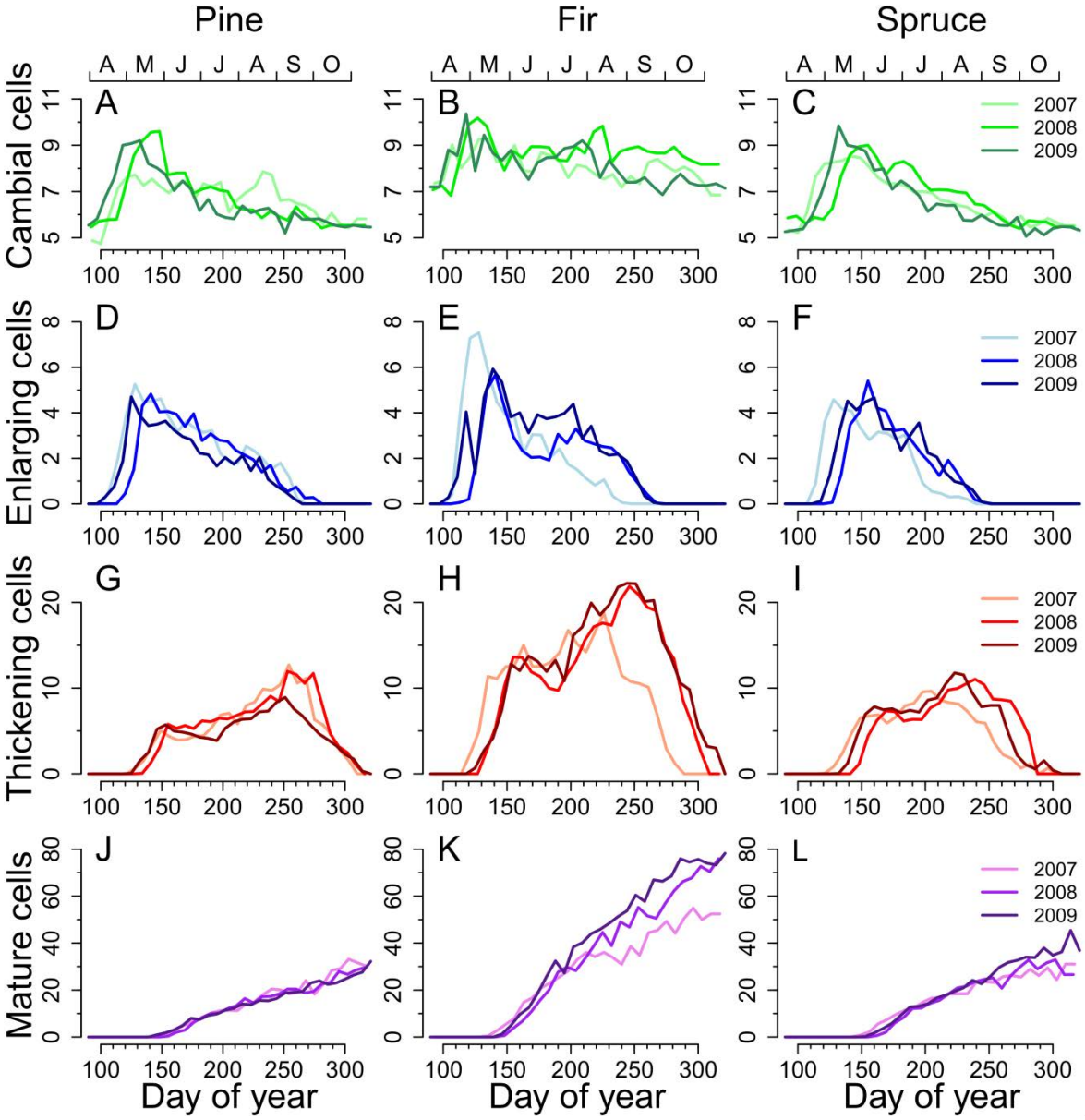

Figure V.1: Number of cells in the cambial, enlargement, thickening, and mature zones of wood formation for Scots pine, silver fir, and Norway spruce. Lines represent the mean of five trees per species per year. Upper x-axis represents the months.

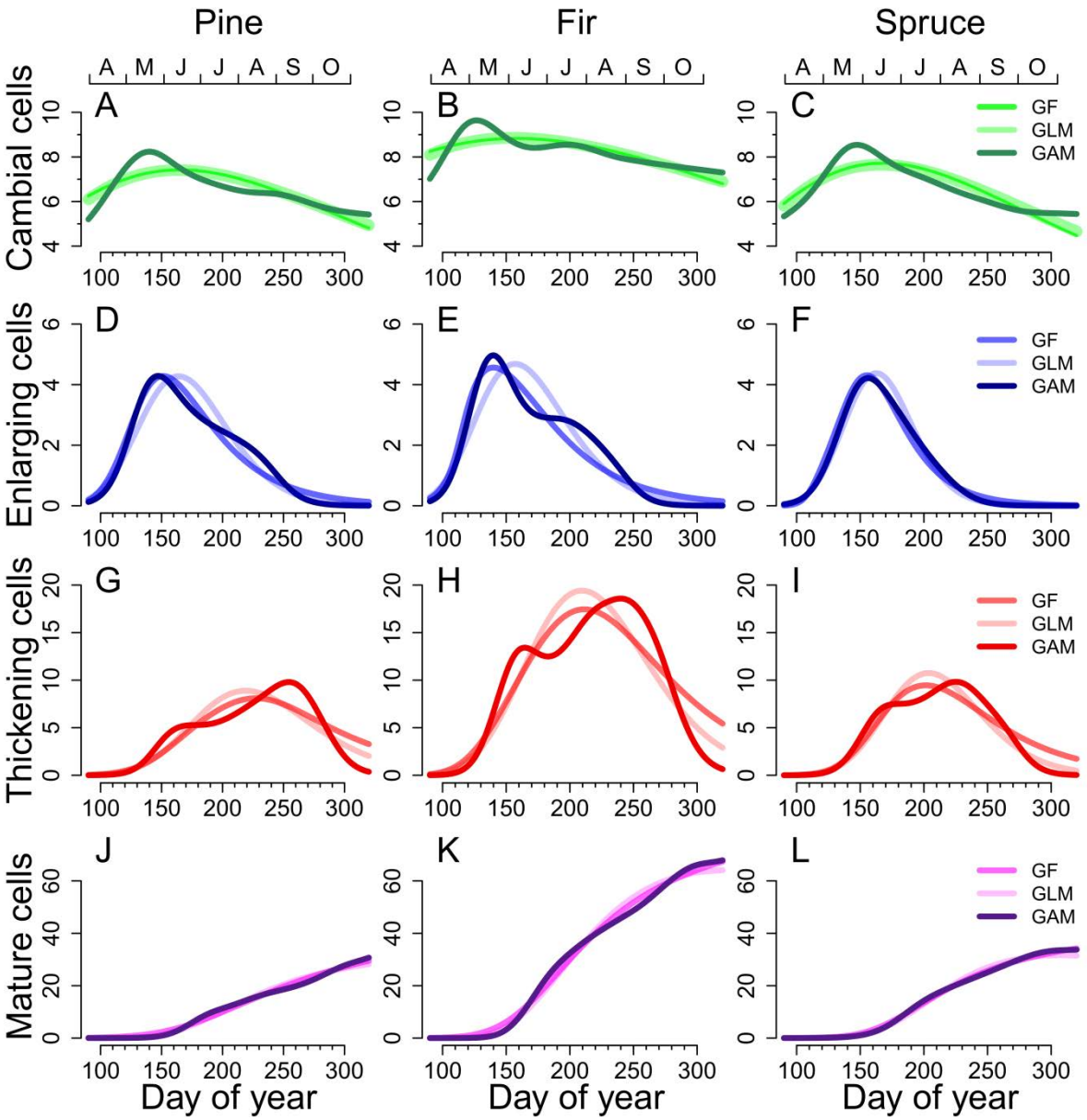

Figure V.2: Gompertz functions (GFs), and generalised linear and additive models (GLMs and GAMs) fitted to the weekly cell count in the cambial, enlargement, thickening, and mature zones for Scots pine, silver fir, and Norway spruce (n = 5 per species) over 3 years (2007, 2008, 2009). Upper x-axis represents the months.

Cell development duration

All three modelling approaches allowed calculation of the time a particular tracheid spends in each zone of xylogenesis during the course of its differentiation (Figure V.S2). All methods agreed on the general trends in cell development duration through a tree ring, showing that cells spent less time in the enlargement zone (d_E) and more time in the thickening zone (d_T) from the beginning to the end of a ring (Figure V.S3). Furthermore, since d_E was always less than or equal to d_T, the total duration of tracheid formation (d_F) increased from the beginning to the end of a ring.

Table V.2: Maximum number (nx) and date of occurrence of the maximum number (tx) of cells in the cambial (CZ), diameter enlargement (EZ), and wall thickening (TZ) zones of wood formation, computed from the fittings of the Gompertz functions (GFs), and generalised linear and additive models (GLMs and GAMs) for Scots pine, Norway spruce, and silver fir (n = 5 per species) during 2007, 2008, and 2009 (means ± standard errors).

Zone	Sp	n_x (cell)			t_x (day of year)		
		GF	GLM	GAM	GF	GLM	GAM
CZ	Pine	7.6 ± 0.3	7.7 ± 0.3	8.5 ± 0.3	158 ± 9	156 ± 8	148 ± 10
	Fir	9.1 ± 0.3	9.1 ± 0.3	10.0 ± 0.5	162 ± 15	161 ± 15	148 ± 14
	Spruce	7.8 ± 0.2	7.7 ± 0.2	8.8 ± 0.3	163 ± 6	162 ± 4	151 ± 3
EZ	Pine	4.5 ± 0.3	4.4 ± 0.3	4.5 ± 0.3	153 ± 2	164 ± 2	151 ± 4
	Fir	5.3 ± 0.5	5.1 ± 0.4	5.5 ± 0.5	150 ± 4	161 ± 3	149 ± 6
	Spruce	4.8 ± 0.3	4.7 ± 0.3	4.6 ± 0.3	152 ± 3	162 ± 3	154 ± 2
TZ	Pine	8.7 ± 0.9	9.2 ± 0.8	10.7 ± 1.2	218 ± 4	218 ± 3	247 ± 6
	Fir	18.8 ± 1.8	20.6 ± 2.1	21.3 ± 2.1	208 ± 5	211 ± 4	229 ± 9
	Spruce	10.2 ± 0.9	11.6 ± 1.0	11.4 ± 1.2	198 ± 4	202 ± 4	216 ± 7

However, a more detailed look showed that the three approaches presented contrasting results. GFs and GLMs, which returned similar curves when fitting cell numbers in the different zones of xylogenesis, exhibited contrasting monotonous patterns, which were always convex for GFs and always concave for GLMs. In contrast, GAMs gave an accurate fit, capturing realistic patterns of cell development durations. The lack of fit of GFs and GLMs resulted in a systematic underestimation of cell development duration (30% and 10%, respectively) compared to GAMs.

The GAMs showed that d_E was longest in pine (13 ± 4 days), approximately 30% shorter in spruce (9 ± 3 days), and 50% shorter in fir (6 ± 2 days). d_E was also maximal for the first-formed cells of the year, around 20 days in pine, and 14 days in fir and spruce (Figure V.3). It decreased by approximately two-thirds along the tree ring (with final durations of 6 days in pine, 5 days in fir, and 4 days in spruce). However, while d_E decreased progressively in pine and spruce, in fir it decreased rapidly in the first 30% of cells, and then remained stable around its minimal value for the following cells.

The GAMs also showed that the ring could be separated into three distinct groups of cells according to d_T (Figure V.3D, E, F). The first group corresponded to the first 40% of cells, for which d_T remained at a steady minimum of approximately 20 days (regardless of species). The second group corresponded to the middle 40% of cells, which showed a strong increase in d_T; the first cells in this second group entered thickening at the end of June, when the number of cells in this zone started to increase again (Figure V.2). The third group corresponded to the last 20% of cells, which had the maximal d_T (53 ± 1 days in pine, 51 ± 1

days in fir, and 45 ± 2 days in spruce); the cells belonging to this third group entered thickening in August and/or September, when the number of cells in this zone was maximal. On average, d_T was 10% shorter in fir and spruce than in pine (32 ± 14, 31 ± 11, and 36 ± 14 days, respectively).

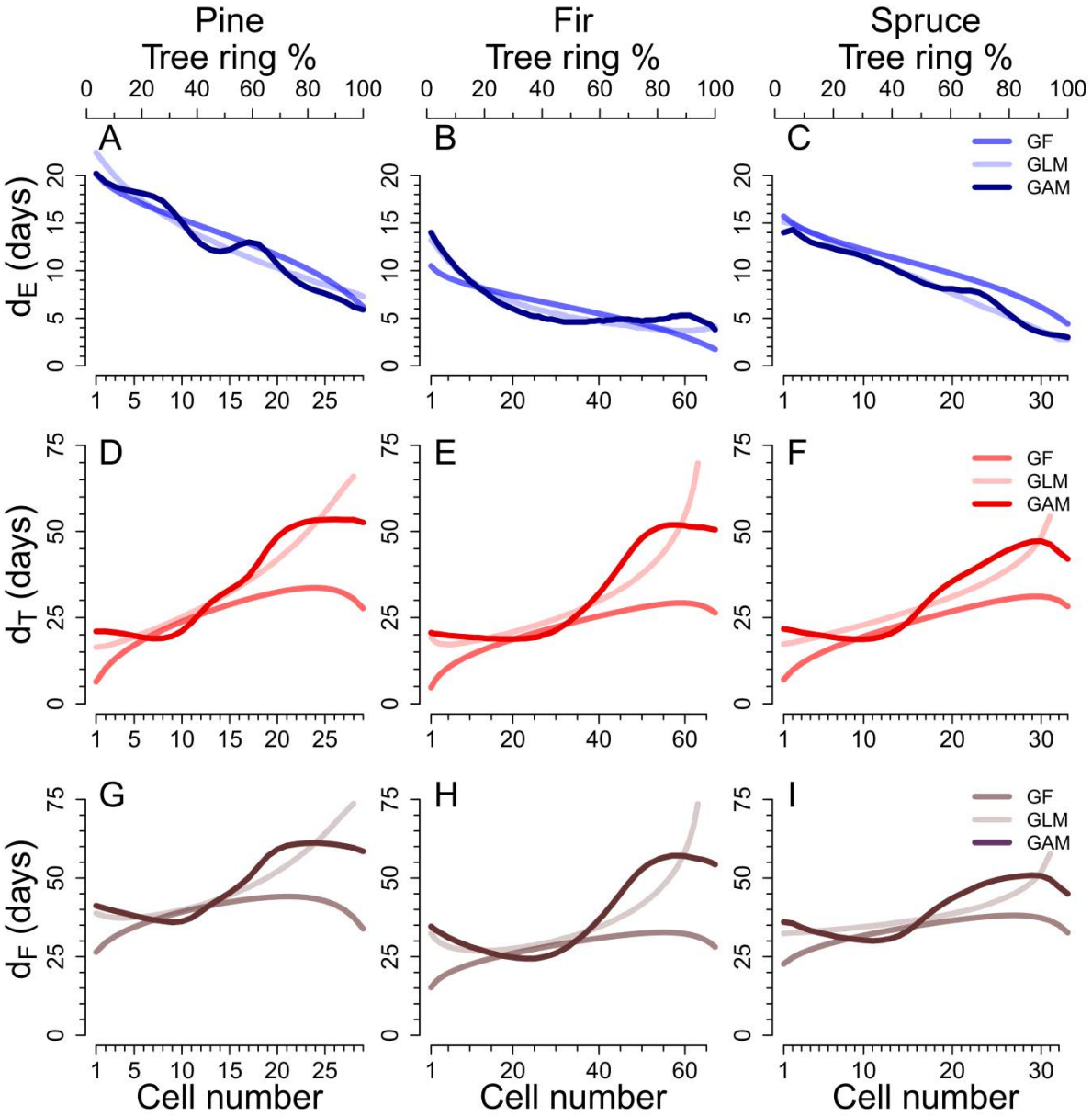

Figure V.3: Cell residence durations in the enlargement (d_E) and thickening (d_T) zones, and total duration of formation (d_F) of tracheids along tree rings in Scots pine, silver fir, and Norway spruce as computed from Gompertz functions (GFs), and generalised linear and additive models (GLMs and GAMs).

The longer d_E and d_T in pine cells meant that d_F was also 20% longer in pine than in fir and spruce (49 ± 10, 38 ± 13, and 40 ± 8 days, respectively). d_F followed a complex pattern resulting from the combination of d_E and d_T. In the first 40% of cells, d_F decreased slightly (from 41 to 36 days in pine, 37 to 30 days in spruce, and 35 to 24 days in fir). It then increased rapidly to reach its maximum at approximately 80% of a ring (61 days in pine, 57 days in fir, and 51 days in spruce). In the last 20% of cells, d_F decreased slightly for a few days.

On average, 20% of d_F was explained by d_E and 80% by d_T, with little variation between species in these proportions (15 vs. 85% in fir, 20 vs. 80% in spruce, and 25 vs. 75% in pine). However, these relative contributions varied greatly according to the position of the cells along the ring: the relative contribution of d_E to d_F in the first 40% of cells was approximately 50% in pine, 40% in spruce, and 30% in fir, but this fell to approximately 10% for the last 20% of cells in a ring, regardless of species.

Entry rates into the different zones

Cell entry rates into the successive zones of xylogenesis exhibited more complex seasonal patterns when calculated using GAMs than the classic bell-shaped curves depicted when using GFs or GLMs (Figure V.4). The cell division rates (and so also the entry rates) depended on the productivity of the species studied, with fir reaching approximately 0.7 cells day^{-1}, spruce reaching 0.35 cells day^{-1}, and pine remaining at about 0.25 cells day^{-1}.

Despite these contrasting levels, the three species presented similar changes in their rates of entry into the different zones of xylogenesis during the growing period. Moreover, the division rate, and the enlargement and thickening entry rates followed close to parallel patterns, only being staggered by a few days. These three rates presented a bimodal pattern: the first peak occurred at the end of May, around the time when the number of cells culminated in the enlargement zone and slightly before the first peak in the thickening zone; and the second peak occurred 40 days later, in the first half of July, when the number of cells in the enlargement zone was decreasing and at the beginning of the second peak in the thickening zone. In contrast, the entry rate into the mature zone followed a different pattern (Figure V.4J, K, L), reaching a clear maximum at the beginning of July, at the time of the small dip in the number of cells in the thickening zone, and then decreasing but remaining fairly high, before reaching a second peak at the end of the season (October), at the same time as the strong final decrease in the number of cells in the thickening zone.

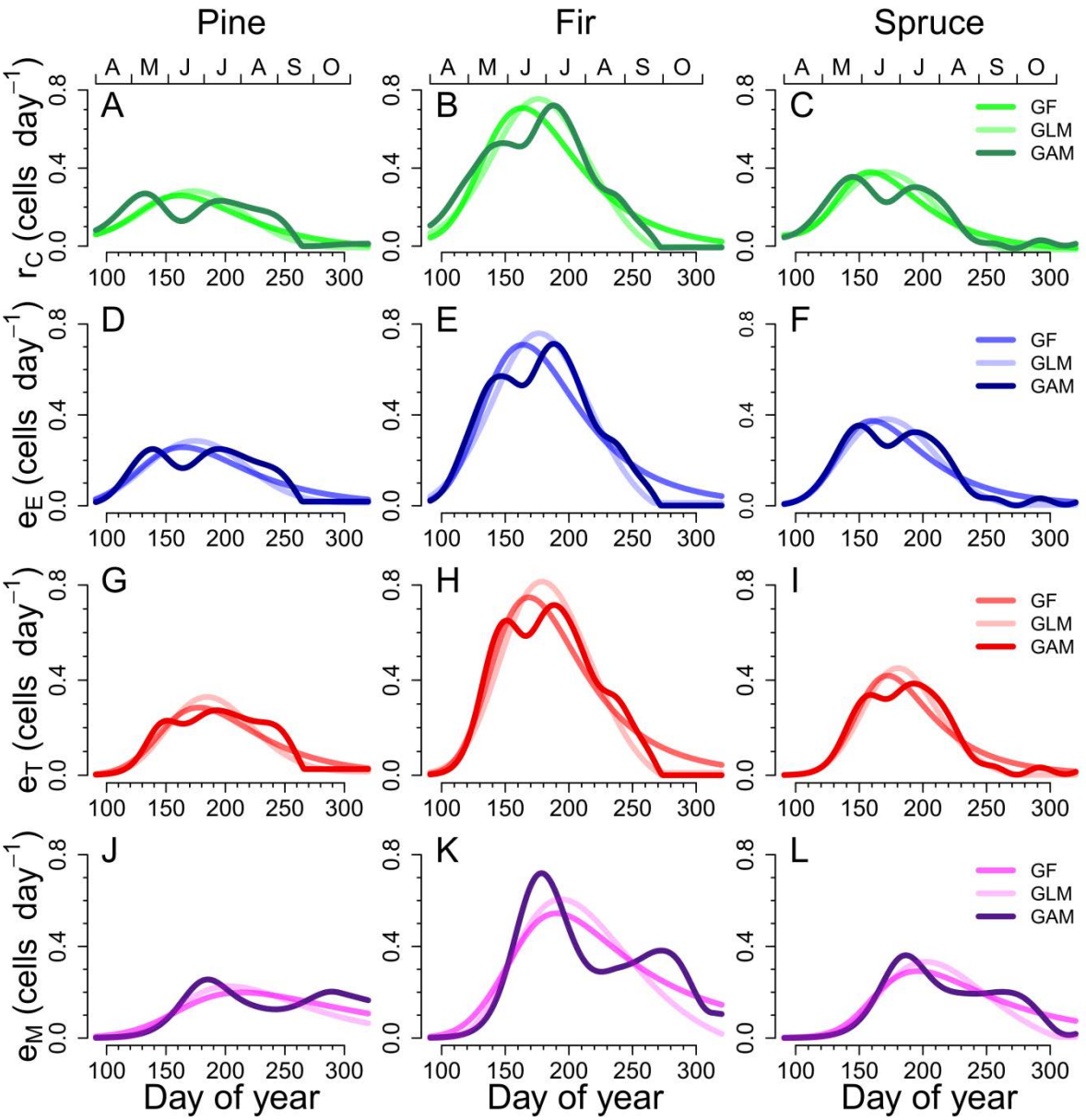

Figure V.4: Rate of cell production (r_C) by the cambial zone, and rates of entrance into the enlargement (e_E), thickening (e_T), and mature (e_M) zones of wood formation as computed from Gompertz functions (GFs), and generalised linear and additive models (GLMs and GAMs). Upper x-axis represents the months.

Discussion

Modelling wood formation dynamics using GFs, GLMs, and GAMs

Numerous studies on the intra-annual dynamics of xylogenesis have been conducted during the last decade, to gain a better understand of the influence of climate change on wood formation (Gričar *et al.*, 2011). The main method used to investigate xylogenesis involves repeated sampling of the stem through a growing season (Rossi *et al.*, 2006a). However, growth is subject to large and sudden variations along and around the stem (Wodzicki & Zajaczkowski, 1970), which makes it difficult to decide whether differences between samples represent the temporal changes in cambial activity (the biological signal of interest) or random within-tree particularities ('noise'). To enhance the desired biological signal, Wodzicki (1971)

sampled a large number of trees (60 in 1967, 216 in 1968) and obtained excellent results on the kinetics of tracheid development. However, such large sampling is exceptional considering the amount of work and cost involved.

In this study, we tested three statistical approaches (GFs, GLMs, and GAMs) to extract a meaningful biological signal from naturally noisy datasets (groups of five trees from three species over 3 years). We found that GFs and GLMs accurately represented the general changes in the number of cells in the enlargement and mature zones, but were inaccurate concerning the cambial and thickening zones. Therefore, we argue that GFs and GLMs could be used to compare general growth patterns between groups of trees – GFs can be used to extract meaningful biological parameters like the final number of produced cells and the value and occurrence of the maximal rate of cell production (see, for example, Cuny *et al.*, 2012) – but we argue that they are unsuitable for accurately characterising intra-annual dynamics of the wood formation process (zone entry rates and/or cell timings).

In contrast, GAMs captured in detail the intrinsic complexity of intra-annual wood formation dynamics, making them the only sound approach that is currently available for accurately characterising this process. Their use solves the basic but thorny issues of sampling date heterogeneity, sampling frequency variability, and missing data. GAMs allow trees and groups of trees (e.g. across species, sites, or years) to be compared or pooled. One possible problem, however, is that GAMs can produce results that are 'biologically incoherent' (e.g. negative zone entry rates), in which case the degree of smoothing must be increased until coherent results are obtained (Wood, 2006).

Because of their high flexibility, GAMs could be adapted to a wide range of conditions where GFs are inappropriate, e.g. accounting for an additional resting period during the summer drought period in Mediterranean regions (de Luis *et al.*, 2007; Camarero *et al.*, 2010), or fitting more complex growth patterns as found in ring-porous deciduous trees (Michelot *et al.*, 2012). Moreover, mixed-effect generalised additive models (GAMMs) could accurately account for the non-independence of weekly cell count data (Zuur *et al.*, 2009), providing a more robust description of the system.

Intra-annual wood formation dynamics

Intra-annual wood formation dynamics is generally described as three delayed bell-shaped curves for the numbers of cells in the cambial (CZ), enlargement (EZ), and thickening (TZ) zones, followed by an S-shaped curve for the mature (MZ) zone (Rossi *et al.*, 2006a; Lupi *et al.*, 2010; Cuny *et al.*, 2012). However, this traditional view, which has been shaped by the use of GFs, did not stand the test of a GAM approach. Rather, we demonstrated that, for conifers in temperate forests, the general pattern of intra-annual wood formation dynamics is composed of two slightly delayed left-skewed bell-shaped curves representing CZ and EZ, followed by a right-skewed bimodal curve representing TZ, and a double sigmoid curve representing MZ.

We used the extensive dataset of Wodzicki's seminal work (1971) to plot the changes in

intra-annual cell numbers in the enlargement, thickening, and mature zones for Scots pine trees grown in Poland (Figure V.S3). The patterns thus established were in full agreement with those highlighted in our study, with the curve for enlarging cells being clearly shifted to the left and culminating early (mid-May), while the curve for thickening cells reached a plateau (June) and then increased again to reach a late maximum (September), and the accumulation of mature cells clearly followed a double sigmoid curve. In the 1960s, some authors also observed that the number of cells culminated early in the season for enlargement and late for thickening (Wodzicki & Peda, 1963; Whitmore & Zahner, 1966), which is supported by our findings.

Our calculations showed that enlargement duration (d_E) decreased from 2–3 weeks to less than 1 week as the season progressed, while thickening duration (d_T) increased from 3 weeks to nearly 2 months. These values match those of Wodzicki (1971), whereas Horacek *et al.* (1999) found longer d_E but similar d_T. Both Wodzicki (1971) and Horacek *et al.* (1999) also described the same characteristic changes in d_T: steady minimal durations for the first 40% of cells in a ring, a strong increase for the following 40%, and a new plateau around the maximum duration for the last 20%. Conversely, studies based on GFs have found pseudo-linear variations in the differentiation durations between the successive cells of a ring (Deslauriers *et al.*, 2003; Rossi *et al.*, 2006a) and, moreover, have calculated shorter d_T, from 1–3 weeks for the first tracheids to 4–5 weeks for the last tracheids. It should be noted that these studies were performed in colder environments (boreal or subalpine zone), which may explain the discrepancies, but we also obtained pseudo-linear variations and under-estimated values of d_T by using GFs.

The developing xylem is a dynamic biological system

Our results show that the developing xylem is a dynamic biological system, justifying the analogy we made with hydrological system modelling. We have demonstrated that the cell flow through the different zones of xylogenesis is not only controlled by the production rate of the cambium (the source), but also by the cell residence times in each 'reservoir' (Figure V.S4A), creating the complex pattern described above (Figure V.S4B), and resulting in strong differences in the computation of the timing of cell development (Figure V.S4C). The early culmination of cells in the enlargement reservoir can be related to both (1) the high flow from the source (demonstrated by the high division rate in the cambium and the high entry rates into the enlarging reservoir); and (2) the long cell residence times in this reservoir at the beginning of the season. The enlargement reservoir then progressively emptied, because of the decreasing residence times in this reservoir.

The early peak in cells in the thickening reservoir can also be related to the intense flow from the source at the beginning of the growing season: the many cells born in the cambium passed quite rapidly through the enlarging reservoir, before entering the thickening reservoir, where they accumulated because of structurally longer residence times. After this first peak, the number of cells in the thickening reservoir remained quasi-stable for a while, indicating that the entry and exit rates were at equilibrium. At the end of summer, despite a rapid decrease in the entry rate, the thickening reservoir reached its maximum cell number, because

of an abrupt increase in the cell residence times.

The complex dynamics of the thickening reservoir was demonstrated by the accumulation of mature cells, which had two periods of rapid increase separated by a slower transition period. The first rapid accumulation echoed the intense cell flow generated by the cambium in the first part of the season, which cascaded through the successive reservoirs. In summer, the period of slower accumulation corresponded to the increasing residence times in the thickening reservoir, resulting in a diminution of mature reservoir entry rate. In autumn, the last period of rapid accumulation of mature cells occurred during the final rapid emptying of the thickening reservoir.

Relationships between the intra-annual dynamics of xylogenesis and wood anatomy

Conifer tree rings can be divided into two parts: earlywood, containing large-diameter, thin-walled tracheids produced at the beginning of the growing season; and latewood, containing narrow-diameter, thick-walled tracheids produced towards the end of the season. In our dataset, the first latewood cell — identified according to Mork's criterion (Denne, 1988) — was estimated to enter the thickening zone around the beginning of the second peak in thickening cells. Therefore, the bimodal curve describing the number of cells in the thickening zone can be interpreted as two juxtaposed bell-shaped curves, corresponding to two distinct populations of tracheids (earlywood and latewood) exhibiting contrasting behaviours. The higher proportion of latewood in pine (45%) compared with spruce (30%) and fir (27%) explains the greater difference in amplitude between the two peaks in the pine thickening zone.

The observed patterns for cell differentiation durations are consistent with the anatomical profiles of conifer tree rings (Mäkinen *et al.*, 2003; Park & Spiecker, 2005; Rathgeber *et al.*, 2006). Indeed, the final diameter of a tracheid, which is acquired during the enlargement phase of its differentiation, progressively decreases along a ring, mimicking the changes in d_E; and the final wall thickness, which is acquired during the thickening phase, remains around a steady minimum in the first part of a ring, increases in the middle part, and reaches a steady maximum in the last part, mimicking the changes in d_T. Moreover, the sizes of tracheids are proportional to the time they spent in the different zones of differentiation: in earlywood tracheids, diameters are two to three times larger and d_E two to three times longer than in latewood tracheids; whereas in latewood tracheids, walls are two to three times thicker and d_T two to three times longer than in earlywood tracheids. It is also striking that the changes in d_F along a ring strongly resembled a classic intra-ring wood density profile (Rathgeber *et al.*, 2006).

Conclusion

Our study shows that GAMs provide an improved approach for modelling intra-annual wood formation dynamics, which is generally represented by changes in the number of cells in the different development stages of xylogenesis: cambial (CZ), enlargement (EZ), wall thickening (TZ), and mature (MZ) zones. Indeed, only GAMs captured the complexity of intra-annual wood formation dynamics, making them suitable for further characterising this

dynamics by computing both the cell entry rates and the cell residence times in the different zones.

We argue that the developing xylem must be seen as a dynamic biological system in which the cell production rate interplays with the cell residence time in each zone, resulting in complex intra-annual patterns: two left-skewed bell-shaped curves for CZ and EZ, followed by a right-skewed bimodal curve for TZ and a double sigmoid curve for MZ. These patterns have the advantage of truly reflecting the data and explaining some anatomical features of a tree ring, separating, for example, earlywood and latewood into two distinct cell populations.

We believe that this approach has great potential and will help us to better understand wood formation. It allows a fine assessment of the dynamics of the processes that can be compared directly with observations; for example, a comparison of cell residence times in each of the zones with tracheid anatomical characteristics shows that the change in cell size along a ring is closely related to the change in d_E through the growing season, whereas the change in cell-wall thickness is closely related to the change in d_T.

Acknowledgements

We thank E. Cornu, E. Farré, C. Freyburger, P. Gelhaye, and A. Mercanti for fieldwork and monitoring; M. Harroué for sample preparation in the laboratory; P. Santenoise for his help with the statistics; and M. Dassot for his help with editing the figures.

References

Abe H, Funada R, Ohtani J, Fukazawa K. 1997. Changes in the arrangement of cellulose microfibrils associated with the cessation of cell expansion in tracheids. *Trees-Structure and Function* **11**(6): 328-332.

Akaike H 1973. Information theory and an extension of the maximum likelihood principle.In Petrov BN, Csaki F. *2nd International Symposium on Information Theory*. Akademiai Kiado, Budapest. 267-281.

Armstrong JS, Collopy F. 1992. Eror measures for generalizing about forecasting methods: empirical comparions. *International Journal of Forecasting* **8**(1): 69-80.

Bates D, Chambers J 1992. Nonlinear models. In: Chambers J, Hastie T eds. *Statistical models in S.* Pacific Grove, CA: Wadsworth and Brooks/Cole.

Camarero JJ, Guerrero-Campo J, Gutierrez E. 1998. Tree-ring growth and structure of *Pinus uncinata* and *Pinus sylvestris* in the Central Spanish Pyrenees. *Arctic and Alpine Research* **30**(1): 1-10.

Camarero JJ, Olano JM, Parras A. 2010. Plastic bimodal xylogenesis in conifers from continental Mediterranean climates. *New Phytologist* **185**(2): 471-480.

Chaffey N. 2002. Why is there so little research into the cell biology of the secondary vascular system of trees? *New Phytologist* **153**(2): 213-223.

Cuny HE, Rathgeber CBK, Lebourgeois F, Fortin M, Fournier M. 2012. Life strategies in intra-annual dynamics of wood formation: example of three conifer species in a temperate forest in north-east France. *Tree Physiology* **32**(5): 612-625.

de Luis M, Gričar J, Čufar K, Raventós J. 2007. Seasonal dynamics of wood formation in *Pinus halepensis* from dry and semi-arid ecosystems in Spain. *Iawa Journal* **28**(4): 389-404.

Denne MP. 1988. Definition of latewood according to Mork (1928). *Iawa Bulletin* **10**(1): 59-62.

Deslauriers A, Morin H, Begin Y. 2003. Cellular phenology of annual ring formation of *Abies balsamea* in the Quebec boreal forest (Canada). *Canadian Journal of Forest Research - Revue Canadienne De Recherche Forestière* **33**(2): 190-200.

Gričar J, Rathgeber CBK, Fonti P. 2011. Monitoring seasonal dynamics of wood formation. *Dendrochronologia* **29**(3): 123-125.

Guisan A, Edwards TC, Hastie T. 2002. Generalized linear and generalized additive models in studies of species distributions: setting the scene. *Ecological Modelling* **157**(2-3): 89-100.

Hastie T, Tibshirani R. 1986. Generalized additive models. *Statistical Science* **1**(3): 297-318.

Horacek P, Slezingerova J, Gandelova L 1999. Effects of environment on the xylogenesis of Norway spruce (*Picea abies* L. Karst.). In: Wimmer R, Vetter RE eds. *Tree-ring analysis: biological, methodological and environmental aspects.* Wallingford, UK: CABI Publishing, 33-53.

Kutscha NP, Hyland F, Schwarzmann JM. 1975. Certain seasonal changes in balsam fir cambium and its derivatives. *Wood Science and Technology* **9**(3): 175-188.

Larson PR. 1994. *The vascular cambium: development and structure*. Berlin Heidelberg: Springer-Verlag.

Lupi C, Morin H, Deslauriers A, Rossi S. 2010. Xylem phenology and wood production: resolving the chicken-or-egg dilemma. *Plant Cell and Environment* **33**(10): 1721-1730.

Mäkinen H, Nöjd P, Saranpää P. 2003. Seasonal changes in stem radius and production of new tracheids in Norway spruce. *Tree Physiology* **23**(14): 959-968.

Mayer DG, Butler DG. 1993. Statistical validation. *Ecological Modelling* **68**(1-2): 21-32.

McCullagh P, Nelder JA. 1983. *Generalized Linear Models*. First ed. London: Chapman and Hall.

Michelot A, Simard S, Rathgeber C, Dufrêne E, Damesin C. 2012. Comparing the intra-annual wood formation of three European species (*Fagus sylvatica*, *Quercus petraea* and *Pinus sylvestris*) as related to leaf phenology and non-structural carbohydrate dynamics. *Tree Physiology* **32**(8): 1033-1045.

Park Y-I, Spiecker H. 2005. Variations in the tree-ring structure of Norway spruce (*Picea abies*) under contrasting climates. *Dendrochronologia* **23**(2): 93-104.

Plomion C, Leprovost G, Stokes A. 2001. Wood formation in trees. *Plant Physiology* **127**(4): 1513-1523.

R Development Core Team 2011. R: A language and environment for statistical computing. Vienna, Austria: R Foundation for Statistical Computing. http://www.R-project.org/.

Rathgeber CBK 2012. Cambial activity and wood formation: data manipulation, visualisation and analysis using R. R package version 1.4-1. http://CRAN.R-project.org/package=CAVIAR.

Rathgeber CBK, Decoux V, Leban J-M. 2006. Linking intra-tree-ring wood density variations and tracheid anatomical characteristics in Douglas fir (*Pseudotsuga menziesii* (Mirb.) Franco). *Annals of Forest Science* **63**(7): 699-706.

Rathgeber CBK, Rossi S, Bontemps J-D. 2011. Cambial activity related to tree size in a mature silver-fir plantation. *Annals of Botany* **108**(3): 429-438.

Rossi S, Deslauriers A, Anfodillo T. 2006a. Assessment of cambial activity and xylogenesis by microsampling tree species: An example at the alpine timberline. *Iawa Journal* **27**(4): 383-394.

Rossi S, Deslauriers A, Anfodillo T, Morin H, Saracino A, Motta R, Borghetti M. 2006b. Conifers in cold environments synchronize maximum growth rate of tree-ring formation with day length. *New Phytologist* **170**(2): 301-310.

Rossi S, Deslauriers A, Gričar J, Seo J-W, Rathgeber CBK, Anfodillo T, Morin H, Levanic T, Oven P, Jalkanen R. 2008. Critical temperatures for xylogenesis in conifers of cold climates. *Global Ecology and Biogeography* **17**(6): 696-707.

Rossi S, Deslauriers A, Morin H. 2003. Application of the Gompertz equation for the study of xylem cell development. *Dendrochronologia* **21**(1): 33-39.

Rossi S, Morin H, Deslauriers A, Plourde P-Y. 2011. Predicting xylem phenology in black spruce under climate warming. *Global Change Biology* **17**(1): 614-625.

Skene DS. 1969. The period of time taken by cambial derivatives to grow and differentiate into tracheids in *Pinus radiata* D. Don. *Annals of Botany* **33**(2): 253-262.

Skene DS. 1972. The kinetics of tracheid development in *Tsuga canadensis* Carr. and its relation to tree vigour. *Annals of Botany* **36**(1): 179-187.

Vaganov EA, Anchukaitis KJ, Evans MN 2011. How well understood are the processes that create dendroclimatic records? A mechanistic model of the climatic control on conifer tree-ring growth dynamics. In: Hughes MK, Swetnam TW, Diaz HF eds. *Dendroclimatology*. London: Springer-Verlag, 37-75.

Whitmore FW, Zahner R. 1966. Development of the Xylem Ring in Stems of Young Red Pine Trees. *Forest Science* **12**(2): 198-210.

Willmott CJ, Matsuura K. 2005. Advantages of the mean absolute error (MAE) over the root mean square error (RMSE) in assessing average model performance. *Climate Research* **30**(1): 79-82.

Wilson BF, Wodzicki TJ, Zahner R. 1966. Differentiation of cambial derivatives: proposed terminology. *Forest Science* **12**(4): 438-440.

Wodzicki TJ. 1971. Mechanism of xylem differentiation in *Pinus sylvestris* L. *Journal of Experimental Botany* **22**(72): 670-687.

Wodzicki TJ, Peda T. 1963. Investigation on the annual ring of wood formation in European silver fir (*Abies pectinata* D.C.). *Acta societatis botanicorum poloniae* **32**: 609-618.

Wodzicki TJ, Zajaczkowski S. 1970. Methodical problems in studies on seasonal production of cambial xylem derivatives. *Acta societatis botanicorum poloniae* **39**(3): 509-520.

Wood SN. 2006. *Generalized additive models: an introduction with R*. Boca Raton, FL: Chapman and Hall/CRC.

Zuur AF, Ieno EN, Walker NJ, Saveliev AA, Smith GM. 2009. *Mixed effects models and extensions in ecology with R*. New York: Springer-Verlag.

Supplementary material

Table V.S1: Main characteristics (means ± standard errors) of the monitored trees from the three studied species (Scots pine, silver fir, and Norway spruce; *n* = 5 per species) illustrated by the age, diameter at breast height (DBH), height (H) , crown area (CA), final ring cell number (RCN), and tree-ring width (TRW).

	Age (years)	DBH (cm)	H (m)	CA (m²)	RCN	TRW (mm)
Pine	119 ± 3	53 ± 2	27 ± 1	29 ± 2	29.7 ± 3.0	1.1 ± 0.1
Fir	73 ± 3	57 ± 3	31 ± 1	37 ± 6	67.9 ± 7.5	2.5 ± 0.2
Spruce	74 ± 4	55 ± 4	33 ± 1	30 ± 7	33.9 ± 4.4	1.3 ± 0.1

Table V.S2: List of the variables.

Notation	Variable	Unit
n_C	Number of cells in the cambial zone	number
n_E	Number of cells in the enlargement zone	number
n_T	Number of cells in the wall thickening zone	number
n_M	Number of cells in the mature zone	number
t_E	Date of cell entry in the enlargement zone	day of
t_T	Date of cell entry in the wall thickening zone	day of
t_M	Date of cell entry in the mature zone	day of
d_E	Cell residence duration in the enlargement zone	day
d_T	Cell residence duration in the wall thickening zone	day
d_F	Total duration of tracheid formation	day
r_C	Rate of cell production by the cambial zone	cell day^{-1}
e_E	Entry rate of cell in the enlargement zone	cell day^{-1}
e_T	Entry rate of cell in the wall thickening zone	cell day^{-1}
e_M	Entry rate of cell in the mature zone	cell day^{-1}

Table V.S3: Number of cells in the cambial (n_C), enlargement (n_E), thickening (n_T), and mature (n_M) zones of xylogenesis during the growing season (mean ± standard deviation). Relative standard deviations are given in brackets.

	n_C	n_E	n_T	n_M
Pine	6.6 ± 1.5 (23%)	1.6 ± 1.8 (113%)	4.5 ± 4.3 (96%)	12.0 ± 11.3 (94%)
Fir	8.3 ± 1.7 (20%)	1.8 ± 2.2 (122%)	9.7 ± 8.9 (92%)	30.3 ± 30.0 (99%)
Spruce	6.6 ± 1.4 (21%)	1.2 ± 1.8 (150%)	4.4 ± 4.9 (111%)	14.4 ± 14.4 (100%)

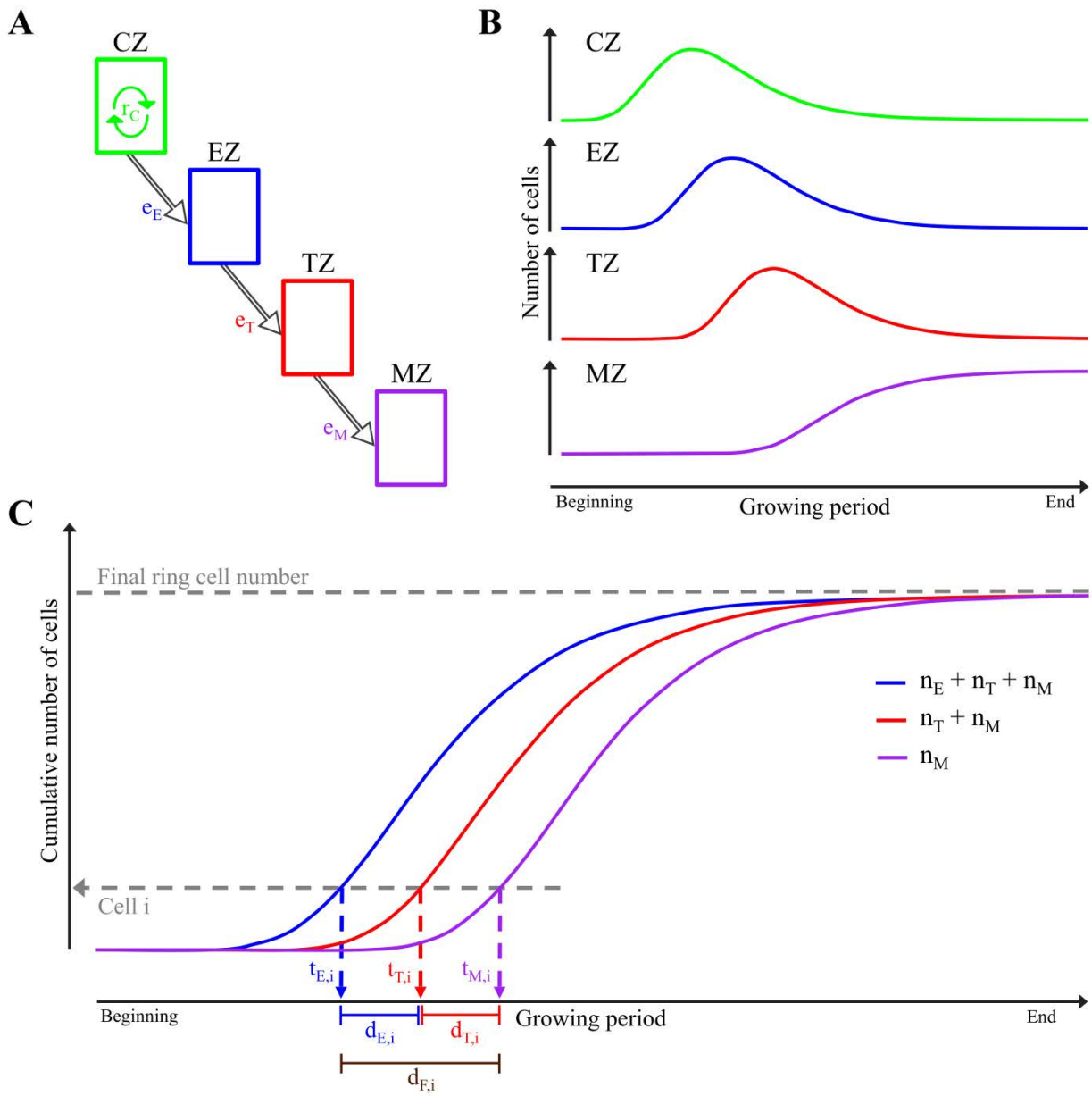

Figure V.S1: Illustration of the classical view of the wood formation dynamics. In A, the diagram describes the developmental zones of xylogenesis as interconnected reservoirs. Cells are generated in the cambial zone (CZ) according to a rate of cell production r_C, and then successively enter the enlargement (EZ), thickening (TZ), and mature (MZ) zones at rates e_E, e_T, and e_M. In this case, the dynamics of r_C in CZ drives the dynamics of the subsequent zones, with e_E, e_T, and e_M echoing r_C. Figure IV.S1B presents the intra-annual dynamics resulting from r_C, with three delayed bell-shaped curves for CZ, EZ, and TZ, and one S-shaped curve for MZ. Figure IV.S1C shows the sums of the cell numbers simulated with Gompertz function used to compute the timing of cell development. The dates of entrance and the duration spent in the enlargement ($t_{E,i}$ and $d_{E,i}$) and thickening ($t_{T,i}$ and $d_{T,i}$) zones, as well as the date of entrance into the mature zone ($t_{M,i}$) and the total duration of tracheid formation ($d_{F,i}$) are computed for cell i.

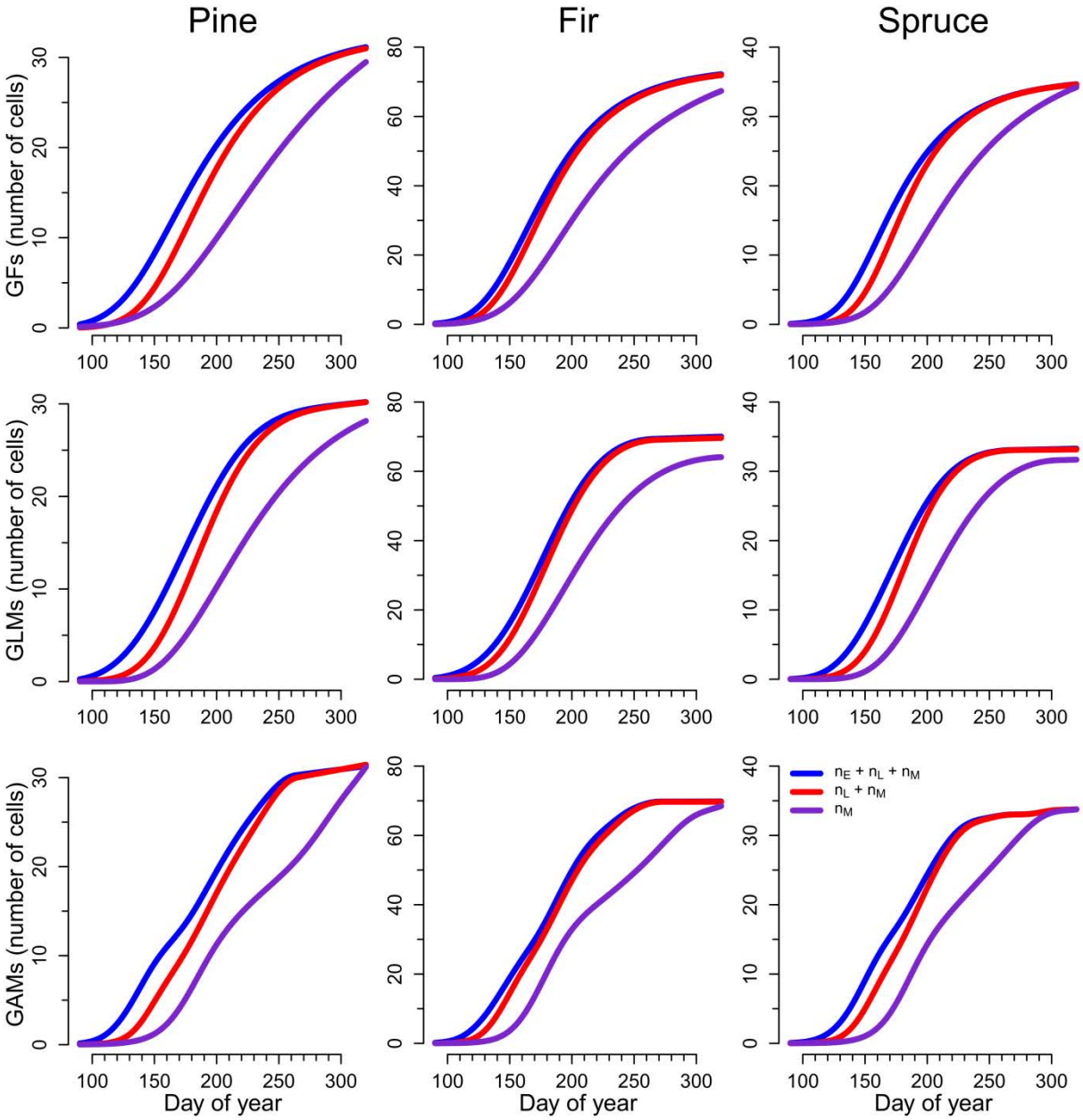

Figure V.S2: Sums of the cell numbers in the wood formation zones simulated by Gompertz functions (GFs), and generalised linear and additive models (GLMs and GAMs) for Scots pine, silver fir and Norway spruce. Lines represent means of five trees during 3 years (2007-2009).

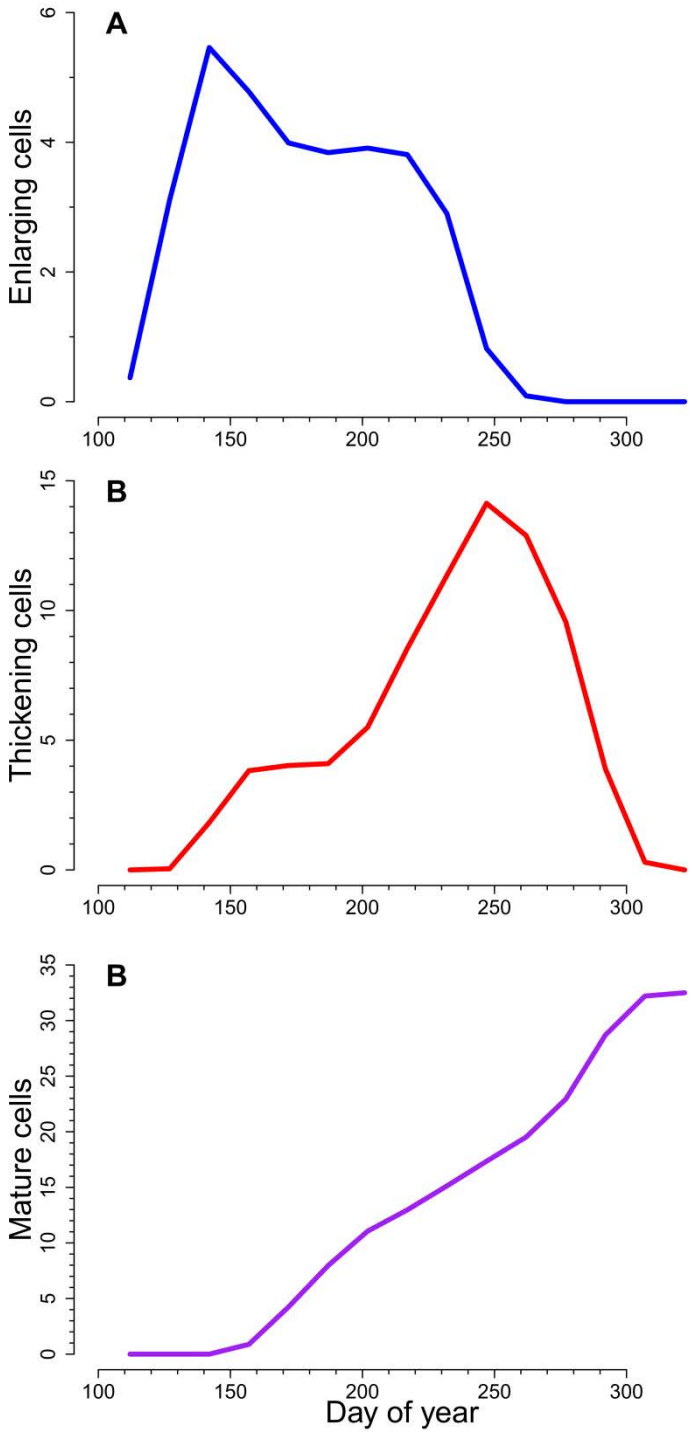

Figure V.S3: Number of cells in the enlargement, thickening, and mature zones of Scots pine trees grown in Poland. Lines correspond to the means of 276 trees (60 in 1967 and 216 in 1968). Data from Wodzicki (1971).

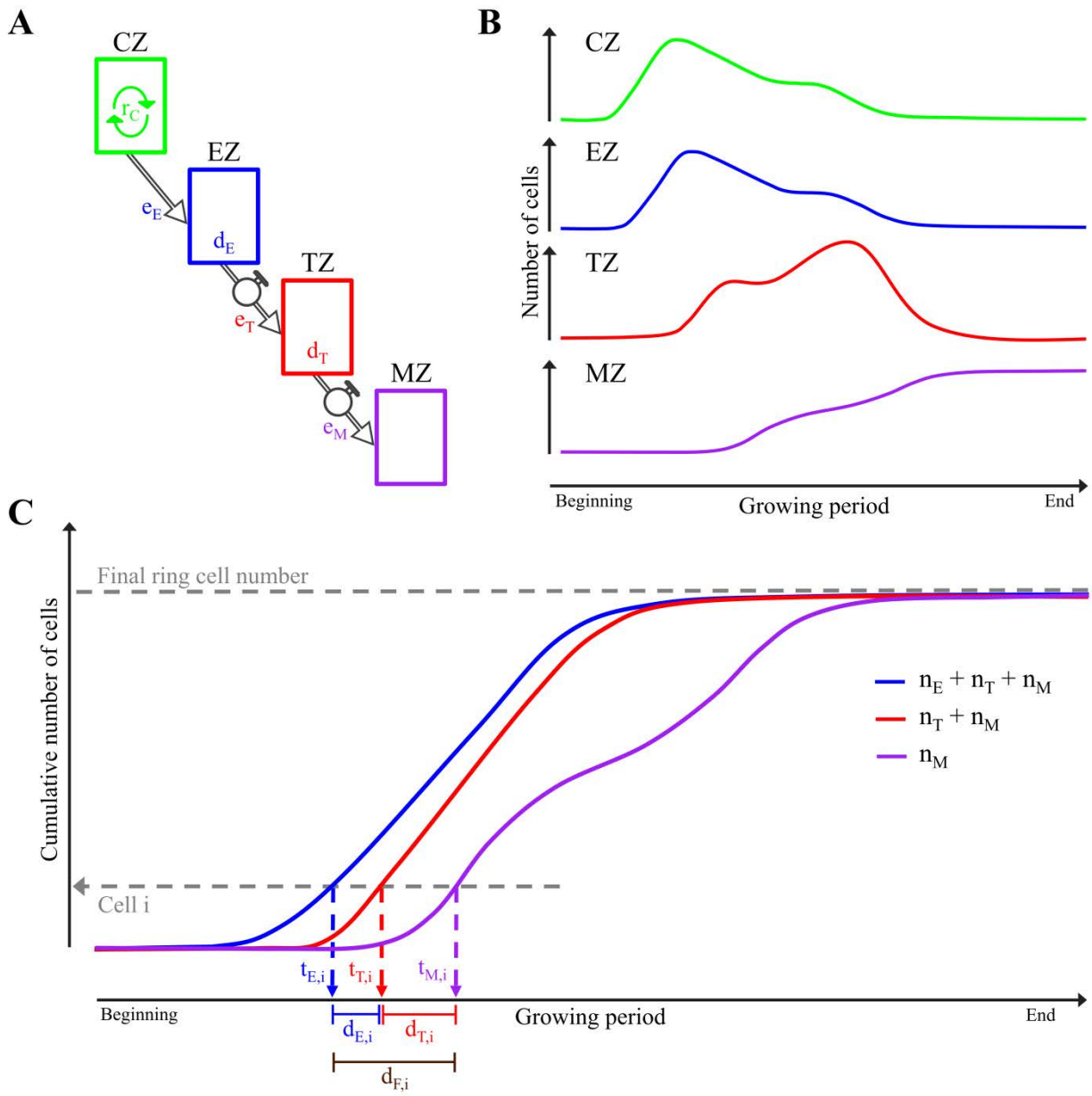

Figure V.S4: Updated conceptual view of the wood formation dynamics. In A, the diagram describes the developmental zones of xylogenesis as interconnected reservoirs. Cells are generated in the cambial zone (CZ) according to a rate of cell production r_C, and then successively enter the enlargement (EZ), thickening (TZ), and mature (MZ) zones at rates e_E, e_T, and e_M. Valves below EZ and TZ indicate the possibility for the cell residence durations in EZ and TZ (d_E and d_T) to change independently during the season. Consequently, EZ and TZ can have their own dynamics, which in turn influence the dynamics of e_T, e_M, and MZ. Figure IV.S4B presents the complex intra-annual dynamics resulting from the interplay of r_C with decreasing d_E and increasing d_T during the season: two left-skewed bell-shaped curves for CZ and EZ, a right-skewed bimodal curve for TZ, and a double sigmoid curve for MZ. Figure IV.S4C shows the sums of the cell numbers simulated with generalised additive models used to compute the timing of cell development. The dates of entrance and the duration spent in the enlargement ($t_{E,i}$ and $d_{E,i}$) and thickening ($t_{T,i}$ and $d_{T,i}$) zones, as well as the date of entrance into the mature zone ($t_{M,i}$) and the total duration of tracheid formation ($d_{F,i}$) are computed for cell i.

VI EXPLICATION DE LA STRUCTURE DU CERNE PAR LES PROCESSUS DE DIFFÉRENCIATION CELLULAIRE

Les deux parties précédentes ont permis une caractérisation précise de la dynamique intra-annuelle de la formation du bois. Dans cette partie, nous proposons d'explorer les mécanismes par lesquels cette dynamique donne forme à la structure du cerne annuel de croissance. Pour cela, nous recherchons la contribution relative des changements dans la durée et la vitesse des processus (élargissement et formation de la paroi) sur les changements de la morphologie des cellules (diamètre cellulaire et épaisseur de paroi) et de la densité du bois typiquement observés le long du cerne. Au contraire des deux parties précédentes, les données utilisées englobent les trois sites du gradient, avec les 45 arbres des 3 espèces et les 3 années (2007 – 2009) de suivi. Cette partie est constituée d'un article scientifique (article 3) en préparation.

Wide cells, thin walls; narrow cells, thick walls: How cell differentiation processes shape conifer tree-ring structure

Henri E. Cuny[1*], Cyrille B.K. Rathgeber[1], Meriem Fournier[2]

(In preparation)

[1] INRA, UMR1092, Laboratoire d Etude des Ressources Foret Bois (LERFoB), Centre INRA de Nancy, F-54280 Champenoux, France

[2] AgroParisTech, UMR1092, Laboratoire d Etude des Ressources Foret Bois (LERFoB), ENGREF, 14 rue Girardet, F-54000 Nancy, France

Summary

Wood anatomy is characterized by key functional traits that determine tree performance and survival. Trees produce wood during xylogenesis; newly produced xylem cells undergo two successive differentiation phases (enlargement and wall thickening) that form their final functional shape. Here, we aim to understand how cell differentiation creates patterns of cell features and wood density along conifer rings. Xylogenesis was monitored weekly over 3 years (2007–2009) in 45 trees of three conifer species (*Abies alba Mill.*, *Picea abies* (L.) Karst., *Pinus sylvestris* L.) in north-eastern France. Generalized additive models were used to describe wood-formation dynamics and to calculate rate and duration of enlargement and thickening for each cell. Tracheid dimensions and wood density were measured after each growing season. Enlargement duration was the main determinant of changes in cell diameter along tree rings, while rate and duration of cell wall deposition contributed equally to changes in the quantity of cell wall. However, because cell size also influences cell wall thickness, the duration of enlargement proved to be the main driver of cell morphology, tree-ring structure, and wood density profiles. Our results demonstrate the importance of duration over rate in processes of xylogenesis, suggesting strong developmental control of wood formation.

Keywords: cambial activity – conifers – generalised additive models (GAMs) – tree-ring structure – xylogenesis – quantitative wood anatomy – wood density

Introduction

Wood performs three essential functions in trees: (1) it supports the photosynthetic tissues via the particular biomechanical properties of stems and branches (Fournier *et al.*, 2006); (2) it conducts water and nutrients from the roots to the leaves (Sperry *et al.*, 2008); and (3) it stores food, water, and defensive compounds (Kozlowski & Pallardy, 1997). Because it performs a diversity of functions, wood is required to accommodate conflicting demands that are continuously modified according to changing environmental cues (Chave *et al.*, 2009). The 'multitasking' aspect of wood is even more critical in conifers than in angiosperms because more than 90% of conifer wood is composed of tracheid cells, which function in both water transport and mechanical support (Brown *et al.*, 1949). Large-diameter tracheids are more efficient at transporting water than those with smaller diameter, but are also more prone to cavitation (Pratt *et al.*, 2007). Tracheids with thick, lignified secondary walls contain less volume for transporting water but provide strong support to the plant body and prevent the conduit from imploding under tension exerted by water transport (Cochard *et al.*, 2004). Such structural and physiological trade-offs, which result from the morphology of individual tracheids, determine the anatomical structure of a tree ring. The wood density profile provides a synthetic and affordable measurement of whole tree-ring anatomical structure. Well-established relationships that link tracheid features and wood density have shown that wood density is primarily related to cell-wall thickness and secondarily to cell-lumen diameter (Rathgeber *et al.*, 2006). Wood density has thus emerged as a key functional trait that integrates changes in cell features and is widely discussed in the ecological literature (e.g. Hacke *et al.*, 2001; King *et al.*, 2006; Chave *et al.*, 2009; Larjavaara & Muller-Landau, 2010).

Xylogenesis is the key process during which trees implement these physiological and structural trade-offs, fixing them permanently in the resulting wood. Xylogenesis is a highly plastic process that allows trees to adjust or adapt to various growth conditions (Fonti *et al.*, 2010). In temperate or cold forests, trees experience contrasting physiological and environmental conditions over the year and produce cells with contrasting features and functions. These differences among cells result in the typical changes in cell dimensions along a tree ring, from the wide, thin-walled cells of light earlywood produced at the beginning of the growing season, to the narrow, thick-walled cells of dense latewood produced toward the end of the growing season (Figure VI.S1 available as Supplementary material).

During xylogenesis, cells pass through three successive phases of production and differentiation before reaching their final, functional shapes: (1) cambial cell division, (2) cell radial enlargement, and (3) secondary cell wall formation and lignification (Wilson *et al.*, 1966). Division of cambial cells produces xylem cells inwards (toward the pith) and phloem cells outwards (toward the bark). Xylem cells then enter the 'enlargement' phase during which they increase in radial diameter through wall loosening, osmotic-driven water uptake, and deposition of new primary wall material (Cosgrove, 2000a; Cosgrove, 2000b). During the enlargement phase, the radial diameter of earlywood tracheids increases seven to eight times (final diameter of 30–50 µm), while this of latewood tracheids increases two to three times (final diameter of 10–25 µm).

Following enlargement, cells enter the 'thickening' phase, during which they build a rigid, waterproof, multi-layered secondary cell wall composed of cellulose, hemicellulose, and lignin (Zhong & Zheng-Hua, 2009). Secondary cell wall formation begins with deposition of a dense matrix of helicoidal cellulose and hemicellulose microfibrils against the primary wall, which limits further radial expansion (Abe *et al.*, 1997). Lignin is deposited within the carbohydrate matrix between microfibrils, cementing them together by chemical bonds (Boerjan *et al.*, 2003). Lignification begins at the cell corners in the middle lamella and primary wall and eventually spreads across the secondary wall towards the lumen. Secondary walls are two to three times thicker in latewood (4–6 µm) than in earlywood (2–3 µm). Programmed cell death (apoptosis) marks the passage of xylem cells to their mature functional state. Apoptosis is triggered by a calcium flux that provokes vacuoles to collapse and release hydrolases that degrade the cellular contents but not the secondary wall (Bollhöner *et al.*, 2012). Thus, mature tracheids are dead, empty, elongated cells; in conifers they are about 100 times longer (2.5–5 mm) than wide (10–60 µm), are tapered at the ends, and have thick, lignified secondary walls.

Our understanding of wood-formation processes has been greatly improved at the cellular and genetic levels in recent years (Plomion *et al.*, 2001; Oda *et al.*, 2005; Mellerowicz & Sundberg, 2008). However, the subject of how the remarkable changes in xylem cell features and wood density along a tree ring are related to changes in intra-annual dynamics of xylogenesis has received little attention since the early seventies. In the pioneering work of Skene (1969), the final radial diameter of a tracheid is described as the result of time spent in the expansion phase and the rate of expansion experienced by the cell; the amount of

secondary cell wall deposited is a function of time spent in the thickening phase and the rate of deposition of wall material. Most experimental results from studies of wood formation have confirmed Skene's (1969) early findings that (1) final radial diameter is not related to the rate of expansion, but rather to the duration of the enlargement phase; and (2) final wall thickness is not related to the rate of deposition but rather to the duration of the thickening phase (Wodzicki, 1971; Denne, 1972; Skene, 1972; Dodd & Fox, 1990; Horacek *et al.*, 1999).

Despite this long-lasting consensus, xylogenesis processes in general, and duration of xylem cell differentiation in particular, are not commonly discussed in environmental (Briffa *et al.*, 1998; Bouriaud *et al.*, 2005; Gagen *et al.*, 2006), ecophysiological (Helle & Schleser, 2004; Offermann *et al.*, 2011), or modelling (Deleuze & Houllier, 1998; Fritts *et al.*, 1999; Ogée *et al.*, 2009; Drew *et al.*, 2010; Eglin *et al.*, 2010) studies, probably because these processes are still not adequately understood. In cambial-activity and wood-formation models, constant durations are typically assigned to processes of xylogenesis. For example, in the model presented by Deleuze & Houllier (1998), expansion and thickening occur during a 5-day period, while the rates of these processes vary according to the plant's physiological state and environmental conditions: cell-expansion rate depends on water potential and wall-deposition rate depends on sugar concentration.

From experimental studies of the kinetics of wood formation (Wodzicki, 1971; Denne, 1972; Skene, 1972; Dodd & Fox, 1990; Horacek *et al.*, 1999), we formulated the following hypotheses: (1) variation in tracheid radial diameter along a tree ring is principally determined by the duration, and not by the rate, of tracheid enlargement; (2) variation in tracheid wall thickness is principally determined by the duration of wall thickening and not by the rate of wall deposition; and (3) the resulting variation in wood density is determined primarily by the duration of thickening and secondarily by the duration of tracheid enlargement, rather than by rates of expansion or cell wall deposition. In order to test these hypotheses and improve our understanding of the determinants of xylem cell development, we assessed the kinetics (duration and rate) of tracheid differentiation processes (enlargement and secondary wall formation), and the relationships between these kinetics and the resulting tracheid features and wood structure (cell diameter, cell wall thickness, and wood density). We used an extensive dataset from 45 trees from three species, Norway spruce [*Picea abies* (L.) Karst.], Scots pine (*Pinus sylvestris* L.), and silver fir (*Abies alba* Mill.). The trees were grown in three mixed stands in the Vosges Mountains (France) and monitored over 3 years (2007–2009). We analysed the data using a novel statistical approach (Cuny *et al.*, 2013).

Material and Methods

Study sites, wood sampling, and anatomical slide preparation

Three plots were selected in three comparable mixed stands composed of silver fir, Norway spruce, and Scots pine located between 350 and 650 m asl in the Vosges Mountains (northeast France). Complete inventories of the stands were used to select mature, dominant, healthy tree specimens (n = 5 of each species in each plot), for a total of 45 trees (5 trees × 3

species × 3 sites) (Table VI.S1).

Tree-ring formation was monitored in each of the selected trees from April to November 2007, 2008, and 2009. Microcores were collected weekly from tree stems and prepared in the laboratory. Transverse sections (5 to 10 µm thick) were cut with a rotary microtome (HM 355S, MM France); sections were stained with cresyl violet acetate and permanently mounted on glass slides using Histolaque LMR® (see Cuny *et al.*, 2012 for details on sampling strategy and microcore preparation).

Tracheid dimension measurements

For each tree, a well-preserved section of the entire ring was selected at the end of each growing season to measure the dimensions of tracheids produced during the year (Figure VI.S2). Digital images of the selected rings were analysed using WinCell (Regent Instruments, Canada) and tracheid dimensions were measured along at least three radial files. The following variables (Table VI.S2, Figure VI.S2) were recorded: (1) lumen radial diameter (LumRD); (2) wall radial thickness (WallRT); (3) lumen cross-sectional area (LumCA); and (4) lumen tangential diameter (LumTD).

During the enlargement phase, cell size increases mainly in the radial direction while the tangential diameter and length remain almost constant (Skene, 1972). Therefore, we used the cell radial diameter (CellRD) as a measure of the final outcome of the enlargement phase. CellRD was calculated as the sum of LumRD and WallRT for both sides (Table VI.S2, Figure VI.S2). Additionally, cell cross-sectional area (CellCA) was estimated based on a rectangular-shaped tracheid and a constant ratio of 1.2 between the tangential and radial wall thickness (Rathgeber *et al.*, 2006) (Table VI.S2, see Method VI.S1 for a detailed explanation).

In contrast, cell wall thickening involves the entire cell wall surface; the final wall thickness depends on the amount of wall material deposited and the volume of the cell to be covered (Skene, 1969). Moreover, although cell volume is constant after enlargement, deposition of material on the inner side of the cell wall reduces the volume of the lumen and hence the surface of deposition. Therefore, we used the wall cross-sectional area (WallCA)—a direct estimate of the amount of deposited material per cell—as the final outcome of the wall-thickening phase, instead of wall thickness as typically used.

To show variation in tracheid dimension along a ring, cell morphological measurements are grouped by radial file in profiles called tracheidograms (Vaganov, 1990). However, because the number of cells varied among radial files within and between trees, tracheidograms could not be directly averaged. A standardization method that allows modification of profile length (cell numbers) without changing profile shape (cell dimensions) was applied (Vaganov, 1990) using a dedicated function of the R package CAVIAR (R Core Team, 2012; Rathgeber, 2012). This method normalized all tracheidograms of a species to the mean number of cells produced by that species. The standardized tracheidograms were then averaged for the three plots and over the 3 years to obtain representations of each species's general tree-ring structure.

Mature tracheids were classified into different types of wood according to Mork's criterion (MC) (Denne, 1988) which is computed as the ratio between four times WallRT and LumRD (see Table VI.S2 for the formula). Cells were classified as follows: MC ≤ 0.5 = earlywood; MC >0.5 and <1.0 = transition wood; and MC ≥ 1 = latewood (Park & Spiecker, 2005).

Wood density measurements

At the end of 2009, two standard cores were taken from each tree, one from each side of the stem (at breast height and perpendicular to the slope), using a Pressler increment borer. A radial strip was cut from each core and exposed to X-ray radiation (Polge & Nicholls, 1972) to obtain a digital map of wood density along the sample. From this map, the CERD software indexes tree-ring boundaries from the density contrast between one ring's latewood and the adjacent ring's earlywood (Mothe *et al.*, 1998). Each annual ring was divided radially into 20 zones and the mean density of each zone was calculated. Thus, from each ring of each core, we obtained 20 values that described density variation along the ring (i.e. a 'microdensity' profile). The microdensity data of the two cores for each tree were averaged to obtain individual series. The individual microdensity profiles were then averaged for the three stands over the 3 years of study to obtain general, species-specific microdensity profiles.

Tracheid allometry and morphometric density calculation

To explore relationships between cell wall thickness, cell size, and the amount of wall material deposited within the cell, we developed a geometric model of tracheid dimensions expressing WallRT as a function of CellRD, cell tangential diameter (CellTD), and WallCA (see development in Method VI.S1)

To assess the influence of changes in tracheid dimension on wood microdensity profile, we used the geometric model of Rathgeber *et al.* (2006), which allowed calculation of morphometric density (MMD) from WallCA, CellRD, and CellTD (Method VI.S2).

Microscopic observations of xylem cell differentiation

Approximately 4300 anatomical sections were observed using an optical microscope (AxioImager.M2; Carl Zeiss SAS, France) under visible and polarized light at ×100–400 magnification to count cells in the different phases of development. The temporal succession of xylem cells developmental phases formed pattern of characteristic strips along the tree ring as it formed (Figure VI.S3a). Cells in the radial enlargement zone were larger than cambial cells but still had thin walls (Figure VI.S3c). Under polarized light, enlarging cells presented dark primary walls (Figure VI.S3d), while thickening cells exhibited birefringent secondary walls (Figure VI.S3e); the birefringence was caused by the orientation of cellulose microfibrils orientation (Abe *et al.*, 1997). Cresyl violet acetate, which stains cellulose in purple and lignin in blue (Kutscha *et al.*, 1975), was used to track the process of lignification; thickening cell walls appeared violet and blue, indicating that lignification was in progress (Figure VI.S3f). Mature tracheids had entirely lignified (completely blue) walls; these cells had large diameters and thin walls in earlywood (Figure VI.S3g), and small diameters and thick walls in latewood (Figure VI.S3h).

The cell number of the previous year was counted on three radial files per sample and used to standardize the raw cell number of the current year to reduce variability in the data (Rossi *et al.*, 2003). A dedicated function of the R package CAVIAR (R Core Team, 2012; Rathgeber, 2012) was used to apply this standardization to all samples.

Wood formation dynamics description

To describe the dynamics of wood formation and the kinetics of tracheid differentiation accurately, we used a novel statistical approach (Cuny *et al.*, 2013). Generalized additive models (GAMs) were fitted to the standardized number of cells in the cambial, enlargement, wall-thickening, and mature zones for each year on each individual tree, using the R mgcv package (Wood, 2006). The values of the fitted models were averaged for the monitored plots over the 3-year period to calculate means representing the general wood-formation dynamics of each species.

For each species, we used the average cell numbers predicted by the GAMs to calculate the date of entrance of each cell into each development zone. From these dates, the residence time of each cell *i* in the cambial ($d_{C,i}$), enlargement ($d_{E,i}$), and thickening ($d_{T,i}$) zones, and the total duration of that cell's formation ($d_{F,i}$), were computed.

The daily rate of cell production by the cambial zone for a day *t* ($r_{C,t}$) was calculated as the difference between the total number of cells predicted at day *t* and at day *t*-1. The rate of division of each cambial cell on a day *t* ($r_{D,t}$) was estimated by dividing $r_{C,t}$ by the number of cambial cells predicted at day *t*. We attributed a rate of division to each tree-ring cell *i* ($r_{D,i}$) by averaging the rate of division (r_D) for the period when the cell was in the cambial zone. The inverse of r_D gives an estimate of the cell cycle length (CCL).

The mean rates of cell radial diameter enlargement ($r_{E,i}$), cell swelling ($r_{S,i}$), wall thickening ($r_{T,i}$), and wall deposition ($r_{W,i}$) were computed for each cell *i* by dividing a cell's final dimensions by the duration it spent in the corresponding phases (Table VI.S2).

To explore the relationship between the kinetics of the processes and the produced cell features, we expressed the final tracheid dimensions (CellRD and WallCA) as functions of the durations (d_E and d_T) and rates (r_E and r_W) of the corresponding phases of differentiation:

$$\text{CellRD} = d_E \times r_E \quad (1)$$

$$\text{WallCA} = d_T \times r_W \quad (2)$$

Data analysis

Analyses of covariance were carried out using R (R Core Team, 2012) to assess relationships between kinetics of tracheid differentiation and the resulting tree-ring structure by species.

Sensitivity analyses were performed to estimate the relative contributions of input variables to results of the different mechanistic models. These analyses measured differences in model output when values of input variables were changed one at a time within a range of

twice their standard deviations, holding the other variables constant at their mean values (Cariboni *et al.*, 2007). We used the results of the sensitivity analyses to quantify the relative contributions of duration and rate of cell enlargement and thickening to tree-ring structure (CellRD, WallCA, wall thickness, and wood density).

Results

Tree ring structure

Earlywood represented approximately 40% of the tree rings (Figure VI.1). However, pine had two times less transition wood than fir or spruce (12% vs. 22% and 21%, respectively) and thus a larger proportion of latewood (52% vs. 40% and 39%, respectively). The division of rings into earlywood, transition wood, and latewood based on MC did not allow definite cell types to be distinguished; the transition in tracheid features was rather smooth.

The first cells were 3 to 4 times larger (approximately 45 µm) than the last ones (10–20 µm); thus, CellRD decreased progressively from the beginning to the end of the rings (Figure VI.1a, b, c). Because the tangential diameter was almost constant (35 ± 2 µm, mean ± SD), the changes in cell cross-sectional area followed those of CellRD.

Tracheid wall thickness followed a hook curve from the beginning to the end of the rings (Figure VI.1d, e, f). Wall thickness was minimal (2.5–3.0 µm) in the first 25% of the rings, after which it increased to a maximum of 6 µm in latewood and decreased abruptly to about 4–5 µm in the last cells. The shape of the wall cross-sectional area (WallCA) curves resembled an anticline fold with a gentle slope on the left side and a steep slope, just after the top, on the right side. In the first 75% of the rings, WallCA increased by 8% in pine (from 520 to 560 µm²) and by 30% in fir and spruce (from about 500 to 650 µm²), and then decreased abruptly to its minimum (about 300 µm2).

Sensitivity analysis of the geometric model of cell wall thickness (Method VI.S1) showed that 67% of the changes in wall thickness along a ring could be attributed to changes in CellRD, and only 33% to changes in WallCA (Table VI.S3).

S-shaped wood density profiles (Figure VI.1g, h, i) presented minimal values in earlywood (approximately 450 kg m-3 in pine, and 375 kg m-3 in fir and spruce). Density then increased and reached its maximum values in latewood (900, 800, 930 kg m-3 in pine, fir, and spruce, respectively). Only in pines, density decreased slightly in the last 15% of the rings.

Highly significant correlations were found between measured tracheid features and X-ray-measured wood density (Table VI.S4, Figure VI.S4). The morphometric density computed from the tracheid dimensions was in agreement with the X-ray density (Figure VI.1g, h, i). Sensitivity analysis of the geometric model of wood morphometric density (Methods VI.S2)

suggested that changes in CellRD accounted for 75% of the changes in wood density along the rings and variation in WallCA accounted for the remaining 25% (Table VI.S5).

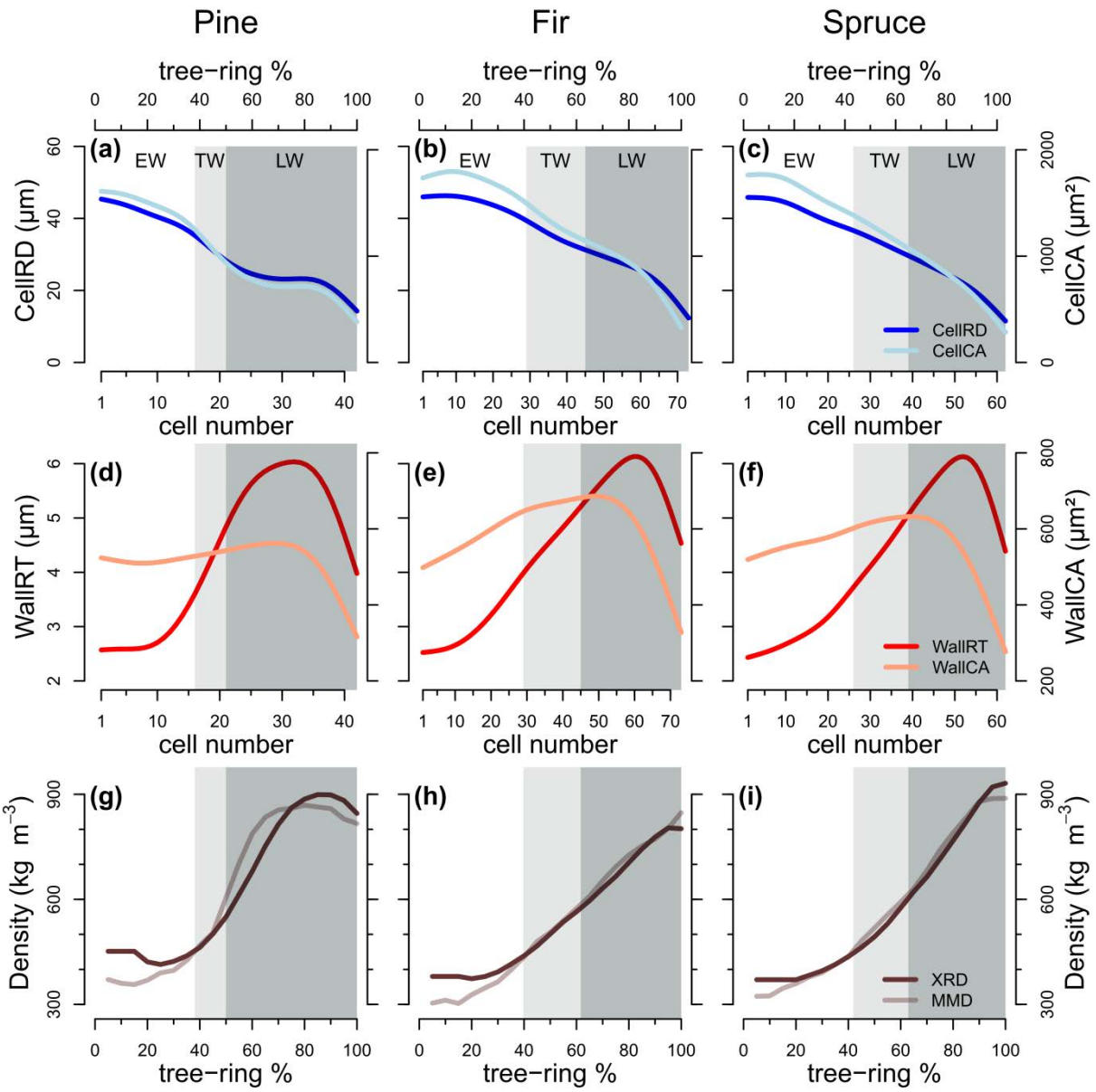

Figure VI.1: Variation in cell (CellCA) and wall (WallCA) cross-sectional area, cell radial diameter (CellRD), cell wall radial thickness (WallRT), and x-ray measured density (XRD) and morphometric wood density (MMD) along tree rings of three conifer species (Scots pine, silver fir, and Norway spruce). For each species, lines represent the mean values for 15 trees over 3 years (2007–2009). White, light-grey, and dark-grey areas represent earlywood (EW), transition wood (TW), and latewood (LW), respectively.

Wood formation calendar and dynamics

The change in the number of cambial cells (n_C) during the growing season followed a flat, bell-shaped curve skewed to the left (Figure VI.2a, b, c). At the beginning of the year, the resting cambium cell counts were about 6-7 cells. In early April, n_C increased rapidly after the onset of cambial activity, reaching a maximum of 9-10 cells in May. From June until the end of summer, n_C decreased slowly, returning to its resting value in mid-September.

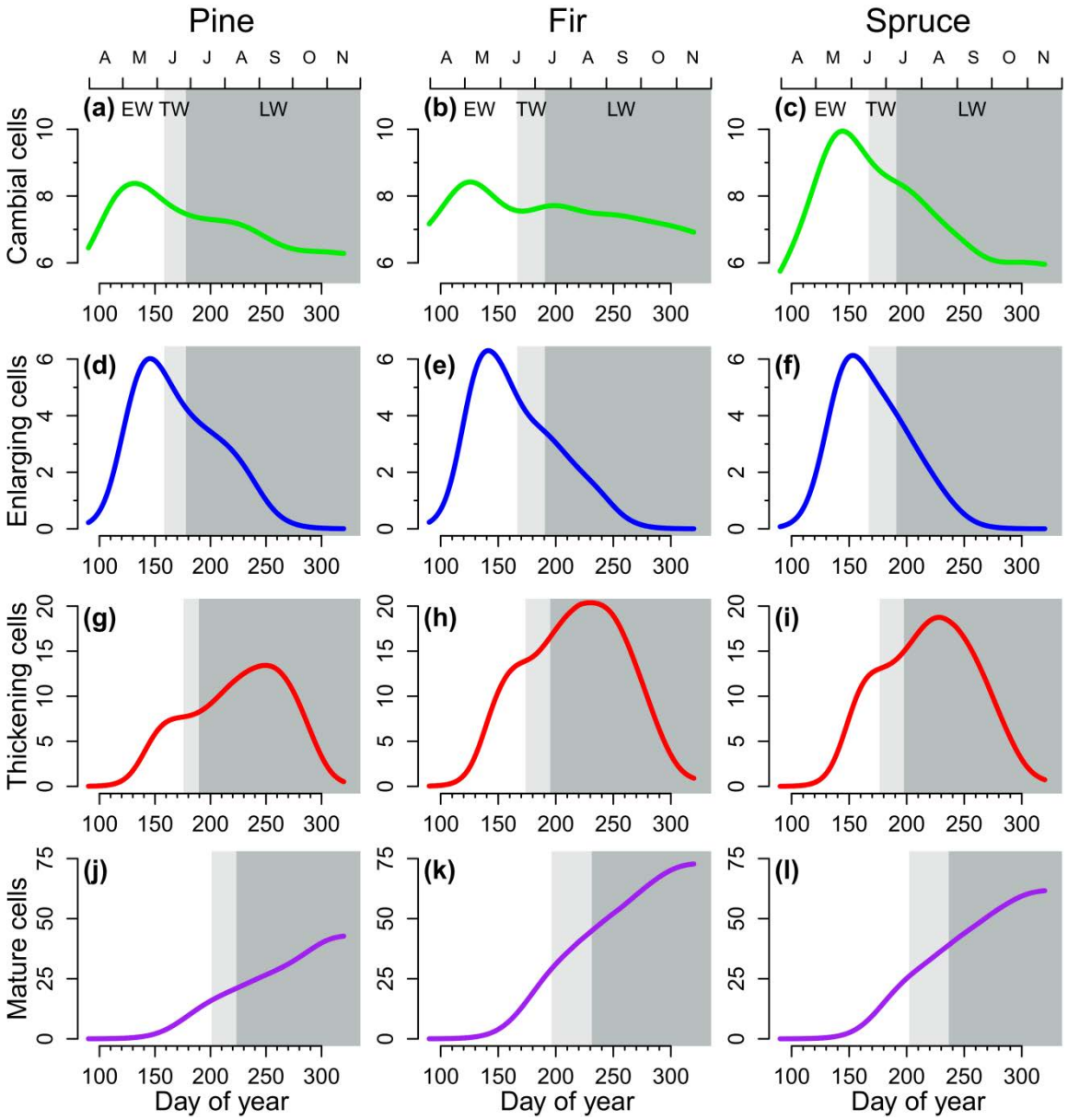

Figure VI.2: Generalized additive models (GAMs) fitted to the weekly cell count in the cambial, enlargement, secondary wall formation, and mature zones for Scots pine, silver fir, and Norway spruce (n = 15 per species) over 3 years (2007–2009). White, light-grey, and dark-grey areas represent earlywood (EW), transition wood (TW), and latewood (LW), respectively..

The change in number of enlarging cells (n_E) also followed a left-skewed, bell-shaped curve (Figure VI.2d, e, f). Cells entered the enlargement zone in mid-April and began to accumulate. The increase in n_E in spring was more pronounced than that of n_C, and slightly shifted in time, culminating at about 6 cells at the end of May. The slow decrease in n_E, from June to mid-September, was also more regular than that for cambial cells.

The change in number of thickening cells (n_T) followed a bimodal, right-skewed curve (Figure VI.2g, h, i). The first cells entered the thickening zone in late April or early May. An initial rapid increase in spring led to a first high point (about 7 cells in pine and 13 cells in fir and spruce) in the first half of June; n_T increased rapidly again to reach a second high point and maximum (about 16 cells in pine and 22 cells in fir and spruce) in summer. Finally, a

rapid decrease in n_T led to emptying of the thickening zone in early November. Interestingly, the dip in n_T between the spring and summer high points corresponded to the passing of the future transition wood cells through the thickening zone.

The change in number of mature cells (n_M) followed a double-sigmoid curve consisting of two periods of rapid accumulation separated by a period of slower accumulation (Figure VI.2j, k, l). The first mature cells were completed during the second half of May. Earlywood cells became mature during the rapid period of accumulation from spring until mid-July. Additional transition wood cells matured during the slowest period (mid-July to mid-August). Finally, latewood cells were completed between late August and late October.

Cell residence times in each development phases

Newly formed xylem cells spent an average of 4 days in the cambial zone (mean ± SE = 4 ± 2 days in pine, 2 ± 1 days in fir, and 6 ± 2 days in spruce). This duration decreased along consecutive cells of the rings, declining from 6 to 3 days in pine, from 3 to 1 days in fir, and from 10 to 5 days in spruce (Figure VI.3a, b, c).

Differentiating xylem cells took an average of 9 days to enlarge, and required 40% more time in pine than in fir and spruce (13 ± 5, 7 ± 3, and 8 ± 3 days, respectively). Residence time in the enlargement zone followed a trend that paralleled that in the cambial zone, decreasing from the first to the last cells produced (from 18 to 6 days in pine, 14 to 5 days in fir, and 12 to 4 days in spruce) (Figure VI.3d, e, f). These trends resulted in strong, linear, species-specific relationships between residence times in the cambial and enlargement zones ($P < 0.001$, $r^2 = 0.85$, Figure VI.S5).

Maturing tracheids required slightly more than 1 month (35 ± 13 days) to build their secondary wall. Residence time in the thickening zone generally increased along successively produced cells, following a stretched, S-shaped curve (Figure VI.3g, h, i). Secondary wall formation of earlywood, transition wood, and latewood tracheids required approximately 4, 5, and 7 weeks, respectively.

The average total duration of tracheid formation was 44 days (49.6 ± 8.4, 40.9 ± 10.6, and 42.2 ± 10.9 days for pine, fir, and spruce, respectively); it increased, following a muted S-shaped curve, over the course of cell production (Figure VI.3j, k, l). Tracheid formation took approximately 1 month for the first half of cells produced and increased to 2 month by 80% of tracheid production, after which it decreased slightly in pine and increased slightly in fir and spruce.

Interestingly, the duration of differentiation better discriminated the different types of tracheids than the morphological characteristics originally used to define them. In the first part of the tree ring, cells with short, stable thickening duration corresponded to earlywood (Figure VI.3g, h, i). In the second part of the ring, cells in which thickening duration increased but enlargement duration rapidly decreased corresponded to transition wood. In the last part of the ring, cells with long thickening duration and short, stable enlargement duration

corresponded to latewood.

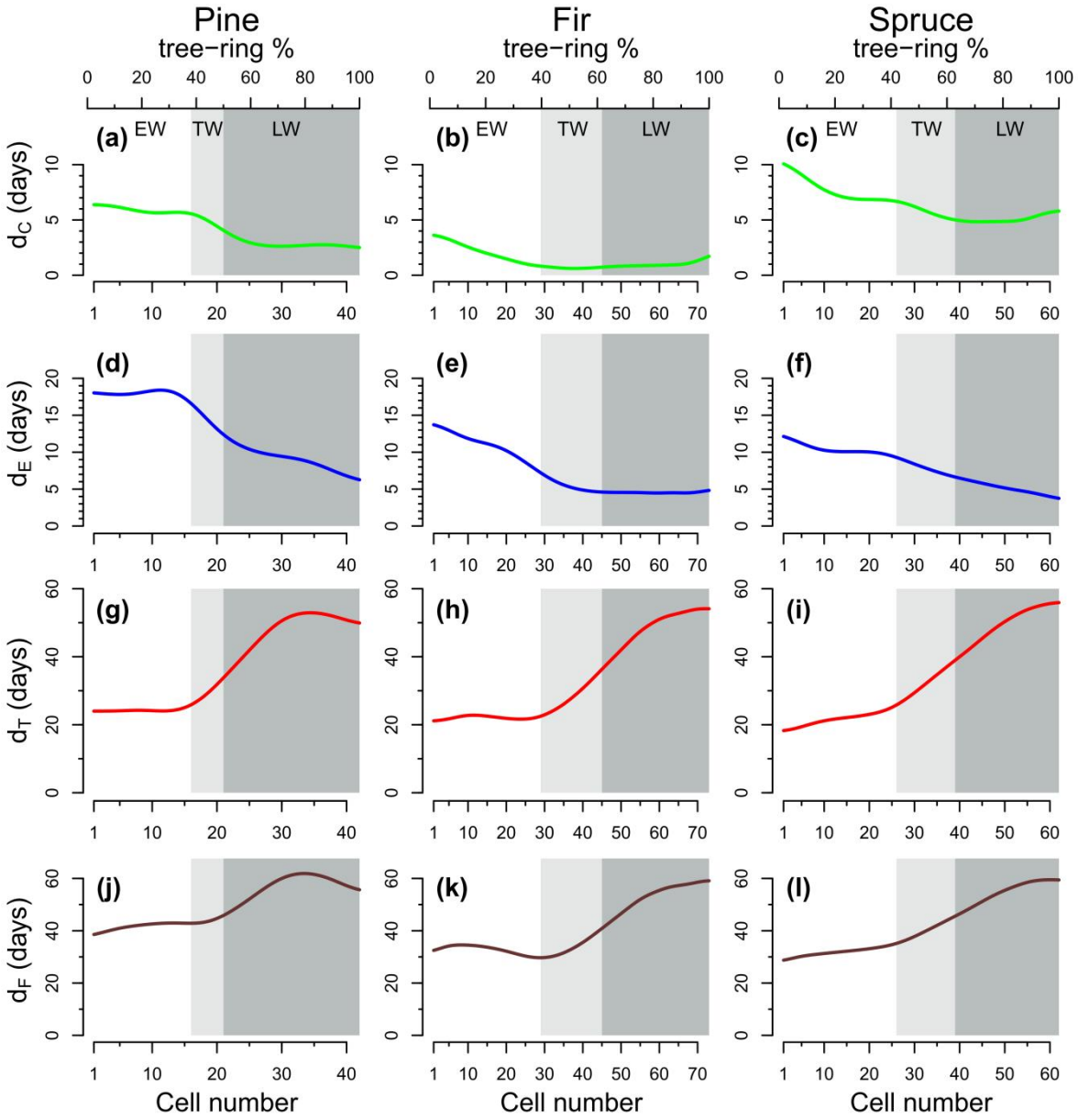

Figure VI.3: Cell residence duration in the cambial (d_C), enlargement (d_E), and wall-thickening (d_T) zones, and total duration of formation (d_F) of tracheids along tree rings of Scots pine, silver fir, and Norway spruce. White, light-grey, and dark-grey areas represent earlywood (EW), transition wood (TW), and latewood (LW), respectively.

Cell differentiation rates

The rates of cell division followed bimodal patterns of variations (Figure VI.4a, b, c). Cambial cells divided at an average rate (r_D) of 0.05 day^{-1}, indicating that it took nearly 20 days for a mother cell to produce a new daughter cell. Cell division in pine was 45% slower than that in fir and 30% slower than in spruce (r_D = 0.04 ± 0.01, 0.07 ± 0.02, and 0.05 ± 0.01 day^{-1}, respectively), which was also reflected in the longer CCL in pine (28 ± 8, 15 ± 9, and 19 ± 10 days in pine, fir, and spruce, respectively).

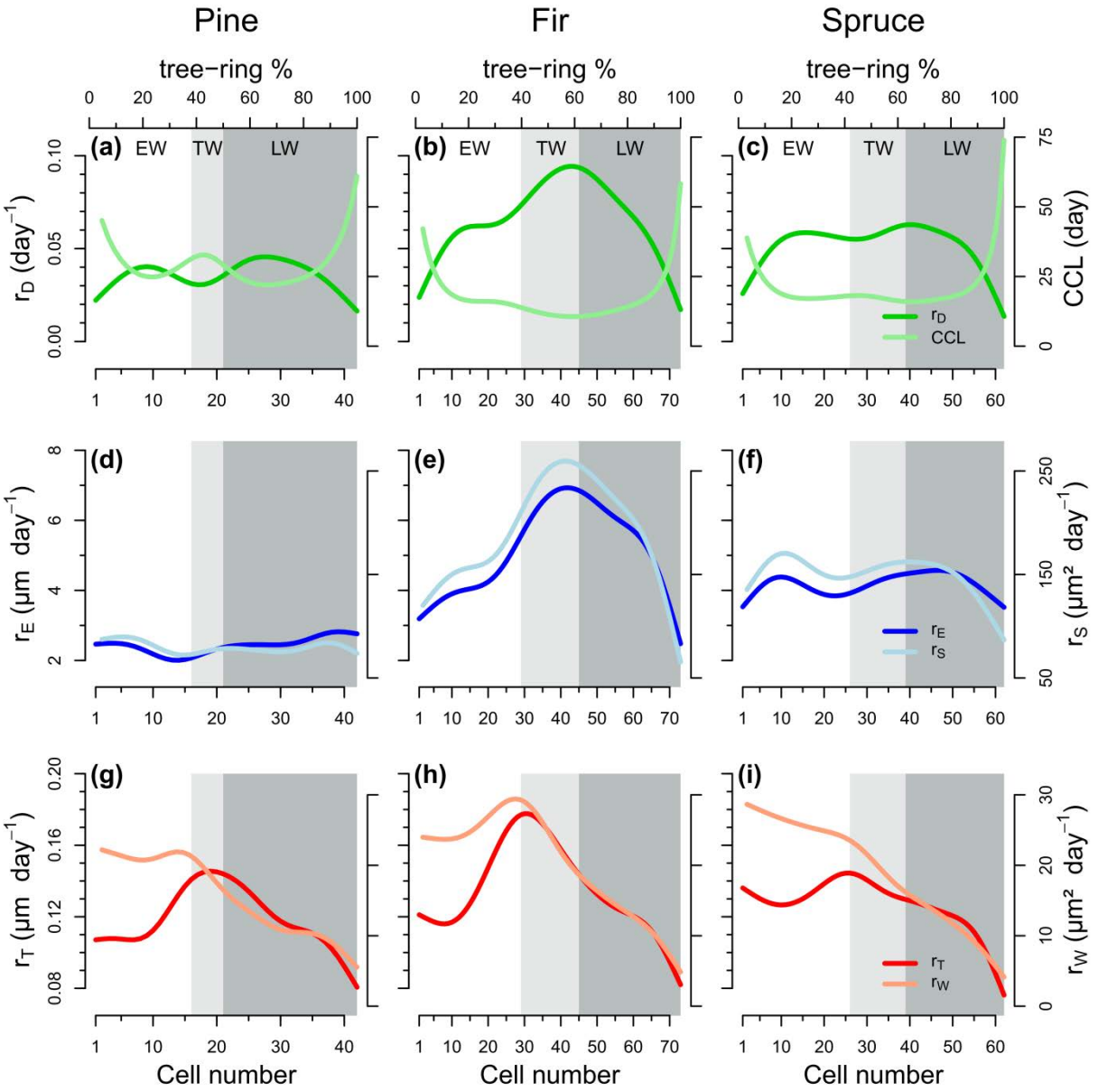

Figure VI.4: Rates of division (r_d), cell cycle length (CCL), radial diameter enlargement (r_E), increase in cell size (r_S), wall thickening (r_T), and wall deposition (r_W) of tracheids along tree rings of Scots pine, silver fir, and Norway spruce. White, light-grey, and dark-grey areas represent earlywood (EW), transition wood (TW), and latewood (LW), respectively.

The rates of cell enlargement (r_E) and cross-sectional-area expansion (r_S) varied along the ring in patterns that resembled those observed for r_D (Figure VI.4d, e, f). On average, cell diameter enlarged at a rate of 4.2 µm day^{-1}. Similar differences were observed between species as for r_D; r_E in pine was 50% slower than in fir and 40% slower than in spruce (r_E = 2.4 ± 0.2, 5.1 ± 0.3, and 4.2 ± 0.3 µm day^{-1}, respectively). Moreover, a highly significant relationship was found between r_E and r_D ($r^2 = 0.78$, $P < 0.001$, n=177, Figure VI.S5).

The rates of wall deposition (r_W) exhibited characteristic 'slide-shaped' curves that differed considerably from the bell-shaped curves corresponding to rates of thickening (r_T) (Figure VI.4g, h, i). In earlywood cells, r_W remained stable between 20–30 µm² day^{-1}, and then decreased continuously during production of transition wood and latewood cells to a

minimum of approximately 5 µm² day^{-1} for the very last cells.

Relationship between dynamics of wood formation and tree-ring structure

The radial diameter (CellRD) of a tracheid was closely related to the duration (d_E), but not to the rate (r_E) of its enlargement (Figure VI.5a, b). A highly significant, linear, species-specific relationship was obtained between d_E and CellRD ($P < 0.001$, r^2=0.85, n=177, Table VI.S6), whereas no significant relationship was found between r_E and CellRD. Sensitivity analysis of the elementary model of cell enlargement (CellRD = $d_E \times r_E$) allowed us to estimate that variation in d_E along the tree ring contributed to 75% of the changes in CellRD, while r_E contributed to only 25% of the changes (Table VI.S7). However, some differences in the relative contributions of d_E and r_E to CellRD were observed between species. The influence of d_E was lower in fir than in pine or spruce (65%, 78%, and 81% respectively), and hence the influence of r_E was higher in fir (35%, 22%, and 19%, respectively).

On the other hand, the wall cross-sectional area (WallCA) was not linearly related to the duration of thickening ($P > 0.1$, $r^2 = 0.06$, n = 177), and was only poorly related to deposition rate ($P < 0.01$, $r^2 = 0.20$, n = 177) (Figure VI.5c, d). Sensitivity analysis of the elementary model of wall thickening (WallCA = $d_T \times r_W$), suggested that variation in thickening duration and deposition rate along the rings contributed equally to changes in WallCA (Table VI.S8). As expected, a highly significant, non-species-specific relationship was observed between d_T and wall thickness ($P < 0.001$, $r^2 = 0.78$, n = 177); however, the relationship stood for only half of the cells, as the first 35% and the last 15% of cells clearly moved away from the regression line (Figure VI.5e). The most striking result was a very significant, negative, non-species-specific relationship between d_T and r_W ($P < 0.001$, $r^2 = 0.91$, n = 177), which was broken only for the last-produced cells, when d_T stopped increasing and r_W strongly decreased (Figure VI.5f).

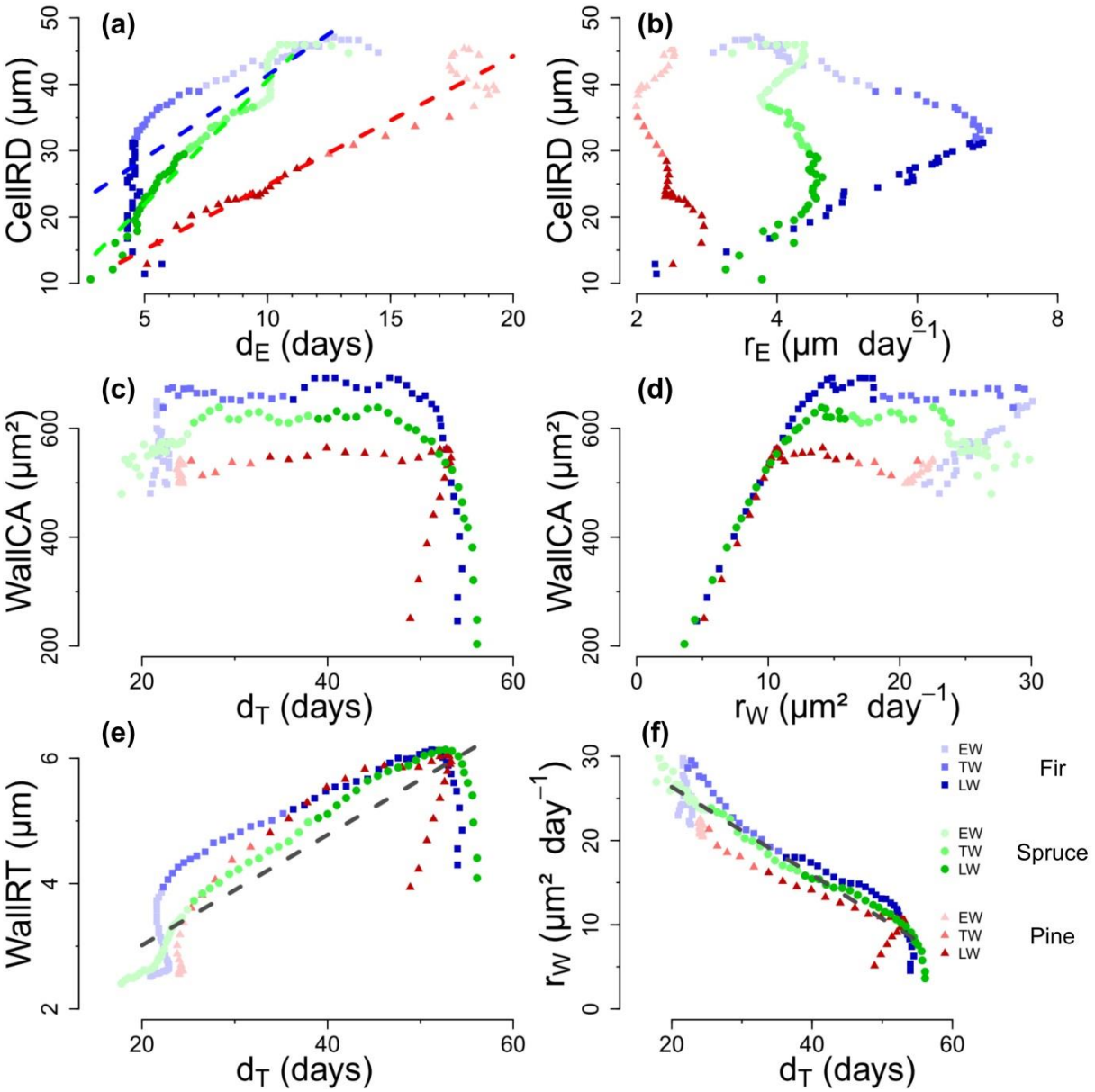

Figure VI.5: Relationships between the durations (d_E and d_T) and rates (r_E and r_w) of tracheid differentiation (enlargement and wall formation) with the resulting cell radial diameter (CellRD), wall cross-sectional area (WallCA), and radial thickness (WallRT) of tracheids along rings of three conifer species (Scots pine, silver fir, and Norway spruce). For each species, each point represents a single cell along an average ring (mean values for 15 trees over 3 years). Light-tone, middle-tone, and dark-tone points represent earlywood (EW), transition wood (TW), and latewood (LW) cells, respectively.

Discussion

Complex intra-annual dynamics of wood formation

The results of the present study, conducted over 3 years in three mixed stands of silver fir, Norway spruce, and Scots pine in north-eastern France, closely matched complex intra-annual dynamics patterns that we observed in a previous study at a single site (Cuny *et al.*, 2013). The results presented here validated our previous hypothesis that the kinetics of xylogenesis processes discriminate the different types of xylem cells (earlywood, transition

wood, and latewood cells) (Cuny *et al.*, 2013). Indeed, we observed that the duration of enlargement decreased throughout the growing season but fell more abruptly when transition wood cells were produced (Figure VI.6a). The duration of wall thickening, which remained remarkably stable during earlywood cell production, increased abruptly during the production of transition wood cells. Considering the rates of cell differentiation, it was clearly apparent that after small variations around a maximum during earlywood production, the rate of cell wall deposition decreased abruptly during transition wood and latewood production (Figure VI.6b). The rate of cell expansion could be generally described as flat at its minimum during earlywood production, increasing during transition-wood production, and falling back to its minimum during latewood formation. Thus, our results demonstrate that the kinetics (the rates and especially the durations) of tracheid differentiation are relevant, process-based drivers of tree-ring structure.

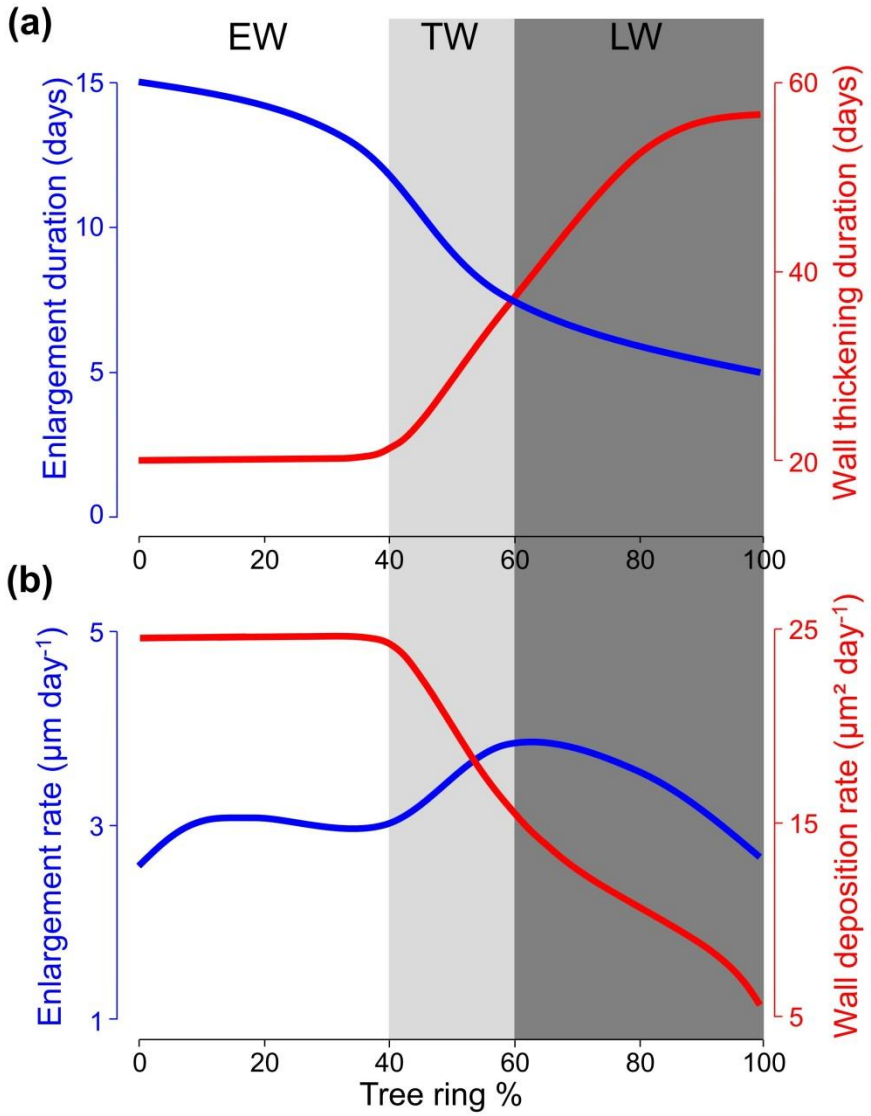

Figure VI.6: Typical evolution of the duration and rate of cell enlargement, and wall thickening duration during tracheid differentiation along a conifer ring, separated into earlywood (EW), transition wood (TW), and latewood (LW).

Relationships between kinetics and final dimensions of tracheids

Our initial hypothesis, that the final size of a cell is principally determined by the duration of its enlargement, was confirmed by our results (Figure VI.7). Our findings are in agreement with most experimental studies on the kinetics of tracheid differentiation, which show that the typical decrease in cell size along the ring parallels an overall decrease in duration of enlargement phase, whereas the rate of enlargement varies less and more irregularly (Wodzicki, 1971; Skene, 1972; Horacek *et al.*, 1999). Moreover, several authors have found that the tapering of tracheid diameter along the stem is related to changes in the duration of enlargement (Denne, 1972; Dodd & Fox, 1990; Ridoutt & Sands, 1993; Anfodillo *et al.*, 2012). This evidence leads us to conclude that whatever the studied axis of variation (e.g. along a radial file in an annual tree-ring, or along a vascular element/route in the stem), the final size of a functional tracheid is mainly controlled by the duration of its enlargement.

Our second hypothesis, that the final thickness of the cell wall is principally determined by the duration of the thickening phase, was not supported by our results. Rather, we showed that the final wall thickness depended primarily on cell size and secondarily on the amount of wall material deposited, which depended on the duration of thickening as much as on the rate of deposition (Figure VI.7). Thus, cell wall thickness is principally determined by the duration of enlargement (75% × 67% = 50%) and secondarily by the duration of thickening and the rate of cell wall deposition. However, several authors have associated the increase in cell wall thickness along an annual ring with increasing duration of the thickening phase (Wodzicki, 1971; Skene, 1972; Horacek *et al.*, 1999). We also found a strong correlation between cell wall thickness and duration of thickening, but we argue that this is not a causal relationship because wall thickness is not a direct outcome of the dynamics of wall deposition.

The duration and rate of cell wall deposition were highly correlated, in agreement with Skene's pioneering work Skene's pioneer work (Skene, 1969), which found no difference in volume of wall material deposited in earlywood and latewood cells and concluded that the increasing duration of secondary wall formation throughout the growing season was accompanied by decreasing rates of wall material deposition. Indeed, our observation of a moderate increase in cell wall material deposited along most of the produced cells indicated that the seasonal increase in duration of thickening for these cells more than counter-balanced the decrease in deposition rate. The duration of thickening levelled off or decreased only in the last quarter of the ring, at which point it no longer balanced the decline in rate of cell wall deposition; hence, a dramatic collapse occurred in the amount of material deposited for the last latewood cells of the ring.

Our third hypothesis, that wood density is determined principally by the duration of thickening, was thus refuted by our results. We showed that wood density depended primarily on radial diameter, and to a much lesser degree on the cross-sectional area of tracheid walls (Figure VI.7). As the duration of the enlargement phase contributed to the majority of the changes in cell diameter, it can be said that it also contributed to the majority (75% × 75% = 56%) of the changes in wood density. These results highlighted that the duration of enlargement is the key determinant of a tracheid's final shape: it is the main predictor of cell

diameter, which in turn is the main driver of cell wall thickness. Therefore, the duration of the enlargement period is the primary determinant of wood density and tree-ring structure.

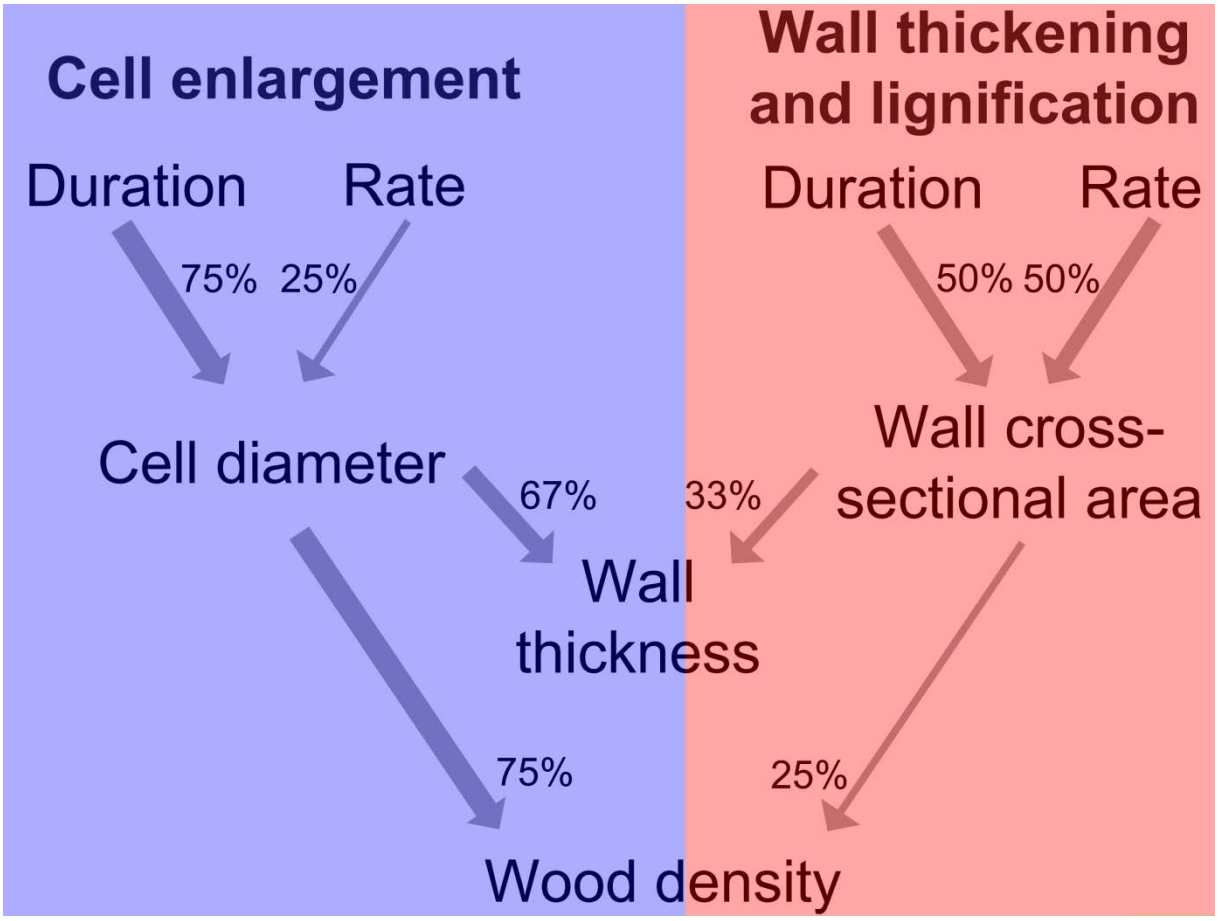

Figure VI.7: Relative contribution of the different components of wood formation to the resulting tracheid dimensions and wood density.

Metabolic regulation vs. developmental control of xylogenesis

Secondary growth represents the most important carbon sink in trees, but due to its low priority level for carbon allocation, this growth depends on the adjustment of several key processes of plant functioning (Körner, 2003). Nutrient uptake and photosynthesis are required for production of the carbohydrates involved in primary and secondary cell wall construction. Respiration, water uptake, and translocation of sugars supply the cambial zone and developing xylem with energy and building materials (Taiz & Zeiger, 1998). Xylogenesis thus involves integrated functioning of the entire plant system and is a highly regulated process (Savidge, 2001; Aloni, 2013). Sundberg *et al.* (2000) proposed that the duration and rate of the sub-processes of xylogenesis are controlled by different regulatory mechanisms. Process duration is thought to be genetically controlled, whereas process rates are thought to be related to plant metabolism, which reflects the physiological state of the plant as well as the influence of the environment.

Our results demonstrated the greater importance of process duration than rate in xylogenesis; in particular the duration of the enlargement phase emerged as the main driver of

xylem cell morphology. Therefore, we argue that typical changes in tracheid features along a conifer ring, from the wide, thin-walled cells of light earlywood to the narrow, thick-walled cells of dense latewood, are primarily genetically fixed rather than driven by changes in environmental factors. The parallel changes in the time cells spent in the cambial and enlargement zones throughout the growing season showed that the kinetics of cell division and enlargement were tightly linked, as also pointed out by Vaganov *et al.* (2006; 2011). Both phases involve cell expansion; expansion is slow in dividing cells and ends with division of the mother cell into two daughter cells, while for enlarging cells it is faster and ends with a large, irreversible increase in cell diameter (Cosgrove, 2000a; Perrot-Rechenmann, 2010). A common set of phytohormones (auxins, cytokinins, gibberellins) controls the division and enlargement phases (Taiz & Zeiger, 1998; Matsumoto-Kitano *et al.*, 2008). Auxin in particular is known as a morphogen, and is distributed at a steep concentration gradient across the division and enlargement zones (Uggla *et al.*, 1996; Tuominen *et al.*, 1997; Sundberg *et al.*, 2000). The slope of the auxin gradient determines the width of the zones and the time spent by cells in each zone (Tuominen *et al.*, 1997; Sundberg *et al.*, 2000).

On the other hand, we found that the amount of material deposited during secondary wall formation was influenced by the deposition rate, but that this influence was more than counterbalanced by the duration of cell wall formation except in the last latewood cells. A metabolic limitation to secondary wall formation could be expected, as this process represents the bulk of carbon allocation in trees (Zhong & Zheng-Hua, 2009) , but the way in which developmental control overcomes metabolic limitations to impose regular changes in cell wall thickness along a ring remains an intriguing open question. Groover & Jones (1999) proposed a mechanism coordinating secondary cell wall synthesis and apoptosis that could provide the biological basis for the coupling between rate and duration of secondary wall formation. These researchers observed accumulation of protease in the extracellular matrix during the secretion of wall material (Groover & Jones, 1999). Once a critical concentration of protease is reached, cell death is triggered and secondary wall formation stops. On the basis of this mechanism, the decreasing rate of wall deposition throughout the growing season should be accompanied by decreased secretion of protease in the extracellular matrix. Accordingly, as the growing season progresses, more time should be required for protease to reach the critical level, delaying apoptosis and increasing the duration of wall deposition. It is possible that the concentration of protease is insufficient to reach the critical threshold at the end of the growing season, but that it is replaced by other factors that can trigger apoptosis, such as sucrose concentration or reactive oxygen species (Bollhöner *et al.*, 2012).

In summary, the duration of the differentiation phases is the main driver of cell morphology, tree-ring structure, and wood density profiles. This suggests strong developmental control of wood formation, tree-ring structure, and density profile, which appear to be genetically fixed in conifer species rather than driven by seasonal changes in environmental factors. Our findings also suggest that structural and physiological trade-offs do not generally result in immediate adjustment of xylem cell morphology to current metabolic constraints; rather, structural and physiological trade-offs have developed through long-term evolutionary processes.

Acknowledgements

We thank E. Cornu, E. Farré, C. Freyburger, P. Gelhaye and A. Mercanti for fieldwork and monitoring; M. Harroué for sample preparation in the laboratory; Jana Dlouha for its help in developing the geometric model of tracheid dimension.

References

Abe H, Funada R, Ohtani J, Fukazawa K. 1997. Changes in the arrangement of cellulose microfibrils associated with the cessation of cell expansion in tracheids. *Trees-Structure and Function* **11**(6): 328-332.

Aloni R. 2013. The role of hormones in controlling vascular differentiation. In *Plant Cell Monographs*. Berlin, Heidelberg: Springer pp. 99-139

Anfodillo T, Deslauriers A, Menardi R, Tedoldi L, Petit G, Rossi S. 2012. Widening of xylem conduits in a conifer tree depends on the longer time of cell expansion downwards along the stem. *Journal of Experimental Botany* **63**(2): 837-845.

Boerjan W, Ralph J, Baucher M. 2003. Lignin biosynthesis. *Annual Review of Plant Biology* **54**: 519-546.

Bollhöner B, Prestele J, Tuominen H. 2012. Xylem cell death: emerging understanding of regulation and function. *Journal of Experimental Botany* **63**(3): 1081-1094.

Bouriaud O, Leban JM, Bert D, Deleuze C. 2005. Intra-annual variations in climate influence growth and wood density of Norway spruce. *Tree Physiology* **25**(6): 651-660.

Brown HP, Panshin AJ, Forsaith CC. 1949. *Textbook of wood technology*. New York: McGraw Hill Book Company Inc.

Briffa K, Schweingruber F, Jones P, Osborn T, Harris I, Shiyatov S, Vaganov E, Grudd H. 1998. Trees tell of past climates: but are they speaking less clearly today? *Philosophical Transactions of the Royal Society of London. Series B: Biological Sciences* **353** (1365): 65-73.

Cariboni J, Gatelli D, Liska R, Saltelli A. 2007. The role of sensitivity analysis in ecological modelling. *Ecological Modelling* **203**(1-2): 167-182.

Chave J, Coomes D, Jansen S, Lewis SL, Swenson NG, Zanne AE. 2009. Towards a worldwide wood economics spectrum. *Ecology Letters* **12**(4): 351-366.

Cochard H, Froux F, Mayr FFS, Coutand C. 2004. Xylem wall collapse in water-stressed pine needles. *Plant Physiology* **134**(1): 401-408.

Cosgrove DJ. 2000a. Expansive growth of plant cell walls. *Plant Physiology and Biochemistry* **38**(1-2): 109-124.

Cosgrove DJ. 2000b. Loosening of plant cell walls by expansins. *Nature* **407**(6802): 321-326.

Cuny HE, Rathgeber CBK, Lebourgeois F, Fortin M, Fournier M. 2012. Life strategies in intra-annual dynamics of wood formation: example of three conifer species in a temperate forest in north-east France. *Tree Physiology* **32**(5): 612-625.

Cuny HE, Rathgeber CBK, Senga Kiesse T, Hartmann FP, Barbeito I, Fournier M. 2013. Generalized additive models reveal the intrinsic complexity of wood formation dynamics. *Journal of Experimental Botany*.

Deleuze C, Houllier F. 1998. A simple process-based xylem growth model for describing wood microdensitometric profiles. *Journal of Theoretical Biology* **193**(1): 99-113.

Denne MP. 1972. A Comparison of Root- and Shoot-wood Development in Conifer Seedlings. *Annals of Botany* **36**(3): 579-587.

Denne MP. 1988. Definition of latewood according to Mork (1928). *Iawa Bulletin* **10**(1): 59-62.

Dodd RS, Fox P. 1990. Kinetics of Tracheid Differentiation in Douglas-fir. *Annals of Botany* **65**(6): 649-657.

Donaldson LA. 2001. Lignification and lignin topochemistry—an ultrastructural view. *Phytochemistry* **57**(6): 859-873.

Drew DM, Downes GM, Battaglia M. 2010. CAMBIUM, a process-based model of daily xylem development in Eucalyptus. *Journal of Theoretical Biology* **264**(2): 395-406.

Eglin T, Francois C, Michelot A, Delpierre N, Damesin C. 2010. Linking intra-seasonal variations in climate and tree-ring $\delta^{13}C$: A functional modelling approach. *Ecological Modelling* **221**(15): 1779-1797.

Fonti P, von Arx G, Garcia-Gonzalez I, Eilmann B, Sass-Klaassen U, Gaertner H, Eckstein D. 2010. Studying global change through investigation of the plastic responses of xylem anatomy in tree rings. *New Phytologist* **185**(1): 42-53.

Fournier M, Stokes A, Coutand C, Fourcaud T, Moulia B. 2006. *Tree biomechanics and growth strategies in the context of forest functional ecology*.

Fritts HC, Shashkin A, Downes GM. 1999. *A simulation model of conifer ring growth and cell structure*.

Gagen M, McCarroll D, Edouard JL. 2006. Combining ring width, density and stable carbon isotope proxies to enhance the climate signal in tree-rings: An example from the southern French Alps. *Climatic Change* **78**(2-4): 363-379.

Gordon JC, Larson PR. 1968. Seasonal Course of Photosynthesis, Respiration, and Distribution of C in Young Pinus resinosa Trees as Related to Wood Formation. *Plant Physiology* **43**(10): 1617-1624.

Groover A, Jones AM. 1999. Tracheary element differentiation uses a novel mechanism coordinating programmed cell death and secondary cell wall synthesis. *Plant physiology* **119**(2): 375-384.

Hacke UG, Sperry JS, Pockman WT, Davis SD, McCulloch KA. 2001. Trends in wood density and structure are linked to prevention of xylem implosion by negative pressure. *Oecologia* **126**(4): 457-461.

Helle G, Schleser G. 2004. Beyond CO2-fixation by Rubisco – an interpretation of 13C/12C variations in tree rings from novel intraseasonal studies on broad-leaf trees. *Plant Cell and Environment* **27**(3): 367-380.

Horacek P, Slezingerova J, Gandelova L 1999. Effects of environment on the xylogenesis of Norway spruce (*Picea abies* L. Karst.). In: Wimmer R, Vetter RE eds. *Tree-ring analysis: biological, methodological and environmental aspects*. Wallingford, UK: CABI Publishing, 33-53.

King DA, Davies SJ, Tan S, Noor NSM. 2006. The role of wood density and stem support costs in the growth and mortality of tropical trees. *Journal of Ecology* **94**(3): 670-680.

Körner C. 2003. Carbon limitation in trees. *Journal of Ecology* **91**(1): 4-17.

Kozlowski TT, Pallardy SG. 1997. *Physiology of woody plants (second edition)*: Academic Press.

Kutscha NP, Hyland F, Schwarzmann JM. 1975. Certain seasonal changes in balsam fir cambium and its derivatives. *Wood Science and Technology* **9**(3): 175-188.

Larjavaara M, Muller-Landau HC. 2010. Rethinking the value of high wood density. *Functional Ecology* **24**(4): 701-705.

Larson PR. 1964. Contribution of different-aged needles to growth and wood formation of young red pines *Forest Science* **10**(2): 224-238.

Matsumoto-Kitano M, Kusumoto T, Tarkowski P, Kinoshita-Tsujimura K, Vaclavikova K, Miyawaki K, Kakimoto T. 2008. Cytokinins are central regulators of cambial

activity. *Proceedings of the National Academy of Sciences of the United States of America* **105**(50): 20027-20031.

Mellerowicz EJ, Sundberg B. 2008. Wood cell walls: biosynthesis, developmental dynamics and their implications for wood properties. *Current Opinion in Plant Biology* **11**(3): 293-300.

Mothe F, Duchanois G, Zannier B, Leban JM. 1998. Microdensitometric analysis of wood samples: data computation method used at Inra-ERQB (CERD program). *Annales Des Sciences Forestieres* **55**(3): 301-313.

Oda Y, Mimura T, Hasezawa S. 2005. Regulation of secondary cell wall development by cortical microtubules during tracheary element differentiation in Arabidopsis cell suspensions. *Plant physiology* **137**(3): 1027-1036.

Ogée J, Barbour M, Wingate L, Bert D, Bosc A, Stievenard M, Lambrot C, Pierre M, Bariac T, Loustau D. 2009. A single-substrate model to interpret intra-annual stable isotope signals in tree-ring cellulose. *Plant Cell and Environment* **32**(8): 1071-1090.

Offermann C, Ferrio JP, Holst J, Grote R, Siegwolf R, Kayler Z, Gessler A. 2011. The long way down—are carbon and oxygen isotope signals in the tree ring uncoupled from canopy physiological processes? *Tree Physiology* **31**(10): 1088-1102.

Park Y-I, Spiecker H. 2005. Variations in the tree-ring structure of Norway spruce (*Picea abies*) under contrasting climates. *Dendrochronologia* **23**(2): 93-104.

Perrot-Rechenmann C. 2010. Cellular responses to auxin: division versus expansion. *Cold Spring Harbor perspectives in biology* **2**(5): a001446-a001446.

Plomion C, Leprovost G, Stokes A. 2001. Wood formation in trees. *Plant physiology* **127**(4): 1513-1523.

Polge H, Nicholls JWP. 1972. Quantitative radiography and the densitometric analysis. *Wood Science* **5**: 51-59.

Pratt RB, Jacobsen AL, Ewers FW, Davis SD. 2007. Relationships among xylem transport, biomechanics and storage in stems and roots of nine Rhamnaceae species of the California chaparral. *New Phytologist* **174**(4): 787-798.

R Core Team 2012. R: A language and environment for statistical computing. R Foundation for Statistical Computing, Vienna, Austria. ISBN 3-900051-07-0, URL http://www.R-project.org/.

Rathgeber CBK 2012. Cambial activity and wood formation: data manipulation, visualisation and analysis using R. R package version 1.4-1. http://CRAN.R-project.org/package=CAVIAR.

Rathgeber CBK, Decoux V, Leban J-M. 2006. Linking intra-tree-ring wood density variations and tracheid anatomical characteristics in Douglas fir (*Pseudotsuga menziesii* (Mirb.) Franco). *Annals of Forest Science* **63**(7): 699-706.

Ridoutt BG, Sands R. 1993. Within-tree variation in cambial anatomy and xylem cell differentiation in *Eucalyptus globulus*. *Trees-Structure and Function* **8**(1): 18-22.

Rossi S, Deslauriers A, Morin H. 2003. Application of the Gompertz equation for the study of xylem cell development. *Dendrochronologia* **21**(1): 33-39.

Rossi S, Rathgeber CBK, Deslauriers A. 2009. Comparing needle and shoot phenology with xylem development on three conifer species in Italy. *Annals of Forest Science* **66**(2).

Savidge RA. 2001. Intrinsic regulation of cambial growth. *Journal of Plant Growth Regulation* **20**(1): 52-77.

Skene DS. 1969. The period of time taken by cambial derivatives to grow and differentiate into tracheids in *Pinus radiata* D. Don. *Annals of Botany* **33**(2): 253-262.

Skene DS. 1972. The kinetics of tracheid development in *Tsuga canadensis* Carr. and its relation to tree vigour. *Annals of Botany* **36**(1): 179-187.

Sperry JS, Meinzer FC, McCulloh KA. 2008. Safety and efficiency conflicts in hydraulic architecture: scaling from tissues to trees. *Plant Cell and Environment* **31**(5): 632-645.

Sundberg B, Uggla C, Tuominen H. 2000. Cambial growth and auxin gradients. In *Cell and molecular biology of wood formation* (Savidge R, Barnett JR, Napier R eds). Oxford, UK: BIOS Scientific Publishers Ltd., pp. 169-188.

Taiz L, Zeiger E. 1998. *Plant physiology*.

Tuominen H, Puech L, Fink S, Sundberg B. 1997. A radial concentration gradient of indole-3-acetic acid is related to secondary xylem development in hybrid aspen. *Plant physiology* **115**(2): 577-585.

Uggla C, Magel E, Moritz T, Sundberg B. 2001. Function and dynamics of auxin and carbohydrates during earlywood/latewood transition in Scots pine. *Plant Physiology* **125**(4): 2029-2039.

Uggla C, Moritz T, Sandberg G, Sundberg B. 1996. Auxin as a positional signal in pattern formation in plants. *Proceedings of the National Academy of Sciences of the United States of America* **93**(17): 9282-9286.

Vaganov EA 1990. Vaganov, E.A. 1990. The tracheidogram method in tree-ring analysis and its application. In: Cook ER, Kairiukstis LA eds. *Methods of dendrochronology: applications in the environmental sciences*. Dordrecht, Netherlands: Kluwer Academic Publishers, 63-76.

Vaganov EA, Anchukaitis KJ, Evans MN 2011. How well understood are the processes that create dendroclimatic records? A mechanistic model of the climatic control on conifer tree-ring growth dynamics. In: Hughes MK, Swetnam TW, Diaz HF eds. *Dendroclimatology*. London: Springer-Verlag, 37-75.

Vaganov EA, Hughes MK, Shashkin AV. 2006. *Growth Dynamics of Conifer Tree Rings*. Heidelberg: Springer.

Wilson BF, Wodzicki TJ, Zahner R. 1966. Differentiation of cambial derivatives: proposed terminology. *Forest Science* **12**(4): 438-440.

Wodzicki TJ. 1971. Mechanism of xylem differentiation in *Pinus sylvestris* L. *Journal of Experimental Botany* **22**(72): 670-687.

Wood SN. 2006. *Generalized additive models: an introduction with R*. Boca Raton, FL: Chapman and Hall/CRC.

Zhong R, Zheng-Hua Y 2009. Secondary cell walls. *Encyclopedia of Life Sciences*. Chichester, UK: John Wiley & Sons, Ltd., 1-9.

Supplementary material

Table VI.S1: Main characteristics (mean ± SE) of the monitored trees from the three studied species (silver fir, Norway spruce and Scots pine) illustrated by the age, diameter at breast height (DBH), height (H), projected crown area (CA), and final ring cell number (RCN).

Site	Species	Age	DBH (cm)	H (m)	CA (m²)	RCN (cell)
Walscheid	Fir	94 ± 2	56 ± 1	31 ± 1	43 ± 5	100 ± 9
	Spruce	89 ± 4	53 ± 2	32 ± 1	40 ± 5	85 ± 10
	Pine	95 ± 3	52 ± 3	31 ± 1	41 ± 10	71 ± 6
Abreschviller	Fir	135 ± 2	60 ± 3	36 ± 1	28 ± 5	51 ± 12
	Spruce	85 ± 7	41 ± 2	32 ± 1	16 ± 2	70 ± 6
	Pine	162 ± 3	33 ± 3	36 ± 1	20 ± 5	27 ± 4
Grandfontaine	Fir	73 ± 3	57 ± 3	31 ± 1	37 ± 6	69 ± 8
	Spruce	74 ± 4	55 ± 4	33 ± 1	30 ± 7	32 ± 3
	Pine	119 ± 3	53 ± 2	27 ± 1	29 ± 2	30 ± 2
Means	Fir	101 ± 6	58 ± 2	33 ± 1	36 ± 3	73 ± 6
	Spruce	83 ± 3	49 ± 2	32 ± 1	29 ± 4	62 ± 5
	Pine	126 ± 8	56 ± 2	32 ± 1	30 ± 4	42 ± 4

Table VI.S2: List of the variables used in this work.

Notation	Variable	Unit	Acquisition
LumRD	Lumen radial diameter	µm	Measured
LumTD	Lumen tangential diameter	µm	Measured
LumCA	Lumen cross-area	µm²	Measured
WallRT	Wall radial thickness	µm	Measured
WallTT	Wall tangential thickness	µm	$\mathrm{WallTT} = 1.2 \times \mathrm{WallRT}$
WallCA	Wall cross area	µm²	$\mathrm{WallCA} = \mathrm{CellCA} - \mathrm{LumCA}$
CellRD	Cell radial diameter	µm	$\mathrm{CellRD} = \mathrm{LumRD} + 2 \times \mathrm{WallRT}$
CellTD	Cell tangential diameter	µm	$\mathrm{CellTD} = \mathrm{LumTD} + 2.4 \times \mathrm{WallRT}$
CellCA	Cell cross area	µm²	$\mathrm{CellCA} = \mathrm{CellRD} \times \mathrm{CellTD}$
MC	Mork's criterion	NA	$\mathrm{MC} = \frac{4 \times \mathrm{WallRT}}{\mathrm{LumRD}}$
MMD	Morphometric density	kg m^{-3}	$\mathrm{MMD} = \frac{\mathrm{WallCA}}{\mathrm{CellRD} \times \mathrm{CellTD}}$
XRD	X-ray measured density	kg m^{-3}	Measured
n_C	Number of cells in the cambial zone	cell	Counted
n_E	Number of cells in the enlargement zone	cell	Counted
n_T	Number of cells in the wall thickening zone	cell	Counted
n_M	Number of cells in the mature zone	cell	Counted
d_C	Cell residence duration in the cambial zone	day	Calculated
d_E	Cell residence duration in the enlargement	day	Calculated
d_T	Cell residence duration in the thickening	day	Calculated
d_F	Total duration of tracheid formation	day	Calculated
r_C	Rate of cell production by the cambial zone	cell	Calculated
r_D	Rate of division of a cambial cell	day^{-1}	$r_D = \frac{r_C}{n_C}$
r_E	Rate of cell radial enlargement	µm day^{-1}	$r_E = \frac{\mathrm{CellRD}}{d_E}$
r_S	Rate of cell swelling	µm² day^{-1}	$r_S = \frac{\mathrm{CellCA}}{d_E}$
r_T	Rate of wall thickening	µm day^{-1}	$r_T = \frac{\mathrm{CellRT}}{d_T}$
r_W	Rate of wall deposition	µm² day^{-1}	$r_W = \frac{\mathrm{WallCA}}{d_T}$
CCL	Cell cycle length of cambial cells	day	$\mathrm{CCL} = \frac{1}{r_D}$

Table VI.S3: Sensitivity analysis of the geometric model of tracheid dimensions (see Method VI.S1). The table shows the variation of the wall thickness (WallRT) when the cell radial diameter (CellRD) and the wall cross area (WallCA) vary within a range of twice their standard deviation (from low to high). The cell tangential diameter in the model is maintained constant.

			WallRT (µm)	Contribution to total WallRT variation
CellRD (µm)	Low	13	9,5	
	High	52	3	
		WallRT variation	6,5	67%
WallCA (µm²)	Low	382	2,8	
	High	744	6,2	
		WallRT variation	3,4	33%
		Total WallRT variation	9,9	

Table VI.S4: Correlations between x-ray measured wood density (XRD) and cell radial diameter (CellRD), cell tangential diameter (CellTD), wall radial thickness (WallRT), wall cross area (WAllCA), and morphometric density (MMD). Numbers are the calculated Pearson correlation coefficients, with stars indicating significant correlations.

Variable	XRD
CellRD	-0.96*** ($P < 0.001$)
CellTD	-0.92*** ($P < 0.001$)
WallRT	0.88*** ($P < 0.001$)
WallCA	0.27* ($P < 0.05$)
MMD	0.99*** ($P < 0.001$)

Table VI.S5: Sensitivity analysis of the geometric model of wood density (see Method VI.S2). The table shows the variation of the morphometric density (MMD) when the cell radial diameter (CellRD) and wall cross area (WallCA) vary within a range of twice their standard deviation (from low to high). The cell tangential diameter (CellTD) in the model is maintained constant.

			MMD (kg m^{-3})	Contribution to total MMD variation
CellRD (µm)	Low	13	1356	
	High	52	345	
		MMD variation	1011	75%
WallCA (µm²)	Low	382	380	
	High	744	719	
		MMD variation	339	25%
		Total MMD variation	1350	

Table VI.S6: Covariance analysis of the relationship between the duration of enlargement (d_E) and final radial cell diameter (CellRD) among the three species (Sp).

Source	Df	Sum of squares	Mean Squares	F	p-value
d_E	1	7081	7081	483.07	< 0,001 ***
Sp	2	6377	3189	217.53	< 0,001 ***
d_E:Sp	2	891	445	30.39	< 0,001 ***
Residuals	171	2507	15		

Table VI.S7: Sensitivity analysis of the model of tracheid enlargement. The table shows the variation of the radial diameter (CellRD) when the duration (d_E) and the rate (r_E) of enlargement vary within a range of twice their standard deviation (from low to high).

				CellRD (µm)	Contribution to total CellRD variation
Pine	d_E (days)	Low	3,6	9	
		High	22,2	54	
			CellRD variation	45	78%
	r_E (µm day^{-1})	Low	1,9	25	
		High	2,9	38	
			CellRD variation	13	22%
			Total CellRD variation	58	

				CellRD (µm)	Contribution to total CellRD variation
Fir	d_E (days)	Low	0,7	3	
		High	13,8	71	
			CellRD variation	68	65%
	r_E (µm day^{-1})	Low	2,6	19	
		High	7,7	56	
			CellRD variation	37	35%
			Total CellRD variation	105	

				CellRD (µm)	Contribution to total CellRD variation
Spruce	d_E (days)	Low	2,7	11	
		High	13,1	55	
			CellRD variation	44	81%
	r_E (µm day^{-1})	Low	3,5	28	
		High	4,8	38	
			CellRD variation	10	19%
			Total CellRD variation	54	

Table VI.S8: Sensitivity analysis of the model of secondary wall formation. The table shows the variation of the wall cross area (WallCA) when the duration (dT) and the rate (rW) of all deposition vary within a range of twice their standard deviation (from low to high).

			WallCA (µm²)	Contribution to total WallCA variation
d_T (days)	Low	9	169	
	High	61	1129	
		WallCA variation	960	50%
r_W (µm² day^{-1})	Low	4,6	161	
	High	32,7	1136	
		WallCA variation	975	50%
		Total WallCA variation	1935	

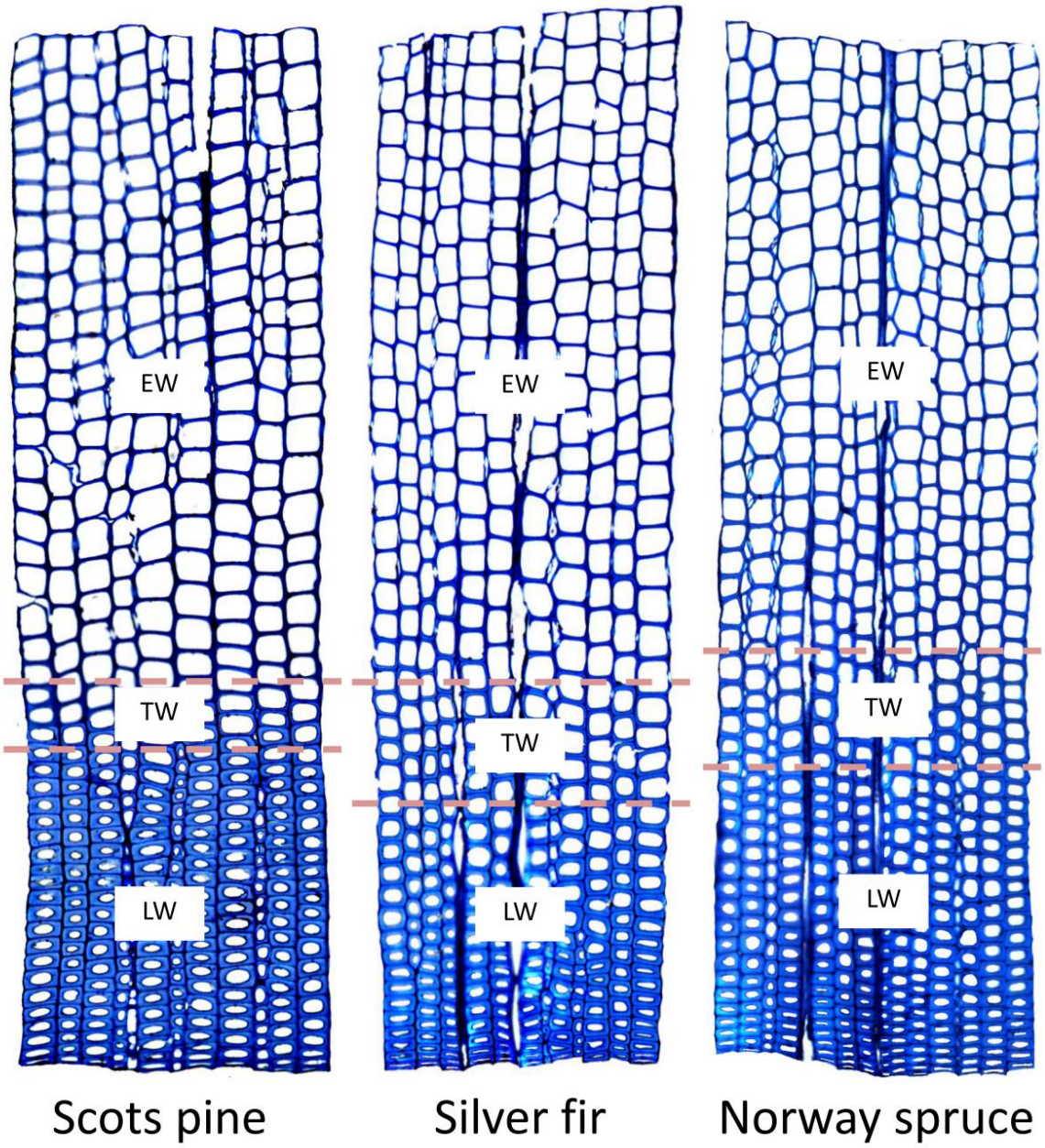

Figure VI.S1: Tree ring structure of the three conifer species, with earlywood (EW), transition wood (TW), and latewood (LW).

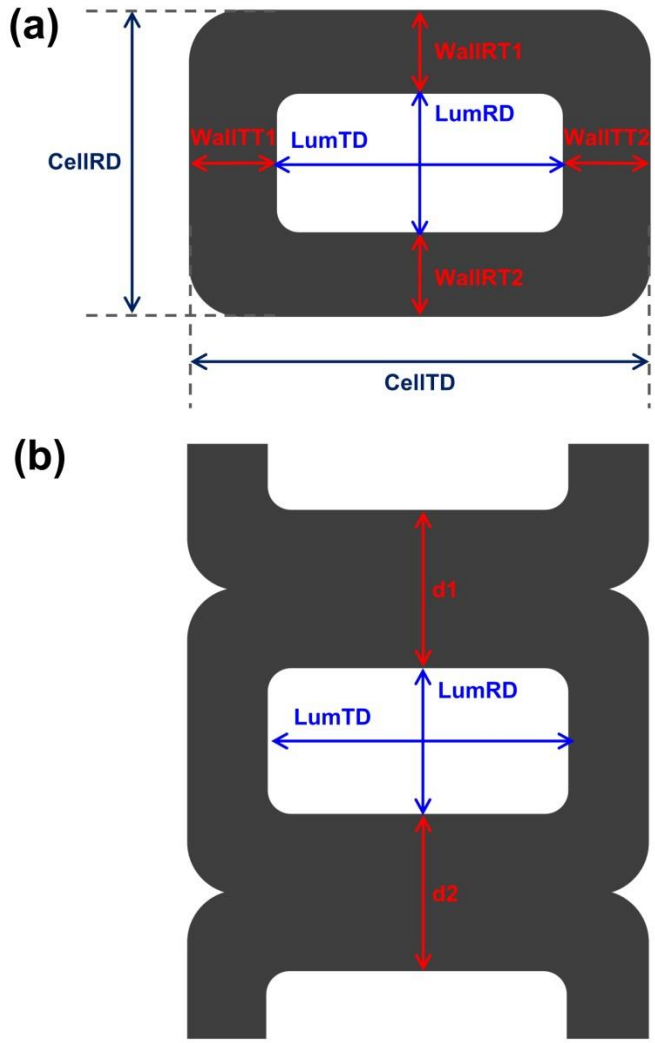

Figure VI.S2: Presentation of tracheid dimensions and their measurement. Figure VI.S2a shows the different dimensions of a tracheid in a transversal plan, with the cell radial (CellRD) and tangential (CellTD) diameters, the lumen radial (LumRD) and tangential (LumTD) diameters, and the double wall radial (WallRT1 and WallRT2) and tangential (WallTT1 and WallTT2) thicknesses. The cell (CellCA), lumen (LumCA) and wall (WallCA) cross-sectional areas are not represented. Figure VI.S1b shows the measurement made by the WinCell software, which, for each cell along a radial file, measures LumRD, LumTD, and the distances between the lumens of the neighbouring cells (d1 and d2). WinCell also measures LumCA.

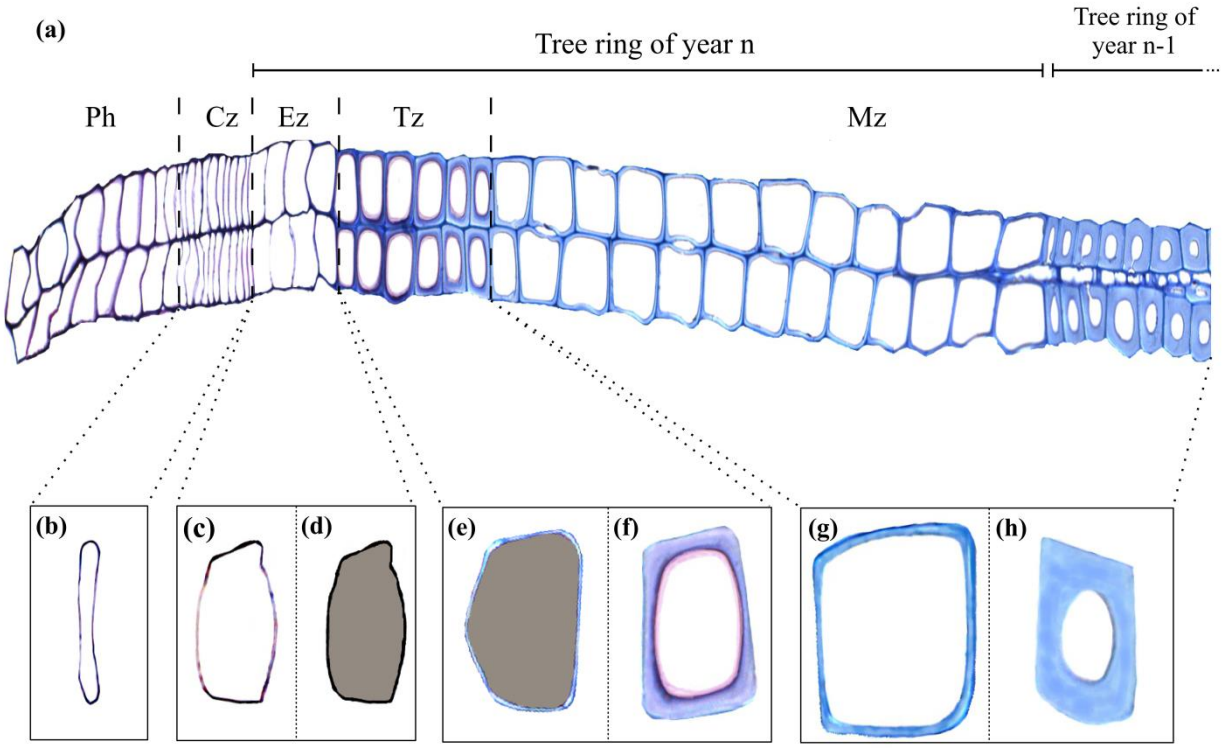

Figure VI.S3: Xylem development observed in Scots pine. Figure VI.S3a shows two radial files isolated from a wood anatomical transverse section (6 µm in thick, stained with cresyl violet acetate) cut from a sample collected the 4th August 2009. They contained the phloem (Ph) and the cambial (Cz), enlargement (Ez), thickening (Tz), and mature (Mz) zones of tracheid differentiation. Figure VI.S3b to VI.S3h illustrate cells isolated from each differentiation zone with a cambial cell (b), an enlarging cell under normal (c) and polarized (d) light, a thickening cell under polarized light (e) and a thickening cell under normal light (f), a mature earlywood cell of the current tree ring (g) and a mature latewood cell of the previous tree ring (h).

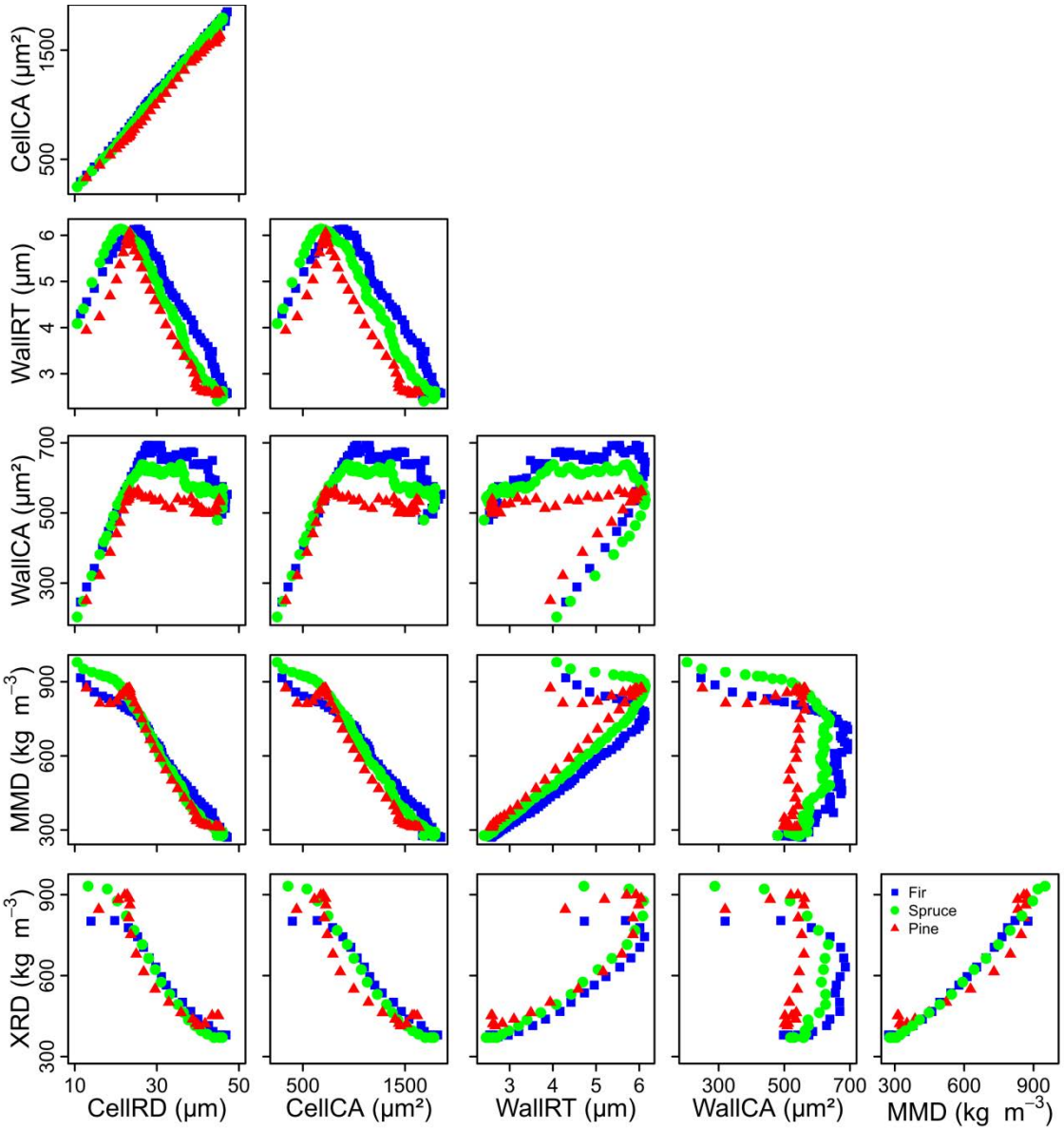

Figure VI.S4: Relationships between the variables of the tree ring structure. Relationships between the tracheid radial diameter (CellRD), cross-sectional area (CellCA), wall thickness (WallRT), wall cross-sectional area (WallCA), the morphometric density (MMD) and the x-ray measured density (XRD).

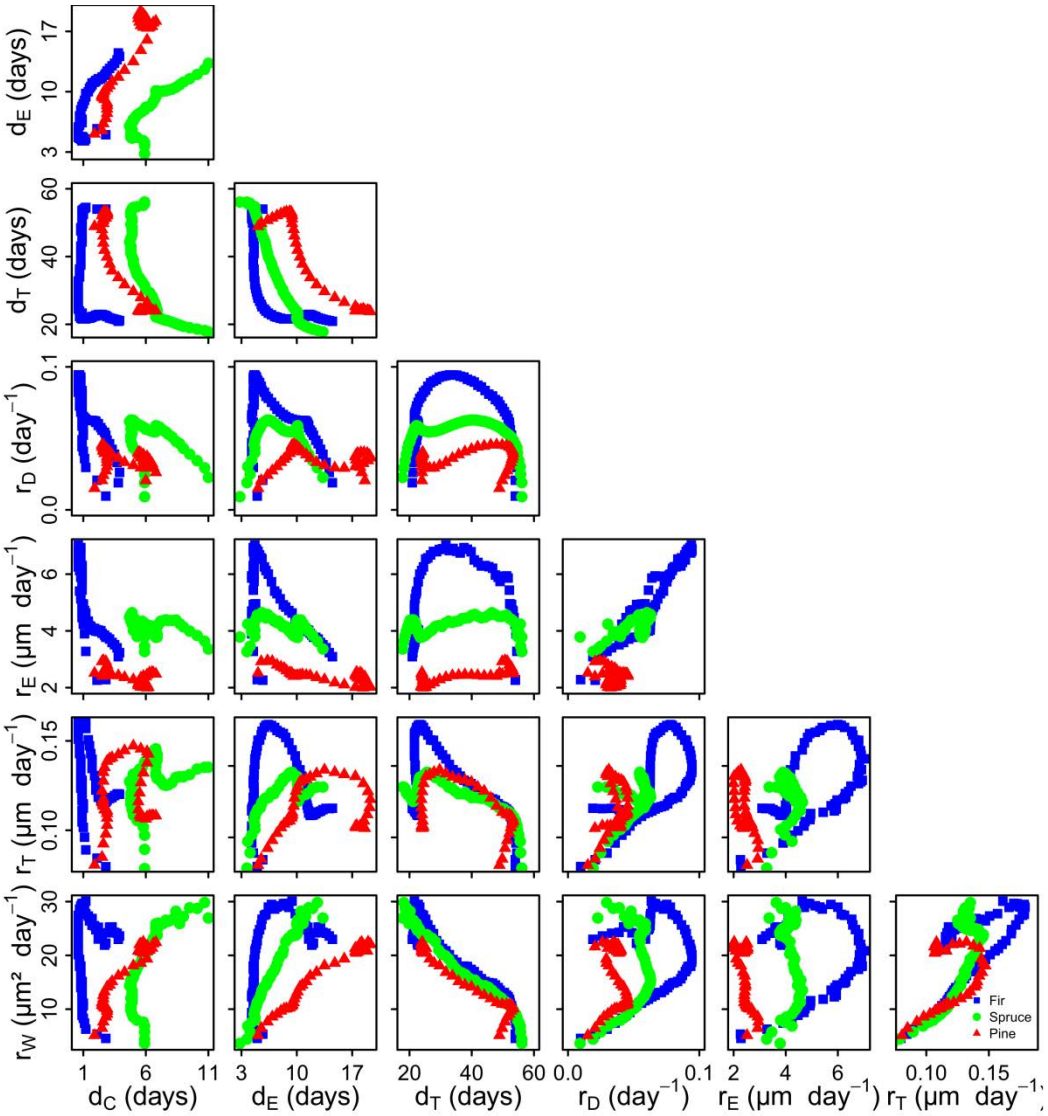

Figure VI.S5: Relationships between the variables of the wood formation dynamics. Relationships between the cell residence duration in the cambial zone (d_C), the duration of cell enlargement (d_E) and wall thickening (d_T), the rate of cambial cell division (r_D), cell enlargement (r_E), wall thickening (r_T) and wall deposition (r_W).

Method VI.S1: Expression of the wall radial thickness (WallRT) as a function of the cell radial and tangential diameters (CellRD and CellTD) and the wall cross area (WallCA).

WallCA can be calculated as the difference between the cell and lumen cross areas (CellCA and LumCA):

$$\mathrm{WallCA} = \mathrm{CellCA} - \mathrm{LumCA}$$

Based on a rectangular shape of tracheids, CellCA can be estimated as:

$$\mathrm{CellCA} = \mathrm{CellRD} \times \mathrm{CellTD}$$

Similarly, LumCA can be estimated from the lumen radial and tangential diameters (LumRD and LumTD), which can themselves be expressed from CellRD, CellTD, WallRT and the wall tangential thickness (WallTT):

$$\mathrm{LumCA} = \mathrm{LumRD} \times \mathrm{LumTD} = (\mathrm{CellRD} - 2\mathrm{WallRT}) \times (\mathrm{CellTD} - 2\mathrm{WallTT})$$

Our expression of WallCA becomes:

$$\mathrm{WallCA} = (\mathrm{CellRD} \times \mathrm{CellTD}) - (\mathrm{CellRD} - 2\mathrm{WallRT}) \times (\mathrm{CellTD} - 2\mathrm{WallTT})$$

By estimating WallTT as 1.2WallRT, our expression becomes:

$$\mathrm{WallCA} = (\mathrm{CellRD} \times \mathrm{CellTD}) - (\mathrm{CellRD} - 2\mathrm{WallRT}) \times (\mathrm{CellTD} - 2.4\mathrm{WallRT})$$

$$\mathrm{WallCA} = (\mathrm{CellRD} \times \mathrm{CellTD}) - (\mathrm{CellRD} \times \mathrm{CellTD} - 2.4\mathrm{CellRD} \times \mathrm{WallRD} - 2\mathrm{WallRT} \times \mathrm{CellTD} + 4.8\mathrm{WallRT}^2)$$

$$\mathrm{WallCA} = 2.4\mathrm{CellRD} \times \mathrm{WalRT} + (2\mathrm{WallRT} \times \mathrm{CellTD} - 4.8\mathrm{WallRT}^2)$$

$$4.8\mathrm{WallRT}^2 - (2.4\mathrm{CellRD} + 2\mathrm{CellTD}) \times \mathrm{WallRT} + \mathrm{WallCA} = 0$$

$$\mathrm{WallRT} = \frac{(2.4\mathrm{CellRD} + 2\mathrm{CellTD}) \pm \sqrt{\Delta}}{2 \times 4.8}$$

With:

$$\Delta = (2.4\mathrm{CellRD} + 2\mathrm{CellTD})^2 - 4 \times 4.8\mathrm{WallCA}$$

$$\Delta = (2.4\mathrm{CellRD} + 2\mathrm{CellTD}) \times (2.4\mathrm{CellRD} + 2\mathrm{CellTD}) - 4 \times 4.8\mathrm{WallCA}$$

$$\Delta = 5.76\mathrm{CellRD}^2 + 4.8\mathrm{CellRD} \times \mathrm{cellTD} + 4.8\mathrm{CellRD} \times \mathrm{CellTD} + 4\mathrm{CellTD}^2 - 19.2\mathrm{WallCA}$$

$$\Delta = 5.76\mathrm{CellRD}^2 + 9.6\mathrm{CellRD} \times \mathrm{cellTD} + 4\mathrm{CellTD}^2 - 19.2\mathrm{WallCA}$$

By replacing Δ in our equation, the final expression of WallRT is:

$$\mathrm{WallRT} = \frac{2.4\mathrm{RellRD} + 2\mathrm{CellTD} \pm \sqrt{5.76\mathrm{CellRD}^2 + 9.6\mathrm{CellRD} \times \mathrm{CellTD} + 4\mathrm{CellTD}^2 - 19.2\mathrm{WallCA}}}{2 \times 4.8}$$

Method VI.S2: Morphometric density (MMD) calculation from tracheid dimensions

The basic expression of MMD is the ratio between the wall (WallCA) and cell (CellCA) cross areas:

$$\mathrm{MMD} = \frac{\mathrm{WallCA}}{\mathrm{CellCA}}$$

Based on a rectangular tracheid shape, the geometric model of wood density can be written using the lumen (LumRD and LumTD) radial and tangential diameters:

$$\mathrm{MMD} = \frac{\mathrm{WallCA}}{\mathrm{CellRD} \times \mathrm{CellTD}}$$

VII LES ARBRES GROSSISSENT AVANT DE PRENDRE DU POIDS

Cette partie se sert de la caractérisation précise de la cinétique des processus du développement cellulaire pour établir la dynamique saisonnière de l'accumulation de la biomasse, en gramme de carbone par jour, dans le bois en formation. Celle-ci est comparée aux dynamiques de la croissance radiale et de l'activité cambiale et mise en relation avec le cycle saisonnier des facteurs climatiques (température, photopériode, radiation lumineuse et disponibilité en eau). Le travail porte sur l'ensemble des données, c'est-à-dire les trois sites du gradient, avec les 45 arbres des 3 espèces et les 3 années (2007 – 2009) de suivi. Cette partie est constituée d'un article scientifique (article 4) en préparation.

Growing is not putting on weight! New insight into carbon accumulation in trees

Henri E. Cuny[1*], Cyrille B.K. Rathgeber[1], Meriem Fournier[2]

(In preparation)

[1] INRA, UMR1092, Laboratoire d Etude des Ressources Foret Bois (LERFoB), Centre INRA de Nancy, F-54280 Champenoux, France

[2] AgroParisTech, UMR1092, Laboratoire d Etude des Ressources Foret Bois (LERFoB), ENGREF, 14 rue Girardet, F-54000 Nancy, France

Summary

- Wood represents more than 20% of the terrestrial biomass on earth. Wood formation fixes half of the carbon photosynthesis captures annually, participating in a lasting carbon sequestration that mitigates climate change. Xylogenesis consist in the production new cells by the cambium, followed by the differentiation (radial enlargement, secondary cell-wall formation, lignification, and programmed cell death) of these cells, in order to form mature functional xylem cells. Whereas division and enlargement determine the number and size of the final mature cells, it is wall formation and lignification that determine the amount of material allocated to each cell. In this study, we build on the development of new statistical methods to describe, at the cellular level, the seasonal dynamics of cambial activity, stem radial growth and biomass accumulation, and to quantify the influence of climatic factors on these processes.
- Wood formation was monitored during 3 years (2007 – 2009) for 45 trees of 3 conifer species (silver fir, Norway spruce, Scots pine) split in 3 mixed stands along an altitudinal gradient (350 – 650m ASL) in northeast France. Rates of cambial activity, secondary growth, and biomass accumulation were calculated from microcores and dendrometers. Meteorological data (temperature, global radiation, and precipitation) were gathered from three weather stations in the studied area.
- Cambial activity presented a slightly bimodal dynamics, reaching a first peak in May, at the very beginning of the brightest period, and a second one in July, during the warmest period. Radial growth followed a left-skewed bell-shaped dynamics that culminates in May (during the brightest period), whereas biomass accumulation presented a bell-shaped dynamics that culminates in July (during the warmest period). A lag of about 1.5 months was observed between the dynamics of radial growth and biomass accumulation.
- Results show that cambial activity, radial growth and biomass accumulation follow different intra-annual dynamics. In particular, the impressive lag between radial growth and biomass accumulation shows that the monitoring of radial growth is not informative of biomass accumulation in trees. This latter process appeared mainly driven by temperature, in agreement with the idea of a limitation of carbon sink activity by temperature.

Keywords: biomass accumulation – carbon cycle – climate changes – dendrometer – tree growth– quantitative wood anatomy – xylogenesis

Introduction

Wood formation is the growth process by which a large part of the biomass of this planet is produced, providing an essential and renewable resource to mankind and playing a central role in the carbon cycle. Indeed, plants fixed by photosynthesis about 120 Gt of atmospheric carbon annually, among which about half is released by respiration (Zhao & Running, 2010). The other half is accumulated as biomass, mainly through the bias of wood formation, which allowed the lasting sequestration of carbon in the forming wood (Lal, 2008). Nowadays, the sequestration is a bit higher than the respiration, which contributes to a carbon sink that mitigates climate change (Canadell & Raupach, 2008). Moreover, wood biomass

promises to be the most abundant renewable source of biofuels in the future (Pauly & Keegstra, 2010). So, there is a tremendous interest in understanding in depth the processes underlying wood biomass production, as well as their mechanisms of regulation, and the influences of the environment. Regulation of biomass production is a hot topic in molecular biology (see review by Demura & Ye, 2010), but needs to be integrated with a more general, process-based, understanding of what drives biomass accumulation in trees.

In temperate ecosystems, wood formation followed regular seasonal patterns of activity, which direct consequence is the formation of annual rings. The formation of a tree ring occurs through the production of new xylem cells by the cambium, the enlargement of these cells and the formation of their secondary wall (Plomion *et al.*, 2001). Cell production and enlargement determine the width of the tree ring, which in turn determines most of tree radial growth, as the increment of wood is generally largely wider than this of the tissues of the bark (Gričar & Čufar, 2008; Gričar *et al.*, 2009). On the other hand, the construction of the thick and highly lignified secondary walls determines most of the biomass accumulated in the tree (Demura & Ye, 2010). Understanding how the seasonal patterns of wood formation are coordinated with the regular cycle of environmental factors can bring new insights about the environmental influence on cambial activity, radial growth and carbon accumulation in trees.

Most of the studies trying to understand environmental influence on wood formation focused on the phenological aspects of the process. These studies have underlined air temperature as a crucial parameter in controlling the beginning, end, and duration of cambial activity and wood formation in the temperate zone and this in various environments, for example in cold environments at high latitudes (Rossi *et al.*, 2008; Lupi *et al.*, 2012) or altitudes (Rossi *et al.*, 2007; Deslauriers *et al.*, 2008; Rossi *et al.*, 2008; Moser *et al.*, 2010), in milder environments at mid-altitude (Gruber *et al.*, 2010; Swidrak *et al.*, 2011) or in central Europe (Horacek *et al.*, 1999), and even in hotter environments characterizing Mediterranean region (Camarero *et al.*, 2010). The crucial importance of temperature in controlling xylogenesis phenology is also visible in the possible induction of cambial reactivation by artificial heating during the quescient stage (Oribe *et al.*, 2001; Gričar *et al.*, 2006; Gričar *et al.*, 2007).

In contrast, only a few studies have investigated the influence of environment on the seasonal evolution of the rate of xylogenesis processes. This aspect of xylogenesis dynamics has been neglected whereas it should be of crucial importance. For example, it has been demonstrated that in a conifer stand, tree ring width is determined mostly by the rate, and not by the duration, of cambial activity (Rathgeber *et al.*, 2011; Cuny *et al.*, 2012). Rossi *et al.* (2006) have investigated the timing of the maximal rate of cambial activity for 8 conifer species of cold environments (boreal and sub-alpine). They found that the occurrence date of the maximal rate to converge toward the time of maximum day length, and not to the time of maximal temperature. Their interpretation is that photoperiod attested a more stable signal in comparison to temperature: the summer solstice acts as a limit after which cambial activity rate decreases, thus allowing plants to safely complete secondary cell wall lignification before winter. By contrast, Mäkinen *et al.* (2003) observed that the maximal rate of cell production

occurred rather in the warmest period, after the summer solstice. However, the way they analyse the data has been criticized and is supposed to explain the shift (Rossi *et al.*, 2006). Camarero *et al.* (2010) have also investigated how the regular cycle of xylogenesis was influenced by environmental conditions under continental Mediterranean climate. He found maximum growth in transitional seasons (spring and autumn) and a low or null growth rate in summer, reflecting the bimodal rainfall distribution in areas with Mediterranean climates. So, the rate of cambial activity seems to be sensitive to environmental factors.

Other studies have tried to relate intra-annual pattern of tree-ring growth to environmental factors based on external measure of stem growth variation using dendrometers (Downes *et al.*, 1999; Worbes, 1999; Deslauriers *et al.*, 2003; Bouriaud *et al.*, 2005; Zweifel *et al.*, 2006). This kind of analyses, however, are complicated by the fact that dendrometer measurements provide time series composed of the rhythm of water storage fluctuations over the year in addition to seasonal xylem and phloem growth (Zweifel *et al.*, 2001; Mäkinen *et al.*, 2003; Deslauriers *et al.*, 2007).

Such attempts to understand how the rate of growth aspects related to wood formation is influenced by external signals are not only scarce, but they concern only cambial activity and tree radial growth, whereas the process responsible of biomass accumulation is rather secondary wall formation. Cambial activity, radial growth and biomass accumulation may have different seasonal dynamics, because, for each cell, secondary walls are formed after its production and enlargement and is longer than these two processes. The most obvious example is at the end of the season, when the produced cells remain almost 2 months in the wall thickening zone (Skene, 1969; Wodzicki, 1971; Skene, 1972; Cuny *et al.*, 2013), which means that some biomass continues to be allocated to the wood during the 2 months following the end of cambial activity and tree radial growth. In the case of delayed dynamics, assessing cambial activity and tree radial growth would give only biased information on the environmental influence on biomass accumulation in trees.

According to Körner (1998; 2003), biomass accumulation in trees under current ambient CO2 concentrations is strongly limited by sink activity (i.e. xylem cell differentiation), and not on source activity (i.e. carbon supply by photosynthesis activity). The main climatic variable at the origin of the sink limitation of biomass accumulation in trees would be temperature, as the processes of xylem cell differentiation are more sensitive to temperature than photosynthesis.

In this study, we aimed to characterize the seasonal dynamics of cambial activity, radial growth and biomass accumulation in the forming wood, and to determine how these seasonal dynamics are driven by the seasonal cycle of environmental factors. Because stem growth and biomass accumulation are supported by different physiological processes, we expect that they have different seasonal dynamics. In particular, we expect that biomass accumulation is shifted from tree radial growth and cambial activity. Based on Körner's hypothesis that temperature limits sink activity, we expect the seasonal dynamics of biomass accumulation to be under the influence of the seasonal cycle of temperature.

To test these hypotheses, cambial activity, tree ring lengthening, and biomass accumulation in the forming wood were assessed during three years (2007 – 2009) for 45 trees of three conifer species (silver fir, Norway spruce, and Scots pine) grown in thee mixed stands along an altitudinal gradient in northeast France.

Material and methods

Study area

Three plots were selected in mixed mature forest-stands composed of silver firs (*Abies alba* Mill.), Norway spruces (*Picea abies* (L.) Karst.) and Scots pines (*Pinus sylvestris* L.) along an altitudinal gradient (from 350 to 650 m ASL) in the Vosges Mountains (northeast France). Based on complete inventories of the stands, five dominant and healthy silvers firs, Norway spruces and Scots pines were selected on each plot, for a total of 45 studied trees (5 trees × 3 species × 3 sites) (Table VII.S1). On each site, vegetation composition and site conditions were described, and two soil pits were dug in order to characterise soil profiles.

Characterization of annual cycle of environmental factors

In order to characterize the annual cycles of environmental factors, daily meteorological data (temperature, precipitation, cumulative global radiation, wind speed, and air relative humidity) of the period 2007-2009 were gathered from three meteorological stations located in the studied area. Moreover, the model Biljou© was used to assess the daily water balance of the three stands (https://appgeodb.nancy.inra.fr/biljou/) (Granier *et al.*, 1999). In addition to the daily meteorological data mentioned above, the model takes as input some soil (e.g., number and depth of layers, and proportion of fine roots per layer), and stand (forest type and maximum leaf area index) parameters, and gives as output the relative extractable water (REW) on a daily scale. The REW is a relative expression of the filling state of the soil: REW is 100% at field capacity, and 0% at the permanent wilting point. Water stress is assumed to occur when the relative extractable soil water (REW) drops below a threshold of 40%, under which transpiration is gradually reduces due to stomata closure (Granier *et al.*, 1999).

Daily meteorological and water balance data were then averaged over the three stations and the three years in order to obtain representative seasonal trends of climatic conditions.

Microscopic observations of the developing tree ring

For each studied tree, wood formation was monitored from April to November during 3 years (2007 – 2009). Microcores were collected weekly on tree stem, prepared in the laboratory, and 5–10-µm-thick transverse sections were cut with a rotary microtome (HM 355S, MM France). Sections were stained with cresyl violet acetate and permanently mounted on glass slides using Histolaque LMR®.

Overall, we analysed 4 300 anatomical sections using an optical microscope (AxioImager.M2, Carl Zeiss SAS, France) under visible and polarized light at ×100–400 magnification to distinguish and count the cells in the different zones of differentiation along

the forming tree ring. Cambial cells had a rectangular shape with small radial diameters and thin primary walls, while cells in the radial enlargement zone were larger but still had thin walls. In contrast to cambial and enlarging cells, cells in the thickening zone had a secondary wall in formation that was birefringent under polarised light (Abe *et al.*, 1997). Cresyl violet acetate staining, whereby cellulose stains purple and lignin stains blue (Kutscha *et al.*, 1975), was used to follow the advancement of lignification. Cells in the thickening zone exhibited violet and blue walls, indicating that lignification was in progress, whereas mature tracheids had entirely lignified and thus completely blue walls.

The number of cells from the previous year was counted on three radial files per sample and used to standardize the raw number of cells of the current year in order to reduce within tree variability (Rossi *et al.*, 2003). A dedicated function of the R package CAVIAR (R Core Team, 2012; Rathgeber, 2012) was used to apply this standardization to all the samples.

Wood formation dynamics description

In order to characterize intra-annual wood formation dynamics, we fitted generalized additive models (GAMs) on the standardized number of cells weekly counted in the cambial, enlargement, wall thickening, and mature zones of xylem differentiation (Cuny *et al.*, 2013). GAMs were fitted in R using the mgcv package (Wood, 2006) for every year on each individual tree. The values of the fitted models were then averaged for the monitored plots over the studied years in order to calculate means representing the general wood formation dynamics of a species.

For each species, the rate of cambial activity at a day t ($r_{C,\,t}$) was calculated as the difference between the total number of cells predicted by GAMs at day t and the total number of cells predicted at day t-1. Moreover, we used the average cell numbers predicted by GAMs to calculate the date of entrance of each cell in each development zone (cambial, enlargement, wall formation and mature zones). From these dates, the residence durations of each cell i in the enlargement ($d_{E,i}$) and wall thickening ($d_{T,i}$) zones were computed. The rate of radial diameter enlargement ($r_{E,i}$) and wall deposition ($r_{W,i}$) were computed for each cell i by dividing its final dimensions (cell radial diameter and wall cross area) – measured from image analysis of the entirely formed tree ring at the end of the season (see Cuny *et al.*, under review, for a detailed description of the tracheid dimension measurements) – by the duration it spent in the corresponding phase ($d_{E,i}$ and $d_{T,i}$) (Table VII.S2).

Cells were also classified in earlywood, transition wood, and latewood on the basis of their dimensions, according to Mork's criterion (Denne, 1988, see Table VII.S2 for formula).

Monitoring stem circumferential variation

Manual band dendrometers (DB-20, EMS Brno, Czech Republic) were installed at breast height in March 2007 on the stem of all monitored trees, after the removal of most part of the bark. They were read weekly thereafter to monitor stem circumference variations. In order to assess the dynamics of stem growth, GAMs were fitted on dendrometer measurements for every year and each individual tree. Fittings were then pooled together over

the three years and the three sites in order to represent the general stem growth dynamics of a species.

Calculating rates of stem radial variation and secondary growth

The daily rate of stem circumferential variation at day t was calculated as the daily differences between the stem circumference variations predicted using GAM. This rate was then converted into a rate of stem radial variation (r_R) assuming a circular cross section.

For each species, a rate of xylem growth (r_G) was also calculated from the rate of cambial activity – assuming that each cambial division leads to the formation of new cells of 7 µm in diameter (unpublished data) – and the individual rates of cell diameter enlargement in the enlarging zone (Method VII.S1).

Calculating a rate of biomass accumulation

The rates of cambial activity, xylem growth, and wall deposition were used to calculate a rate of biomass accumulation in the forming wood (Method VII.S2). The rate of cambial activity was used to calculate a rate of primary wall material deposition in the tangential direction. For that, we assumed that each cambial division leads to the formation of two primary walls of 1µm in thick (unpublished data), and with a length corresponding to the mean width of a radial file. Similarly, the rate of xylem growth was used to calculate a rate of primary wall deposition in the radial direction. A given growth of the xylem was associated with the formation of two primary walls of 1 µm in thick and with a length corresponding to the lengthening of the ring. Moreover, the rate of secondary wall-material deposition at the radial file level was calculated as the sum of the cellular rates of wall deposition.

The global rate of wall deposition in the radial file was calculated as the sum of the rates of primary and secondary wall deposition. This rate was further converted into a rate of biomass accumulation (r_B) in the forming wood at the tree stem level, based on the height and basal stem diameter of the monitored trees, on an apparent density of the wall of 1.100 g cm^{-3} (Decoux *et al.*, 2004), and on a carbon proportion in wood around 50% of dry weight (Lamlom & Savidge, 2003) (Method VII.S2). So, the obtained rate is expressed in gram of carbon per day (gC day^{-1}).

Results

Seasonal patterns of climatic factor variations

From January 2007 to December 2009, a mean annual temperature of 9.4°C was observed. Daily temperature remained at a steady minimum of approximately 2°C in January. It increased slowly to 5°C in mid-March, and more rapidly from mid-March to reach 14°C in mid-May (Figure VII.1a). Daily temperature then increased slowly again to reach its maximum, around 17°C, to occur at the end of July (Table VII.1). The period of maximal temperatures (> 95% of the maximum), however, were quite spread over a period of almost 2 months, from the end of June to the middle of August (Table VII.1). Daily temperature then

decreased steadily until 0°C at the end of the year.

A mean daily cumulative radiation of 1170 J cm^{-2} day^{-1} was observed. The daily radiation started from values below 400 J cm^{-2} at the beginning of January, and increased of about 5 times until the beginning of May (Figure VII.1b). Then, it increased very slightly to reach a maximum a bit above 2000 J m^{-2} at the beginning of June, 2 weeks before the summer solstice (Table VII.1). However, as for temperature, the period of maximal radiation (> 95% of the maximum) was quite long, lasting 2 months, from the beginning of May to the beginning of July (Table VII.1). After what it decreased continuously until returning to a minimal value below 300 J cm^{-2} in December.

Table VII.1: Day of occurrence of the maximum (t_{max}) and period of maximal values (> 95% of the maximum) of radiation and temperature.

Radiation		Temperature	
t_{max}	period max	t_{max}	period max
157	127 - 185	209	175 - 230
(6 June)	(7 May - 4 July)	(28 July)	(24 June - 18 August)

On average, it rained 1350 mm a year (i.e. 3.7 mm day^{-1}). These precipitations were quite steadily distributed during the season, even if two periods with lower precipitations could be distinguished in spring (April-May) and in autumn (September-October) (Figure VII.1c).

Because of regular precipitations well spread over the year, the relative extractable water (REW) remained at a high level during the whole season (Figure VII.1d). It was at 100% in the first quarter of the year, indicating that the soil was at its maximal capacity. REW starts to decrease at the very end of March, when temperatures started to increase significantly, to oscillate between 65-85%, depending on raining events, most of the summertime. it increased to return to 100% during autumn.

Seasonal evolution of cambial activity, cell expansion, xylem growth, and radial growth

New xylem cells were produced during about 5 months, from the middle (pines and firs) or the end (spruces) of April to mid-September. Cambial activity rate exhibited a seasonal evolution close to bimodal shared by the three species (Figure VII.2a,b,c). Thus, a first peak (0.33 cells day^{-1} in pines, 0.52 cells day^{-1} in firs, and 0.60 cells day^{-1} in spruces) was reached early in the season, at mid-May in pines and firs, and two weeks later in spruces (Table VII.2). After this first peak, cambial activity remained high but slightly decreased to reach a minimum (0.24 cells day^{-1} in pines, 0.50 in firs, and 0.52 in spruces) at the middle (pines and firs) or at the end of June (spruces). After what cambial activity increased again to reach a second peak (0.33 cells day^{-1} in pines, 0.73 in firs, and 0.56 in spruces) at the same time for the three species, at the middle of July. Cambial activity then decreased until mid-September. The average rate of cell production during the growing season was lowest in pines (0.26 cells day^{-1}), 60% higher in spruces (0.42 cells day^{-1}), and 75% higher in firs (0.46 cell day^{-1}).

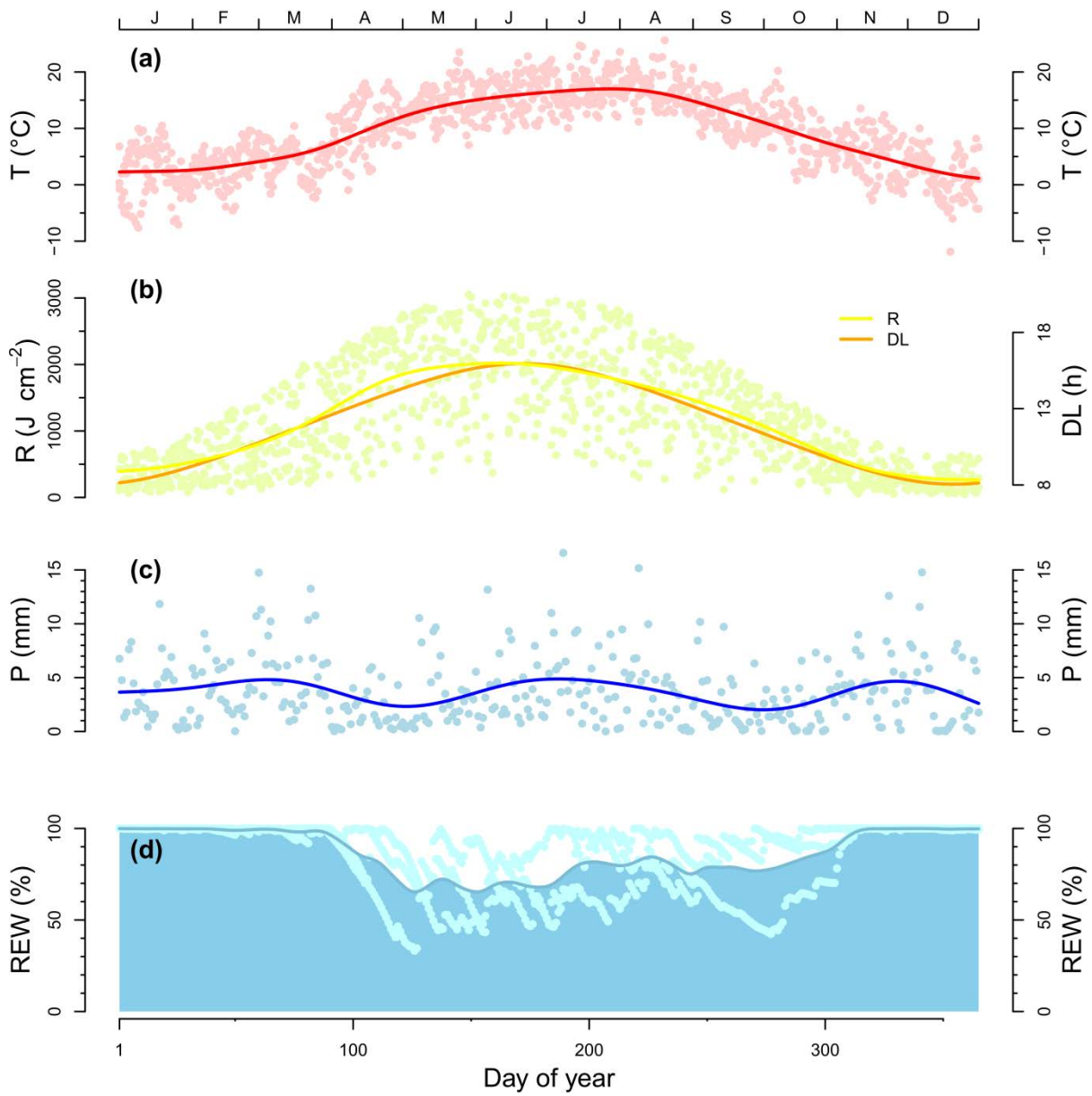

Figure VII.1: Seasonal cycle of temperature (T), radiation (R) and day length (DL), and soil relative extractable water (REW). Points represent daily values for the three years. Lines represent means for the three years.

Xylem growth occurred during 5 months, from the middle (pines and firs) or the end (spruces) of April to mid-September. We estimated that cambial activity accounted for only 20% of the xylem growth, which was mainly (80%) driven by the expansion of the newly produced xylem cells in the enlargement zone. The rate of xylem growth exhibited left-skewed bell-shaped curves (Figure VII.2d,e,f) that culminated early in the season, in the second half of May (Table VII.2), when the number of earlywood cells in the enlargement zone was maximal (Figure VII.2d,e,f). The rate of xylem growth then decreased, but, between mid-June and the beginning of July, a period of slower decrease was observed in pines and spruces, and even the formation of a smaller peak occurred in firs. The rate of xylem growth then decreased until it stopped in mid-September. The rate of xylem growth (r_G) was lowest in pines than in firs and spruces, as visible in its mean (9 µm day^{-1}, 17 µm day^{-1}, and 14 µm day^{-1}, respectively) or maximal value (14 µm day^{-1}, 29 µm day^{-1}, and 27 µm day^{-1}, respectively).

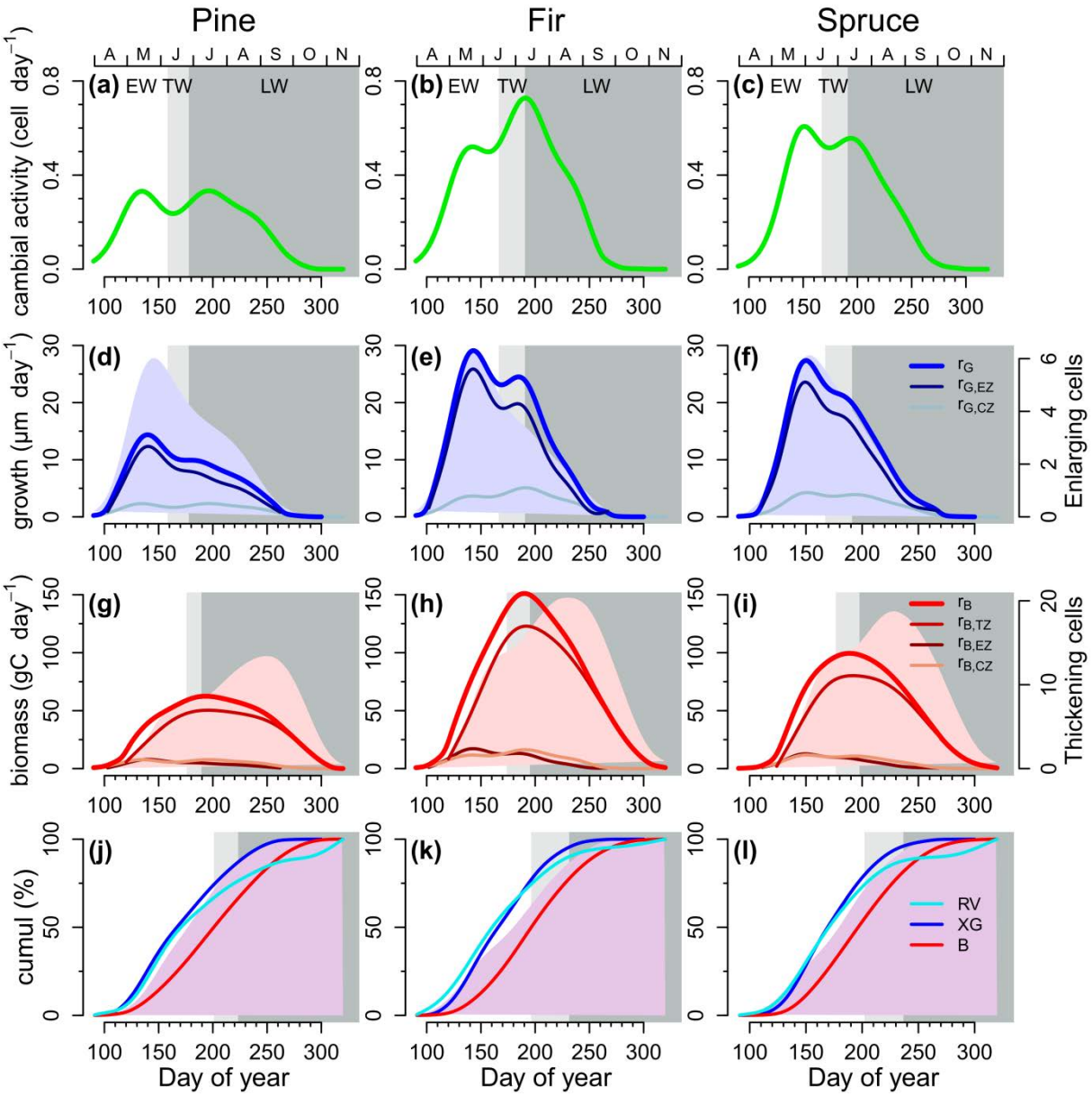

Figure VII.2: Seasonal evolution of the rate of cambial activity, xylem growth, and biomass accumulation in the forming wood tissue for Scots pine, silver fir, and Norway spruce. The rate of xylem growth (r_G) integrates the contribution of the appearance of new xylem cells in the cambial zone ($r_{G,CZ}$) and the expansion of these cells in the enlargement zone ($r_{G,EZ}$). The total rate of biomass accumulation (r_B) in the forming wood corresponds to the rate of biomass accumulation in the secondary walls in the thickening zone ($r_{B,TZ}$) plus the rate of biomass accumulation in the primary walls in the cambial ($r_{B,CZ}$) and enlargement ($r_{B,EZ}$) zones. The last line of the figure gives the cumulated radial variations (RV) – measured from dendrometers – along with the cumulative xylem growth (XG) and biomass accumulation (B) in the forming wood. Blue and red areas represent the number of cells in the enlargement and wall thickening zones, and purple area represents the total number of produced cells.

Seasonal evolution of primary and secondary wall formation, lignification and biomass accumulation

Biomass was allocated to the walls of forming tracheids during almost 7 months, from the middle (pines and firs) or the end (spruces) of April to the beginning of November. For the three species, we estimated the formation of primary walls to account for only 20% of the rate of biomass accumulation in the forming wood (12% for the formation of tangential primary

walls in the cambial zone and 8% for the formation of radial primary walls in the enlargement zone). The rate of biomass accumulation was largely (80%) driven by the secondary walls in formation in the thickening zone (Figure VII.2g,h,i). Thus, the rate of biomass accumulation in wood followed a quite symmetric bell-shaped which followed this of the biomass accumulation in secondary walls. It culminates in the first half of July (Table VII.2), at the time when the cell of transition wood where in the thickening zone (Figure VII.2g,h,i). However, the top of bell-shaped curves was quite flat, in particular in pines. Consequently, the period covered by the maximal rate of biomass accumulation (> 95% of the maximum) was quite long. It lasted one month in firs and spruces, from the end of June to the end of July. It spread about 2 weeks longer in pines, until the beginning of August (Table VII.2). Maximal biomass accumulation in secondary walls – and so on in wood – occurred before the maximal number of cells in the thickening zone was reached. This means that the individual rates of secondary wall deposition were lower at the time of the maximal number of thickening cells, which corresponded to the latewood cells. During the growing season, the rate of biomass accumulation to the forming wood was lowest in pines and highest in firs, as visible in the mean (41 gC day^{-1} in pines, 56 gC day^{-1} in spruces, and 84 gC day^{-1} in firs) and maximal (62 gC day^{-1} in pines, 99 gC day^{-1} in spruces, and 151 gC day^{-1} in firs) values.

Table VII.2: day of occurrence of the first (t_{peak1}) and second (t_{peak2}) peak of cambial activity, day of occurrence of the maximal (t_{max}) rate of xylem growth and biomass allocation, and period of maximal values (> 95% of the maximum) of biomass accumulation.

	Cambial activity		Xylem growth	Biomass accumulation	
	t_{peak1}	t_{peak2}	t_{max}	t_{max}	period max
pine	135 (15 May)	196 (15 July)	140 (20 May)	192 (11 July)	176 - 215 (25 June - 3 August)
fir	139 (19 May)	191 (10 July)	144 (24 May)	190 (9 July)	177 - 204 (26 June - 23 July)
Spruce	151 (31 May)	194 (13 July)	149 (29 May)	188 (7 July)	175 - 207 (24 June – 26 July)

Comparison between radial variations, xylem growth and biomass accumulation

The cumulative xylem growth – calculated from wood tissue sampling – and radial variations – measured from dendrometers – followed an evolution close to this of xylem cell accumulation (Figure VII.2j,k,l). So, the rate of stem radial variations computed from dendrometer measurements was globally in agreement with the rate of xylem growth computed from the microcores (Figure VII.3). The maximal rate of radial growth computed from dendrometer occurred at the end of May ($t_{max,\ fir}$ = 142 d, $t_{max,\ pine}$ = 145 d, $t_{max,\ spruce}$ = 151 d), with a difference of only 2 to 4 days with the occurrence date of the maximal rate of xylem growth calculated from microcore sampling. Only in firs, the second peak exhibited by the rate of xylem growth calculated from microcores was not found on the rate of stem radial growth calculated from dendrometers.

On the other hand, the cumulative biomass allocated in the wood did not followed the increasing in cell number and radial growth (Figure VII.2j,k,l). So, the rate of biomass accumulation in the forming wood presented a dynamics largely delayed with this of the radial growth rate (Figure VII.3). Thus, we observed an impressive lag of 1.5 months between the maximal rate of radial growth – either calculated from dendrometer measurements or wood tissue sampling – and the maximal rate of biomass accumulation in the forming wood. Similarly, at the middle of September, when stem stopped to grow, the biomass accumulation in secondary walls was still at almost 50% of its maximal value. The biomass accumulation in secondary walls finished at the beginning of November, almost 2 months after the end of stem growth.

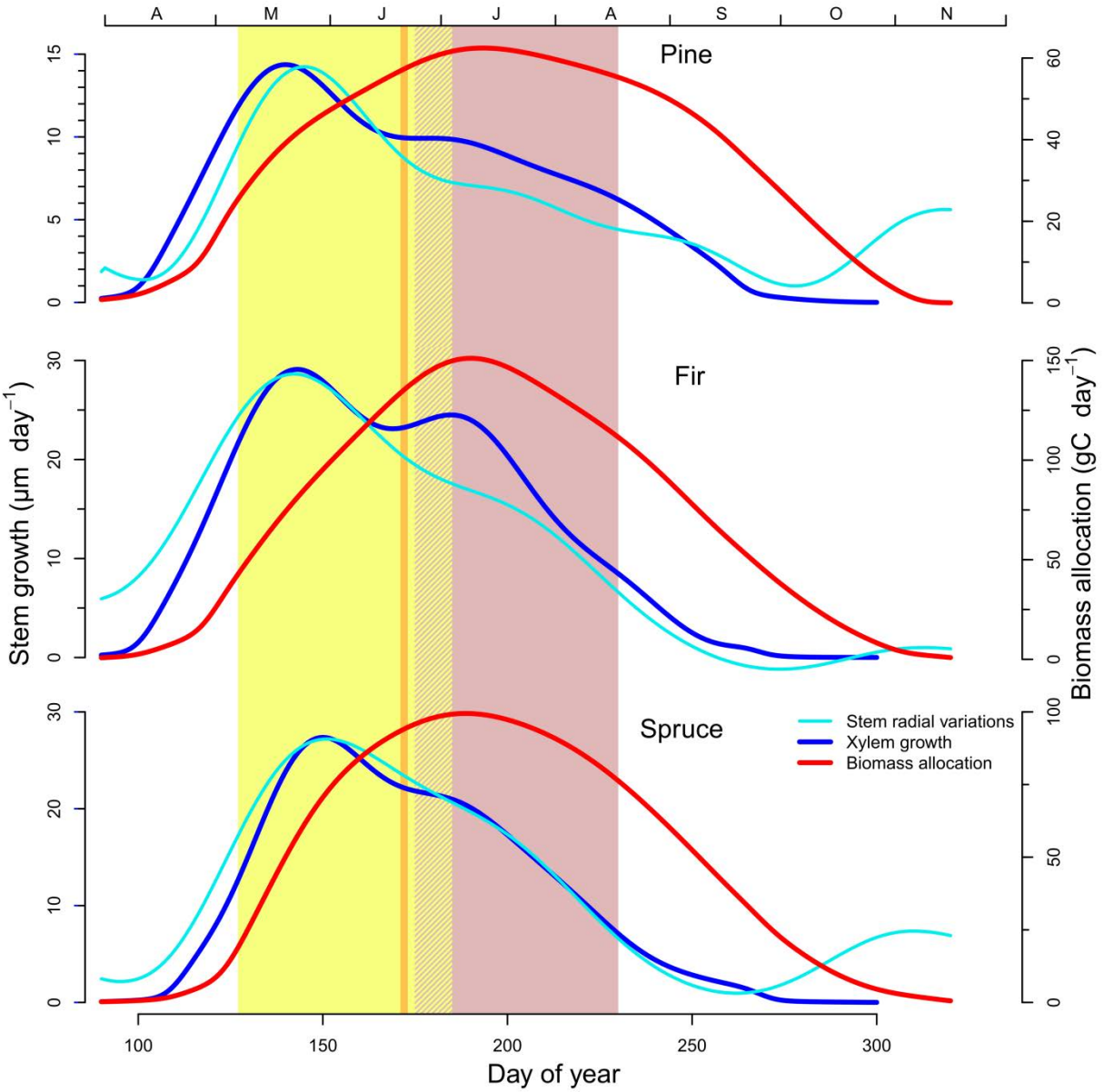

Figure VII.3: Comparison between the seasonal dynamics of stem radial variations, xylem growth and biomass accumulation in the forming wood tissue for Scots pine, silver fir, and Norway spruce. Yellow and red areas represents the period of maximal (> 95% of the maximum) radiation and temperatures, respectively. Orange vertical line represents summer solstice.

Influence of the environment

The maximal rate of xylem growth – which occurred about the same time than the first peak of cambial activity (Figure VII.2, Table VII.2) – occurred at the very beginning of the brightest period (Figure VII.3). So, it was 1 month before summer solstice and the beginning of the warmest period. On the other hand, the maximal rate of biomass accumulation – which occurred about the same time than the second peak of cambial activity (Table VII.2) – was reached at the beginning of the warmest period, 1 month after the occurrence of maximal radiation, and more than 2 weeks after summer solstice. Thus, the period of maximal biomass accumulation (> 95% of the maximum) occurred later than the brightest period, covering only 15% of its right-margin. It was more synchronized with the warmest temperatures, covering about 60% of the period of maximal temperatures on its left-margin.

Discussion

In this study, we used a large dataset – 45 trees of three conifer species (silver fir, Norway spruce, and Scots pine) monitored over three years (2007 – 2009) in three mixed stands along an altitudinal gradient (350 to 650 m ASL) under a temperate climate – to characterize the intra-annual pattern of cambial activity, xylem growth, and biomass accumulation in the forming wood. Each of this xylogenesis component followed a specific intra-annual dynamics. Cambial activity was spread over 5 months, from mid-April to mid-September, and followed a pattern close to bimodal (Figure VII.4). It presented 2 peaks in spring and summer, while high rates were maintained between these two peaks. Xylem growth occurred during the same period than cambial activity, but following a left-skewed bell-shape curve that culminates in spring. By contrast, the rate of biomass accumulation was spread over 7 months, until the beginning of November, and demonstrated a bell-shape curve that culminates in summer. To our knowledge, this study is the first to propose a precise, process-based, characterization of the seasonal dynamics of biomass accumulation in the forming wood, a key aspect of the carbon cycle.

Seasonal dynamics of cambial activity: comparison between various climates

By contrast to our results, studies dealing with cambial activity have described left-skewed bell-shaped curves for the seasonal evolution of the cell production rate (Mäkinen *et al.*, 2003; Rossi *et al.*, 2006; Gruber *et al.*, 2010). An explanation of such a discrepancy is in the methodology used to assess this rate. All authors cited above used the parametric Gompertz function, while we used the more flexible, said “data-driven”, generalized additive models (GAMs). The superiority of GAMs over the Gompertz function to precisely describe intra-annual wood formation dynamics has been demonstrated in Cuny *et al.* (2013). In this previous paper, we compared the performance of the two approaches to describe intra-annual wood formation dynamics on similar data than those of this study (upper site only). Gompertz functions gave only slightly less good fittings on data than GAMs, but this leaded to large differences when characterizing further the dynamics. Thus, concerning cambial activity rate, the Gompertz function revealed bell-shaped patterns that culminate between the two peaks highlighted by GAMs. So, we believe that the use of the Gompertz function constrained

growth to follow bell-shaped patterns that are not necessarily well representative of the underlying data.

Although the dynamics in bell-shape as revealed by Gompertz is open to criticism, there is no doubt that trees of cold environments (high altitudes of latitudes) display a more "explosive" cambial activity dynamics than this found in this study. Indeed, they are constraint to grow in a period about twice shorter (Deslauriers *et al.*, 2008; Makinen *et al.*, 2008; Rossi *et al.*, 2008; Zhai *et al.*, 2012), but reach cell production rates as high than in this study (Mäkinen *et al.*, 2003; Rossi *et al.*, 2006). By contrast, Camarero *et al.* (2010) found for conifers in dry environments (Mediterranean region, north of Spain) that cambial activity was spread over 7 months (May - November) and followed a clear bimodal pattern, with two peaks of cambial activity in spring and autumn separated by a summer period of very low rate. So, the pattern highlights in this study for conifers grown under a temperate climate appears as an intermediate between the wide-spread and marked bimodal pattern observed for conifers of Mediterranean region (Camarero *et al.*, 2010) and the explosive, supposed unimodal, pattern of conifers grown in cold environments (Mäkinen *et al.*, 2003; Rossi *et al.*, 2006). So, in addition to phenology, the seasonal pattern of cambial activity seems to be an aspect of xylogenesis highly variable according to the environment.

Time-lag between stem growth and biomass accumulation

The rate of radial stem variation computed from dendrometer measurement was quite close to the rate of xylem growth computed from microcore sampling. Such a result confirms that xylem growth is the main driver of stem radial growth. On the other hand, the rate of radial growth was not in agreement with the rate of cambial activity, which confirms that cambial activity cannot be assessed on the basis of stem growth measurements (Mäkinen *et al.*, 2003; Deslauriers et al., 2007; Mäkinen *et al.*, 2008).

Similarly, we observed a lag of 1.5 months between the dynamics of radial growth – either assessed from dendrometer or microcore sampling – and this of the biomass accumulation in the forming wood (Figure VII.4). Such a lag means that the monitoring of tree growth does not reflect the dynamics of biomass accumulation in the stem. This result can be explained by the fact that these growth aspects are supported by different processes having different seasonal dynamics. On the one hand, tree radial growth is mainly driven by the expansion of the new cells produced by cambial activity in the enlargement zone. Cells of earlywood develop a large diameter and accumulate in the enlargement zone at the beginning of the season, hence the maximal radial growth rate in spring. Then, despite the maintenance of high cambial activity, cells develop smaller diameter during their enlargement and the radial growth rate decreases.

On the other hand, the rate of biomass accumulation depends on the deposition rate of wall-material to the forming wood, in particular to the thick and highly lignified secondary walls that surround tracheids. Generally, the amount of secondary wall material deposited within tracheids increases among the cells until the beginning of latewood (Cuny *et al.*, under review), which explains why the maximal biomass accumulation is reached later than the

maximal growth rate. Moreover, the duration of secondary wall formation increases during the season, reaching until 2 months for the last cells (Skene, 1969; Wodzicki, 1971; Skene, 1972; Horacek *et al.*, 1999; Cuny *et al.*, 2013). Because of this, many cells accumulate in the wall thickening zone at the end of the season (Cuny *et al.*, 2013), hence the maintenance of a high rate of biomass accumulation at the tissue level after the end of cambial activity and xylem growth.

Zweifel *et al.* (2010) found a tight relationship between the dynamics of stem radial growth measured from dendrometer and this of the net ecosystem productivity measured by eddy covariance, and this at various time-scales (annual and intra-annual). A relationship between stem basal increment and NEP at annual scale as found by Zweifel *et al.* (2010) but also Rocha *et al.* (2006) can be easily explained by the fact that the annual aboveground wood increment represents most of the annual biomass accumulation in a forest ecosystem (Barford *et al.*, 2001). But at a shorter time scale, the relationship is very surprising as we demonstrate that the dynamics of radial growth convey only poor information on the dynamics of biomass accumulation. Anyway, the mechanism at the origin of this association between ecosystem carbon flux measurement and radial growth at short time scale cannot be explained by the carbon accumulation in the forming wood.

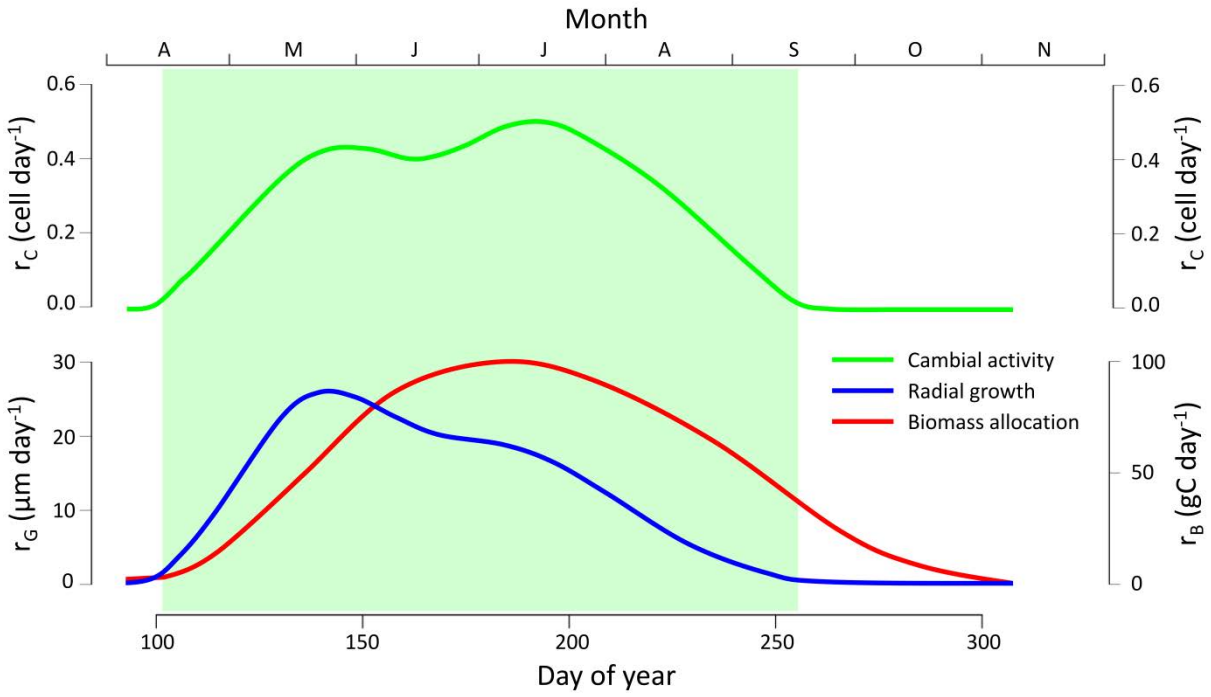

Figure VII.4: Typical seasonal evolution of the rate of cambial activity (rC), tree radial growth (rG), and biomass accumulation (rB) in the forming wood for conifers under a temperate climate.

Environmental influence on cambial activity, tree radial growth and biomass accumulation

The first peak of cambial activity occurred in May, at the very beginning of the brightest period, whereas the second one occurred in July, during the period of warmest temperature. The period of slower growth separating the two peaks covered the maximal day length. So, the idea that the summer solstice acts as a limit after which growth tends to decline (Rossi *et*

al., 2006; Cuny *et al., 2012*) does not stand for conifers grown under mild temperate climates. In addition to the questionable use of the Gompertz function explained above, an additional explanation of such a difference is that growth is less constrained by temperature in our temperate mild study area than in cold environments, so that trees can maintain high rates over a longer period without taking too much risks of cold damage.

We found the second peak of cambial activity and the maximal biomass accumulation in the forming wood to occur rather in the warmest than in the brightest period of the year. So, this suggests temperature is the main driver of biomass accumulation in conifer trees under a temperate climate. According to Körner (1998; 2003), biomass allocation in trees under current ambient CO2 concentrations is limited by sink activity (i.e. xylem cell differentiation), and not by source activity (i.e. carbon supply by photosynthesis activity). Such a sink limitation has been directly related to temperature influence, as the processes of xylem cell differentiation are more sensitive to temperature than photosynthesis. So, our results go in the sense of a biomass accumulation limited by sink activity, itself under the direct influence of temperature, as a limitation by the source would rather result in a limitation by light.

Conclusion

In this study, we applied recent methodological improvement in assessing fine aspects of wood formation dynamics on a valued dataset – 45 trees of three conifer species monitored over three years in a temperate area – in order to characterize together for the first time the intra-annual dynamics of cambial activity, tree radial growth, and biomass accumulation in the forming wood. Results show that these components of xylogenesis have different intra-annual dynamics. Thus, cambial activity presented a quite bimodal pattern with a first peak in spring and a second peak in summer, while radial growth – either calculated from wood tissue sampling or dendrometer – followed a left-skewed bell-shaped dynamics that culminates in spring, and biomass accumulation in the forming wood followed a bell-shaped dynamics that culminates in summer.

Overall, a lag of 1.5 months was observed between the dynamics of stem radial growth and this of biomass accumulation, indicating that the monitoring of stem growth cannot give accurate information about the dynamics of carbon accumulation in tree stem at intra-annual time scales. Such a time lag can be easily explained by the fact that these growth aspects are supported by different processes. Tree radial growth depends mainly on cell enlargement, whereas biomass accumulation mainly depends mainly on secondary wall formation.

The first peak of cambial activity and the spring culmination of radial growth occurred before optimal growth conditions, at the very beginning of the brightest period and far before the warmest period. Moreover, they did not involve high energy costs, suggesting that they are not under a strong environmental determinism. On the other hand, the second peak of cambial activity and maximal rate of biomass accumulation occurred during the warmest period, and not the brightest period. So, temperature appears as the most important environmental factor driving biomass accumulation in wood.

Acknowledgements

We thank E. Cornu, E. Farré, C. Freyburger, P. Gelhaye, and A. Mercanti for fieldwork and monitoring; M. Harroué for sample preparation in the laboratory; Bernard Longdoz of the forest ecology and ecophysiology (EEF) team and the association for the study and monitoring of air pollution in Alsace (ASPA) for the meteorological data. Manuel Nicholas of the French permanent plot network for the monitoring of forest ecosystems (RENECOFOR) for the meteorological data and the description of the soil profiles.

References

Abe H, Funada R, Ohtani J, Fukazawa K. 1997. Changes in the arrangement of cellulose microfibrils associated with the cessation of cell expansion in tracheids. *Trees-Structure and Function* **11**(6): 328-332.

Barford CC, Wofsy SC, Goulden ML, Munger JW, Pyle EH, Urbanski SP, Hutyra L, Saleska SR, Fitzjarrald D, Moore K. 2001. Factors controlling long-and short-term sequestration of atmospheric CO2 in a mid-latitude forest. *Science* **294**(5547): 1688-1691.

Bouriaud O, Leban JM, Bert D, Deleuze C. 2005. Intra-annual variations in climate influence growth and wood density of Norway spruce. *Tree Physiology* **25**(6): 651-660.

Camarero JJ, Olano JM, Parras A. 2010. Plastic bimodal xylogenesis in conifers from continental Mediterranean climates. *New Phytologist* **185**(2): 471-480.

Canadell JG, Raupach MR. 2008. Managing forests for climate change mitigation. *Science* **320**(5882): 1456-1457.

Cuny HE, Rathgeber CBK, Fournier M. under review. Big cells, thin walls; small cells, thick walls: how xylem cell differentiation process shapes conifer tree-ring structure.

Cuny HE, Rathgeber CBK, Lebourgeois F, Fortin M, Fournier M. 2012. Life strategies in intra-annual dynamics of wood formation: example of three conifer species in a temperate forest in north-east France. *Tree Physiology* **32**(5): 612-625.

Cuny HE, Rathgeber CBK, Senga Kiesse T, Hartmann FP, Barbeito I, Fournier M. 2013. Generalized additive models reveal the intrinsic complexity of wood formation dynamics. *Journal of Experimental Botany*.

Decoux V, Varcin E, Leban JM. 2004. Relationships between the intra-ring wood density assessed by X-ray densitometry and optical anatomical measurements in conifers. Consequences for the cell wall apparent density determination. *Annals of Forest Science* **61**(3): 251-262.

Demura T, Ye Z-H. 2010. Regulation of plant biomass production. *Current Opinion in Plant Biology* **13**(3): 298-303.

Denne MP. 1988. Definition of latewood according to Mork (1928). *Iawa Bulletin* **10**(1): 59-62.

Deslauriers A, Morin H, Urbinati C, Carrer M. 2003. Daily weather response of balsam fir (*Abies balsamea* (L.) Mill.) stem radius increment from dendrometer analysis in the boreal forests of Quebec (Canada). *Trees-Structure and Function* **17**(6): 477-484.

Deslauriers A, Rossi S, Anfodillo T. 2007. Dendrometer and intra-annual tree growth: What kind of information can be inferred? *Dendrochronologia* **25**(2): 113-124.

Deslauriers A, Rossi S, Anfodillo T, Saracino A. 2008. Cambial phenology, wood formation and temperature thresholds in two contrasting years at high altitude in southern Italy. *Tree Physiology* **28**(6): 863-871.

Downes G, Beadle C, Worledge D. 1999. Daily stem growth patterns in irrigated Eucalyptus globulus and E. nitens in relation to climate. *Trees* **14**(2): 102-111.

Granier A, Breda N, Biron P, Villette S. 1999. A lumped water balance model to evaluate duration and intensity of drought constraints in forest stands. *Ecological Modelling* **116**(2-3): 269-283.

Gričar J, Čufar K. 2008. Seasonal dynamics of phloem and xylem formation in silver fir and Norway spruce as affected by drought. *Russian Journal of Plant Physiology* **55**(4): 538-543.

Gričar J, Krze L, Čufar K. 2009. Number of cells in xylem, phloem and dormant cambium in silver fir (*Abies alba*), in trees of different vitality. *Iawa Journal* **30**(2): 121-133.

Gričar J, Zupančič M, Čufar K, Koch G, Schmitt U, Oven P. 2006. Effect of local heating and cooling on cambial activity and cell differentiation in the stem of Norway spruce (*Picea abies*). *Annals of Botany* **97**(6): 943-951.

Gričar J, Zupančič M, Čufar K, Oven P. 2007. Regular cambial activity and xylem and phloem formation in locally heated and cooled stem portions of Norway spruce. *Wood Science and Technology* **41**(6): 463-475.

Gruber A, Strobl S, Veit B, Oberhuber W. 2010. Impact of drought on the temporal dynamics of wood formation in *Pinus sylvestris*. *Tree Physiology* **30**(4): 490-501.

Horacek P, Slezingerova J, Gandelova L 1999. Effects of environment on the xylogenesis of Norway spruce (*Picea abies* L. Karst.). In: Wimmer R, Vetter RE eds. *Tree-ring analysis: biological, methodological and environmental aspects.* Wallingford, UK: CABI Publishing, 33-53.

Körner C. 1998. A re-assessment of high elevation treeline positions and their explanation. *Oecologia* **115**(4): 445-459.

Körner C. 2003. Carbon limitation in trees. *Journal of Ecology* **91**(1): 4-17.

Kutscha NP, Hyland F, Schwarzmann JM. 1975. Certain seasonal changes in balsam fir cambium and its derivatives. *Wood Science and Technology* **9**(3): 175-188.

Lal R. 2008. Sequestration of atmospheric CO2 in global carbon pools. *Energy & Environmental Science* **1**(1): 86-100.

Lamlom S, Savidge R. 2003. A reassessment of carbon content in wood: variation within and between 41 North American species. *Biomass and Bioenergy* **25**(4): 381-388.

Lupi C, Morin H, Deslauriers A, Rossi S. 2012. Xylogenesis in black spruce: does soil temperature matter? *Tree Physiology* **32**(1): 74-82.

Mäkinen H, Nöjd P, Saranpää P. 2003. Seasonal changes in stem radius and production of new tracheids in Norway spruce. *Tree Physiology* **23**(14): 959-968.

Mäkinen H, Seo JW, Nöjd P, Schmitt U, Jalkanen R. 2008. Seasonal dynamics of wood formation: a comparison between pinning, microcoring and dendrometer measurements. *European Journal of Forest Research* **127**(3): 235-245.

Moser L, Fonti P, Büntgen U, Esper J, Luterbacher J, Franzen J, Frank D. 2010. Timing and duration of European larch growing season along altitudinal gradients in the Swiss Alps. *Tree Physiology* **30**(2): 225-233.

Oribe Y, Funada R, Shibagaki M, Kubo T. 2001. Cambial reactivation in locally heated stems of the evergreen conifer *Abies sachalinensis* (Schmidt) Masters. *Planta* **212**(5-6): 684-691.

Pauly M, Keegstra K. 2010. Plant cell wall polymers as precursors for biofuels. *Current Opinion in Plant Biology* **13**(3): 304-311.

Plomion C, Leprovost G, Stokes A. 2001. Wood formation in trees. *Plant Physiology* **127**(4): 1513-1523.

R Core Team 2012. R: A language and environment for statistical computing. R Foundation for Statistical Computing, Vienna, Austria. ISBN 3-900051-07-0, URL http://www.R-project.org/.

Rathgeber CBK 2012. Cambial activity and wood formation: data manipulation, visualisation and analysis using R. R package version 1.4-1. http://CRAN.R-project.org/package=CAVIAR.

Rathgeber CBK, Rossi S, Bontemps J-D. 2011. Cambial activity related to tree size in a mature silver-fir plantation. *Annals of Botany* **108**(3): 429-438.

Rocha AV, Goulden ML, Dunn AL, Wofsy SC. 2006. On linking interannual tree ring variability with observations of whole-forest CO2 flux. *Global Change Biology* **12**(8): 1378-1389.

Rossi S, Deslauriers A, Anfodillo T, Carraro V. 2007. Evidence of threshold temperatures for xylogenesis in conifers at high altitudes. *Oecologia* **152**(1): 1-12.

Rossi S, Deslauriers A, Anfodillo T, Morin H, Saracino A, Motta R, Borghetti M. 2006. Conifers in cold environments synchronize maximum growth rate of tree-ring formation with day length. *New Phytologist* **170**(2): 301-310.

Rossi S, Deslauriers A, Gričar J, Seo J-W, Rathgeber CBK, Anfodillo T, Morin H, Levanic T, Oven P, Jalkanen R. 2008. Critical temperatures for xylogenesis in conifers of cold climates. *Global Ecology and Biogeography* **17**(6): 696-707.

Rossi S, Deslauriers A, Morin H. 2003. Application of the Gompertz equation for the study of xylem cell development. *Dendrochronologia* **21**(1): 33-39.

Skene DS. 1969. The period of time taken by cambial derivatives to grow and differentiate into tracheids in *Pinus radiata* D. Don. *Annals of Botany* **33**(2): 253-262.

Skene DS. 1972. The kinetics of tracheid development in *Tsuga canadensis* Carr. and its relation to tree vigour. *Annals of Botany* **36**(1): 179-187.

Swidrak I, Gruber A, Kofler W, Oberhuber W. 2011. Effects of environmental conditions on onset of xylem growth in Pinus sylvestris under drought. *Tree Physiology* **31**: 483–493.

Wodzicki TJ. 1971. Mechanism of xylem differentiation in *Pinus sylvestris* L. *Journal of Experimental Botany* **22**(72): 670-687.

Wood SN. 2006. *Generalized additive models: an introduction with R*. Boca Raton, FL: Chapman and Hall/CRC.

Worbes M. 1999. Annual growth rings, rainfall - dependent growth and long - term growth patterns of tropical trees from the Caparo Forest Reserve in Venezuela. *Journal of Ecology* **87**(3): 391-403.

Zhai L, Bergeron Y, Huang J-G, Berninger F. 2012. Variation in intra-annual wood formation, and foliage and shoot development of three major Canadian boreal tree species. *American Journal of Botany* **99**(5): 827-837.

Zhao M, Running S. 2010. Drought-Induced Reduction in Global Terrestrial Net Primary Production from 2000 Through 2009. *Science* **329**(5994): 940-943.

Zweifel R, Eugster W, Etzold S, Dobbertin M, Buchmann N, Hasler R. 2010. Link between continuous stem radius changes and net ecosystem productivity of a subalpine Norway spruce forest in the Swiss Alps. *New Phytologist* **187**(3): 819-830.

Zweifel R, Item H, Häsler R. 2001. Link between diurnal stem radius changes and tree water relations. *Tree Physiology* **21**(12-13): 869-877.

Zweifel R, Zimmermann L, Zeugin F, Newbery DM. 2006. Intra-annual radial growth and water relations of trees: implications towards a growth mechanism. *Journal of Experimental Botany* **57**(6): 1445-1459.

Supplementary material

Table VII.S1: Main characteristics (mean ± SE) of the monitored trees from the three studied species (silver fir, Norway spruce and Scots pine) illustrated by the age, diameter at breast height (DBH), height (H), and projected crown area (CA).

Site	Species	Age	DBH (cm)	H (m)	CA (m²)
Walscheid	Fir	94 ± 2	56 ± 1	31 ± 1	43 ± 5
	Spruce	89 ± 4	53 ± 2	32 ± 1	40 ± 5
	Pine	95 ± 3	52 ± 3	31 ± 1	41 ± 10
Abreschviller	Fir	135 ± 2	60 ± 3	36 ± 1	28 ± 5
	Spruce	85 ± 7	41 ± 2	32 ± 1	16 ± 2
	Pine	162 ± 3	33 ± 3	36 ± 1	20 ± 5
Grandfontaine	Fir	73 ± 3	57 ± 3	31 ± 1	37 ± 6
	Spruce	74 ± 4	55 ± 4	33 ± 1	30 ± 7
	Pine	119 ± 3	53 ± 2	27 ± 1	29 ± 2
Means	Fir	101 ± 6	58 ± 2	33 ± 1	36 ± 3
	Spruce	83 ± 3	49 ± 2	32 ± 1	29 ± 4
	Pine	126 ± 8	56 ± 2	32 ± 1	30 ± 4

Table VII.S2: List of the variables used in this work

Notation	Variable	Unit	Acquisition
LumRD	Lumen radial diameter	µm	Measured
LumTD	Lumen tangential diameter	µm	Measured
LumCA	Lumen cross-area	µm²	Measured
WallRT	Wall radial thickness	µm	Measured
WallTT	Wall tangential thickness	µm	$\mathrm{WallTT} = 1.2 \times \mathrm{WallRT}$
WallCA	Wall cross area	µm²	$\mathrm{WallCA} = \mathrm{CellCA} - \mathrm{LumCA}$
CellRD	Cell radial diameter	µm	$\mathrm{CellRD} = \mathrm{LumRD} + 2 \times \mathrm{WallRT}$
CellTD	Cell tangential diameter	µm	$\mathrm{CellTD} = \mathrm{LumTD} + 2.4 \times \mathrm{WallRT}$
CellCA	Cell cross area	µm²	$\mathrm{CellCA} = \mathrm{CellRD} \times \mathrm{CellTD}$
MC	Mork's criterion	NA	$\mathrm{MC} = \frac{4 \times \mathrm{WallRT}}{\mathrm{LumRD}}$
d_C	Cell residence duration in the cambial zone	day	Calculated
d_E	Cell residence duration in the enlargement	day	Calculated
d_T	Cell residence duration in the thickening	day	Calculated
d_F	Total duration of tracheid formation	day	Calculated
r_E	Rate of cell radial enlargement	µm day^{-1}	$r_E = \frac{\mathrm{CellRD}}{d_E}$
r_W	Rate of wall deposition	µm² day^{-1}	$r_W = \frac{\mathrm{WallCA}}{d_T}$
r_R	Rate of stem radial variation	µm day^{-1}	Measured
r_C	Rate of cell production by the cambial zone	cell day^{-1}	Calculated
$r_{G,CZ}$	Growth rate provided by the cambial zone	µm day^{-1}	$r_{G,CZ} = r_C \times 7$
$r_{G,EZ}$	Growth rate provided by the enlargement zone	µm day^{-1}	Calculated (Method VII.S1)
r_G	Rate of xylem growth	µm day^{-1}	$r_G = r_{G,CZ} + r_{G,EZ}$
$r_{B,CZ}$	Rate of biomass accumulation in the cambial zone	gC day^{-1}	Calculated (Method VII.S2)
$r_{B,EZ}$	Rate of biomass accumulation in the enlargement zone	gC day^{-1}	Calculated (Method VII.S2)
$r_{B,TZ}$	Rate of biomass accumulation in the thickening zone	gC day^{-1}	Calculated (Method VII.S2)
r_B	Rate of biomass accumulation in the forming wood	gC day^{-1}	$r_B = r_{B,CZ} + r_{B,EZ} + r_{B,TZ}$
T	Temperature	°C	Measured
P	Precipitations	mm	Measured
R	Cumulative global radiation	J cm^{-2}	Measured
DL	Day length	h	Calculated
REW	Soil relative extractable water	%	Calculated

Method VII.S1: Calculation of a rate of xylem growth

For each species, a rate of xylem growth was also calculated from the rate of cambial activity and the individual rates of cell diameter enlargement in the enlarging zone.

We assumed that the division of a cambial cell leads to the appearance of a new cell of 7 µm in diameter. So, the rate of xylem provided by the cambial zone ($r_{G,CZ}$) is calculated simply by multiplying the rate of cambial activity by 7:

$$r_{G,CZ} = r_C \times 7$$

Moreover, the the rate of xylem growth provided by the enlargement zone ($r_{G,EZ,t}$)was calculated as the sum of the individual rates of cell enlargement:

$$r_{G,EZ,t} = \sum_{i=1}^{n_{E,t}} r_{E,i}$$

where $n_{E,t}$ is the number of cells in the enlargement zone at day t, $r_{E,i}$ is the enlargement rate of the cell i of the $n_{E,t}$ cells.

The rate of xylem growth (r_G) can then be calculated as the sum of the contributions of cambial activity and enlargement:

$$r_G = r_{G,CZ} + r_{G,EZ}$$

Method VII.S2: Calculation of a rate of biomass accumulation in tree stem

At a day t, the rate of tangential primary walls formation in the dividing cells of the cambial zone ($r_{W,CZ,t}$) is calculated from the rate of cambial activity. For that, we assume that the division of a cambial cell generates 2 primary walls of 1µm in thick and equal in length to the width of the radial file width:

$$r_{W,CZ,t} = r_{C,t} \times 2 \times 1 \times RF_w$$

where $r_{C,t}$ is the rate of cambial activity at day t, RF_w is the width of the radial file.

At a day t, the rate of radial primary walls formation in the enlarging cells of the enlargement zone ($r_{W,EZ}$) is calculated from the rate of xylem growth. For that, we assume that a given xylem growth generates 2 primary walls of 1 µm in thick and equal in length to the lengthening of the xylem:

$$r_{W,EZ,t} = r_{G,t} \times 2 \times 1$$

where $r_{G,t}$ is the rate of xylem growth at day t.

At a day t, the rate of secondary wall deposition in the thickening zone ($r_{W,TZ}$) – is calculated as the sum of the individual rates of wall deposition calculated for each cell i:

$$r_{W,TZ,t} = \sum_{i=1}^{n_{T,t}} r_{W,i}$$

where $n_{T,t}$ is the number of cell in the thickening zone at day t, $r_{W,i}$ is the wall deposition rate of the cell i of the $n_{T,t}$ cells.

The total rate of wall deposition in the radial file ($r_{W,RF,t}$) is calculated as the sum of the rates of primary and secondary wall deposition.

After measuring the mean width of a radial file and the mean circumference at breast height of the studied trees, we can estimate the number of radial files composing a tree ring at the periphery of the base of the stem. So, the total rate of wall deposition at the tree ring level ($r_{W,TR,t}$) can be estimated as:

$$r_{w,TR,t} = r_{w,RF,t} \times n_{RF}$$

where n_{RF} is the estimated number of radial files composing a tree ring at the periphery at the base of the stem.

The total rate of wall deposition at the stem level ($r_{W,S,t}$) is obtained on the basis of a cone and from the height of the studied trees (H):

$$r_{W,S,t} = \frac{1}{3} \times H \times r_{W,TR,t}$$

Based on an apparent density of the wall of 1.100 g cm^{-3}, and on a carbon percentage in wood of 50% of dry weight, we converted our volumetric wall deposition rate at the stem level in a rate of biomass accumulation ($r_{B,t}$):

$$r_{B,t} = 1.100 \times r_{W,S,t} \times 0.5$$

This rate is expressed in gram of carbon per day (gC day^{-1}).

Proceeding this way, the rates of tangential primary wall deposition in the cambial zone ($r_{W,CZ}$), radial primary wall deposition in the enlargement zone ($r_{W,EZ}$), and secondary wall deposition in the thickening zone ($r_{W,TZ}$) can also be extended at the tree stem level and converted into biomass accumulation (the obtained rates are called $r_{B,CZ}$, $r_{B,EZ}$, and $r_{B,TZ}$, respectively). The relative contribution of these different rates on the global rate of biomass accumulation in the forming wood can then be evaluated.

.

VIII LES PROCESSUS DE LA DIFFÉRENCIATION CELLULAIRE RELIÉS AUX VARIABLES CLIMATIQUES

Dans cette partie, nous utilisons les connaissances acquises dans les parties V (« caractérisation de la cinétique des processus de différenciation cellulaire ») et VI (« mécanismes par lesquels la cinétique des processus donne forme à la structure du cerne ») pour développer une approche mécaniste de l'influence du climat sur les processus du développement cellulaire et la structure du cerne résultante. Pour cela, le travail présenté recherche l'influence des variables climatiques (température, rayonnement et disponibilité en eau) sur la durée et la vitesse des processus de différenciation cellulaire et les dimensions des cellules formées au cours de la saison. Comme dans les deux parties précédentes, le travail porte sur l'ensemble des données, avec les 45 arbres des 3 espèces répartis dans les 3 sites et suivis pendant 3 années (2007 – 2009). Cette partie est constituée d'un article scientifique (article 5) en préparation.

Xylem cell differentiation processes related to climatic factors in conifers

Henri E. Cuny[1*], Cyrille B.K. Rathgeber[1], Meriem Fournier[2]

(In preparation)

[1] INRA, UMR1092, Laboratoire d Etude des Ressources Foret Bois (LERFoB), Centre INRA de Nancy, F-54280 Champenoux, France

[2] AgroParisTech, UMR1092, Laboratoire d Etude des Ressources Foret Bois (LERFoB), ENGREF, 14 rue Girardet, F-54000 Nancy, France

Summary

- Tree rings provide detailed natural archives of crucial importance in reconstructing past climates. They consist of the accumulation, in long-lasting and climate-sensitive structures, of dead xylem cells throughout a growing season. However, which, when and how climate factors influence xylogenesis processes remain unclear. Here, we investigated the influence of climatic factors on xylem cell differentiation processes (enlargement and thickening) which shape conifer tree-ring structure and wood properties.
- Xylogenesis was monitored over 3 years (2007 – 2009) for 45 trees of three species (Norway spruce, Scots pine, and silver fir) grown in three mixed stands in northeast France. Final tracheid dimensions were measured and their differentiation kinetics was calculated. Daily meteorological data were used to characterize climatic conditions experienced during the different phases of tracheid differentiation.
- Cell-wall deposition rate was under climatic influences (solar radiation and temperatures), while secondary wall formation duration and cell expansion rate and duration were not. The climate influences recorded by the wall deposition rate were not engraved on tree-ring structure because they were counterbalanced by cell-wall deposition duration except for the last latewood cells.
- Our results show that xylogenesis is mainly under developmental control. Environmental influences are mainly mediated by the cell-wall deposition rate. The lack of compensation by the wall deposition duration in latewood is a clue to explain the capacity of maximal latewood density to record thermal conditions.

Keywords: cambial activity – climatic factors – quantitative wood anatomy – tree ring structure – xylogenesis

Introduction

A remarkable aspect of xylogenesis is its plasticity, i.e. its capacity to generate various growth forms in response to environmental changes (Rowe & Speck, 2005). The environmental factors, by influencing the dynamics (when, how long and how fast) of xylogenesis processes (division, cell radial enlargement and secondary wall formation), leave permanent imprints in the wood formed (Schweingruber, 1996; Vaganov *et al.*, 1999; Wodzicki, 2001; Fonti *et al.*, 2010). Thus, the structure of an annual ring represents a natural archive of environmental changes, with the tree-ring width, wood density, and cell anatomical features providing valuable bio-indicators used to reconstruct past environmental conditions in general and past climate in particular (see, for example, Hughes *et al.*, 1984; Esper *et al.*, 2002; Treydte *et al.*, 2006; Trouet *et al.*, 2009; Fonti *et al.*, 2010). Such retrospective analyses, however, still lack a precise understanding of the detailed mechanisms by which environmental changes influence tree-ring structure (Vaganov *et al.*, 2011). Such information is crucial, because it is the only way to ensure the reliability of past-climatic reconstructions and climate change impact assessments. So, a more detailed mechanistic understanding of the influence of the environmental influence on xylogenesis is needed, which implies to evaluate the influence of ecological climatic factors not only on the final tree-ring structure, but also on the processes responsible for the making of this structure (Gričar *et al.*, 2011).

Environmental influence on xylem cell differentiation is complex, because the growth processes involved are coupled with other physiological processes in the living tree (e.g., photosynthesis, respiration, plant nutrition, water uptake, carbon allocation) which are also subject to environmental influences (Denne & Dodd, 1981). Thus, the influence of environmental factors on xylem differentiation may either be direct, through physical inhibition or stimulation of xylogenesis processes, or indirect, e.g. mediated through the synthesis and transport of growth substrates and/or regulators. Another question is about the target of environmental influence. Antonova & Stasova (1993; 1997) supposed that each process (division, enlargement, and secondary wall formation) can be affected by the environmental conditions during the time-window it occurred. On the other hand, Vaganov *et al.* (2006; 2011) argue that the target of environmental influence is the cambial zone, and the signal is then transformed into further processes of cell differentiation.

Moreover, environmental influence is supposed to be specific to each process, according to the nature of the physiological events involved. The new xylem cells produced by division in the cambial zone enter in the enlargement phase where they undergo a marked increase in radial diameter through wall loosening, osmotic-driven water uptake, and deposition of new primary wall material (Cosgrove, 2000a; Cosgrove, 2000b). The basic element for cell enlargement is water, which exerts the pressure to extend the wall, and plays on the wall extensibility itself (Nonami & Boyer, 1990b; Cosgrove, 1997). So, cell expansion has long-term been depicted as one of the plant processes most sensitive to water stress, if not the most sensitive of all (Hsiao, 1973). Following enlargement, cells enter the wall formation phase, where they build a rigid, waterproof, and multi-layered secondary cell wall composed of cellulose, hemicellulose, and lignin (Zhong & Zheng-Hua, 2009). The secondary walls involved high energy costs and represent the bulk of biomass allocation in trees (Demura & Ye, 2010). So, it should depends on the quantity of carbohydrates produced by photosynthesis, for which light is the indispensable energy source (Kozlowski & Pallardy, 1997).

In the 1960s and 1970s, a confusing variety of experimental results has produced a diversity of interpretations (see Denne & Dodd, 1981 for synthesis). Experimentations have been conducted under controlled conditions on seedlings of various species in order to investigate the influence of temperature (Richardson, 1964; Larson, 1967; Denne, 1971), light intensity (Denne, 1974; Smith, 1974; Doley, 1979), photoperiod (Wodzicki, 1964; Denne & Smith, 1971; Smith, 1975), and water supply (Larson, 1963; Zahner *et al.*, 1964; Doley & Leyton, 1968) on xylogenesis. Such studies provide interesting clues on the potential influence of each factor on tree ring formation, but the obtained results do not allow drawing clear conclusions on the environmental control of xylem differentiation in situ. Indeed, each of the studied factors is important, and so possibly affects whole tree physiology and xylogenesis when it is forced to vary beyond critical thresholds. For example, Balatinecz & Farrar (1968) observed that short days alone were sufficient to bring about latewood differentiation, as were water deficits. Moreover, this kind of experimentations on seedlings allowed looking at the influence of environmental factors on ring structure, but not on the processes that determine this structure.

Temperate and boreal regions are characterized by regular seasonal cycles of environmental factors. In parallel, typical changes of cell dimensions occurred along the ring, from the large thin-walled cells of earlywood mainly devoted to water transport, produced at the beginning of the season, to the narrow thick-walled cells of latewood that provide biomechanical strength, produced toward the end of the season (Wilson, 1984). So, another way to study the influence of environmental factors on wood formation is to see how the seasonal cycles of environmental factors influence xylem cell differentiation and the resulting cell dimensions along the ring for mature trees in situ. Antonova & Stasova (1993; 1997) and Wodzicki (1971) chose this option. Both found the main climatic influence to be this of temperature on the wall deposition rate, but they did not have information about light and soil water supply, so that the relationships they drew might be blurred with the influence of other uncontrolled important factors.

Based on the idea that cell enlargement primarily depends on water, we expect that the changes in the kinetic of cell enlargement and resulting diameter along the ring are mainly related to changes in soil water content during the season. Considering that the formation of secondary wall depends on the availability of carbohydrates, we rather expect that the changes in the kinetic of wall deposition and resulting amount of wall deposited in the cells are primarily influenced by changing light conditions during the season. We also test the hypothesis that the sensor of environment influence is the cambial zone (Vaganov *et al.*, 2006; Vaganov *et al.*, 2011).

In this study, we aimed to understand the detailed mechanisms by which seasonal cycle of environmental factors (temperature, water and light balance) influence tree-ring structure under a temperate climate. For that, the wood formation dynamics and resulting tree ring structure were assessed over 3 years (2007-2009) for 45 trees belonging to three conifer species (Norway spruce, Scots pine, and Silver fir) and grown in three mixed stands along an altitudinal gradient (from 350 to 650 m ASL) in the Vosges Mountains (France). In parallel, the environmental conditions were monitored by 3 weather stations in the studied area. For each cell along the ring, the kinetics (duration and rate) of each developmental phase (enlargement and wall thickening) and its final result (cell radial diameter and wall cross area) were related to the climatic factors occurring during the corresponding time-window.

Materials and Methods

Study area

Three sites were selected along an altitudinal gradient (350 to 650 m ASL) in mixed stands composed of silver firs (*Abies alba* Mill.), Norway spruces (*Picea abies* (L.) Karst.) and Scots pines (*Pinus sylvestris* L.) in north-east France, in the temperate forest of the Vosges Mountains. Based on complete inventories of the stands, five dominant and healthy silvers firs, Norway spruces and Scots pines were selected on each site, for a total of 45 studied trees (5 trees × 3 species × 3 sites) (Table VIII.S1). On each site, two soil pits were dug in order to assess soil characteristics (soil type, number of layers and their depth,

proportion of fine roots in each layer).

Meteorological variables recording and soil water balance modeling

In order to characterize the annual cycle of environmental factors, daily meteorological data (temperature, precipitation, cumulative global radiation, wind speed, and relative humidity) of the period 2007-2009 were gathered from three meteorological stations spread along the altitudinal gradient, following the disposition of the selected sites. Moreover, the model Biljou© was used to assess the daily water balance of the three studied stands. In addition to the daily meteorological data mentioned above, the model takes as input some soil (e.g., number and depth of layers, and proportion of fine roots per layer), and stand (forest type and maximum leaf area index) parameters, and gives as output the relative extractable water (REW) on a daily scale. The REW is a relative expression of the filling state of the soil: REW is 100% at field capacity, and 0% at the permanent wilting point. Water stress is assumed to occur when the relative extractable soil water (REW) drops below a threshold of 40%, under which transpiration is gradually reduces due to stomata closure (Granier *et al.*, 1999).

Daily temperature, cumulative global radiation, and REW were aggregated over the three stations and the three years to obtain some means representing a typical annual cycle of environmental factors for the studied area.

Sampling, preparation, and microscopic observations of the developing xylem

For each studied tree, tree-ring formation was monitored from April to November during the 3 years (2007-2009). Microcores were collected weekly on tree stem, prepared in the laboratory, and 5–10-µm-thick transverse sections were cut with a rotary microtome (HM 355S, MM France). Sections were stained with cresyl violet acetate and permanently mounted on glass slides using Histolaque LMR®. Overall, about 4 300 anatomical sections were observed using an optical microscope (AxioImager.M2, Carl Zeiss SAS, France) under visible and polarized light at ×100–400 magnification to distinguish the different phases of development among the cells. Cambial cells had thin primary walls and small radial diameters. Cells in the radial enlargement zone were larger than cambial cells but still had thin primary walls. Contrariwise to enlarging cells, cells in the thickening zone developed secondary walls that shined under polarized light because of the orientation of cellulose microfibrils (Abe *et al.*, 1997). Cresyl violet acetate staining, which stains cellulose in purple and lignin in blue (Kutscha *et al.*, 1975), was used to follow the advancement of lignification. Advanced thickening cells exhibiting violet and blue walls, indicating that lignification was in progress, whereas mature tracheids had entirely lignified and thus completely blue walls.

The number of cells from the previous year was counted on three radial files per sample and used to standardise the raw number of cells of the current year in order to reduce within tree growth variability (Rossi *et al.*, 2003), using a dedicated function of the R package CAVIAR (R Core Team, 2012; Rathgeber, 2012).

Tracheid dimensions measurements

For each tree, at the end of each year, a well-preserved section of the entirely formed tree ring was selected to characterize the dimensions of the cells produced during the year. Digital images of the selected tree rings were analysed with WinCell (Regent instruments, Canada) in order to measure, in the radial direction, the lumen diameter (LumRD), and the wall thickness (WallRT) of tracheids along at least three radial files. The lumen tangential diameter (LumTD) and cross area (LumCA) were also measured. From these measurements, the cell radial diameter (CellRD) and the wall cross area (WallCA) were calculated (see Cuny *et al.*, under review, for details on measurement and calculation of tracheid dimensions) and considered as the final results of the enlargement and wall thickening phase, respectively (Cuny *et al.*, under review).

Profiles of cell size variation along radial files of xylem are called tracheidograms (Vaganov, 1990). Because the number of cells varied between radial files within and between trees, averages could not be calculated directly from raw tracheidograms. So, a standardization method that allows modifying the length of the profiles (cell numbers) without changing their shape (cell sizes) was applied on each tracheidogram (Vaganov, 1990). This standardization was used to normalize all the tracheidograms of a species to the mean number of cells of this species. In this way, the tracheidograms can be averaged (for the three plots and over the three years) in order to obtain mean profiles of cell dimensions variation representing the general tree ring structure of a species.

Mature tracheids were classified in the different types of wood according to Mork's criterion (MC) (Denne, 1988), which discriminates cells according the ratio between radial wall thickness and lumen diameter (see Table S2 for formula). Cells presenting a MC inferior or equal to 0.5 were classified as earlywood (EW), cells having a MC between 0.5 and 1 were classified as transition wood (TW), and cells having a MC superior or equal to 1 belonged to latewood (LW) (Park & Spiecker, 2005).

Assessing the kinetics of tracheid development

In order to describe accurately wood formation dynamics, generalised additive models (GAMs) were fitted on the standardised numbers of cells in each phase of xylem development (Cuny *et al.*, 2013). GAMs were fitted using the R mgcv package (Wood, 2006; R Core Team, 2012) for every year on each individual tree. The values of the fitted models were then averaged for the monitored plots over the studied years in order to calculate means representing the general wood formation dynamics of a species.

For each species, we used the average cell numbers predicted by GAMs to calculate the date of entrance of each cell in each development zone (cambial, enlargement, wall formation and mature zones) using the method described in Cuny *et al.* (2013). From these dates, the residence durations of each cell i in the cambial ($d_{C,i}$) enlargement ($d_{E,i}$) and wall thickening ($d_{T,i}$) zones and its total duration of formation ($d_{F,i}$) were computed. In order to have a complete characterisation of the development kinetic of each cell i, we also estimated the rate of enlargement ($r_{E,i}$) and wall deposition ($r_{W,i}$) by dividing its final dimensions ($CellRD_i$ and $WallCA_i$) by the duration ($d_{E,i}$ and $d_{T,i}$) it spent in the corresponding phase (enlargement and

wall thickening) (Table VIII.S2).

Assessing the environmental influence on tracheid development and final dimensions

In order to study the fine mechanisms by which the studied environmental factors (temperature, cumulative radiation and relative extractable water) influence wood formation, the kinetics (duration and rate) and the results (cell radial diameter or wall cross area) of a phase (enlargement or wall thickening) were associated with the mean environmental conditions acting during the time-window occupied by this phase. For example, the duration and rate of enlargement and resulting cell radial diameter of a cell were related to the mean environmental factors that were occurring during the enlargement of this same cell. Similarly, the duration and the rate of wall deposition and resulting final wall cross area of a cell were related to the mean environmental factors that were occurring during the wall thickening phase of this cell.

Moreover, in order to test the hypothesis that the target of environment influence is the cambial zone (Vaganov *et al.*, 2006; Vaganov *et al.*, 2011), the environmental factors were also averaged for the period when the cell was in the cambial zone, and then related to the kinetics of the successive phases of its development and resulting final dimensions.

Results

Annual cycle of environmental factors

A mean annual temperature of 9.4°C was observed. Daily temperature followed a right-skewed bell-shape curve during the year (Figure VIII.1a), reaching maximal values around 17°C in summer (end of July - beginning of August). The annual mean daily radiation was 1170 J cm^{-2}. Daily radiation followed a left-skewed bell-shape curve which culminates at values around 2000 J cm^{-2}, 2 weeks before the summer solstice (Figure VIII.1b). On average, it rained 1350 mm a year, with two periods with lower precipitations detectable in spring (April-May) and in autumn (September-October) (Figure VIII.1c). Because of the abundant rains, the relative extractable water maintained at a high level (< 60%) all along the year (Figure VIII.1d). It was minimal in May, at the time of the accelerated increasing in temperature and during the period of lower precipitation.

Timing of xylem cell development

Overall, xylem cells developed from mid-April to mid-November (Figure VIII.2). Because each consecutive cell along the ring was produced at a specific time during the season, each successive phase of its differentiation occupied a specific time-window during the year. However, as this time-window was always longer than the lag separating the production of one or more successive cells, it partially overlapped with the time-windows occupied by development phases of one or more successive cells. On average, cells resided 4 days in the cambial zone, 9 days in enlargement zone and 35 days in the wall thickening zone, indicating that the development of a xylem cell occupied a time-window of about 48 days. However, the residence durations in the cambial and enlargement zones decreased of about 3

to 4 times along the successive cells of the ring (from 2-3 weeks to 5 days), whilst the residence durations in the thickening zone increased of 2 to 3 times (from 3 to 7-8 weeks). Thus, for the last cells of the ring, d_T could be more than 10 times longer than d_C and d_E. Because of this, cells were in the cambial and enlargement zones from mid-April to mid-September, whereas there were some cells in the wall thickening zone from the very beginning of May until the beginning of November.

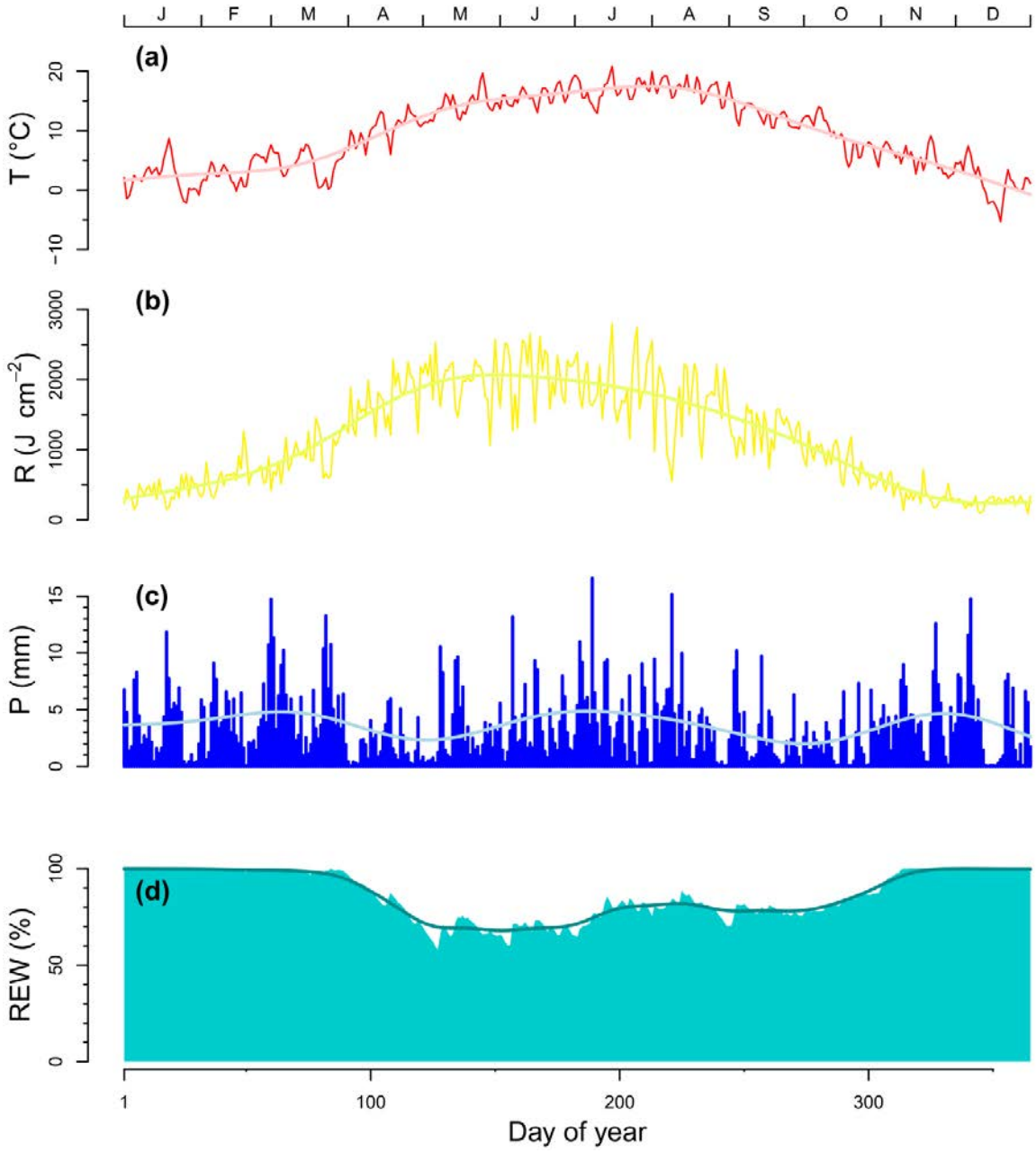

Figure VIII.1: Annual evolution of the monitored environmental factors with the temperature (T), global radiation (R), precipitations (P), and soil relative extractable water (REW). For each factor, daily values averaged for the 3 years (2007 – 2009) are plotted along with the global seasonal tendencies as revealed by generalized additive models.

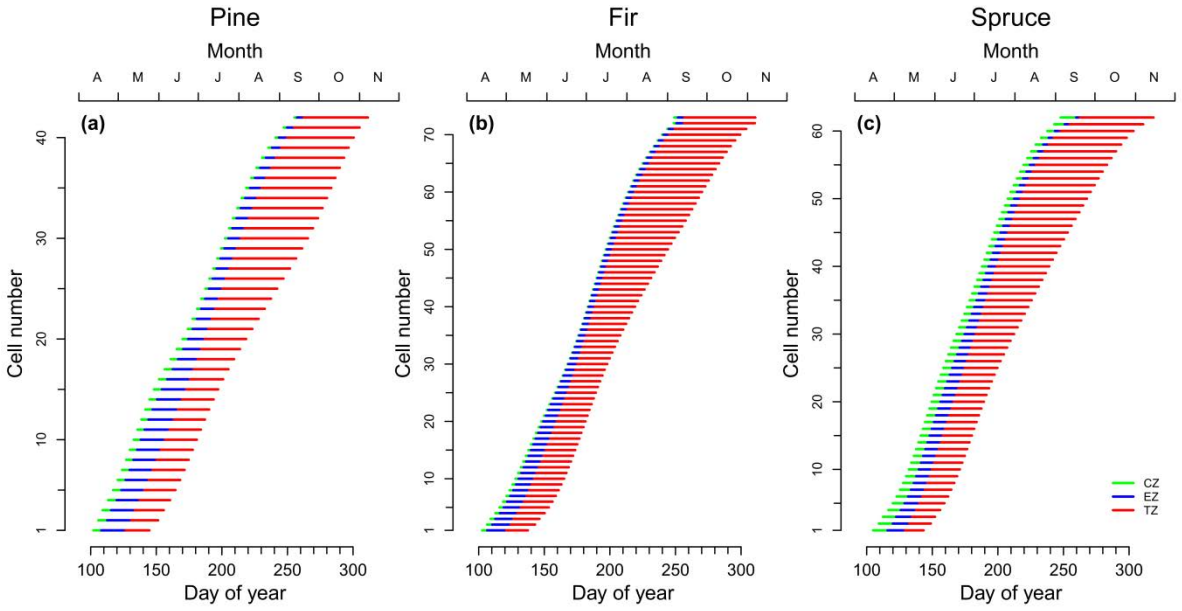

Figure VIII.2: Timing of tracheid development, with, for each cell along the ring of the three species, the periods when it was in the cambial, enlargement, and wall thickening zones.

Environmental conditions experienced during xylem cell development

Each cell experienced a unique combination of environmental factors signals during its lifetime (Figure VIII.3). In particular, for each cell, the exit from the cambial zone and the consecutive enlargement took a few times and so underwent environmental conditions that only slightly differed, whereas the later wall thickening occurred during a longer time-window and so experienced environmental conditions that differed sharply.

The mean temperature acting when cells were in the cambial and enlargement zones increased along the ring, except for the last 20% of cells for which it decreased abruptly (Figure VIII.3a,b,c). Thus, first earlywood cells enlarged at a temperature between 10 and 13°C, whereas the first latewood cells enlarged at a temperature superior to 16°C, and the last latewood cells enlarged at 13°C. By contrast, the temperature perceived during wall thickening increased only for the first 50% (pines) or 60% (firs and spruces) of cells produced, and then decreased abruptly exactly at the beginning of latewood. Thus, earlywood cells build their wall at a mean temperature of 13-14°C, while transition wood cells build their wall at 16-17°C. The temperature perceived during wall thickening was reduced by 2 in latewood, passing from approximately 17°C to 8-9°C between the first and last latewood cells. Cells of earlywood and transition wood experienced higher temperatures in the wall thickening than in the cambial and enlargement zones, whereas the contrary was observed for latewood cells.

Solar radiations received during division and enlargement increase slowly for EW-cells before to decrease rapidly for TW- and LW-cells. Solar radiations received during thickening remained stable for earlywood cells, and then decreased continuously along the successive cells (Figure VIII.3d,e,f). The decreased, however, was more pronounced when considering the time cell spent in the thickening phase. So, light radiation received by tree when cell was in the wall thickening zone was about 2 times higher for earlywood cells (around 2000 J cm^{-2})

than for the last latewood cells (around 1000 J cm^{-2}).

The relative extractable water (REW) exhibited little changes and remained relatively high for the successive cells of the ring (Figure VIII.3g,h,i). The REW available when cells were in the cambial and enlargement zones decreased for the first 10% produced cells. Then, the REW remained at 70% until half of the ring, and increased to about 80% for latewood cells. So, the REW was even higher for latewood cells than for earlywood cells.

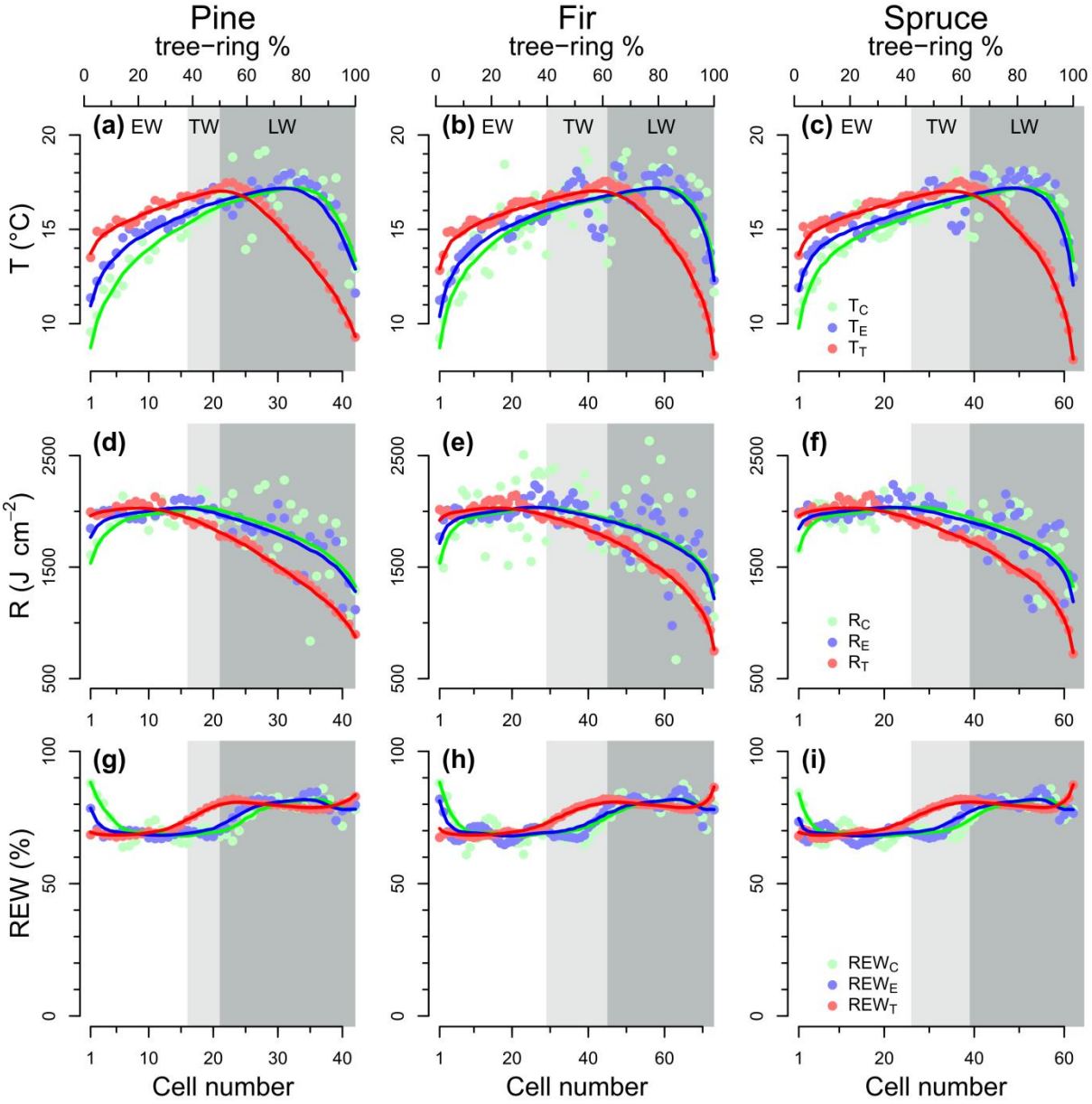

Figure VIII.3: Temperature, global radiation, and relative extractable water when cells were in the cambial (T_C, R_C, and REW_C), enlargement (T_E, R_E, and REW_E) and wall thickening (T_T, R_T, and REW_T) zones. For each species, each point represents a single cell along an average ring (means of 15 trees over three years). Lines represent the global tendencies as revealed by generalized additive models. White, light-grey and dark-grey areas represent earlywood (E_W), transition wood (T_W), and latewood (L_W), respectively.

Environmental influence on xylem cell sizes

Highly significant relationships were found between the temperature, relative extractable water, and radiation acting during enlargement and cell radial diameter (CellRD), but these relationships were complex and clearly not linear (Figure VIII.4a,b,c). Thus, a highly significant and positive relationship was obtained between light radiation and CellRD ($R^2 = 0.4$, $P > 0.001$), but the relationship did not stand for earlywood cells (Figure VIII.4b). A highly significant relationship was obtained between the relative extractable water and CellRD ($R^2=0.5$, $P < 0.001$), but this relationship was negative, meaning that increasing water availability was associated with decreasing CellRD (Figure VIII.4c).

On the other hand, a strong relationship was found between the wall cross area (WallCA) and the temperature when the cell was in wall thickening ($R^2=0.71$, $P < 0.001$) (Figure VIII.4d). However, this relationship was mainly due to latewood cells, and thus was stronger when considering only latewood ($R^2=0.80$, $P < 0.001$) A highly significant relationship was also found between WallCA and the radiation acting during wall thickening ($R^2=0.2$, $P < 0.001$), but again the relationship was clearly linear only for latewood cells ($R^2=0.80$, $P < 0.001$) (Figure VIII.4e). By contrast, no relationship was found between the relative extractable water available during wall thickening and WallCA (Figure VIII.4f).

In general, the relationships were decreased when using the values of environmental factors when cells were in the cambial zone (Figure VIII.S1). For example, the strong relationship found between the radiation and the cell diameter remained highly significant but was reduced ($R^2=0.12$ $P<0.001$), as well as the relationship between the temperature and the wall cross area was considerably reduced ($R^2=0.12$, $P<0.001$).

Environmental influence on the kinetic of tracheid development

No simple linear relationship was observed between the environmental factors and the duration or the rate of cell enlargement (Figure VIII.S2). On the other hand, a highly significant and positive relationship was found between the mean daily radiation received by tree when the cell was in the wall thickening zone and the wall deposition rate in this cell ($R^2 = 0.85$, $P < 0.001$) (Figure VIII.5a). The positive relationship, however, was accompanied by a relationship of the same order, but negative, between the daily radiation and the duration of wall deposition ($R^2=0.85$, $P < 0.001$) (Figure VIII.5b). Consequently, a very strong and negative relationship was found between the rate and the duration of wall deposition ($R^2=0.92$, $P < 0.001$). Only for the last latewood cells, the duration of wall deposition stopped increasing while the rate continued to fall.

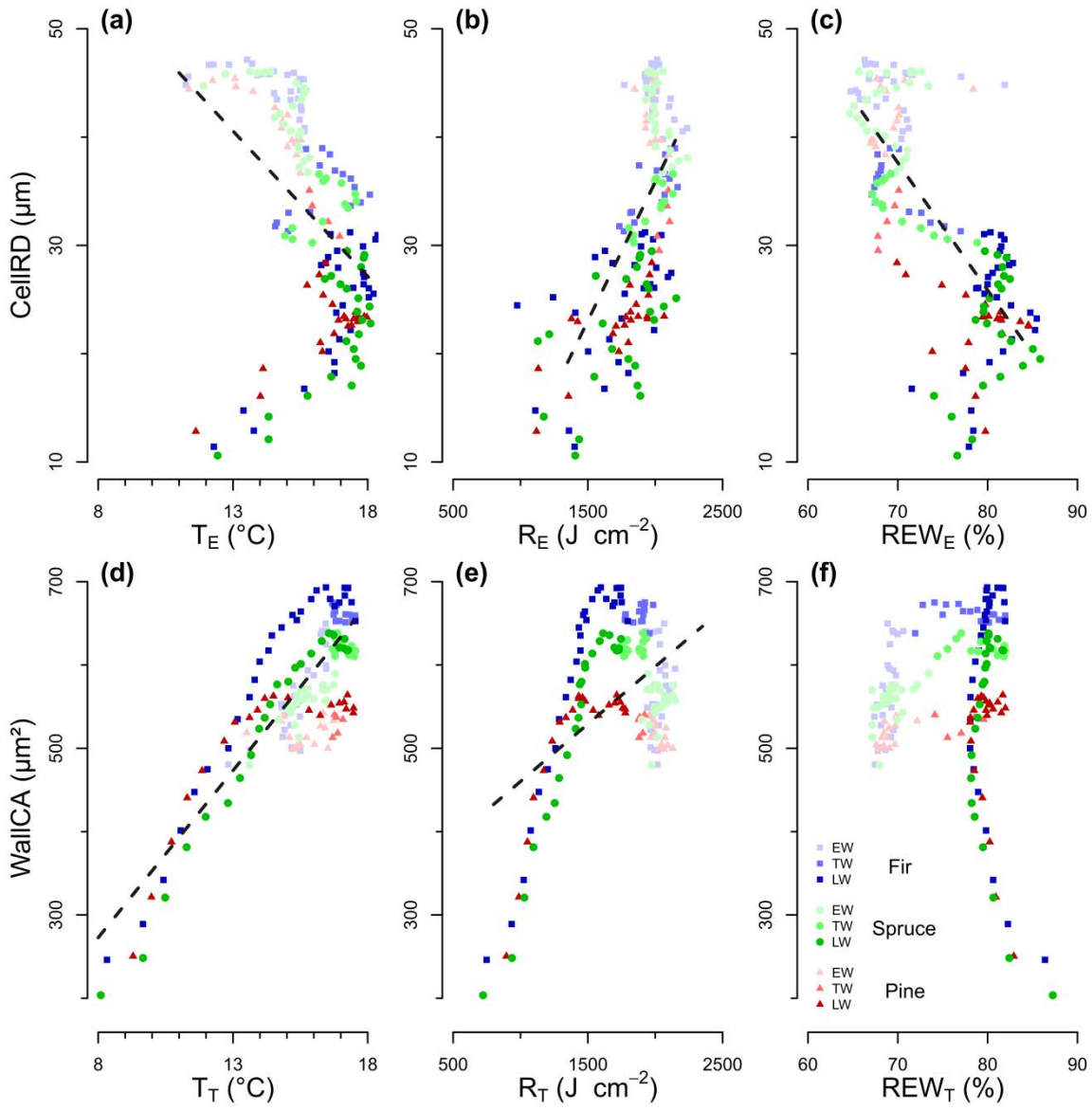

Figure VIII.4: Relationships between climatic factors and tracheid features. Relationships between the temperature (T_E), global radiation (R_E), and relative extractable water (REW_E) occurring during cell enlargement and the final cell radial diameter (CellRD). Relationships between the temperature (T_T), global radiation (R_T), and relative extractable water (REW_T) occurring during wall thickening and the final wall cross area (WallCA). For each species, each point represents a single cell along an average ring (means of 15 trees over three years). Light-tone, middle-tone, and dark-tone points represent earlywood (EW), transition wood (TW) and latewood (LW) cells, respectively.

A highly significant and positive relationship was observed between the temperature and the rate of wall deposition, but the relationship was clearly not linear when considering all the cells of the ring (R^2=0.32, $P < 0.001$). But when considering only latewood cells, the relationship appeared very strong and linear (R^2=0.90, $P < 0.001$) (Figure VIII.5c). On the contrary, no significant linear relationship was found between temperature and the wall deposition duration, and the points cloud did not allow detecting any clear relationship (Figure VIII.5d).

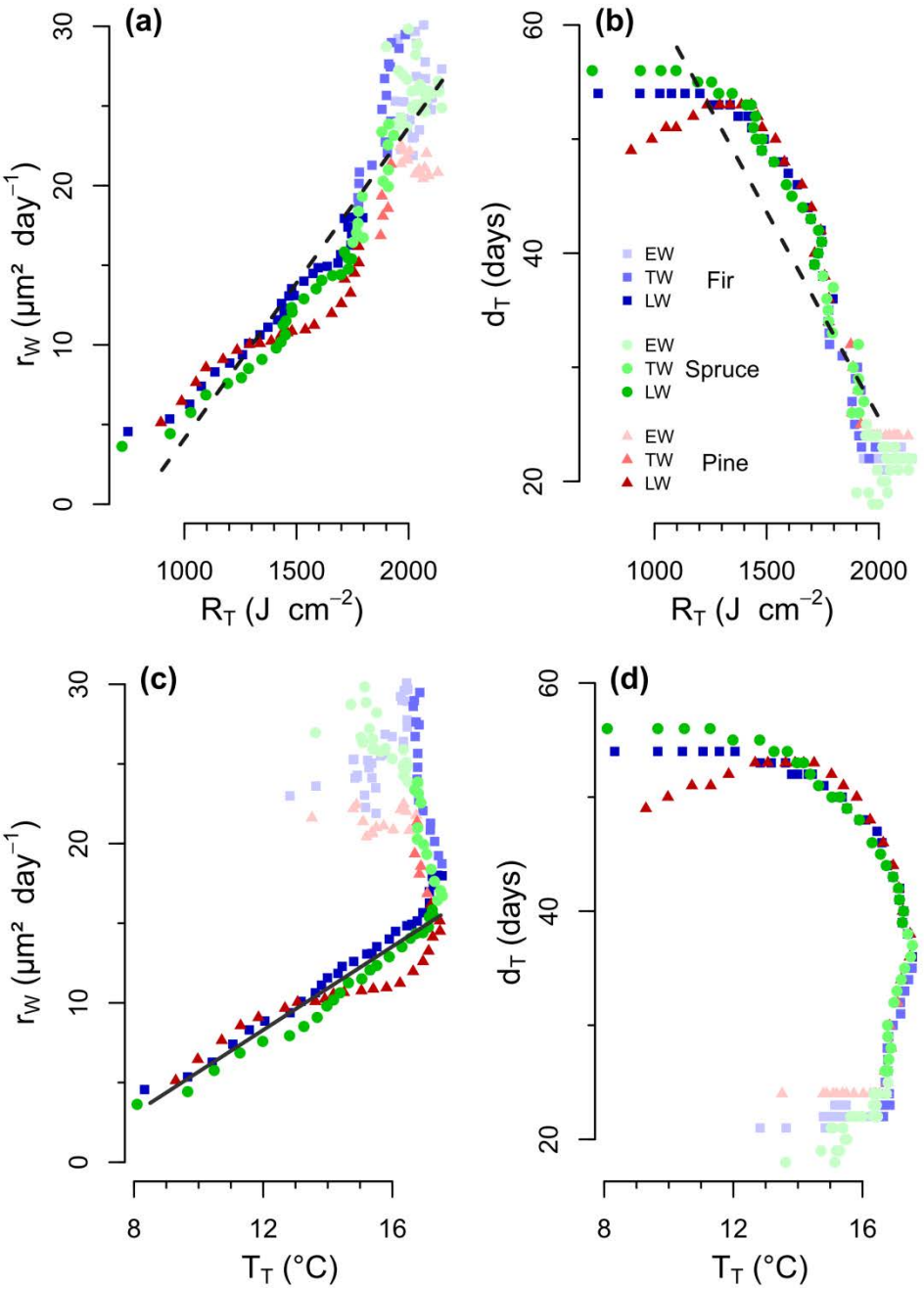

Figure VIII.5: Relationships between the global radiation (R_T) and the temperature (T_T) acting during wall thickening and the rate (r_W) and duration (d_T) of wall deposition. For each species, each point represents a single cell along an average ring (means of 15 trees over three years). Light-tone, middle-tone, and dark-tone points represent earlywood (EW), transition wood (TW) and latewood (LW) cells, respectively. Dashed lines in a and b present the regression for all the cells, whereas continuous line in c presents the regression only for latewood cells.

The environmental influence on the kinetics of tracheid differentiation was reduced when using the environmental factors acting when cells were in the cambial zone. The relationships between the environmental factors (light radiation and temperature) and the wall deposition rate remained significant ($P < 0.05$), but were considerably weakened (R^2=0.22 and R^2=0.15, respectively), as was the relationship between temperature and the wall deposition rate in latewood cells ($P < 0.01$; R^2=0.08).

Discussion

Control of xylem cell enlargement and tracheid final diameter

Based on the evidence that turgor is the essential condition for cells to enlarge (Nonami & Boyer, 1989), we expected water availability would have a strong influence on xylem cell radial enlargement and tracheid final diameter. Surprisingly, we found no relationship between the amount of extractable water in the soil and the rate and duration of cell enlargement, or the final diameter of tracheids. The simplest explanation of this result is that our study took place in a well-watered region (1350 mm regularly distributed through the year on average for the 3 sites and the 3 years), so that the soil water supply remains sufficient throughout the growing season and does not limit cell enlargement. These results refutes the hypothesis that latewood formation is systematically triggered by the entrance of trees in drought conditions (Kramer, 1964), but they are in agreement with the observation that narrow latewood cells are formed even for irrigated trees (Zahner *et al.*, 1964). So, we can conclude that the typical decrease of xylem cell size along conifer tree ring in temperate forest is not related to water shortage.

A relationship was obtained between the light radiation received during enlargement and the final diameter of cells. Positive influence of light conditions on cell diameter has been experimentally found (Larson, 1962; Richardson, 1964; Balatinecz & Farrar, 1968). Light influence is thought to be mediated by the growth regulator balance, with long days inducing large diameters by promoting the synthesis of molecular substances that stimulate enlargement (Larson, 1962; Larson, 1964). However, the relationship we found was not linear as it did not work for earlywood cells. Similarly, the influence of light radiation on the kinetic of enlargement appeared complex and far from linear. So, light radiation alone could not explain the decrease of xylem cell size along conifer ring. We also found significant influence of temperature on enlargement and cell diameter, but relationships appeared even less linear and more complex than those obtained with light. So, we conclude that no single environmental factor explains the reduction in xylem cell size along conifer rings under a temperate climate.

Control of secondary wall formation and wall amount in tracheids

Because secondary wall formation represents high investments of carbohydrates (Demura & Ye, 2010), we expected that light, as the primary energy source for photosynthesis, would have a major influence on this process. We actually found a strong positive and linear relationship between the wall deposition rate and the amount of light received when cells were in the thickening phase. Such a relationship confirms a light effect mediated by the photosynthetic tissue on secondary wall formation (Richardson, 1964; Vaganov *et al.*, 2011). Throughout the season, the decrease of light availability induces a decrease in sugar production by photosynthesis, which induces a decrease in the supply of the wall material substrates transported to the forming wood, decreasing wall deposition rate in xylem cells.

Wodzicki (1971) and Antonova & Stasova (1993; 1997) found a positive relationship

between temperature and the wall deposition rate, and have thus attributed the seasonal changes of wall deposition rate to the temperature regime. However, they did not have information about light, so that the relationship they found may be confused with light influence. Nevertheless, an effect of temperature on the wall deposition rate was also found in our study, but only for latewood cells for which we observed a strong, positive, and linear relationship between the temperature occurring during the thickening phase and the wall deposition rate in the cell.

Throughout the growing season, except for the last cells 5-10 cells of latewood, increasing durations of secondary cell-wall formation counterbalanced decreasing wall deposition rates. Such a compensatory effect by the wall deposition duration has already been emphasized (Wodzicki, 1971; Doley, 1979; Antonova & Stasova, 1993; Antonova & Stasova, 1997; Cuny *et al.*, under review). Its direct consequence is to delete the registration of the environmental signal on the result of the process, i.e. the amount of wall material deposited in the cell. Thus, despite the strong influence of the light radiation on the wall deposition rate, the actual amount of deposited wall material was only related to the light radiation in the last latewood cells, when the compensatory effect of the duration were no more sufficient.

Negative influence of high temperatures on the amount of wall material deposited has been experimentally observed and has been associated to the increase in the expenditure of photoassimilates on respiration (Richardson, 1964; Larson, 1967). But as we found, all authors found a positive influence of temperature on the rate of wall deposition, whatever the temperature range considered (Denne, 1971; Wodzicki, 1971; Antonova & Stasova, 1993; Antonova & Stasova, 1997). Such a result implies that the decreasing wall amount under high temperature is due to decreasing durations, and not to decreasing rates of wall deposition, which disagrees with the idea of a photoassimilates depletion. The decreasing durations under high temperatures could be associated to the stimulation of enzymes of programmed cell death (Antonova & Stasova, 1997). But neither we nor Wodzicki (1971) found a significant influence of temperature on the wall deposition duration. So, whatever the mechanisms behind, temperature influences on wall deposition is complex because of the balance between the rate and the duration of the process. The most evident effect of temperature appeared in latewood, in which the brutal decrease of temperature is associated to a drop of the wall deposition rate, probably because of a drop of the metabolic activity, which is not compensated by the duration, hence the drop in the amount of wall material deposited.

Sensor of environmental influence

Vaganov *et al.* (2006; 2011) present a theory according to which the main target of environmental control of tree-ring formation is the cambial zone, and then this signal is transformed into further processes of cell differentiation (enlargement and cell wall thickening). According to this theory, the environmental factors influence the final morphology of xylem cells only when they are in the cambial zone, and cannot influence the successive stages of xylogenesis independently. Our results contest this theory. Indeed, using the environmental factors acting when the cell was in the cambial zone decreased the relationships between the environmental factors and wood formation dynamics, in particular

the strong relationships between the temperature and the quantity of wall deposited, and between the radiation and the rate of wall deposition. As already defended by Antonova & Stasova (1993; 1997), such a result suggests that the environmental factors can affect each process of xylogenesis separately, depending on the nature of the physical and physiological events involved and the moment when the process takes place.

Environmental vs. developmental control of tree ring structure

We showed in a previous study that the final tracheid diameter depends primarily on the duration of enlargement, whereas the rate exhibits few changes during the season (Cuny *et al.*, under review). We associated the high importance of the enlargement duration to a developmental control, in which auxin would be of primary importance. This hormone is distributed as a steep gradient across the cambial and enlargement zones, which serves as a positional signal for the developing cells (Uggla *et al.*, 1996). The widest the gradient, the longest the duration of enlargement is (Tuominen *et al.*, 1997; Sundberg *et al.*, 2000). Such hormonal gradients have been supposed to change rapidly in response to environmental cues (Schrader *et al.*, 2003), in which case the environmental influence on the enlargement process and final diameter is indirect.

Many observations argue for a strong environmental influence on cell enlargement and resulting diameter under more constraining conditions, in particular concerning water availability. Indeed, there is a broad range of water potential values over which the radial diameters do not vary significantly, but an accelerating decline in cell sizes occurred below some critical value of water potential (Von Wilpert, 1991). Cell enlargement is physically inhibited and its rate collapses (Nonami & Boyer, 1990b; Nonami & Boyer, 1990a), hence the rapid reduction in diameter when a drought occurs (Abe *et al.*, 2003; Rossi *et al.*, 2009). So, differences in cell diameter generally occurred when comparing sites or years with contrasted water conditions (Gruber *et al.*, 2010). But the drastic reduction in cell size along tree ring does not result of changing water conditions.

Cell size is a crucial determinant of the whole ring structure, being the main determinant of the final wall thickness, and so of the transition from earlywood to latewood and wood density (Cuny *et al.*, under review). So, by showing that cell enlargement is not under a strong cliamtic control, our results shows that the environmental influence on the whole tree ring structure should be rather limited. This is in agreement with the idea that, in our temperate area, tree ring structure is highly fixed in tree ontogeny as it provides a good compromise between water conductivity and mechanical strength (Cuny *et al.*, under review).

Influence of environmental factors (light and temperature) was found mainly on the kinetics of secondary wall formation and the amount of wall material deposited in cells. This result confirms that cell enlargement and secondary wall formation are under different physiological control (Cuny *et al.*, under review). The environmental influence on secondary wall formation is mediated by the metabolism, which direct translation is the wall deposition rate. Along most of the ring, however, the environmental influence on the final results is complicated because of a compensation effect by the duration. This compensation effect

ceases in latewood, opening the door for a direct registration of the environmental signal, in particular the strong positive effect of temperature on the wall deposition rate. Moreover, secondary wall formation takes almost 2 months at the end of the season, meaning that the final amount of wall material in the cell integrates 2 months of environmental influence. Such a result is a clue to explain why maximum latewood density is one of the most valuable tree-ring proxy for climate reconstruction (see, for example, Hughes *et al.*, 1984; Briffa *et al.*, 1998; Barber *et al.*, 2000), even if it does not explain the strong relationship between maximum latewood density and the temperature for the whole season.

Conclusion

In this study, we investigated how the changes of climatic conditions during the season influence the differentiation and resulting dimensions of xylem cells along conifer tree ring. Seasonal variations of temperature, radiation, and water availability did not explain the seasonal changes in the kinetic of cell enlargement and so the regular decrease of the tracheid radial diameter along the ring. Environmental influence was found mainly on the process of secondary wall formation, with a linear and strong relationship between the light radiation and the wall deposition rate. An evident positive effect of temperature was also observed on the wall deposition rate in latewood cells.

Environmental influence on the wall deposition rate, however, was offset by the wall deposition duration, which complicated the registration of the environmental signal on the amount of wall deposited. Only in latewood, because the duration did not increase enough to compensate the rate fall, the environmental influence on the wall deposition rate was directly recorded in the resulting amount of wall material deposited in the cells.

The absence of a clear environmental determinism of tracheid final diameters, a crucial determinant of the whole ring structure, agrees with the idea that tree ring structure of conifers grown under temperate climate is under a strong developmental control. On the other hand, the strong influence of light and temperature on the wall deposition rate suggests an environmental influence mediated by the metabolism. The lack of a compensatory effect of the wall deposition duration for the last latewood cells is a clue to explain the usefulness of maximum latewood density as a recorder of environmental conditions.

Acknowledgements

We thank E. Cornu, E. Farré, C. Freyburger, P. Gelhaye, and A. Mercanti for fieldwork and monitoring; M. Harroué for sample preparation in the laboratory; Bernard Longdoz of the forest ecology and ecophysiology (EEF) team and the association for the study and monitoring of air pollution in Alsace (ASPA) for the meteorological data. Manuel Nicholas of the French permanent plot network for the monitoring of forest ecosystems (RENECOFOR) for the meteorological data and the description of the soil profiles.

References

Abe H, Funada R, Ohtani J, Fukazawa K. 1997. Changes in the arrangement of cellulose microfibrils associated with the cessation of cell expansion in tracheids. *Trees-Structure and Function* **11**(6): 328-332.

Abe H, Nakai T, Utsumi Y, Kagawa A. 2003. Temporal water deficit and wood formation in *Cryptomeria japonica*. *Tree Physiology* **23**(12): 859-863.

Antonova GF, Stasova VV. 1993. Effects of environmental factors on wood formation in Scots pine stems. *Trees-Structure and Function* **7**(4): 214-219.

Antonova GF, Stasova VV. 1997. Effects of environmental factors on wood formation in larch (Larix sibirica Ldb.) stems. *Trees-Structure and Function* **11**(8): 462-468.

Balatinecz J, Farrar J 1968. Tracheid development and wood quality in larch seedlings under controlled environment. *Proceedings of the Eighth Lake States Forest Tree Improvement Conference; Res. Pap. NC-23. St. Paul, MN: US Forest Service, North Central Forest Experiment Station. 28-36*.

Barber VA, Juday GP, Finney BP. 2000. Reduced growth of Alaskan white spruce in the twentieth century from temperature-induced drought stress. *Nature* **405**(6787): 668-673.

Briffa K, Schweingruber F, Jones P, Osborn T, Shiyatov S, Vaganov E. 1998. Reduced sensitivity of recent tree-growth to temperature at high northern latitudes. *Nature* **391**(6668): 678-682.

Cosgrove DJ. 1997. Relaxation in a high-stress environment: the molecular bases of extensible cell walls and cell enlargement. *The Plant Cell* **9**(7): 1031.

Cosgrove DJ. 2000a. Expansive growth of plant cell walls. *Plant Physiology and Biochemistry* **38**(1-2): 109-124.

Cosgrove DJ. 2000b. Loosening of plant cell walls by expansins. *Nature* **407**(6802): 321-326.

Cuny HE, Rathgeber CBK, Fournier M. under review. Big cells, thin walls; small cells, thick walls: cell differentiation processes determine tree-ring structure in conifers.

Cuny HE, Rathgeber CBK, Senga Kiesse T, Hartmann FP, Barbeito I, Fournier M. 2013. Generalized additive models reveal the intrinsic complexity of wood formation dynamics. *Journal of Experimental Botany*.

Demura T, Ye Z-H. 2010. Regulation of plant biomass production. *Current Opinion in Plant Biology* **13**(3): 298-303.

Denne M. 1971. Temperature and tracheid development in Pinus sylvestris seedlings. *Journal of Experimental Botany* **22**(2): 362-370.

Denne M. 1974. Effects of light intensity on tracheid dimensions in Picea sitchensis. *Annals of Botany* **38**(2): 337-345.

Denne M, Dodd R 1981. The environmental control of xylem differentiation. *Xylem cell development*. Tunbridge Wells: Castle House Publications 236-255.

Denne M, Smith C. 1971. Daylength effects on growth, tracheid development, and photosynthesis in seedlings of *Picea sitchensis* and *Pinus sylvestris*. *Journal of Experimental Botany* **22**(2): 347-361.

Denne MP. 1988. Definition of latewood according to Mork (1928). *Iawa Bulletin* **10**(1): 59-62.

Doley D. 1979. Effects of shade on xylem development in seedlings of *Eucalyptus grandis Hill* Ex. Maiden. *New Phytologist* **82**(2): 545-555.

Doley D, Leyton L. 1968. Effects of growth regulating substances and water potential on the development of secondary xylem in *Fraxinus*. *New Phytologist* **67**(3): 579-594.

Esper J, Cook ER, Schweingruber FH. 2002. Low-frequency signals in long tree-ring chronologies for reconstructing past temperature variability. *Science* **295**(5563): 2250-2253.

Fonti P, von Arx G, Garcia-Gonzalez I, Eilmann B, Sass-Klaassen U, Gaertner H, Eckstein D. 2010. Studying global change through investigation of the plastic responses of xylem anatomy in tree rings. *New Phytologist* **185**(1): 42-53.

Granier A, Breda N, Biron P, Villette S. 1999. A lumped water balance model to evaluate duration and intensity of drought constraints in forest stands. *Ecological Modelling* **116**(2-3): 269-283.

Gričar J, Rathgeber CBK, Fonti P. 2011. Monitoring seasonal dynamics of wood formation. *Dendrochronologia* **29**(3): 123-125.

Gruber A, Strobl S, Veit B, Oberhuber W. 2010. Impact of drought on the temporal dynamics of wood formation in *Pinus sylvestris*. *Tree Physiology* **30**(4): 490-501.

Hsiao TC. 1973. Plant responses to water stress. *Annual review of plant physiology* **24**(1): 519-570.

Hughes MK, Schweingruber FH, Cartwright D, Kelly PM. 1984. July-August temperature at Edinburgh between 1721 and 1975 from tree-ring density and width data. *Nature* **308**(5957): 341-344.

Kozlowski TT, Pallardy SG. 1997. *Physiology of woody plants (second edition)*: Academic Press.

Kramer P 1964. The role of water in wood formation. In: Zimmermann MH ed. *The formation of wood in forest trees*. New York, London: Academic Press, 519-532.

Kutscha NP, Hyland F, Schwarzmann JM. 1975. Certain seasonal changes in balsam fir cambium and its derivatives. *Wood Science and Technology* **9**(3): 175-188.

Larson PR. 1962. The indirect effect of photoperiod on tracheid diameter in *Pinus resinosa*. *American Journal of Botany*: 132-137.

Larson PR. 1963. The indirect effect of drought on tracheid diameter in red pine. *Forest Science* **9**(1): 52-62.

Larson PR 1964. Some indirect effects of environment on wood formation. In: Zimmermann MH ed. *The formation of wood in forest trees*. New York, London: Academic Press.

Larson PR. 1967. Effects of temperature on the growth and wood formation of ten Pinus resinosa sources. *Silvae Genet* **16**(2): 58-65.

Nonami H, Boyer JS. 1989. Turgor and growth at low water potentials. *Plant Physiology* **89**(3): 798-804.

Nonami H, Boyer JS. 1990a. Primary events regulating stem growth at low water potentials. *Plant Physiology* **93**(4): 1601-1609.

Nonami H, Boyer JS. 1990b. Wall extensibility and cell hydraulic conductivity decrease in enlarging stem tissues at low water potentials. *Plant Physiology* **93**(4): 1610-1619.

Park Y-I, Spiecker H. 2005. Variations in the tree-ring structure of Norway spruce (*Picea abies*) under contrasting climates. *Dendrochronologia* **23**(2): 93-104.

R Core Team 2012. R: A language and environment for statistical computing. R Foundation for Statistical Computing, Vienna, Austria. ISBN 3-900051-07-0, URL http://www.R-project.org/.

Rathgeber CBK. 2012. Cambial activity and wood formation: data manipulation, visualisation and analysis using R. R package version 1.4-1. http://CRAN.R-project.org/package=CAVIAR.

Richardson S 1964. The external environment and tracheid size in conifers. In: Zimmermann MH ed. *The formation of wood in forest trees*. New York, London: Academic Press, 367-388.

Rossi S, Deslauriers A, Morin H. 2003. Application of the Gompertz equation for the study of xylem cell development. *Dendrochronologia* **21**(1): 33-39.

Rossi S, Simard S, Deslauriers A, Morin H. 2009. Wood formation in *Abies balsamea* seedlings subjected to artificial defoliation. *Tree Physiology* **29**(4): 551-558.

Rowe N, Speck T. 2005. Plant growth forms: an ecological and evolutionary perspective. *New Phytologist* **166**(1): 61-72.

Schrader J, Baba K, May S, Palme K, Bennett M, Bhalerao R, Sandberg G. 2003. Polar auxin transport in the wood-forming tissues of hybrid aspen is under simultaneous control of developmental and environmental signals. *Proceedings of the National Academy of Sciences* **100**(17): 10096-10101.

Schweingruber FH. 1996. *Tree rings and environment: dendroecology*.

Smith C. 1974. Light intensity and substrate availability in relation to tracheid development in *Picea sitchensis*. *Annals of Botany* **38**(2): 347-358.

Smith C. 1975. Substrate availability in relation to daylength effects on tracheid development in *Picea sitchensis* (Bong) Carr. *Annals of Botany* **39**(1): 101-111.

Sundberg B, Uggla C, Tuominen H. 2000. *Cambial growth and auxin gradients*.

Treydte KS, Schleser GH, Helle G, Frank DC, Winiger M, Haug GH, Esper J. 2006. The twentieth century was the wettest period in northern Pakistan over the past millennium. *Nature* **440**(7088): 1179-1182.

Trouet V, Esper J, Graham NE, Baker A, Scourse JD, Frank DC. 2009. Persistent Positive North Atlantic Oscillation Mode Dominated the Medieval Climate Anomaly. *Science* **324**(5923): 78-80.

Tuominen H, Puech L, Fink S, Sundberg B. 1997. A radial concentration gradient of indole-3-acetic acid is related to secondary xylem development in hybrid aspen. *Plant physiology* **115**(2): 577-585.

Uggla C, Moritz T, Sandberg G, Sundberg B. 1996. Auxin as a positional signal in pattern formation in plants. *Proceedings of the National Academy of Sciences of the United States of America* **93**(17): 9282-9286.

Vaganov EA 1990. The tracheidogram method in tree-ring analysis and its application. In: Cook ER, Kairiukstis LA eds. *Methods of dendrochronology: applications in the environmental sciences*. Dordrecht, Netherlands: Kluwer Academic Publishers, 63-76.

Vaganov EA, Anchukaitis KJ, Evans MN. 2011. How well understood are the processes that create dendroclimatic records? A mechanistic model of the climatic control on conifer tree-ring growth dynamics. In: Hughes MK, Swetnam TW, Diaz HF eds. *Dendroclimatology*. London: Springer-Verlag, 37-75.

Vaganov EA, Hughes MK, Kirdyanov AV, Schweingruber FH, Silkin PP. 1999. Influence of snowfall and melt timing on tree growth in subarctic Eurasia. *Nature* **400**(6740): 149-151.

Vaganov EA, Hughes MK, Shashkin AV. 2006. *Growth Dynamics of Conifer Tree Rings*. Heidelberg: Springer.

Von Wilpert K. 1991. Intraannual variation of radial tracheid diameters as monitor of site specific water stress. *Dendrochronologia* **9**: 95-113.

Wilson BF. 1984. *The growing tree*. Amherst: The university of Massachusetts press.

Wodzicki TJ. 1964. Photoperiodic control of natural growth substances and wood formation in larch (*Larix decidua* D.C.). *Journal of Experimental Botany* **15**(3): 584-599.

Wodzicki TJ. 1971. Mechanism of xylem differentiation in *Pinus sylvestris* L. *Journal of Experimental Botany* **22**(72): 670-687.

Wodzicki TJ. 2001. Natural factors affecting wood structure. *Wood Science and Technology* **35**(1-2): 5-26.

Wood SN. 2006. *Generalized additive models: an introduction with R*. Boca Raton, FL: Chapman and Hall/CRC.

Zahner R, Lotan JE, Baughman WD. 1964. Earlywood-latewood features of red pine grown under simulated drought and irrigation. *Forest Science* **10**(3): 361-370.

Zhong R, Zheng-Hua Y 2009. Secondary cell walls. *Encyclopedia of Life Sciences*. Chichester, UK: John Wiley & Sons, Ltd., 1-9.

Supplementary material

Table VIII.S1: Main characteristics (mean ± SE) of the monitored trees from the three studied species (silver fir, Norway spruce and Scots pine) illustrated by the age, diameter at breast height (DBH), height (H), and projected crown area (CA).

Site	Species	Age	DBH (cm)	H (m)	CA (m²)
Walscheid	Fir	94 ± 2	56 ± 1	31 ± 1	43 ± 5
	Spruce	89 ± 4	53 ± 2	32 ± 1	40 ± 5
	Pine	95 ± 3	52 ± 3	31 ± 1	41 ± 10
Abreschviller	Fir	135 ± 2	60 ± 3	36 ± 1	28 ± 5
	Spruce	85 ± 7	41 ± 2	32 ± 1	16 ± 2
	Pine	162 ± 3	33 ± 3	36 ± 1	20 ± 5
Grandfontaine	Fir	73 ± 3	57 ± 3	31 ± 1	37 ± 6
	Spruce	74 ± 4	55 ± 4	33 ± 1	30 ± 7
	Pine	119 ± 3	53 ± 2	27 ± 1	29 ± 2
Means	Fir	101 ± 6	58 ± 2	33 ± 1	36 ± 3
	Spruce	83 ± 3	49 ± 2	32 ± 1	29 ± 4
	Pine	126 ± 8	56 ± 2	32 ± 1	30 ± 4

Table VIII.S2: List of the variables used in this work.

Notation	Variable	Unit	Acquisition
LumRD	Lumen radial diameter	µm	Measured
LumTD	Lumen tangential diameter	µm	Measured
LumCA	Lumen cross-area	µm²	Measured
WallRT	Wall radial thickness	µm	Measured
WallTT	Wall tangential thickness	µm	$\mathrm{WallTT} = 1.2 \times \mathrm{WallRT}$
WallCA	Wall cross area	µm²	$\mathrm{WallCA} = \mathrm{CellCA} - \mathrm{LumCA}$
CellRD	Cell radial diameter	µm	$\mathrm{CellRD} = \mathrm{LumRD} + 2 \times \mathrm{WallRT}$
CellTD	Cell tangential diameter	µm	$\mathrm{CellTD} = \mathrm{LumTD} + 2.4 \times \mathrm{WallRT}$
CellCA	Cell cross area	µm²	$\mathrm{CellCA} = \mathrm{CellRD} \times \mathrm{CellTD}$
MC	Mork's criterion	NA	$\mathrm{MC} = \frac{4 \times \mathrm{WallRT}}{\mathrm{LumRD}}$
d_C	Cell residence duration in the cambial zone	day	Calculated
d_E	Cell residence duration in the enlargement zone	day	Calculated
d_T	Cell residence duration in the thickening zone	day	Calculated
d_F	Total duration of tracheid formation	day	Calculated
r_C	Rate of cell production by the cambial zone	cell day^{-1}	Calculated
r_D	Rate of division of a cambial cell	day^{-1}	$r_D = \frac{r_C}{n_C}$
r_E	Rate of cell radial enlargement	µm day^{-1}	$r_E = \frac{\mathrm{CellRD}}{d_E}$
r_W	Rate of wall deposition	µm² day^{-1}	$r_W = \frac{\mathrm{WallCA}}{d_T}$
T	Mean daily temperature	°C	measured
R	Daily cumulative radiation	J cm^{-2}	measured
P	Daily cumulative precipitation	mm	measured
REW	Relative extractable water	%	calculated

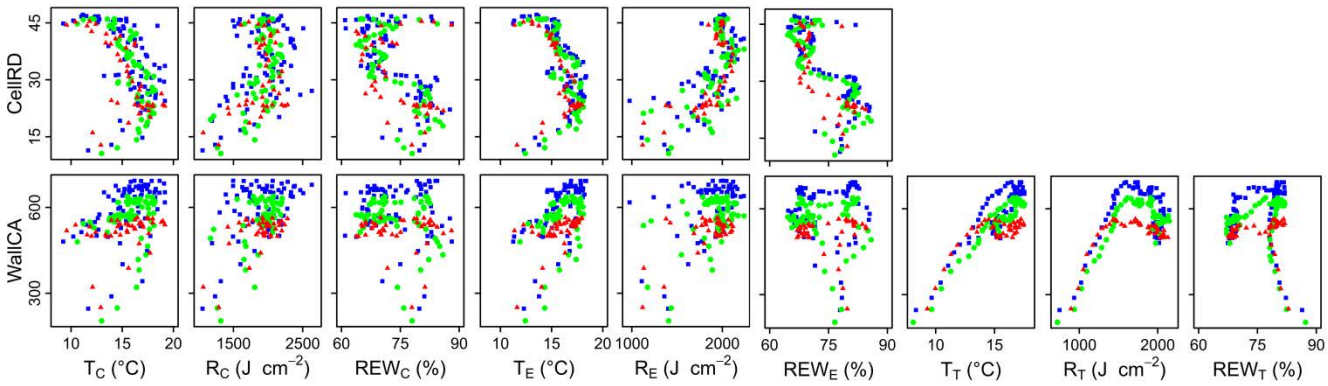

Figure VIII.S1: Relationships between climatic factors and final tracheid dimensions. Relationships between the temperature, radiation and relative extractable water when cells were in the cambial (T_C, R_C, and REW_C), enlargement (T_E, R_E, and REW_E), and wall thickening phase (T_T, R_T, and REW_T) of their differentiation and the final cell radial diameter (CellRD) and wall cross area (WallCA). Red, blue, and green points are for Scots pine, silver fir, and Norway spruce, respectively. For each species, each point represents a single cell along an average ring (means of 15 trees over three years).

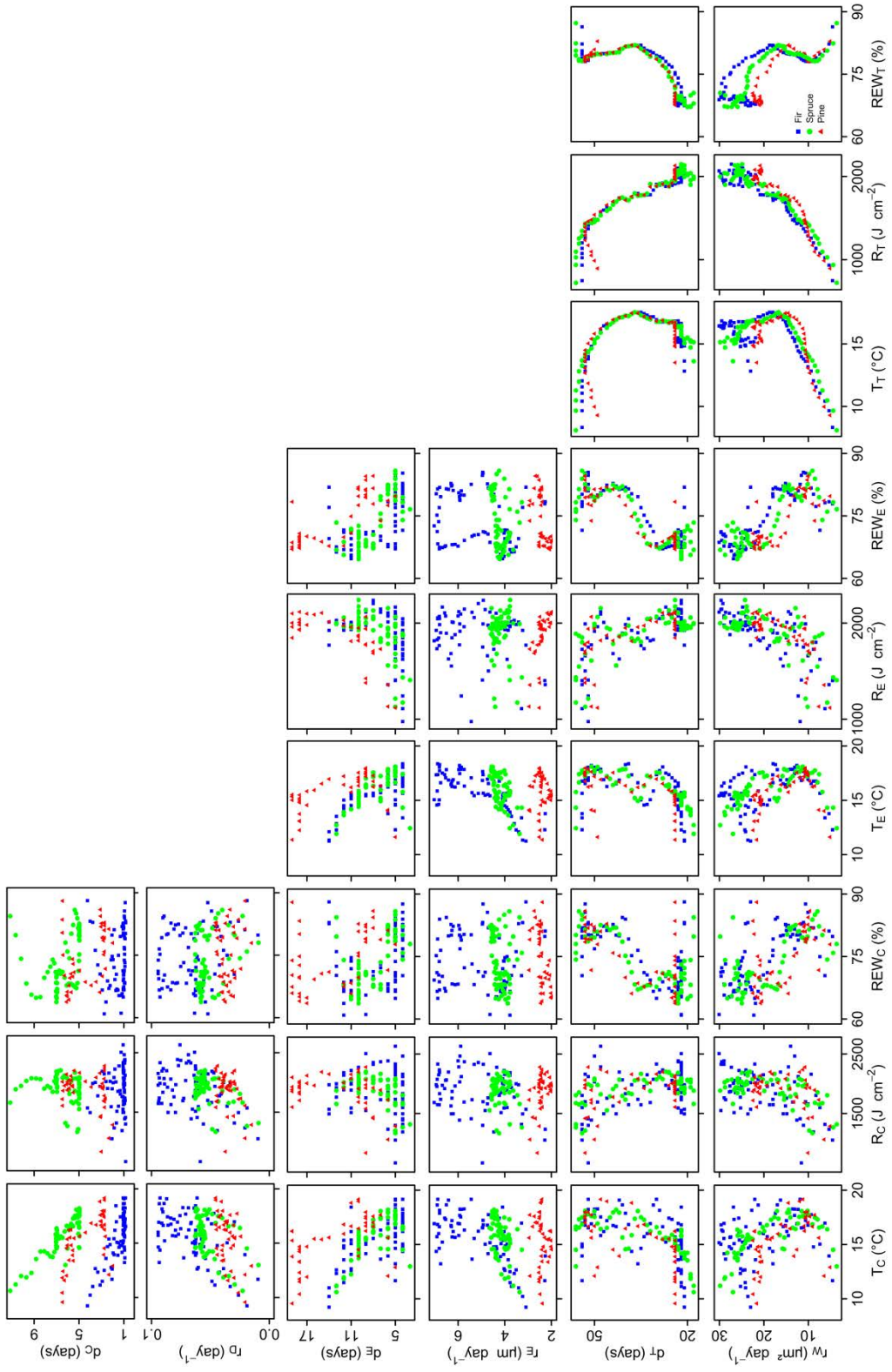

Figure VIII.S2: Relationships between climatic factors and tracheid differentiation kinetics. Relationships between the temperature, radiation and relative extractable water when cells were in the cambial (T_C, R_C, and REW_C), enlargement (T_E, R_E, and REW_E), and wall thickening phase (T_T, R_T, and REW_T) of their differentiation, the residence times of these cells in the cambial, enlargement and wall thickening zone (d_C, d_E, d_T), and the corresponding rates of division, enlargement and wall deposition (r_D, r_E, and r_W). Red, blue, and green points are for Scots pine, silver fir, and Norway spruce, respectively. For each species, each point represents a single cell along an average ring (means of 15 trees over three years).

IX DISCUSSION GÉNÉRALE

IX.1 Apports méthodologiques de cette thèse

IX.1.1 Caractérisation de la phénologie de la formation du bois

Une difficulté pour caractériser la dynamique intra-annuelle de la xylogénèse tient en la définition des variables utilisées pour décrire sa phénologie. Face à ce problème, cette thèse a contribué à l'établissement de définitions claires et objectives des principaux évènements phénologiques de l'activité cambiale et de la formation du bois au cours de l'année : début et fin de l'élargissement des cellules, début et fin de la phase d'épaississement et lignification et début de la phase mature. Les définitions ont été établies à partir d'observations anatomiques claires (présence/absence de cellules dans une phase donnée) et traduites en algorithmes efficaces basés sur des régressions logistiques (utilisées pour calculer la date à laquelle il y a une probabilité de 50% que la phase ait démarrée ou soit arrêtée). Le package CAVIAR, qui calcule automatiquement ces dates à partir du jeu de données de comptage cellulaire, a été développé par Rathgeber (2012) pour le logiciel R (R Core Team, 2012). Une utilisation généralisée de cette méthode homogénéiserait le traitement des données et rendrait donc les résultats de différentes études directement comparables. Pour plus de détails sur les définitions et la méthode, se référer à l'article de Rathgeber *et al.* (2011a) disponible en annexe (annexe 3). La méthode a notamment été appliquée dans la partie IV (article 1) pour caractériser avec rigueur la phénologie de la formation du bois pour chaque arbre de nos trois espèces. C'est grâce à cette caractérisation rigoureuse que nous avons pu comparer nos trois espèces et interpréter les différences phénologiques en termes de stratégies écologiques.

IX.1.2 Caractérisation de la dynamique intra-annuelle de la formation du bois

Un obstacle majeur au suivi de la xylogénèse est qu'elle est « cachée » dans le tronc (Chaffey, 2002). En conséquence, un suivi du processus n'est possible que par des prélèvements ponctuels de tissus au cours de la saison. Chaque prélèvement contient une « photographie » du cerne en formation et la dynamique de la mise en place du cerne doit être reconstruite a posteriori à partir de ces « photographies » successives. De plus, la formation du bois n'est pas homogène tout autour du tronc (Wodzicki & Zajaczkowski, 1970), ce qui rend difficile de savoir si les différences entre les « photographies » successives sont représentatives de la dynamique du processus (signal biologique d'intérêt) ou de sa variabilité à l'intérieur de l'arbre (bruit).

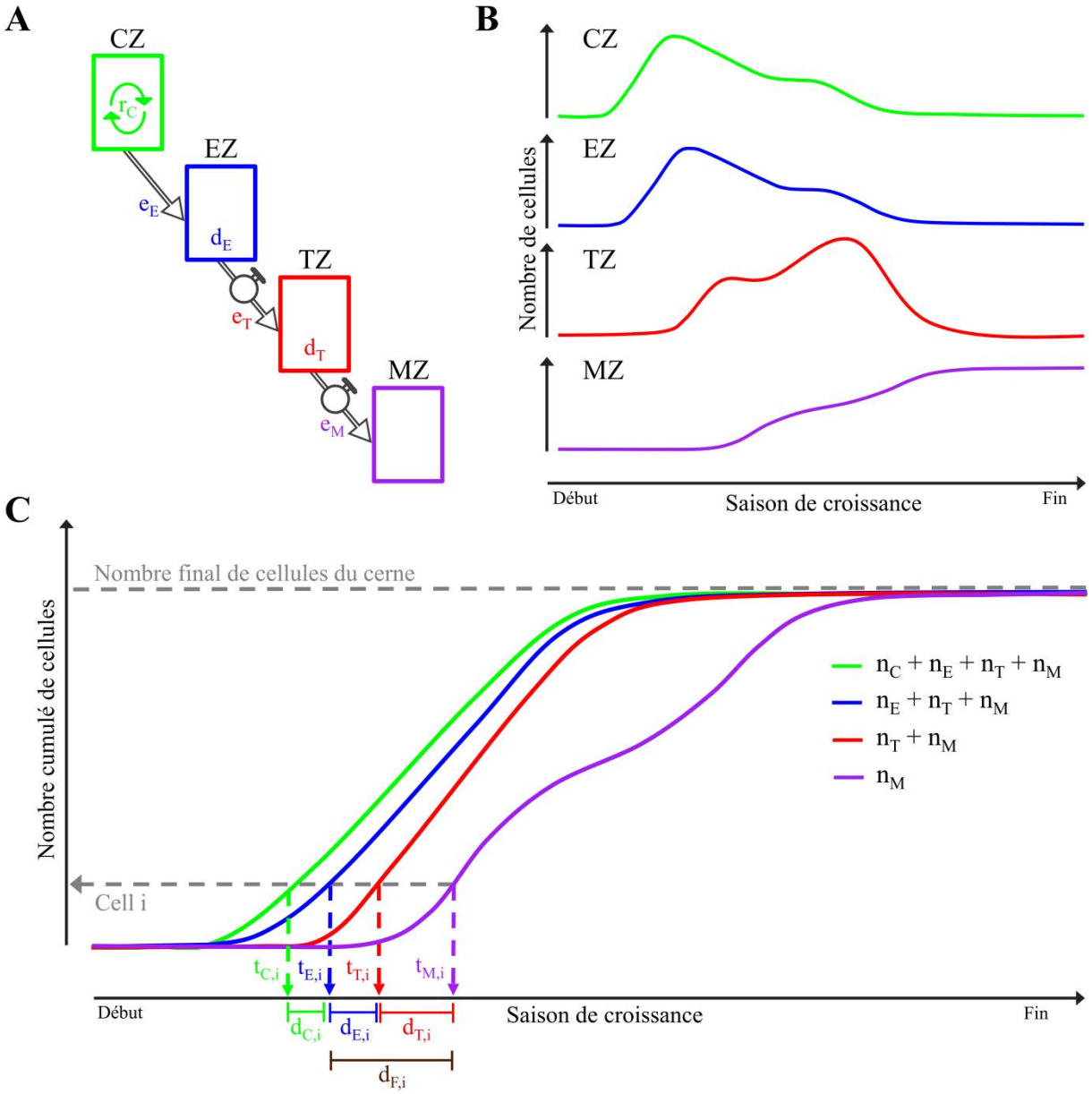

Figure IX.1: Utilisation des modèles additifs généralisés (GAMs) pour caractériser la dynamique intra-annuelle de la formation du bois. Les différentes zones de différenciation des cellules – zones cambiale (CZ), d'élargissement (EZ), d'épaississement (TZ) et mature (MZ) – sont vues comme des réservoirs interconnectés (A). L'ajustement des GAMs sur l'évolution du nombre de cellules dans ces zones (n_C, n_E, n_T et n_M) au cours de la saison (B) permet de calculer la vitesse de production des cellules dans la zone cambiale (r_C) ainsi que la vitesse à laquelle les cellules produites entrent dans les zones d'élargissement (e_E), d'épaississement (e_T) et mature (e_M). La méthode permet également de calculer pour chaque cellule i les dates d'entrée dans chaque zone ($t_{C,i}$, $t_{E,i}$, $t_{T,t}$, $t_{M,i}$), dates à partir desquelles sont déterminées les durées de résidence dans les zones cambiale ($d_{C,i}$), d'élargissement ($d_{E,i}$) et d'épaississement de la paroi ($d_{T,i}$), ainsi que la durée totale de différenciation ($d_{F,i}$).

Face à ce problème, une nouvelle méthode statistique, basée sur l'utilisation des modèles additifs généralisés (GAMs), a été développée dans cette thèse pour caractériser de façon précise la dynamique de la xylogénèse (Figure IX.1). La méthode a été décrite dans la partie V (article 2) et une description plus détaillée des GAMs est disponible en annexe (annexe 2). A notre connaissance, ceci constitue la première méthode statistique qui permette une caractérisation précise de la dynamique intra-annuelle de la formation du bois à travers :

- La description de l'évolution du nombre de cellules dans les zones de différenciation au cours de la saison ;
- Le calcul du flux de cellules entre les zones : taux de production cellulaire par la zone cambiale et taux d'entrée dans les zones d'élargissement, d'épaississement et mature ;
- Le calcul de la cinétique des processus du développement cellulaire : timing, durée et vitesse de l'élargissement et de la formation de la paroi secondaire.

Cette méthode représente donc une avancée significative dans l'analyse des données de la dynamique intra-annuelle de la formation du bois. En particulier, l'accès aux aspects cruciaux mais encore peu étudiés – car très difficilement accessibles – relatifs au développement cellulaire est un point fort, car il permet une caractérisation plus complète de la dynamique. En plus, cette méthode est robuste : elle ne fait pas d'hypothèse quant à la distribution des données et peut donc être utilisée pour n'importe quelle espèce dans n'importe quel biome.

IX.2 Synthèse des résultats

Les paragraphes suivants proposent une synthèse des principaux résultats obtenus dans cette thèse :

- Tout d'abord, nous rassemblons les résultats obtenus dans la description du timing, la durée et la vitesse des différents composants de la dynamique ;
- Ensuite, nous présentons les résultats qui concernent les mécanismes de la formation de la structure du cerne annuel par la dynamique ;
- Enfin, nous discutons des mécanismes de l'influence des facteurs climatiques sur la formation du bois.

IX.2.1 Dynamique intra-annuelle de la xylogénèse

Pour nos trois espèces sous un climat tempéré en moyenne-montagne (350 à 650 m d'altitude) dans les Vosges, nous avons vu que l'activité cambiale durait environ 4-5 mois, de avril-mai à aout-septembre, tandis que la xylogénèse durait 6-7 mois, jusqu'à octobre-début novembre. Des dates et durées très semblables ont été observées pour ces trois espèces dans de nombreuses régions au climat comparable à celui de notre étude : pour le pin sylvestre dans le nord de la France (Michelot *et al.*, 2012) et en Pologne (Wodzicki, 1971; Wodzicki, 2001), pour le pin sylvestre et le sapin pectiné en plaine du nord-est de la France (Rathgeber *et al.*, 2011a; Rathgeber *et al.*, 2011b), et pour l'épicéa commun et le sapin pectiné en Slovénie (Gričar, 2007). En revanche, l'analyse des données de la littérature montre pour de nombreuses espèces de conifères en forêt boréale (Mäkinen *et al.*, 2003; Schmitt *et al.*, 2004; Makinen *et al.*, 2008; Rossi *et al.*, 2008b; Lupi *et al.*, 2010; Rossi *et al.*, 2011; Seo *et al.*, 2011; Zhai *et al.*, 2012) ou d'altitude (Rossi *et al.*, 2006; Rossi *et al.*, 2007; Deslauriers *et al.*, 2008; Rossi *et al.*, 2008a; Rossi *et al.*, 2008b) que l'activité cambiale et la xylogénèse y commencent 2 à 4 semaines plus tard, y finissent 2 à 4 semaines plus tôt et y sont donc plus

courtes de 1 à 2 mois qu'en forêt tempérée. De telles différences dans le début, la fin et la durée entre des environnements froids et doux traduisent l'influence cruciale de la température dans le contrôle de la phénologie de la formation du bois (Rossi *et al.*, 2007; Deslauriers *et al.*, 2008; Rossi *et al.*, 2008b; Lupi *et al.*, 2012), avec une augmentation des durées estimée de 1 à 1,5 semaines par degré (Moser *et al.*, 2010; Rossi *et al.*, 2011).

Pour du pin sylvestre à moyenne altitude (750 m) dans les Alpes, dans une vallée caractérisée par une température similaire à notre étude (7,3°C de moyenne annuelle) mais avec des conditions hydriques beaucoup plus limitantes (715 mm par an), l'activité cambiale commençait à des dates très similaires à celles décrites dans cette thèse mais finissait deux mois et demi plus tôt, au tout début de l'été (Gruber *et al.*, 2010; Swidrak *et al.*, 2011). Cette différence apporte une nuance à l'influence cruciale de la température. Ainsi, dans les régions caractérisées par des forts déficits hydriques estivaux, la fin de l'activité cambiale apparait principalement déterminée par la disponibilité en eau et est d'autant plus précoce que la sécheresse estivale est marquée (Eilmann *et al.*, 2011 ; Gruber *et al.*, 2010).

Durant la saison de croissance, la vitesse moyenne de production des cellules était de 0,3-0,5 cellules jour^{-1} et suivait une évolution bimodale, avec un premier maximum au printemps et un second en été (Figure IX.2A). Dans la littérature, beaucoup moins d'informations sur les taux sont disponibles car les études se sont pour la plupart focalisées sur la phénologie. Cependant, les rares valeurs données pour des climats similaires à celui de notre région d'étude sont très proches de celles que nous avons obtenues. Pour le sapin pectiné et l'épicéa commun en Slovénie, Gričar (2007) donne des taux entre 0,3 et 0,7 cellules jour^{-1}, tandis que Rathgeber *et al.* (2011b) trouvent des taux de 0,15 à 0,5 cellules jour^{-1} pour le sapin en plaine du nord-est de la France. Gruber *et al.* (2010) ont obtenu des taux très faibles, autour de 0,1 cellules jour^{-1} pour le pin sylvestre en conditions sèches, ce qui suggère qu'en plus d'affecter la fin, le déficit hydrique limite la vitesse de l'activité cambiale. Au contraire, les données de la littérature suggèrent que les taux observés en environnements froids sont au moins aussi importants que ceux observés en forêt tempérée. En effet, Rossi *et al.* (2008a) calculent des taux de 0,1 à 0,7 cellules jour^{-1} à plus de 2000 m d'altitude dans les Alpes, tandis que Deslauriers & Morin (2005) présentent des taux de production supérieurs à 0,5 cellules jour^{-1} en forêt boréale au Québec. Enfin, Mäkinen *et al.* (2003) ont observé des taux très élevés, entre 0.5 et 1 cellule jour^{-1}, en Finlande.

Une hypothèse pourrait même être que les taux sont plus élevés pour les arbres contraints à des durées plus courtes en environnements froids. Gregory & Wilson (1968) ont comparé la dynamique de l'activité cambiale d'épinettes blanches entre l'Alaska et la Nouvelle-Angleterre. En Alaska, les arbres disposaient d'une saison de végétation deux fois plus courtes (45 vs. 95 jours) mais réussissaient à produire le même nombre de cellules (60 à 70) en compensant par des taux de division dans la zone cambiale deux fois plus élevés (1.4 vs. 0.7 cellules par jour). Les auteurs suggèrent alors que les épinettes d'Alaska se sont adaptées à leur saison de croissance plus courte par un taux de division plus grand. Cependant, une compensation d'une telle amplitude par la vitesse de production apparait improbable car des productions faibles (< 30 trachéides) sont souvent rapportées pour les

environnements froids (Rossi *et al.*, 2006; 2007 ; 2011; Deslauriers *et al.*, 2008; Lupi *et al.*, 2010). Une analyse à large échelle, en regroupant des données de la dynamique de l'activité cambiale à des latitudes et/ou altitudes variées, permettrait de confirmer ou d'infirmer cette hypothèse.

L'intensité de l'activité cambiale dépend du nombre de cellules cambiales et de la longueur du cycle cellulaire, c'est-à-dire la durée nécessaire à une cellule pour se diviser et donner naissance à une nouvelle cellule du xylème (Vaganov *et al.*, 2006). Nous avons estimé qu'une cellule cambiale met, en moyenne, 20 à 30 jours pour se diviser (de 45 jours maximum à 15 jours minimum dans la saison) (Figure IX.2A). Skene (1969; 1972) donne des valeurs comparables, avec des cycles cellulaires estimés à 28 jours pour le pin de Monterey (*Pinus radiata*) en Australie, entre 10 et 35 jours pour la pruche du Canada (*Tsuga canadensis*) aux États-Unis. Ces durées apparaissent très longues. Pour prendre un exemple à l'extrême opposé, la durée est réduite à 90 minutes pour les levures et à moins de 30 minutes pour des cellules embryonnaires (Cooper, 2000). De nombreux cycles cellulaires se font en 24h : c'est le cas pour une cellule typique de mammifère (Alberts *et al.*, 2002; Bernard & Herzel, 2006) ou pour une cellule d'un méristème primaire végétal (Tardieu & Granier, 2000; West *et al.*, 2004). Les durées très longues du cycle cellulaire des cellules cambiales pourraient être liées à leur forme très allongée extrêmement particulière. Lors de la division d'une cellule cambiale, la cytocinèse (division du cytoplasme) se fait sur toute la longueur de la cellule, ce qui implique de former de la paroi en grande quantité. La surface à couvrir est ainsi plusieurs centaines de fois plus grandes que dans les cellules des méristèmes primaires (Lachaud *et al.*, 1999). Donc, la déposition de la plaque cellulaire périclinale puis de la paroi primaire limitent probablement la fréquence des divisions cambiales. Lorsqu'il faut de grandes vitesses de production cellulaire, l'arbre doit augmenter la taille de la population de cellules cambiales (Mellerowicz *et al.*, 2001), d'où les très bonnes relations obtenues entre nombre de cellules cambiales et taux de production exposées dans ce manuscrit (partie IV, article 1) ou dans la littérature (Gregory & Wilson, 1968; Gričar *et al.*, 2009).

Après avoir été produite par l'activité cambiale, les futures trachéides poursuivent leur programme de différenciation avec tout d'abord l'élargissement radial puis la formation de la paroi secondaire. Nous avons calculé qu'en moyenne, l'élargissement prend 9 jours à une vitesse de 4 µm jour^{-1}. Toutefois, au contraire de la vitesse, la durée d'élargissement présente une évolution marquée au cours de la saison : elle diminue de 3 à 4 fois, passant de 2-3 semaines à environ 5 jours (Figure IX.2B). Après l'élargissement, la formation de la paroi dure 7 semaines en moyenne, avec un taux de déposition du matériel pariétal autour de 19 µm² jour^{-1}. Tout comme la durée d'élargissement, la durée de formation de la paroi présente une évolution caractéristique au cours de la saison (Figure IX.2C). Elle reste minimale et stable dans le bois initial (3 semaines), puis augmente brutalement de 2 à 3 fois pour culminer à près de 8 semaines pour les dernières cellules du bois final. Le taux de déposition présente une évolution opposée : il est maximal et stable dans le bois initial (20-30 µm² jour^{-1}), puis diminue de 4 à 6 fois pour atteindre un minimum à la toute fin du bois final (5 µm² jour^{-1}).

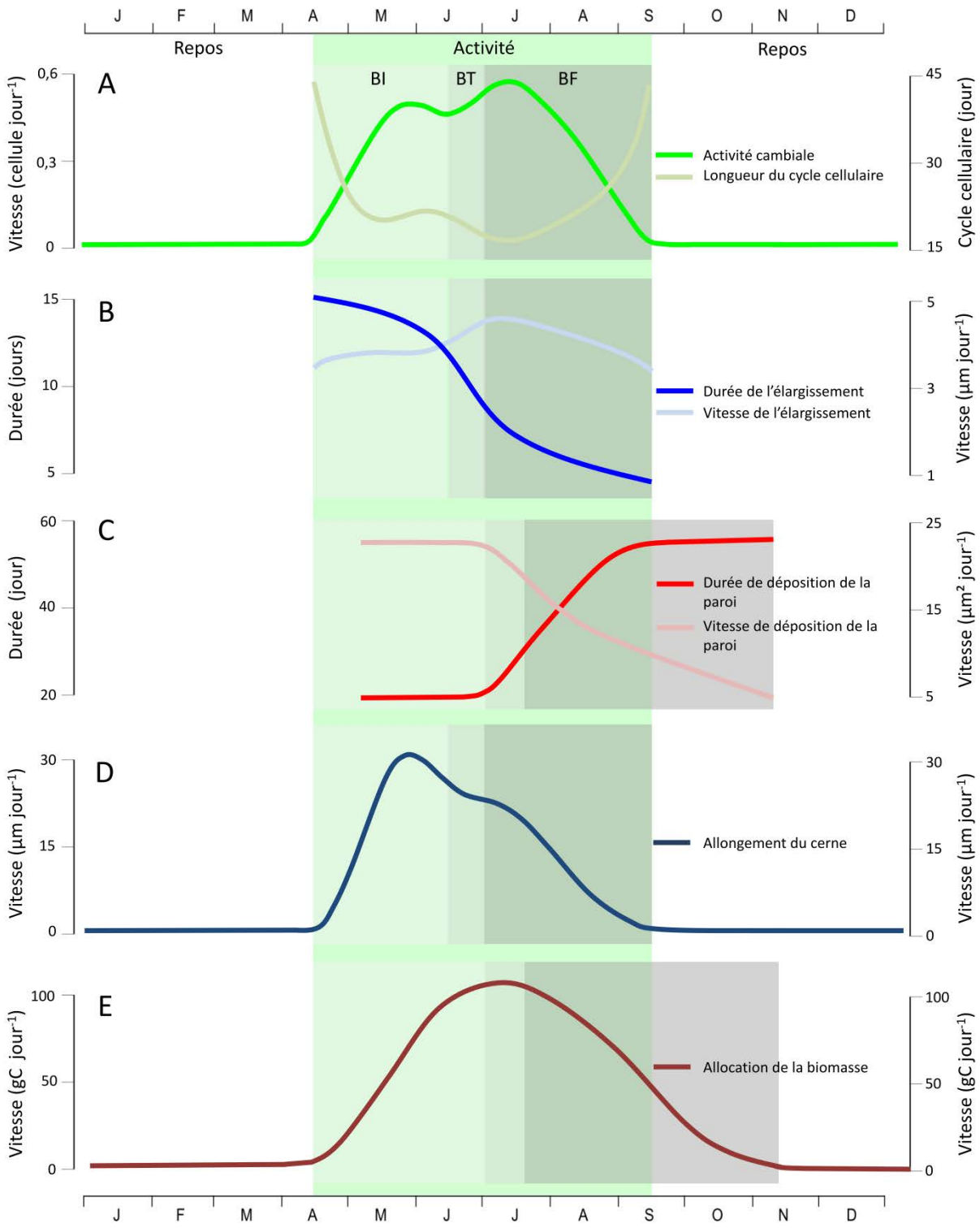

Figure IX.2 : Dynamique intra-annuelle de la formation du bois des conifères en forêt tempérée. La figure synthétise les différents résultats obtenus dans la thèse relatifs à la dynamique de la formation du bois. Au contraire des représentations données dans les parties de résultats, les durées et vitesses de l'élargissement cellulaire et de la formation de la paroi secondaire ne sont pas représentées en fonction de la position de la cellule dans le cerne mais en fonction du temps. A un certain temps, la valeur donnée correspond à la moyenne pour l'ensemble des cellules qui se trouve dans la phase correspondante. Pour chaque courbe, les aires colorées avec différents tons représentent le bois initial (BI), le bois de transition (BT) et le bois final (BF). En A, B, et D, la date de passage à un certain type de bois correspond à la date où la première cellule de ce type de bois est produite. En C et E, le passage à un certain type de bois correspond à la date où la première cellule de ce type de bois entre en phase d'épaississement de la paroi et lignification.

Au contraire des patrons généraux de la xylogénèse, qui sont documentés dans une littérature récente (dernière décennie), la dynamique de différenciation cellulaire est principalement décrite dans une littérature ancienne (années 1960 – 1970 surtout) et difficilement accessible. Cependant, l'analyse de cette littérature donne des valeurs et une évolution des durées de différenciation cellulaire pour des conifères en climat tempéré qui sont très similaires à celles que nous avons obtenues. Ainsi, la compilation des données recueillies pour le pin de Monterey en Australie (Skene, 1969), la pruche du Canada aux États-Unis (Skene, 1972), le pin sylvestre en Pologne (Wodzicki, 1971) et l'épicéa commun en République Tchèque (Horacek *et al.*, 1999) donne une durée d'élargissement qui diminue de 2-4 semaines à 5-10 jours au cours de la saison, alors que la durée d'épaississement augmente de 2-3 semaines à 7-10 semaines. Il est intéressant de noter que les valeurs et tendances sont très proches alors que la diversité des espèces et des régions géographiques est très grande. Donc, quelle que soit l'espèce ou la position géographique considérée, les conifères en climat tempéré partagent une dynamique intra-annuelle de la formation du bois très semblable, que ce soit dans les patrons généraux de la croissance ou dans la cinétique de différenciation cellulaire.

Rossi *et al.* (2006), à haute altitude (> 2000 m), trouvent aussi des durées d'élargissement qui diminuent de 2-4 semaines à moins de 1 semaine, tandis que Deslauriers *et al.* (2003) en forêt boréale calculent des durées d'élargissement autour de 1 semaine pour toutes les cellules. Ces durées sont donc très proches de celles déterminées pour nos arbres. Ces deux études donnent des durées de formation de la paroi qui augmentent de 1-3 à 4-5 semaines et qui sont donc inférieures à celles décrites pour la forêt tempérée. Cependant, ces auteurs ont utilisé la fonction de Gompertz. Hors, nous avons démontré que l'utilisation de cette méthode conduisait à sous-estimer la durée de formation de la paroi (voire partie V, article 2). En l'utilisant, nous avons également trouvé des durées qui augmentaient de 1 à 4 semaines. Donc, en utilisant la même méthode, nous retrouvons les mêmes valeurs entre notre zone d'étude et les environnements froids, ce qui laisse à penser que contrairement à la phénologie cambiale, la cinétique de différenciation cellulaire est similaire entre les différents biomes de la zone tempérée.

L'intégration de la cinétique des processus à un niveau arbre a permis de calculer la vitesse de croissance du xylème et de l'accumulation de la biomasse dans le bois en formation. Au cours de la saison, la vitesse moyenne de la croissance radiale du xylème était de 15 µm jour^{-1} et suivait une courbe en cloche qui culminait au printemps (Figure IX.2D). Les mesures externes de variations de la circonférence par les dendromètres donnaient le même patron. Par contraste, l'accumulation de la biomasse dans le bois en maturation, qui était en moyenne de 60 grammes de carbone par jour, suivait une courbe en cloche symétrique qui culminait en été (Figure IX.1E). Un tel établissement de la dynamique saisonnière de l'accumulation de la biomasse dans le bois, sur la base des processus, est inédit. Le résultat est important car il montre que la croissance radiale et l'accumulation de la biomasse dans le bois sont largement décalées dans le temps. En conséquence, la dynamique de l'accumulation du carbone dans l'arbre ne peut pas être calculée à partir de mesures externes de la croissance du tronc.

IX.2.2 Mécanismes de la formation de la structure du cerne annuel par la dynamique

L'étude des relations entre durée, vitesse de l'activité cambiale et incrément annuel de bois dans la partie IV (article 1) a montré que, dans nos peuplements mélangés de conifères, la variabilité de la largeur de cerne observée entre les arbres est principalement expliquée par des changements dans la vitesse de production des cellules, alors que la longueur de la saison de végétation à une influence plus faible (Figure IX.3). Rathgeber *et al.* (2011b) ont trouvé le même résultat pour expliquer la variabilité de la largeur du cerne entre des arbres appartenant à différents statuts sociaux dans une plantation de sapin. Donc, dans un peuplement de conifères, la vitesse de production des cellules est le principal déterminant de la variabilité de la largeur du cerne annuel entre les arbres. Ce résultat démontre l'importance de la vitesse de l'activité cambiale, un aspect qui a pourtant été largement négligé par rapport à la phénologie du processus.

Michelot *et al.* (2012) ont obtenu un résultat discordant pour des pins sylvestre dans le nord de la France (près de Paris). Ils ont trouvé que la variabilité de l'incrément de xylème était principalement expliquée par des changements dans la durée de l'activité cambiale, eux-mêmes exclusivement expliqués par la variabilité de la fin de l'activité cambiale. Leur zone d'étude se caractérise par des précipitations de moitié inférieures à celles observées dans les Vosges (750 mm vs.1350 mm). Leur hypothèse est que le fort déficit hydrique estival cause la variabilité dans la fin de la croissance, et donc dans l'incrément final. Ce résultat rejoint d'ailleurs le point discuté précédemment sur l'influence majeur des conditions hydriques dans le contrôle de la fin de l'activité cambiale dans les environnements plus secs.

Les résultats de la partie VI (article 3) ont clairement démontré que la variabilité de la taille des cellules le long du cerne est principalement expliquée par des changements dans la durée de l'élargissement cellulaire, la vitesse ayant une influence plus faible (Figure IX.3). Plusieurs études ont déjà montré que la diminution du diamètre des cellules observée le long du cerne va de pair avec une diminution de la durée élargissement, tandis que la vitesse varie de façon plus irrégulière (Skene, 1969; Wodzicki, 1971; Denne, 1972; Skene, 1972). Cependant, jamais l'influence relative de la durée et de la vitesse d'élargissement sur les changements de taille des cellules n'avait été clairement quantifiée. Cette thèse a donc dévoilé pour la première fois le mécanisme de la diminution de la taille des cellules le long du cerne.

La variabilité dans l'épaisseur de la paroi le long du cerne était en retour principalement expliquée par les changements dans la taille des cellules : l'épaisseur de la paroi augmente avant tout parce que la taille des cellules diminue. Cet effet géométrique était déjà connu, puisque certains auteurs ont calculé la surface transversale de la paroi pour en tenir compte (Skene, 1969; Wodzicki, 1971; Skene, 1972; Dodd & Fox, 1990). Toutefois, il y existe dans la littérature une contradiction entre la reconnaissance de cet effet fort de la taille des cellules et l'attribution de la variation de l'épaisseur de la paroi à la cinétique de déposition du matériel pariétal, en particulier à la durée de déposition (Wodzicki, 1971; Denne, 1972; Dodd & Fox,

1990; Horacek *et al.*, 1999). A cause de cette contradiction, l'idée que l'épaisseur de la paroi dépend principalement de la durée d'épaississement s'est durablement ancrée dans les esprits (voir, par exemple, Uggla *et al.*, 2001; Bouriaud *et al.*, 2005; Vaganov *et al.*, 2011). Dans cette thèse, nous avons donc clarifié le mécanisme des changements dans l'épaisseur de la paroi le long du cerne : ils sont surtout dus à la diminution de la taille des cellules qui est elle-même principalement pilotée par la durée d'élargissement ; ils ne sont qu'en second lieu expliqués par la quantité de paroi déposée dans la cellule, qui elle-même dépend autant de la durée que de la vitesse de déposition.

Au vu des résultats précédents, nous sommes maintenant capables d'expliquer les changements de dimensions des trachéides le long du cerne par la cinétique des processus de différenciation, avec la durée d'élargissement en facteur principal. Hors, les relations entre les dimensions des trachéides et la densité du bois sont clairement établies à l'aide de modèles géométriques (Decoux *et al.*, 2004; Rathgeber *et al.*, 2006) et ont également été établies dans la partie VI (article 3). Nous sommes dons capables d'expliquer les changements de densité le long du cerne par la cinétique des processus. Ainsi, comme les changements dans la durée d'élargissement expliquent la majorité des changements dans la morphologie des cellules (taille et épaisseur de la paroi) le long du cerne, ce sont majoritairement eux qui pilotent l'évolution de la densité le long du cerne.

Le fait que la dynamique de la xylogénèse donne forme à la structure du cerne était déjà fortement pressentit avant cette thèse. Par exemple, le cerne en lui-même résulte directement de l'activité saisonnière du cambium. Par contre, jamais les contributions relatives des différents composants de la dynamique sur la structure du cerne formé n'avaient été évaluées. Donc, pour la première fois, cette thèse dévoile les mécanismes fins par lesquels la dynamique intra-annuelle de différenciation cellulaire forme la structure d'un cerne annuel. Deux résultats principaux peuvent être mis en exergue :

- **la vitesse de l'activité cambiale est le principal déterminant de la variabilité de la largeur du cerne ;**
- **la durée de l'élargissement cellulaire est le principal déterminant des changements dans la morphologie des trachéides (diamètre radial et épaisseur de paroi) et la densité du bois le long du cerne.**

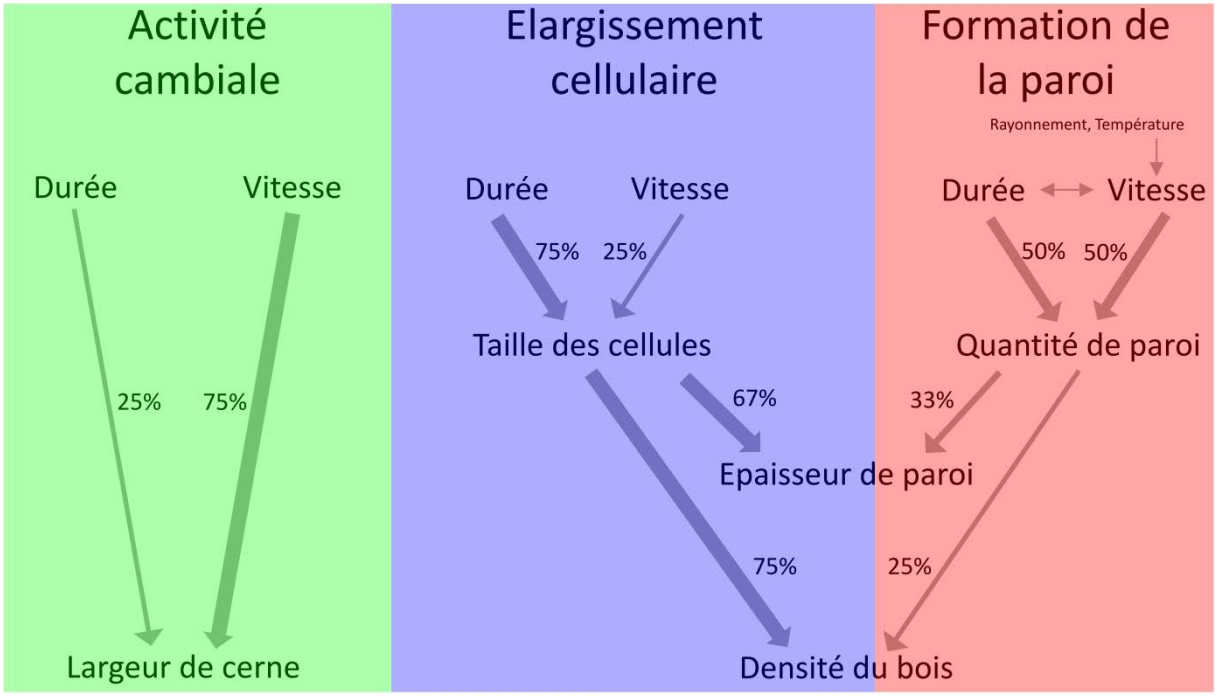

Figure IX.3 : Mécanismes par lesquels la dynamique intra-annuelle de la formation du bois forme la structure du cerne. Les pourcentages donnent la contribution relative des différents composants de la dynamique intra-annuelle de la formation du bois sur les différentes caractéristiques de la structure du cerne. Pour l'activité cambiale, les pourcentages donnent la contribution relative de la durée et de la vitesse sur la variabilité de la largeur de cerne entre les arbres dans un peuplement. Pour l'élargissement et la formation de la paroi secondaire, on observe la contribution des différents composants sur la variabilité des dimensions cellulaires et de la densité le long du cerne. Par exemple pour l'élargissement, les changements de taille des cellules le long du cerne sont expliqués à 75% par les changements dans la durée et 25% par les changements dans la vitesse.

IX.2.3 Régulation de la dynamique de la xylogénèse

Durant la dernière décennie, la plupart des études sur la dynamique intra-annuelle de la formation du bois ont cherché à comprendre l'influence des facteurs environnementaux sur la xylogénèse en se focalisant sur la phénologie des processus. La phénologie est un aspect important, car elle traduit un compromis entre l'optimisation de la durée pour la croissance et la reproduction et l'évitement des évènements climatiques extrêmes (Richardson & O'Keefe, 2009). La phénologie a donc une influence sur la croissance, la reproduction et la survie des individus. Cependant, nous avons vu que la durée de la saison de végétation n'avait qu'une influence limitée sur la croissance. De plus, c'est la dynamique de différenciation cellulaire qui détermine la morphologie des cellules et la densité du bois, un déterminant majeur des propriétés du bois pour l'industrie (Bowyer *et al.*, 2007) et un trait fonctionnel très important largement discuté dans la littérature (voir par exemple Hacke *et al.*, 2001; King *et al.*, 2006; Chave *et al.*, 2009; Larjavaara & Muller-Landau, 2010). Il faut donc s'intéresser également à ces aspects de la dynamique pour évaluer pleinement l'influence des facteurs environnementaux sur la formation du bois.

Ainsi dans cette thèse, par contraste avec l'approche « classique » – qui consiste à regarder l'influence des facteurs environnementaux sur la phénologie de l'activité cambiale et de la xylogénèse – nous avons regardé l'influence des variables climatiques sur les processus de la différenciation des cellules du xylème. Pour cela, nous nous sommes servis des deux étapes (1) « caractérisation de la cinétique des processus du développement cellulaire » et (2) « mécanismes de la formation de la structure du cerne par les processus ». Tout d'abord, une bonne connaissance du timing des processus du développement cellulaire permet de les associer aux facteurs climatiques correspondants et ainsi de s'assurer de la causalité des relations. A partir de là, on peut regarder l'influence des variables climatiques sur la durée et la vitesse de chaque processus pour chaque cellule. Comme on a établi les mécanismes par lesquels la durée et la vitesse des processus influencent les caractéristiques du xylème, on peut finalement accéder aux mécanismes de l'influence des variables climatiques sur la structure du cerne.

Dans ce manuscrit, nous avons associé les deux composantes « durée » et « vitesse » de la cinétique des processus à des mécanismes de régulation différents (Sundberg *et al.*, 2000). D'un côté, la durée des cellules reflète le laps de temps laissé à chaque cellule pour se développer, que nous avons associé plutôt à un contrôle développemental. D'un autre côté, la vitesse des processus traduit un potentiel instantané à la croissance que nous avons en conséquence plutôt associé au métabolisme. En partant de cette conception, nous avons déjà conclu dans la partie VI (article 3) que l'influence cruciale de la durée d'élargissement suggérait un contrôle développemental fort de la taille des cellules qui, étant donnée l'influence de la taille des cellules sur les autres caractéristiques du xylème (épaisseur de la paroi et densité), devrait limiter l'influence des variables climatiques sur la structure du cerne. Cette idée a été confirmée dans la partie VIII (article 5), dans laquelle nous montrons que les variations de la durée et de la vitesse de l'élargissement cellulaire, ainsi que du diamètre final de la trachéide qui en résulte, ne sont pas associées aux variations saisonnières des facteurs climatiques considérés (température, réserve hydrique et radiation).

En utilisant une approche similaire à la nôtre, Wodzicki (1971) sur du pin sylvestre en Pologne ou Antonova & Stasova (1993; 1997) sur du pin sylvestre et du mélèze en Sibérie n'ont également pas retrouvé un déterminisme climatique fort de l'élargissement cellulaire et de la diminution du diamètre des trachéides le long du cerne. Donc, la diminution drastique de la taille des cellules typiquement observée le long du cerne des conifères n'est pas déterminée par les changements dans les variables climatiques au cours de la saison. Un tel résultat réfute l'idée persistante – reprise par exemple dans la conception de modèles de la formation du bois (Deleuze & Houiller, 1998) – que la diminution de la taille des cellules résulte de la diminution de la disponibilité en eau au cours de la saison (Kramer, 1964).

L'auxine a été largement impliquée dans la régulation de l'élargissement cellulaire (Uggla *et al.*, 1996; Tuominen *et al.*, 1997; Sundberg *et al.*, 2000). Cette hormone est distribuée selon un gradient abrupt de concentration entre les zones cambiales et d'élargissement et jouerait le rôle de morphogène (c'est-à-dire une molécule de signal qui induit des réponses cellulaire spécifique en fonction de sa concentration locale). La taille du

gradient contrôlerait la taille de la zone d'élargissement et ainsi la durée de résidence des cellules en élargissement (Tuominen *et al.*, 1997; Uggla *et al.*, 1998; Sundberg *et al.*, 2000; Mellerowicz *et al.*, 2001).

Une influence directe des facteurs environnementaux sur l'élargissement cellulaire apparait néanmoins évidente dans des milieux plus limitants, en particulier vis-à-vis de l'eau. En effet, l'eau est l'élément crucial pour l'élargissement car elle exerce la pression nécessaire à l'extension de la paroi et joue sur l'extensibilité de la paroi elle-même (Nonami & Boyer, 1990b; Cosgrove, 1997). L'élargissement cellulaire est ainsi connu pour être l'un des processus végétaux les plus sensibles au stress hydrique (Hsiao, 1973). Il semble y avoir une large gamme de potentiels hydriques dans laquelle le diamètre ne change pas significativement, mais la taille des cellules diminuent ensuite rapidement en dessous d'un seuil critique de potentiel hydrique (Von Wilpert, 1991). C'est pourquoi une diminution rapide des diamètres est généralement observée lors d'une sécheresse (Abe *et al.*, 2003; Rossi *et al.*, 2009), ou encore que les diamètres sont différents lorsque l'on compare des sites ou des années avec des conditions hydriques différentes (Gruber *et al.*, 2010).

L'influence des facteurs climatiques (température et rayonnement) sur la différenciation du xylème étaient néanmoins clairement visible sur le taux de déposition du matériel pariétal (Figure IX.3). Tout d'abord, un tel résultat montre bien que l'élargissement cellulaire et la formation de la paroi secondaire sont régulés par des mécanismes physiologiques différents. Au contraire de la paroi primaire formée durant la division ou l'élargissement cellulaire, la déposition de la paroi secondaire et la lignification représentent le puits dominant de l'investissement des carbohydrates dans l'arbre au cours de la saison (Demura & Ye, 2010). L'influence forte des facteurs climatiques sur le taux de déposition de la paroi suppose donc une action via le métabolisme. D'un côté, la lumière fournit l'énergie pour la production des carbohydrates par la photosynthèse. Son action est donc sans doute liée à l'activité photosynthétique. Au cours de la saison, la radiation lumineuse diminue, ce qui pourrait réduire l'approvisionnement du matériel pariétal produit par la photosynthèse, d'où la réduction du taux de déposition. Pour la température, l'influence apparait plus complexe. La température influence la vitesse du métabolisme de la plante. Au niveau de la formation des parois, l'influence de la température peut donc être sur la photosynthèse ou/et le transport ou/et l'assemblage des constituants dans la cellule. Cependant, la différenciation des cellules du xylème est reconnue pour être plus sensible à la température que la photosynthèse (Körner, 2003; Rossi et *al.*, 2008b), ce qui suggère que l'influence de la température se fait plutôt sur les mécanismes directement responsables de la formation de la paroi dans la cellule.

Cependant, pour la majorité des cellules, l'influence des facteurs climatiques sur le taux de déposition est contrebalancée par la durée de déposition. La conséquence d'une telle compensation est qu'elle empêche l'enregistrement du signal climatique dans la structure du cerne. Par exemple, l'influence de la lumière sur la diminution du taux ne se retrouve pas sur la structure du cerne car dans le même temps, la durée de déposition augmente. Il n'y a qu'à la fin du bois final que la durée cesse d'augmenter et ne compense plus la chute du taux. Dans cette portion très réduite du cerne, l'influence des facteurs environnementaux sur le taux de

déposition peut alors être directement enregistrée dans la structure du cerne (c'est-à-dire dans la quantité de paroi déposée). De plus, comme la déposition de la paroi prend jusqu'à deux mois pour les dernières cellules du cerne, cela signifie que le « capteur » enregistre 2 mois de conditions environnementales. Un tel résultat peut expliquer pourquoi la densité maximale du bois final est l'un des proxies les plus utilisés pour les reconstructions des températures estivales.

IX.3 Références

Abe H, Nakai T, Utsumi Y, Kagawa A. 2003. Temporal water deficit and wood formation in *Cryptomeria japonica*. *Tree Physiology* **23**(12): 859-863.

Alberts B, Johnson A, Lewis J, Raff M, Roberts K, Walter P 2002. The cell cycle and programmed cell death. *Molecular Biology of the cell*. New York: Garland Science, 984-1026.

Antonova GF, Stasova VV. 1993. Effects of environmental factors on wood formation in Scots pine stems. *Trees-Structure and Function* **7**(4): 214-219.

Antonova GF, Stasova VV. 1997. Effects of environmental factors on wood formation in larch (*Larix sibirica* Ldb.) stems. *Trees-Structure and Function* **11**(8): 462-468.

Bernard S, Herzel H. 2006. Why do cells cycle with a 24 hour period? *Genome informatics. International Conference on Genome Informatics* **17**(1): 72-79.

Bouriaud O, Leban JM, Bert D, Deleuze C. 2005. Intra-annual variations in climate influence growth and wood density of Norway spruce. *Tree Physiology* **25**(6): 651-660.

Bowyer JL, Shmulsky R, Haygreen JG. 2007. *Forest products and wood science*: Wiley-Blackwell.

Camarero JJ, Olano JM, Parras A. 2010. Plastic bimodal xylogenesis in conifers from continental Mediterranean climates. *New Phytologist* **185**(2): 471-480.

Chaffey N 2002. An introduction to the problems of working with trees. In: Chaffey N ed. *Wood formation in trees - Cell and molecular biology techniques*. London: Taylor & Francis.

Chave J, Coomes D, Jansen S, Lewis SL, Swenson NG, Zanne AE. 2009. Towards a worldwide wood economics spectrum. *Ecology Letters* **12**(4): 351-366.

Cooper GM 2000. The eukaryotic cell cycle. In: Cooper GM, Hausmann RE eds. *The cell. A molecular approach*: ASM Press, Washington, Sinauer associates, Sunderland, 653-692.

Cosgrove DJ. 1997. Relaxation in a high-stress environment: the molecular bases of extensible cell walls and cell enlargement. *The Plant Cell* **9**(7): 1031.

Decoux V, Varcin E, Leban JM. 2004. Relationships between the intra-ring wood density assessed by X-ray densitometry and optical anatomical measurements in conifers. Consequences for the cell wall apparent density determination. *Annals of Forest Science* **61**(3): 251-262.

Deleuze C, Houllier F. 1998. A simple process-based xylem growth model for describing wood microdensitometric profiles. *Journal of Theoretical Biology* **193**(1): 99-113.

Demura T, Ye Z-H. 2010. Regulation of plant biomass production. *Current Opinion in Plant Biology* **13**(3): 298-303.

Denne MP. 1972. A comparison of root- and shoot-wood development in conifer seedlings. *Annals of Botany* **36**(3): 579-587.

Deslauriers A, Morin H. 2005. Intra-annual tracheid production in balsam fir stems and the effect of meteorological variables. *Trees-Structure and Function* **19**(4): 402-408.

Deslauriers A, Morin H, Begin Y. 2003. Cellular phenology of annual ring formation of *Abies balsamea* in the Quebec boreal forest (Canada). *Canadian Journal of Forest Research - Revue Canadienne De Recherche Forestière* **33**(2): 190-200.

Deslauriers A, Rossi S, Anfodillo T, Saracino A. 2008. Cambial phenology, wood formation and temperature thresholds in two contrasting years at high altitude in southern Italy. *Tree Physiology* **28**(6): 863-871.

Dodd RS, Fox P. 1990. Kinetics of Tracheid Differentiation in Douglas-fir. *Annals of Botany* **65**(6): 649-657.

Gregory RA, Wilson BF. 1968. A comparison of cambial activity of white spruce in Alaska and New England. *Canadian Journal of Botany* **46**(6): 733-734.

Gričar J. 2007. *Xylo- and phloemogenesis in silver fir (Abies alba Mill.) and Norway spruce (Picea abies (L.) Karst.).* University of Ljubljana Ljubljana.

Gričar J, Krze L, Čufar K. 2009. Number of cells in xylem, phloem and dormant cambium in silver fir (*Abies alba*), in trees of different vitality. *Iawa Journal* **30**(2): 121-133.

Gruber A, Strobl S, Veit B, Oberhuber W. 2010. Impact of drought on the temporal dynamics of wood formation in *Pinus sylvestris*. *Tree Physiology* **30**(4): 490-501.

Hacke UG, Sperry JS, Pockman WT, Davis SD, McCulloch KA. 2001. Trends in wood density and structure are linked to prevention of xylem implosion by negative pressure. *Oecologia* **126**(4): 457-461.

Horacek P, Slezingerova J, Gandelova L 1999. Effects of environment on the xylogenesis of Norway spruce (*Picea abies* L. Karst.). In: Wimmer R, Vetter RE eds. *Tree-ring analysis: biological, methodological and environmental aspects*. Wallingford, UK: CABI Publishing, 33-53.

Hsiao TC. 1973. Plant responses to water stress. *Annual review of plant physiology* **24**(1): 519-570.

King DA, Davies SJ, Tan S, Noor NSM. 2006. The role of wood density and stem support costs in the growth and mortality of tropical trees. *Journal of Ecology* **94**(3): 670-680.

Körner C. 2003. Carbon limitation in trees. *Journal of Ecology* **91**(1): 4-17.

Kramer P. 1964. The role of water in wood formation. In: Zimmermann MH ed. *The formation of wood in forest trees*. New York, London: Academic Press, 519-532.

Lachaud S, Catesson AM, Bonnemain JL. 1999. Structure and functions of the vascular cambium. *Comptes Rendus de l'Académie des Sciences - Series III - Sciences de la Vie* **322**(8): 633-650.

Larjavaara M, Muller-Landau HC. 2010. Rethinking the value of high wood density. *Functional Ecology* **24**(4): 701-705.

Lupi C, Morin H, Deslauriers A, Rossi S. 2010. Xylem phenology and wood production: resolving the chicken-or-egg dilemma. *Plant Cell and Environment* **33**(10): 1721-1730.

Lupi C, Morin H, Deslauriers A, Rossi S. 2012. Xylogenesis in black spruce: does soil temperature matter? *Tree Physiology* **32**(1): 74-82.

Mäkinen H, Nöjd P, Saranpää P. 2003. Seasonal changes in stem radius and production of new tracheids in Norway spruce. *Tree Physiology* **23**(14): 959-968.

Makinen H, Seo JW, Nojd P, Schmitt U, Jalkanen R. 2008. Seasonal dynamics of wood formation: a comparison between pinning, microcoring and dendrometer measurements. *European Journal of Forest Research* **127**(3): 235-245.

Mellerowicz EJ, Baucher M, Sundberg B, Boerjan W. 2001. Unravelling cell wall formation in the woody dicot stem. *Plant Molecular Biology* **47**(1-2): 239-274.

Michelot A, Simard S, Rathgeber C, Dufrêne E, Damesin C. 2012. Comparing the intra-annual wood formation of three European species (*Fagus sylvatica*, *Quercus petraea* and *Pinus sylvestris*) as related to leaf phenology and non-structural carbohydrate dynamics. *Tree Physiology* **32**(8): 1033-1045.

Moser L, Fonti P, Büntgen U, Esper J, Luterbacher J, Franzen J, Frank D. 2010. Timing and duration of European larch growing season along altitudinal gradients in the Swiss Alps. *Tree Physiology* **30**(2): 225-233.

Nonami H, Boyer JS. 1990. Wall extensibility and cell hydraulic conductivity decrease in enlarging stem tissues at low water potentials. *Plant Physiology* **93**(4): 1610-1619.

R Core Team 2012. R: A language and environment for statistical computing. R Foundation for Statistical Computing, Vienna, Austria. ISBN 3-900051-07-0, URL http://www.R-project.org/.

Rathgeber CBK 2012. Cambial activity and wood formation: data manipulation, visualisation and analysis using R. R package version 1.4-1. http://CRAN.R-project.org/package=CAVIAR.

Rathgeber CBK, Decoux V, Leban J-M. 2006. Linking intra-tree-ring wood density variations and tracheid anatomical characteristics in Douglas fir (*Pseudotsuga menziesii* (Mirb.) Franco). *Annals of Forest Science* **63**(7): 699-706.

Rathgeber CBK, Longuetaud F, Mothe F, Cuny H, Le Moguedec G. 2011a. Phenology of wood formation: Data processing, analysis and visualisation using R (package CAVIAR). *Dendrochronologia* **29**(3): 139-149.

Rathgeber CBK, Rossi S, Bontemps J-D. 2011b. Cambial activity related to tree size in a mature silver-fir plantation. *Annals of Botany* **108**(3): 429-438.

Richardson AD, O'Keefe JF 2009. Phenological differences between understory and overstory: A case study using the long-term Harvard Forest records. In: Noormets A ed. *Phenology of Ecosystem Processes*. New York: Springer, 87-117.

Rossi S, Deslauriers A, Anfodillo T. 2006. Assessment of cambial activity and xylogenesis by microsampling tree species: An example at the alpine timberline. *Iawa Journal* **27**(4): 383-394.

Rossi S, Deslauriers A, Anfodillo T, Carraro V. 2007. Evidence of threshold temperatures for xylogenesis in conifers at high altitudes. *Oecologia* **152**(1): 1-12.

Rossi S, Deslauriers A, Anfodillo T, Carrer M. 2008a. Age-dependent xylogenesis in timberline conifers. *New Phytologist* **177**(1): 199-208.

Rossi S, Deslauriers A, Gričar J, Seo J-W, Rathgeber CBK, Anfodillo T, Morin H, Levanic T, Oven P, Jalkanen R. 2008b. Critical temperatures for xylogenesis in conifers of cold climates. *Global Ecology and Biogeography* **17**(6): 696-707.

Rossi S, Morin H, Deslauriers A, Plourde P-Y. 2011. Predicting xylem phenology in black spruce under climate warming. *Global Change Biology* **17**(1): 614-625.

Rossi S, Simard S, Deslauriers A, Morin H. 2009. Wood formation in Abies balsamea seedlings subjected to artificial defoliation. *Tree Physiology* **29**(4): 551-558.

Schmitt U, Jalkanen R, Eckstein D. 2004. Cambium dynamics of Pinus sylvestris and Betula spp. in the northern boreal forest in Finland. *Silva Fennica* **38**(2): 167-178.

Schrader J, Baba K, May S, Palme K, Bennett M, Bhalerao R, Sandberg G. 2003. Polar auxin transport in the wood-forming tissues of hybrid aspen is under simultaneous control of developmental and environmental signals. *Proceedings of the National Academy of Sciences* **100**(17): 10096-10101.

Seo J-W, Eckstein D, Jalkanen R, Schmitt U. 2011. Climatic control of intra- and inter-annual wood-formation dynamics of Scots pine in northern Finland. *Environmental and Experimental Botany* **72**(3): 422-431.

Skene DS. 1969. The period of time taken by cambial derivatives to grow and differentiate into tracheids in *Pinus radiata* D. Don. *Annals of Botany* **33**(2): 253-262.

Skene DS. 1972. The kinetics of tracheid development in *Tsuga canadensis* Carr. and its relation to tree vigour. *Annals of Botany* **36**(1): 179-187.

Sundberg B, Uggla C, Tuominen H. 2000. *Cambial growth and auxin gradients*.

Swidrak I, Gruber A, Kofler W, Oberhuber W. 2011. Effects of environmental conditions on onset of xylem growth in *Pinus sylvestris* under drought. *Tree Physiology* **31**: 483–493.

Tardieu F, Granier C. 2000. Quantitative analysis of cell division in leaves: methods, developmental patterns and effects of environmental conditions. *Plant Molecular Biology* **43**(5-6): 555-567.

Tuominen H, Puech L, Fink S, Sundberg B. 1997. A radial concentration gradient of indole-3-acetic acid is related to secondary xylem development in hybrid aspen. *Plant Physiology* **115**(2): 577-585.

Uggla C, Magel E, Moritz T, Sundberg B. 2001. Function and dynamics of auxin and carbohydrates during earlywood/latewood transition in Scots pine. *Plant Physiology* **125**(4): 2029-2039.

Uggla C, Mellerowicz EJ, Sundberg B. 1998. Indole-3-acetic acid controls cambial growth in Scots pine by positional signaling. *Plant Physiology* **117**(1): 113-121.

Uggla C, Moritz T, Sandberg G, Sundberg B. 1996. Auxin as a positional signal in pattern formation in plants. *Proceedings of the National Academy of Sciences of the United States of America* **93**(17): 9282-9286.

Vaganov EA, Anchukaitis KJ, Evans MN 2011. How well understood are the processes that create dendroclimatic records? A mechanistic model of the climatic control on conifer tree-ring growth dynamics. In: Hughes MK, Swetnam TW, Diaz HF eds. *Dendroclimatology*. London: Springer-Verlag, 37-75.

Vaganov EA, Hughes MK, Shashkin AV. 2006. *Growth nynamics of conifer tree rings*. Heidelberg: Springer.

Von Wilpert K. 1991. Intraannual variation of radial tracheid diameters as monitor of site specific water stress. *Dendrochronologia* **9**: 95-113.

West G, Inze D, Beemster GTS. 2004. Cell cycle modulation in the response of the primary root of Arabidopsis to salt stress. *Plant physiology* **135**(2): 1050-1058.

Wodzicki TJ. 1971. Mechanism of xylem differentiation in *Pinus sylvestris* L. *Journal of Experimental Botany* **22**(72): 670-687.

Wodzicki TJ. 2001. Natural factors affecting wood structure. *Wood Science and Technology* **35**(1-2): 5-26.

Wodzicki TJ, Zajaczkowski S. 1970. Methodical problems in studies on seasonal production of cambial xylem derivatives. *Acta societatis botanicorum poloniae* **39**(3): 509-520.

Zhai L, Bergeron Y, Huang J-G, Berninger F. 2012. Variation in intra-annual wood formation, and foliage and shoot development of three major Canadian boreal tree species. *American Journal of Botany* **99**(5): 827-837.

X CONCLUSIONS : CE QUE CETTE THÈSE APPORTE À L'ÉTUDE DE LA DYNAMIQUE DE LA XYLOGÉNÈSE

La formation du bois est un processus biologique important car il produit une large partie de la biomasse de la planète et une ressource essentielle pour l'Homme. La dynamique est un aspect fondamental du processus : c'est elle qui définit la structure du cerne (quantité et qualité du bois produit) et c'est elle qui sert de levier à l'influence des facteurs intrinsèques (gènes, hormones, etc.) et extrinsèques (environnement) de régulation. Pourtant, nos connaissances de la dynamique de la formation du bois sont encore limitées car cet aspect a été négligé ou considéré de façon fragmentaire. Dans cette thèse, nous nous sommes servis d'un jeu de données large et original – 45 arbres de 3 espèces de conifères (sapin pectiné, épicéa commun et pin sylvestre) suivis pendant 3 ans (2007-2009) et répartis dans 3 peuplements mélangés le long d'un gradient altitudinal dans le nord-est de la France – pour arriver à une meilleure compréhension de la dynamique de la xylogénèse. Les contributions majeures de la thèse à cet objectif sont les suivantes :

- Tout d'abord, les informations données tout au long de ce manuscrit – obtenues grâce au développement d'une méthode statistique innovante et performante – donnent une description précise de quand, combien de temps et à quelle vitesse les différents processus de la xylogénèse prennent place durant l'année. **Une telle caractérisation exhaustive de la dynamique, en particulier vis-à-vis des aspects relatifs au développement cellulaire, est extrêmement rare. Cette thèse apporte donc des informations précieuses qui améliorent nos connaissances sur la dynamique intra-annuelle de la xylogénèse.** Ainsi, pour nos trois espèces de conifères en forêt tempérée, nous montrons que la production des nouvelles cellules du cerne par l'activité cambiale dure environ 4-5 mois, d'avril-mai à août-septembre. La différenciation des dernières cellules produites se poursuit jusqu'à fin octobre-début novembre, ce qui porte la durée totale de la xylogénèse à 6-7 mois. Les cellules sont produites à une vitesse moyenne de 0,3-0,5 cellules $jour^{-1}$. Après avoir été produite par l'activité cambiale, chaque cellule du cerne met environ 6 semaines à atteindre sa forme finale fonctionnelle : 1 semaine pour s'élargir (à une vitesse de 4 µm $jour^{-1}$), 5 semaines pour former sa paroi secondaire (vitesse de déposition de 20 μm^2 $jour^{-1}$). Cependant, ces durées changent au cours de la saison. Ainsi, la durée d'élargissement est maximale (2-3 semaines) au début de la saison puis diminue progressivement (jusqu'à 4-5 jours), alors que la durée de formation de la paroi reste minimale (à environ 3 semaines) durant la première partie de la saison puis augmente rapidement (jusqu'à 8 semaines).

- Sur la base de cette caractérisation, **cette thèse dévoile les mécanismes – jamais établis auparavant – par lesquels la dynamique de la xylogénèse donne forme à la structure du cerne** (partie VI, article 3)**.** Nous montrons que la variation de l'incrément annuel de xylème (égal au nombre de cellules ou à la largeur du cerne) est principalement due à des différences dans la vitesse et non dans la durée de l'activité cambiale. D'un autre côté, nous montrons que les changements dans la taille des cellules le long du cerne sont majoritairement expliqués par les changements dans la durée d'élargissement. En retour, les changements dans la taille des cellules sont les principaux déterminants des changements dans l'épaisseur de la paroi : le long du

cerne, l'épaisseur de la paroi augmente avant tout parce que la surface à tapisser (c'est-à-dire la taille des cellules) diminue. La variation de l'épaisseur de la paroi n'est expliquée qu'en second lieu par les changements dans la quantité de paroi déposée, qui dépendent eux-mêmes autant de variations dans la durée que dans la vitesse de déposition du matériel pariétal. La durée de l'élargissement ressort donc comme un aspect clé de la dynamique vis-à-vis de son influence cruciale sur la structure du cerne : elle influence la forme globale des cellules (diamètre et épaisseur de paroi), pilotant ainsi les changements dans la densité du bois et la transition du bois initial au bois final.

- La caractérisation précise de la cinétique des processus du développement cellulaire a également permis d'accéder à la dynamique de l'accumulation de la biomasse dans le bois en formation (partie VII, article 4). **Une telle caractérisation, sur la base des processus, de la dynamique saisonnière de l'accumulation de la biomasse dans le bois en formation – le puits dominant de carbone dans les écosystèmes forestiers – est une première. Cette thèse améliore donc notre compréhension d'une partie importante du cycle du carbone dans les écosystèmes forestiers.** L'accumulation de la biomasse – principalement supportée par la formation des parois secondaires – présente une dynamique en forme de cloche qui est décalée de 1,5 mois par rapport à la dynamique de la croissance radiale – qui elle est principalement supportée par l'élargissement cellulaire ; en résumé, l'arbre grossit avant de prendre de la biomasse, si bien qu'un suivi de la croissance radiale ne renseigne pas sur la dynamique de l'accumulation du carbone dans le bois en formation. L'accumulation de la biomasse dans le bois culmine en été (juillet), durant la période la plus chaude et non durant la période la plus lumineuse, ce qui suggère qu'elle est principalement pilotée par la température.

- La caractérisation précise de la dynamique et des mécanismes par lesquels elle donne naissance au cerne ont également permis de développer une approche mécaniste de l'influence du climat sur la xylogénèse (partie VIII, article 5). **Les résultats obtenus par cette approche améliorent donc notre compréhension des mécanismes de l'influence du climat sur la xylogénèse.** Dans notre région tempérée, nous ne retrouvons pas une influence climatique forte sur les changements dans la durée et la vitesse de l'élargissement cellulaire et donc sur la diminution de la taille des cellules le long du cerne. Etant donné l'influence prépondérante de l'élargissement (sa durée en particulier) et de la taille des cellules sur les autres caractéristiques du xylème (épaisseur de paroi et densité), nous supposons que la structure du cerne est sous un contrôle développemental fort qui limite l'influence des variables climatiques au cours de la saison. L'influence des facteurs climatiques (température et radiation lumineuse) apparait néanmoins clairement sur la vitesse de déposition de la paroi secondaire – le puits dominant de biomasse dans l'arbre –, en accord avec l'idée que l'influence du climat sur la différenciation du xylème se fait principalement via le métabolisme. Mais le long du cerne, l'influence du climat sur le taux de déposition est contrebalancée par les variations dans la durée de déposition qui empêchent l'enregistrement du signal

climatique dans la structure du cerne. Il n'y a qu'à la fin du bois final où l'effet compensatoire de la durée s'arrête et ouvre la porte à un enregistrement du signal climatique, ce qui pourrait expliquer pourquoi la densité maximale du bois final est un bio-indicateur privilégié des changements environnementaux.

Au final, cette thèse propose une exploration approfondie du fonctionnement dynamique de la xylogénèse et s'inscrit donc largement à la volonté d'une meilleure compréhension de ce processus extrêmement complexe. Avoir réussi à accéder à la cinétique des processus du développement cellulaire constitue l'édifice et la force du travail. En effet, la prise en compte de ces aspects encore très peu documentés – car très difficilement accessibles – a permis une caractérisation plus complète de la dynamique de la xylogénèse et la compréhension des mécanismes par lesquels cette dynamique donne forme à la structure du cerne. A partir de là, nous avons pu accéder à la dynamique de l'accumulation du carbone dans le bois et arriver aux mécanismes de l'influence du climat sur la formation du bois, deux contributions originales à des thématiques centrales de la recherche scientifique actuelle.

XI ANNEXES

XI.1 Annexe 1 : liste des publications et communications

Liste à jour du 10/09/2013

Publications acceptées dans des revues internationales à comité de lecture

Life strategies in intra-annual dynamics of wood formation: example of three conifer species in a temperate forest in north-east France

H.E. CUNY, C.B.K. RATHGEBER, F. LEBOURGEOIS, M. FORTIN, M. FOURNIER

Tree Physiology, volume 32, pages 612-625 (2012)

Generalized additive models reveal the intrinsic complexity of wood formation dynamics

H.E. CUNY, C.B.K. RATHGEBER, T. SENGA KIESSE, F.P. HARTMAN, I. BARBEITO, M. FOURNIER

Journal of Experimental Botany, volume 64, pages 1983-1994 (2013)

Phenology of wood formation: Data processing, analysis and visualisation using R (package CAVIAR)

C.B.K. RATHGEBER, F. LONGUETAUD, F. MOTHE, **H. CUNY**, G. LE MOGUÉDEC

Dendrochronologia, volume 29, pages 139-149 (2011)

Discrete triangular associated kernel and bandwidth choices in semiparametric estimation for count data

T. SENGA KIESSÉ, **H.E. CUNY**

Journal of Statistical Computation and Simulation, DOI:10.1080/00949655.2013.768995, (2013)

Cambium phenology and growth: linear and nonlinear patterns in conifers of the northern hemisphere

S. ROSSI, T. ANFODILLO, K. ČUFAR, **H.E. CUNY**, A. DESLAURIERS, P. FONTI, D. FRANK, J. GRIČAR, A. GRUBER, G. KING, C. KRAUSE, H. MORIN, W. OBERHUBER, P. PRISLAN, C.B.K. RATHGEBER

Annals of Botany (In press)

Publications en préparation ou en relecture dans des revues internationales à comité de lecture

Wide cells, thin walls; narrow cells, thick walls: How cell differentiation processes shape conifer tree-ring structure

H.E. CUNY, C.B.K. RATHGEBER, M. FOURNIER

Under review in The Plant Journal

On modeling wood formation using parametric, nonparametric and semiparametric regressions for count data

H.E. CUNY, T. SENGA KIESSÉ

Under review in Computational Statistics and Data Analysis.

Growing is not putting on weight! New insight into carbon accumulation in trees

H.E. CUNY, C.B.K. RATHGEBER, M. FOURNIER

In preparation

Xylem cell differentiation processes related to climatic factors in conifers

H.E. CUNY, C.B.K. RATHGEBER, M. FOURNIER

In preparation

Intra-annual dynamics of wood formation and resulting tree-ring structure related to tree social status in a mature silver-fir plantation

N. CLAIRET, C.B.K. RATHGEBER, **H.E. CUNY**

In preparation

Picea mariana saplings machinery under warming and water deficit

L. BALDUCCI, **H.E. CUNY**, A. DESLAURIER, C.B.K. RATHGEBER, A. GIOVANNELLI, S. ROSSI

In preparation

Autres publications

Dynamique intra-annuelle de la formation du bois de trois espèces de conifères (épicéa commun, pin sylvestre et sapin pectine) dans les Vosges

H.E. CUNY, C.B.K. RATHGEBER, M. FOURNIER

Actes du colloque Panorama de la dendrochronologie en France, 8 au 10 Octobre 2009, Collection EDYTEM, Cahiers de Géographie n°11, pages 53-62 (2010)

Suivi intra-annuel de la croissance des arbres – Comparaison des dates de mise en place des feuilles, des rameaux et du cerne de bois

H.E. CUNY, C.B.K. RATHGEBER

Actes du séminaire de l'école doctorale RP2E, 19 Janvier 2012

Communications internationales

Wood formation phenology of three conifer species (Norway spruce, Scots pine and silver fir) in northeast France during 2008 (Communication orale)

H.E. CUNY, C.B.K. RATHGEBER, M. FOURNIER

Tree-Ring in Archeology, Climatology and Ecology (TRACE) meeting, 22-25 April 2010, Freiburg, Deutschland

Intra-annual dynamics of cambial activity: comparison of three conifer species (Norway spruce, Scots pine & silver fir) in north-east France (Poster; presentation: C.B.K. RATHGEBER)

H.E. CUNY, C.B.K. RATHGEBER, F. LEBOURGEOIS, M. FOURNIER

WorldDendro conference, 13-18 June 2010, Rovaniemi, Finland

Life-strategies in intra-annual dynamics of cambial activity: a study case involving three conifer species (Norway spruce, Scots pine and silver fir) in northeast France (Communication orale)

H.E. CUNY, C.B.K. RATHGEBER, F. LEBOURGEOIS, M. FOURNIER

Tree-Ring in Archeology, Climatology and Ecology (TRACE) meeting, 11-14 May 2011, Orléans, France

Life-strategies in intra-annual dynamics of cambial activity: an example for three conifer species (Norway spruce, Scots pine and silver fir) in northeast France (Communication orale)

H.E. CUNY, C.B.K. RATHGEBER, F. LEBOURGEOIS, M. FORTIN, M. FOURNIER

Eurodendro conference, 19-22 September 2011, Engelberg, Switzerland

Xylem cell differentiation processes related to climatic factors in conifers (Poster)

H.E. CUNY, C.B.K. RATHGEBER, F. LEBOURGEOIS, M. FOURNIER

International symposium on wood structure in plant biology and ecology, 15-20 April 2013, Naples, Italy

Communications nationales

Étude de la dynamique saisonnière de la formation du bois de trois espèces de conifères (Épicéa commun, Pin sylvestre et Sapin pectiné) dans le nord-est de la France

H.E. CUNY, C.B.K. RATHGEBER, M. FOURNIER

Panorama de la dendrochronologie en France, 8-10 octobre 2009, Digne-les-Bains, France

Suivi intra-annuel de la croissance des arbres – Comparaison des dates de mise en place des feuilles, des rameaux et du cerne de bois pour trois espèces de conifères (épicéa commun, pin sylvestre et sapin pectiné)

H.E. CUNY, C.B.K. RATHGEBER

Séminaire de l'école doctorale RP2E –19 janvier 2012, Nancy, France

XI.2 Annexe 2 : détails sur les modèles additifs généralisés

Le développement des modèles additifs généralisés (GAMs) a constitué une innovation statistique important des 30 dernières années. Les modèles additifs généralisés sont une extension semi-paramétrique des modèles linéaires généralisés (GLMs), qui sont eux-mêmes une extension mathématique des modèles linéaires.

Partons du modèle linéaire qui a la forme :

$$Y = \alpha + X\beta + \varepsilon \qquad \text{Eq. (1)}$$

où Y désigne la variable de réponse, α est une constante appelée intercept, X = (X1, … Xp) est une matrice de p variables explicatives, β = (β1, …, βp) est le vecteur de p coefficients de régression (un pour chaque variable explicative) et ε est le terme d'erreur. Deux hypothèses principales limitent l'utilisation de ce modèle linéaire : (1) les erreurs sont supposées suivre une distribution normale (Gaussienne) et avoir une variance constante ; (2) les variables explicatives sont supposées avoir un effet linéaire sur la variable de réponse.

En appliquant une transformation mathématique à la variable de réponse Y selon la distribution réelle des erreurs, les GLMs relâchent ces hypothèses et généralisent le modèle linéaire à des réponses non-linéaires (mais la linéarité des paramètres est préservée) et à des variables qui peuvent avoir une distribution différente de la distribution normale (d'où le nom de modèles additifs généralisés), telles que les distributions binomiale, de Poisson ou gamma (McCullagh & Nelder, 1983; Zuur, 2009). Cette généralisation a considérablement amélioré l'analyse des données en écologie car la plupart des données écologiques n'ont pas une distribution normale et de nombreuses réponses ne sont pas linéaires. La fonction mathématique utilisée pour transformer la variable de réponse est appelée « fonction de lie » car elle procure la relation entre le prédicteur linéaire (Xβ) et la valeur attendue de la variable de réponse Y, si bien qu'un GLM prend la forme :

$$g(E(Y)) = \alpha + X\beta + \varepsilon \qquad \text{Eq. (2)}$$

où g() est la fonction de lien, E(Y) est la valeur attendue de Y et α, X, et β sont les mêmes que décrits en Eq. (1).

La fonction de lien dépend de la distribution de la variable de réponse (et donc de son erreur). Dans le cas du suivi de la formation du bois, la variable de réponse correspond typiquement au nombre de cellules compté chaque semaine dans les différentes zones de différenciation. Les données de comptages suivent une distribution de Poisson et dans ce cas la fonction de lien utilisée est la fonction log (on obtient un modèle log-linéaire). Notez que si la variable de réponse suit une distribution normale avec une variance constante, la fonction de lien est la fonction identité g(E(Y))) = Y, si bien que l'on retrouve le modèle linéaire classique de l'Eq. (1), qui peut en fait être considéré comme un cas particulier des GLMs.

Un GAM est un GLM dans lequel le prédicteur linéaire dépend en partie d'une somme de fonction de lissage de variables explicatives. Comme pour les GLMs, la distribution de probabilité de la variable de réponse doit être spécifiée. Donc, les GAMs sont une

généralisation semi-paramétrique des GLMs et prennent la forme :

$$g\big(E(Y)\big) = \alpha + X\beta + \sum s_j(X_j) + \varepsilon \qquad \text{Eq. (3)}$$

où X = (X1, …, Xp) est une matrice pour les composants strictement paramétriques du modèle à laquelle est associée le vecteur de paramètres β, $s_j()$ dont des fonctions de lissage non spécifiées pour les variables explicatives X_j et g(), E(Y) et α sont les mêmes que décrits en Eq. (1) et (2).

Les GAMs sont dits « pilotés par les données » plutôt que « pilotés par le modèle ». En raison de la partie non paramétrique du prédicteur, ils sont en effet plus flexibles que les modèles paramétriques et peuvent mettre en évidence des structure dans la distribution des données qui seraient autrement éludées (Hastie & Tibshirani, 1986; Yee & Mitchell, 1991).

Dans le cas de la dynamique de la formation du bois, on veut exprimer le nombre de cellules compté chaque semaine dans les phases, en fonction du jour de l'année. L'expression des GAMs utilisés devient simplement :

$$\log\big(E(N)\big) = \alpha + s(d) + \varepsilon \qquad \text{Eq. (4)}$$

où N est le vecteur du nombre de cellules comptées dans la phase considérée et DY est le vecteur des jours de l'année correspondants.

Les GAMs peuvent être ajustés dans le logiciel R (R Core Team, 2012) avec le package mgcv (Wood, 2006).

Références

Hastie T, Tibshirani R. 1986. Generalized additive models. *Statistical Science* **1**(3): 297-318.

McCullagh P, Nelder JA. 1983. *Generalized Linear Models*. First ed. London: Chapman and Hall.

R Core Team 2012. R: A language and environment for statistical computing. R Foundation for Statistical Computing, Vienna, Austria. ISBN 3-900051-07-0, URL http://www.R-project.org/.

Wood SN. 2006. Generalized additive models: an introduction with R. Boca Raton, FL: Chapman and Hall/CRC.

Yee TW, Mitchell ND. 1991. Generalized additive models in plant ecology. *Journal of Vegetation Science* **2**(5): 587-602.

Zuur AF, Ieno EN, Walker NJ, Saveliev AA, Smith GM. 2009. *Mixed effects models and extensions in ecology with R*. New York: Springer-Verlag.

XI.3 Annexe 3 : étude de la phénologie de la formation du bois avec le package CAVIAR pour R

Phenology of wood formation: Data processing, analysis and visualization using R (package CAVIAR)

Cyrille B.K. Rathgeber[a,b], Fleur Longuetaud[a,b], Frédéric Mothe[a,b], Henri Cuny[a,b], Gilles Le Moguédec[a,c]

*Dendrochronologia (2011) **29**(3), 139-149*

[a] INRA, UMR1092, Laboratoire d Etude des Ressources Foret Bois (LERFoB), Centre INRA de Nancy, F-54280 Champenoux, France

[b] AgroParisTech, UMR1092, Laboratoire d Etude des Ressources Foret Bois (LERFoB), ENGREF, 14 rue Girardet, F-54000 Nancy, France

[c] INRA, UMR AMAP, F-3400 Montpellier, France

Abstract
Studies of intra-annual dynamics of cambial activity and wood formation share very similar data because they are based on classic concepts of xylem development and well-documented techniques of sample preparation. However, the way the data are produced is specific to each study or group of authors because there is not a real agreement or consensus about critical variable definitions and data processing. The consequence is that despite very similar data, these studies are difficult to compare. In order to improve this point, we proposed objective definitions of the main phenological events (critical dates) occurring during wood formation, i.e. the beginning and ending of the cell enlarging and maturing phases and the beginning of the cell mature phase. The beginning of a given phase was defined as the date at which 50% of the observed radial files show at least one first cell in this phase, while the end of a given phase was defined as the date at which 50% of the observed radial files show at most one last cell in this phase. Dedicated R package CAVIAR was developed in order to apply these definitions to the computation of critical dates, as well as to their visualisation and analysis. Several statistical tests (Student's t-test, Wilcoxon's rank sum test and bootstrap tests on means and medians) were evaluated for comparing critical dates between two groups. Based on theoretical considerations and on study case analyses, it was shown that the bootstrap test on median is the best-suited statistical test for comparing critical dates when considering the peculiarities of the data at hand. Finally, the application of the presented definitions and methods was illustrated by the study of a real dataset obtained from five silver firs and five Scots pines grown under the same conditions and sampled weekly during the 2006 vegetation period. The results of this application showed that wood formation in pines started earlier, finished later and lasted longer than in firs, as documented by previous studies. We believe that the development of such objective definitions accompanied by ready-to-use tools for data processing, analysis and visualization will reinforce the discipline by contributing efficiently to standardise concepts and methodologies.

Keywords: Tree radial growth monitoring – Xylogenesis – Bootstrap test on median – *Abies alba* – *Pinus silvestris*

Introduction

The study of intra-annual dynamics of cambial activity and wood formation is an innovative and fast-growing field in plant science (see this special issue of *Dendrochronologia* for example). Most of surveys done in this field are based on classic concepts of xylem development and well-documented techniques of sample preparation – even if these techniques were only recently adapted to this field. However, the way the results are obtained is specific to each study or group of authors because there is not, at this time, a real agreement or consensus about critical variables definitions and data processing. The consequence is that despite very similar type of raw data, these surveys are still quite difficult to compare. Monitoring wood formation allows studying the phenology (e.g. beginning, end and duration of the development phases) as well as the dynamics of the process (e.g. rates of cell production and maturation). We chose to base this paper on wood formation phenology

only, because it is the most original contribution of wood formation monitoring studies to botany and ecology until now.

Wilson *et al.* (1966) were already concerned that communication among plant scientists was hampered by the use of "conflicting, even inaccurate, terminology to describe the stage of cell differentiation". So, they proposed "a simple, unified terminology, suited to anatomical and physiological studies of cambial activity" to overcome this problem. The first aim of this paper is to link Wilson *et al.* (1966) unified definitions with sound anatomical observations of cell development, in order to translate them into efficient algorithms that compute unambiguous critical dates of the main phenological events occurring during wood formation. The second aim of this paper is to provide to the community an R add-on package dedicated to critical dates computation, visualisation and analysis. R is a very powerful general-purpose public-domain statistical language that provides excellent graphics and data analysis capabilities and that can be easily expanded by writing functions and packages (R Development Core Team, 2007). Finally, the third aim of this paper is to select the best-suited statistical test of significance for comparing critical dates, taking into account the peculiarities of data at hand. Bootstrap test on means and medians as well as classical Student's *t*-test and Wilcoxon's rank sum test were considered.

The application of the presented definitions and methods through the use of the developed R add-on package is illustrated in the paper by the analysis of a real dataset obtained from five silver firs and five Scots pines grown under the same conditions, near Nancy (Northeast France), and sampled weekly during the 2006 vegetation period. This dataset was chosen because it is very representative of datasets provided by intra-annual wood formation monitoring studies on conifers all over the world.

Materials and methods

Terminology

According to Wilson *et al.* (1966), the differentiation of tracheids in the xylem can be divided into four relatively distinct phases. (1) Just after being formed by the cambial initials, xylem mother cells may retain the ability to divide for a certain time, contributing to xylem cell production; they are in the dividing phase (D). Wilson *et al.* (1966) saved the term "cambium" only for the layer of cambial initials and used the term "cambial zone" to regroup all the cells that are able to divide – initial cells plus phloem and xylem mother cells. (2) After dividing, cells usually undergo marked radial diameter increase; they are in the enlarging phase (E). (3) After radial enlargement, cell differentiation continues with the formation of the secondary cell walls; cells are in the maturing phase (L). (4) Cell maturing ends with programmed cell death, i.e. autolysis of the cytoplasm (Plomion et al., 2001); cells are then permanently in the mature phase (M). We would like to acknowledge the fact that this conceptual model is convenient for studying intra-annual dynamics of wood formation, but it may be inaccurate sometimes, for example the different phases might overlap to some extent (Wilson *et al.*, 1966).

All the derivatives produced by a cambial initial constitute a radial file. So, the temporal succession of the differentiation phases undergone by each cell forms a spatial succession of differentiation zones when considering the whole radial file or tree-ring in formation (Fig. 1). Observational criteria for classifying forming xylem cells in the four differentiation phases were reviewed by Rossi *et al.* (2006b). In cross section, cells in the cambial zone are characterized by thin cell walls and small radial diameters (Skene, 1969; Timel, 1980; Antonova and Stasova, 1997). Cells in the radial enlarging zone are larger than those in the cambial zone and present thin, primary cell walls that are not birefringent under polarized light (Kutscha *et al.*, 1975). By opposition, the developing secondary walls of cells in the maturing zone exhibit birefringence under polarized light and are violet and blue under white light after coloration by cresyl fast violet (Antonova and Shebeko, 1981; Abe *et al.*, 1997). Tracheids were considered mature when their cell walls are plain, completely blue for example with cresyl fast violet coloration (Gričar *et al.*, 2005; Rossi *et al.*, 2006b).

Definitions of critical dates

In temperate and cold climate forest, cambium becomes active in spring and the production of new daughter cells by the cambial initial and the xylem and phloem mother cells starts (Wilson, 1970); this is the beginning of cambial activity, tree radial growth and wood formation (xylogenesis). The newly formed cells undergo the successive differentiation phases (E and L) to become fully mature and functional xylem cells – i.e. tracheids for more than 90% of them (Brown *et al.*, 1949; Panshin and de Zeeuw, 1980; Fengel and Wegener, 1989). These processes continue through the whole growing season. At the end of the summer or during autumn, the cambium becomes dormant and cell production stops; this is the end of cambial activity. Then, the last produced cells finish their differentiation. When the last cell goes out the enlarging phase, entering the maturing phase, this is the end of tree radial growth; and when it becomes mature, this is the end of xylogenesis.

We defined a set of critical dates that describe cambium and wood formation phenology at the "tree level": (1) the beginning of the dividing phase (t_iD) is defined as the date at which more than 50% of the observed radial files present at least one additional cell compared to the minimum number of dormant cells; (2) the beginning of the enlarging phase (t_iE) is defined as the date at which more than 50% of the observed radial files present at least one first enlarging cell; (3) the beginning of the maturing phase (t_iL) is defined as the date at which more than 50% of the observed radial files present at least one first thickening cell; (4) the beginning of the mature phase (t_iM) is defined as the date at which more than 50% of the observed radial files present at least one first mature cell; (5) the end of the dividing phase (t_fD) is defined as the date at which less than 50% of the observed radial files present at most one last additional cell compared to the minimum number of dormant cells; (6) the end of the enlarging phase (t_fE) is defined as the date at which less than 50% of the observed radial files present at most one last enlarging cell; and (7) the end of the maturing phase (tfL) is defined as the date at which less than 50% of the observed radial files present at most one last lignifying cell.

These critical dates allowed computing critical durations that describe cambium and wood formation phenology: (1) the duration of the dividing phase: $\Delta tD = t_fD - t_iD$; (2) the duration of the enlarging phase: $\Delta tE = t_fE - t_iE$; and (3) the duration of the maturing phase: $\Delta tL = t_fL - t_iL$. Following the previous definitions and terminology, ΔtD represents also cambial activity duration, while (4) the duration of tree radial growth is: $\Delta tG = tfE - tiD$; and (5) the total duration of xylogenesis is: $\Delta tX = t_fL - t_iD$ (see Appendix A for a list of used variables).

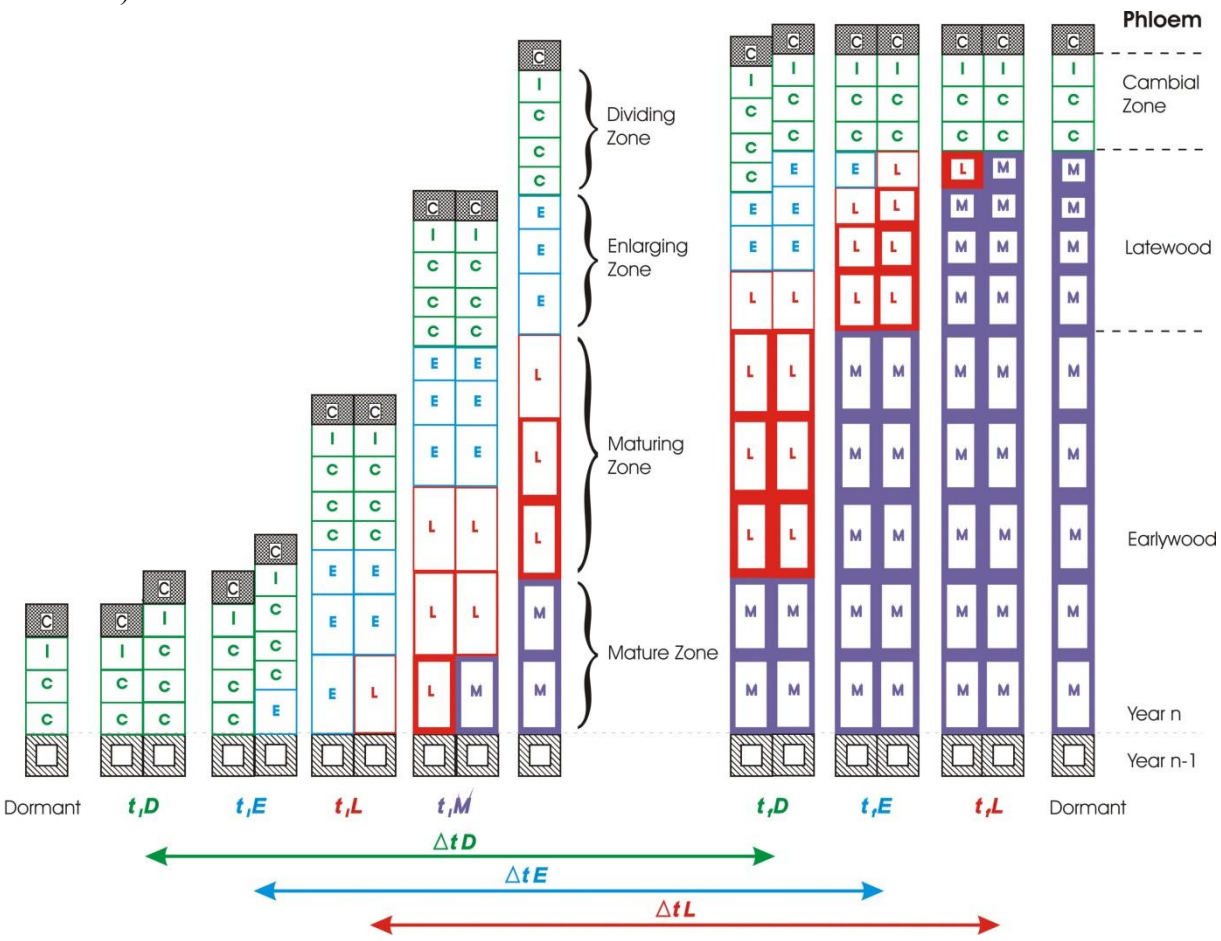

Fig. 1. Illustration of xylem cell development. This drawing illustrates the definitions of critical dates and durations presented in the paper, using two schematic xylem radial files that are developing throughout the growing season. t_iD, t_iE, t_iL and t_iM stands for the beginning of dividing, enlarging, maturing and mature phases respectively; while t_fD, t_fE and t_fL stands for the end of dividing, enlarging, maturing and mature phases respectively; and ΔtD, ΔtE and ΔtL stands for the durations of dividing, enlarging and maturing phases respectively. Cambial cells are noted as C, enlarging cells: E, maturing cells: L and mature cells: M.

It is very important that critical dates and durations are defined and computed at the tree level, and not directly at the level of a group of trees (the stand for example, as it is done most of the time), in order to allow sound statistical analyses and inter-studies comparison.

Computation of critical dates

From the raw data table, critical dates were computed automatically by a dedicated R add-on function of the CAVIAR package. R is a very powerful general-purpose statistical language (R Development Core Team, 2007) that provides excellent graphics and data

analysis tools (Crawley, 2005, 2007; Murrell, 2006). It is public-domain software that is very similar to Splus®. Both programs are popular with statisticians because they can be easily expanded by writing functions and packages of functions. Observations at "the radial file level" (for example, three radial files by tree are counted for each date during the growing season) were used by the *computeCriticalDates* function, to compute critical dates at "the tree level". First, the function "binarised" radial file data by coding 0 when there was no cell in one given phase (phase is not active) and 1 when at least one cell was present (phase is active). Then the function split data for each phase in two dataset, one for detecting the beginning and one for detecting the end. Logistic regressions – the *glm*(*formula, family = binomial*) function in R – were used to compute critical dates (Venables and Ripley, 2002; Crawley, 2005, 2007; R Development Core Team, 2007). The logistic regression takes the general form:

$$\text{Logit}(\pi_d) = \ln\left(\frac{\pi_d}{1-\pi_d}\right) = \beta_0 + \beta_1 d \qquad (1)$$

where π_d is the probability of one phase being active on a given day d of the year. β_0 and β_1 are the intercept and slope of the regression. Critical dates were calculated when the probability of a given phase being active was 50%, i.e. when $\text{Logit}(\pi) = 0$ and $d_{50} = \beta_0/\beta_1$. Therefore, for a date above d_{50}, a given phase was more likely to be active than non-active. Additionally we computed a standard deviation for each critical date by taking the 2.5 and 97.5% probabilities as limits of the 95% confidence interval (see example Fig. 2). Optionally, the function can draw a plot illustrating the computation of each critical date for quick visual verification. From these critical dates, the function finally computed the critical durations defined above (see *computeCriticalDates* help file in the CAVIAR package for a practical description of this function).

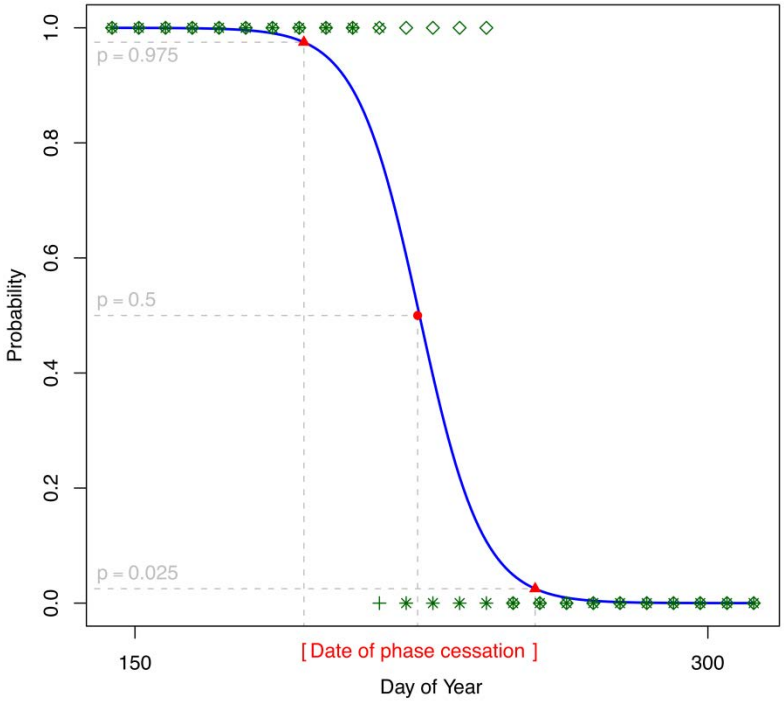

Fig. 2. Computation of critical dates by logistic regression. This figure illustrates the computation of the enlarging phase cessation in Tree 3. The point shows the mean critical date while the triangles indicate the 95% confidence interval.

Visualization of critical dates

Critical dates were first plotted for each individual tree in order to allow a visual check of date consistencies using a dedicated R add-on function – *plotWoodFormationCalendar*. This first checking showed that critical dates associated to the dividing phase were not consistent (see Appendix C). Consistent dates were then used to draw a wood formation calendar using another option of the same function. Xylem development phase onsets (t_iE, t_iL and t_iM) and cessations (t_fE and t_fL) were represented by diamond-crossed-by- a-line marks (Fig. 4a and c). These marks are well adapted for representing groups of five values, which is the most common case in wood formation studies. The left end of the line represents the minimum, the left end of the diamond the first quartile, the middle of the diamond the median, the right end of the diamond the third quartile and the right end of the line the maximum. In fact, most of the time some of the values are tied so the shape of the mark is also very informative: if the mark looks like a cross, for example, it means that three trees start (stop) at the same time, while the two others start (stop) earlier and later; if the mark looks like a play button, for example, it means that all the trees start at the same time but one is late. In addition to critical dates, durations of the phases were also drawn (Fig. 4b and d). A horizontal bar, above which a horizontal line stretches from the minimum to the maximum, represents the median duration; two little vertical lines indicate the first and third quartiles.

The described representations are specially designed for five trees datasets. They also work when more trees are available, but then the graph represents a summary of the dataset and not all the data individually (see *plotWoodFormationCalendar* help file in the CAVIAR package for a practical description of this function).

Comparison of critical dates

Choice of the statistical method

Plotting critical dates already give a visual insight of the differences between two groups of trees. However, what we really want to know is if the observed differences between these two groups are large enough to allow drawing sound conclusions about differences between the two populations they represent. Several statistical tests of significance can be used to compare the central tendencies of two samples. It is important to consider the main characteristics of the dataset at hand in order to select the most appropriated statistical method. Critical date datasets coming from cambial activity and wood formation monitoring studies are characterized by: (1) a very small number of observations per dates; (2) probably non-normally distributed; (3) with regular occurrence of tied values; and (4) with possible presence of extreme values and outliers.

The most common test for comparing two sample means is the parametric Student's t-test. However, this test should only be used when: (1) samples are independent; (2) variances are equal; and (3) samples are normally distributed. The parametric Welch's t-test is an adaptation of Student's t-test intended for use with two samples having possibly unequal variances. The non-parametric Wilcoxon's ranksumtest – extended by Mannand Whitney for non-equal sample sizes, and by Kruskall and Wallis for three samples or more – is designed to

test whether one population has greater observations than the other overall and can be used as an alternative to Student's t-test when variances are not equal and/or samples are not normally distributed. Wilcoxon's family tests are the most appropriated classical tests for data coming from wood formation monitoring studies (Rossi *et al.*, 2009a,b,c). However, it is not recommended to use Wilcoxon's test with tied values because in their presence, tables for critical values are only approximately correct. All these considerations lead us to prefer permutation tests, which are particularly adapted for analyzing the type of datasets we are dealing with (Good, 2004).

We also preferred the median as an estimator of the central tendency rather than the arithmetic mean because the median is not sensitive to extreme values and outliers. Another advantage of permutation tests is that they work as well with mean as with median – and associated measures of dispersion.

Null and alternative hypotheses

The role of a statistical test of significance is to decide whether a null hypothesis (H_0) postulated for the reference population can be rejected or not, based on the available data coming from a representative sample of this population. The null hypothesis is accompanied by the formulation of an alternative hypothesis (H_1) that is the opposite of H_0.
In this study for example, we want to test if there is a difference between the medians of the beginning of enlargement phase of fir and pine populations – $H_0 : t_1\widetilde{E}_f = t_1\widetilde{E}_p$. The common alternative "two-tailed" hypothesis would assume a true difference between population medians – $H_1 : t_1\widetilde{E}_f \neq t_1\widetilde{E}_p$. However, we were more interested in a "one-tailed" alternative hypothesis assuming that fir median is greater than pine one because we think, based on the literature (Rossi *et al.*, 2007, 2008), that pines start earlier than firs – $H_1 : t_1\widetilde{E}_f > t_1\widetilde{E}_p$.

Test statistics

In order to test if two populations present the same central tendency, one would choose a test statistic measuring the difference between the two sample means, or preferably medians in our case:

$D = \bar{x}_f - \bar{x}_p$ (1), or preferably $D = \tilde{x}_f - \tilde{x}_p$, (2)

where $x_f = \{x_{f1}, x_{f2}, \dots, x_{fn_f}\}$, and $x_p = \{x_{p1}, x_{p2}, \dots, x_{pn_p}\}$.

The simple difference between the means works well, assuming that the two population distributions are the same, apart from a possible difference in their means (Manly, 2007). However, it is possible to construct a test without making this assumption (Efron and Tibshirani, 1993) by using a test statistic inspired from Student's t-test and by modifying the bootstrap sampling method (see below). A suitable test statistic for this situation is:

$$t = \frac{\bar{x}_f - \bar{x}_p}{\sqrt{s_f^2/n_f + s_p^2/n_p}}, \quad (3)$$

where $s_j^2 = \sum(x_{ij} - \bar{x}_j)^2/(n_j - 1)$ is the usual unbiased estimator of variance for sample j.

Construction of the reference distribution

In permutation testing, instead of comparing the observed value of a test statistic to a standard statistical distribution, the reference distribution is generated from the data themselves. For constructing the reference distribution for the test statistic, the null hypothesis is assumed to be true, i.e. there is no difference between the two populations. Therefore, the two groups of trees are mixed together to form a combined sample ($x = x_f \cup x_p$).

Here, the reference distribution is produced by using the bootstrap method (Efron and Tibshirani, 1993). From the combined sample, nf trees out of n are drawn at random, with replacement, in order to form the first group (x_f^*); the second group (x_p^*) is formed in the same way. This procedure is sufficient when testing the medians equality; however, when testing means equality, we may need to compute a bootstrap distribution for which the null hypothesis is more strictly made to be true (Efron and Tibshirani, 1993). A simple way to do that consists in centering the values of the two groups around the mean of the combined sample:

$$x'_{ij} = x_{ij} - \bar{x}_j + \bar{x}, \quad (4)$$

where x_{ij} is the *i*th value of the sample *j*, $\bar{x}_j$ is the mean of the sample j, and $\bar{x}$ is the mean of the combined sample.

The desired test statistic is computed between the two bootstrap groups. The operation is repeated a great number of times in order to construct a reference distribution for the test statistic. The justification of this procedure is that re-sampling the original sample approximates a re-sampling of the original population (Efron and Tibshirani, 1993).

Statistical decision and significance level

In bootstrap tests, the decision is made by comparing the observed value of the test statistic to the reference distribution obtained by bootstrap under the null hypothesis. If the observed value of the test statistic is typical of the values obtained under H_0, which states that there is no difference between the two populations, H_0 cannot be rejected; if the observed value is too extreme to be considered as a likely result under H_0, H_0 is rejected and the alternative hypothesis H_1 is accepted.

For one-tailed tests, the achieved significance level (ASL) is the proportion of values in the reference distribution, which are as extreme as, or more extreme than, the observed test statistic. ASL can be interpreted in the same way as the p-value (P) given by conventional tests of significance. As stated by Efron and Tibshirani (1993): “The smaller the value of ASL, the stronger the evidence against H0”.

Number of possible combinations and number of iterations

The number of possible combinations when drawing p elements out of n with replacement is:

$$C_{n-1}^{n+p-1} = \frac{(n+p-1)!}{p!(n-1)!}. \quad (5)$$

In our case (two groups of five trees) it made $C_9^{14} \times C_9^{14} = 4 \times 10^6$ possible combinations, because the drawing of the first group leave the composition of the second group completely undetermined as replacement is allowed. With only two groups of three trees, it will already reach more than 3×10^3 possible combinations, which would be sufficient to draw a statistic distribution.

The precision of the probability estimate is the inverse of the number of combinations performed; for instance, after 1×10^3 combinations, the precision of the probability statement is 0.001 (Legendre and Legendre, 1998). However, it is important to note that because of the random sampling of the possible combinations in the bootstrap method, 1×10^3 iterations does not mean 1×10^3 distinct combinations, as some of them can be redundant. So, the precision of the probability estimate is always weaker than the limit given by the inverse of the number of possible combinations.

The number of iterations that should be performed is always a trade-off between precision and computing time. Legendre and Legendre (1998) suggest that 500–1000 iterations may be sufficient as a first contact with the problem. Then they recommend running more iterations if the computed probability is close to the preselected significance level. And finally, they exhort using even more iterations (e.g. 1×10^4) for final published results.

A dedicated R add-on function was developed in order to compute automatically two-samples bootstrap tests using the different test statistics and data adjustments presented in this paper (see Appendix D for a practical description of this function). Moreover, this function is able to take into account the standard deviation associated with each singular critical date, in order to provide the better estimate of P. This function was first used for comparing the performance of the bootstrap tests with the classical tests in three study cases based on virtual data. Then, it was applied on real data for comparing wood formation calendars obtained for firs and pines.

Presentation of the biological material

The “real” data used in this study were collected from five dominant silver firs (Abies alba Mill.) and five dominant Scots pines (Pinus sylvestris L.) grown in two stands only separated by a ditch and located in the Amance forest near Nancy (48.74°N, 6.32°E, 270m a.s.l., Lorraine, France). These two stands were approximately 40 years old. Sampled trees presented, for firs and pines respectively, a mean height of 23.1 and 21.9 m and a mean diameter at breast height of 36 and 26.4 cm.

In 2006, from the 23 March to the 6 December, wood samples (i.e. microcores of 2mmin diameter and 15–20mmin length) were collected weekly at breast height on the stem of the selected trees using a Trephor® tool (Rossi *et al.*, 2006a) and following an ascending spiral pattern (Deslauriers *et al.*, 2003). Microcores were taken at about 2 cmapart to avoid wounding tissues and resin ducts without increasing toomuchstem circumferential variability (Wodzicki and Zajaczkowski, 1970). Microcores were placed in a solution of ethanol 50%

and stored at 5 °C before being dehydrated by successive immersions in baths of ethanol and d-limonene and embedded in paraffin according to Rossi *et al.* (2006a). Transverse sections, 6–10 µm thick, were cut with a rotary microtome, stained with cresyl violet acetate and mounted on slides.

Sections were observed under white and polarized light at 125–400 magnifications in order to distinguish the cells in the cambial zone and in the differentiating xylem. The number of cells in the cambial zone (nC), enlarging zone (nE), maturing zone (nL), and mature zone (nM) were counted along three radial files according to criteria described above (Rossi *et al.*, 2006b). Finally, 3760 observations (counting) were made and saved, in database-like format, in a raw data table (see Appendix B for an illustration of used data tables). These data are provided with the CAVIAR package as a learning example (see AMA2006 help file in CAVIAR package for a complete description of the dataset).

The obtained dataset is very representative of intra-annual cambial activity and wood formation monitoring studies datasets: one or more groups of approximately five trees, collected from one or more species and for one or more years, in a particular location or along an environmental gradient.

Virtual data

We constructed three "virtual" datasets from our "real" dataset in order to compare the behaviour of the bootstrap tests (on means and medians) and the classical tests (Student's or Welch's t-test and Wilcoxon's rank sum test) for three contrasted study cases: (1) means and medians are different but variances are equal; (2) means and medians are equal but variances are different; (3) means, medians and variances are different.

The three virtual datasets were derived from the original dataset concerning the beginning of the enlargement phase for firs – $w = \{113, 113, 120, 126, 127\}$. For the first one, 30 artificial series were constructed with $x_i = w - i$, with i ranging from 1 to 30. So w and x variances are equals (45.7) but their means (119.8 and 109.8 for w and x_{10}, respectively) and medians (120 and 110 for w and x_{10}, respectively) are different. The second artificial dataset was constructed using the following formula $y = w + w \otimes \{-0.05, -0.025, 0, 0.025, 0.05\}$. So w and y means and medians (120) are equals but variances are different (45.7 and 129.62, respectively). The third artificial dataset was constructed with z = y – 10. So w and z means (119.8 and 110 respectively) and medians (120 and 110 respectively) as well as w and z variances (45.7 and 129.62, respectively) are different. The observed mean difference is 9.8 while the observed median difference is 10.

Results

Study cases with virtual data

Study case 1: means and medians are different but variances are equal

As expected, the results of the bootstrap t-test were close to those of Student's t-test, while the results of the bootstrap test on median differences were close to those of the Wilcoxon rank sum test (Fig. 3). The tests based on mean (Student's and bootstrap t-test) yield lower P than the tests based on rank or median (Wilcoxon's rank sum test and bootstrap test on median). All the tests were able to detect a mean difference of 7 days between the two groups (at the 0.10 significance level), which is quite coherent with the usual sampling time step of one week.

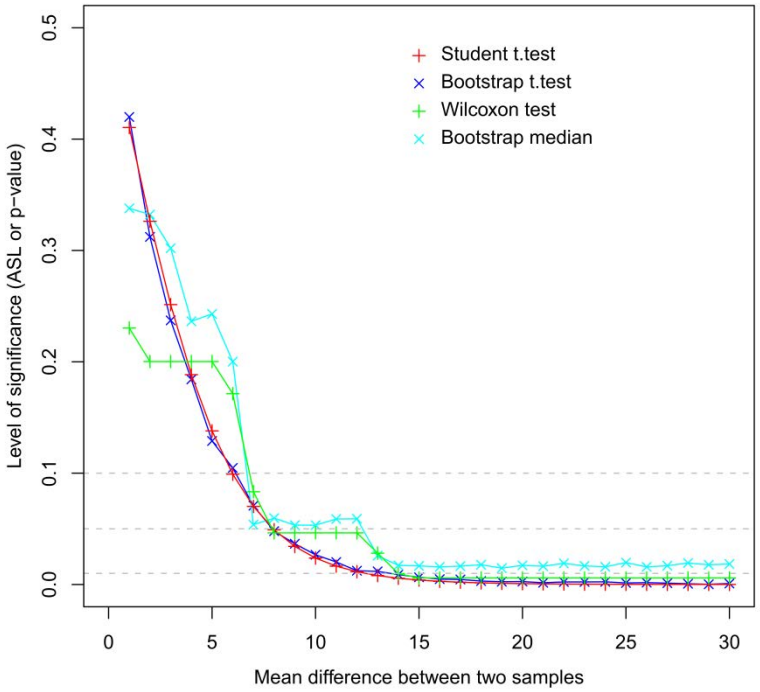

Fig. 3. Comparison between the level of significance of different statistical tests. The tests were done using the virtual datasets w and x presented in the paper ($n_f = n_p = 5$; 10 000 iterations for bootstrap tests).

Study case 2: means and medians are equal but variances are different

Testing the equality of the means of w and y using a onetailed Welch's t-test generated a P of 0.4867, which can be compared to the P of 0.4842 provided by the bootstrap t-test (after 1×10^4 iterations). Testing the equality of the medians using the bootstrap test gave a P of 0.3859 (after 1×10^4 iterations), while using a Wilcoxon rank sum test generated a P of 0.5418.

Study case 3: means, medians and variances are different

Testing the equality of the means of the two populations represented by these two samples using a one-tailed Welch's t-test generated a P of 0.07265, which can be compared to the P of 0.06579 provided by the bootstrap t-test (after 1×10^4 iterations). Testing the equality of the medians using the bootstrap test on median generated and P of 0.1184 (after 1×10^4

iterations), which can be compared to the P of 0.07123 provided by the Wilcoxon rank sum test.

Application on real data

The methods described in the previous sections were then used in order to analyse the real dataset presented in the materials. Xylem cell enlargement started at mid-April for pines, ($t_iE_p = 102 \pm 2$ days – in this paragraph the median is given ± 1 median absolute deviation, $n_p = n_f = 5$) and at the very beginning of May for firs ($t_iE_f = 120 \pm 7$ days) (Fig. 4a,c). Pines started 18 days earlier than firs (the bootstrap test on medians is very significant, $P = 4.47 \times 10^{-2}$, 1×10^4 iterations, Fig. 5a). Secondary cell-wall formation started at the very end of April for pines ($t_iL_p = 120 \pm 4$ days) and at the middle of May for firs ($t_iL_f = 133 \pm 4$ days). Pines started 13 days earlier than firs (the bootstrap test on medians is very significant, $P = 3.2 \times 10^{-2}$, 1×10^4 iterations, Fig. 5b). The first mature cells appeared during the first days of June for pines ($t_iM_p = 155 \pm 4$ days) as well as for firs ($t_iM_f = 155 \pm 6$ days). At this point, firs had completely made up for their initial delay (the bootstrap test on medians is not significant, $P = 4.985 \times 10^{-1}$, 1×10^4 iterations, Fig. 5c). The end of xylem cell enlargement occurred at the middle of September for pines ($t_fE_p = 256 \pm 2$ days) and firs ($t_fE_f = 266 \pm 2$ days). Considering the median, pines stopped only 10 days before firs but this difference is significant (bootstrap test on medians is very significant, $P = 4.64 \times 10^{-2}$, 1×10^4 iterations, Fig. 5d). The end of secondary cell-wall lignification occurred at the end of October for firs ($t_fL_f = 294 \pm 1$ days) and pines ($t_fL_p = 301 \pm 6$ days). So, pines finished only 7 days later than firs but this difference is statistically significant (bootstrap test on medians is significant, $P = 8.829 \times 10^{-2}$, 1×10^4 iterations, Fig. 5e). It is interesting to note that the variability around the medians of the critical dates was very low for firs as well as for pines and remained always under one week, which is the sampling time-step.

The period of xylem cells enlarging lasted more than five months for firs ($\Delta_tE_f = 150 \pm 3$ days) and pines ($\Delta_tE_p = 157 \pm 1$ days) – the bootstrap test on medians was not significant, $P = 1.331 \times 10^{-1}$, 1×10^4 iterations (Fig. 4b,d, 5f). The period of xylem cell maturing lasted around five months and a half for firs ($\Delta_tL_f = 160 \pm 4$ days) and around six months for pines ($\Delta_tL_p = 181 \pm 9$ days); pine cell maturing duration was significantly longer than fir one – the bootstrap test on medians was very significant, $P = 2.34 \times 10^{-2}$, 1×10^4 iterations (Fig. 5g). The total wood formation duration, i.e. the time elapsed between the appearance of the first xylem cell and the death of the last one, was about 6 months for firs ($\Delta_tX_f = 175 \pm 4$ days) and about 6 months and 3 weeks for pines ($\Delta_tX_p = 199 \pm 6$ days). So, the earlier start of pine resulted in a longer period of wood formation of about 3 weeks compared to fir – the bootstrap test on medians is very significant, $P = 2.45 \times 10^{-2}$, 10 000 iterations (Fig. 5h). The variability around the medians of the durations was low (about one week) and comparable for firs and pines.

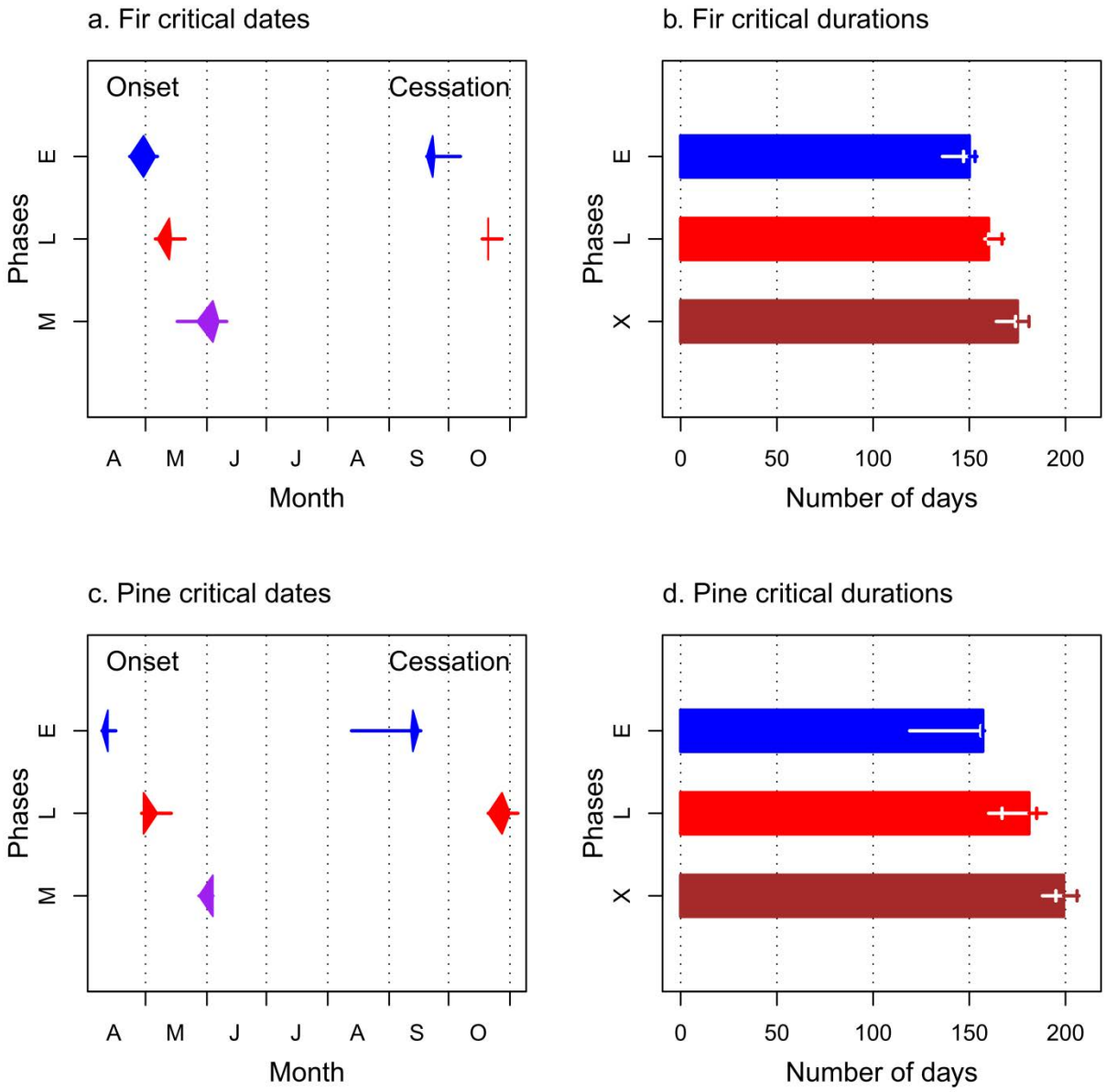

Fig. 4. Firs and pines wood formation calendars. Diamonds shapes represent the critical dates for the 5 trees of a group, while bars and lines represent the durations. E, L and M stand for enlarging, maturing and mature phases respectively, while X stands for xylem formation.

Discussion

Which dates to use for describing wood formation phenology?

We associated to the four conceptual phases of xylem cell differentiation (dividing, enlarging, maturing and mature), the seven critical dates (t_iD, t_iE, t_iL, t_iM, t_fD, t_fE, and t_fL), which mark the beginning and end of each phase (except for mature phase that as no end). These critical dates were used to compute the durations of the three development phases (ΔtD,ΔtE, andΔtL) plus two additional durations of interest (ΔtG, ΔtX).

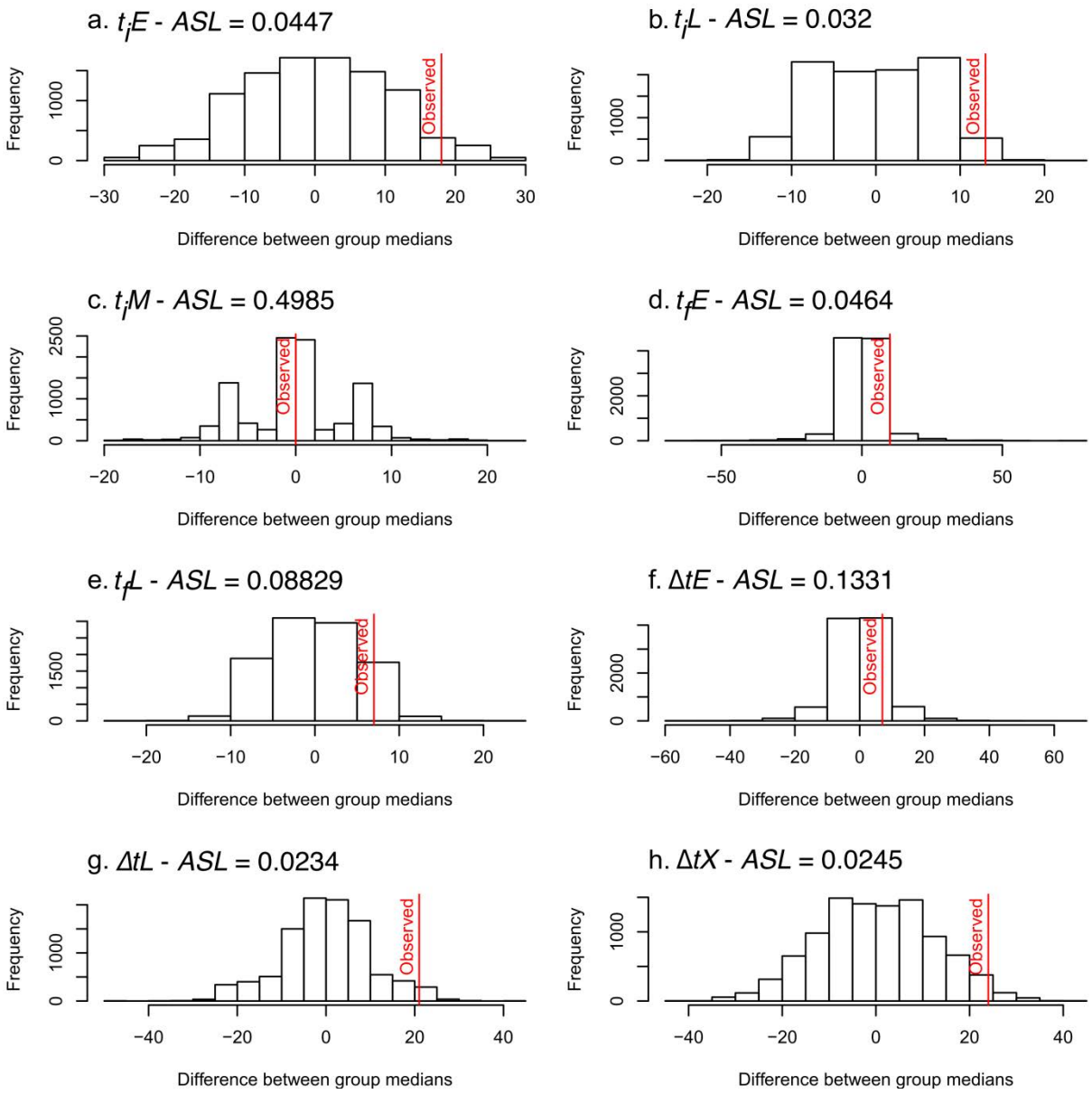

Fig. 5. Comparison between fir and pine critical dates and durations. One tailed two-sample bootstrap tests of significance on medians ($n_f = n_p = 5$; 10 000 iterations)

The beginning of the dividing phase was defined as the date at whichmorethan50%of the observed radial files present at least one additional cell compared to the minimum number of dormant cambial cells (nDC), and the end as the date at which less than 50% of the observed radial files present at maximum one additional cell compared to nDC. This definition and its application posed three main problems that prevented us to compute critical dates for the dividing phase (see Appendix C for an illustration). The first problem is that cambial cells are the less well preserved in the anatomical sections; so counting them is quite tedious and produces nearly all the missing data of the dataset. The second problem is that it is nearly impossible to define nDC without knowing t_iD. This is particularly true because there is usually only very few samples available before the start of the growing season. It is easier to compute nDC at the end of the growing season – it is what we did in our algorithm. However, even for the same tree, nDC may vary between the beginning and the end of the

growing season adding somemore noise in the calculations. The third problem is the relatively high variability of nDC between samples, making practically impossible the detection of the apparition of an additional cell. Given this broad range of problems, we decided not using the number of cells in the cambium to describe cambial activity and we advise colleagues to do the same. We think that workable definitions of the beginning and the end of the dividing phase should be based on other observations than just the number of cells.

The beginning of enlarging, maturing and mature phases (t_iE, t_iL, and t_iM), was defined as the date at which 50% of the observed radial files show at least one first cell in the given phase, while the end of enlarging and maturing phases was defined as the date at which 50% of the observed radial files show at most one last cell in the given phase (t_fE, t_fL). These sound definitions were easily translated in an efficient algorithm that enabled to compute them as well as the related durations. This algorithm, based on logistic regressions, presents the great advantage of computing for each critical date its standard deviation. It also produces plots that make computation checking very easy (see Fig. 2 for an example). Critical dates obtained using these definitions and algorithms proved to be very consistent (see Appendix C for an illustration). So, they were used in this paper to describe wood formation phenology and we recommend their utilisation to our colleagues.

The fact that t_iD and t_fD were not consistent while t_iE, t_iL, t_iM, t_fE and t_fL proved to be very reliable speaks in favour of modifying computations in which t_iD and t_fD were involved. So, we suggest using t_iE, t_fE and ΔtE as proxies for beginning, end and duration of cambial activity and tree-radial growth. We also suggest using t_iE, t_fL and ΔtX as proxies for beginning, end and duration of treering and wood formation. Indeed, several studies shows that the beginning and the end of the dividing phase are very close (less than one week) to the beginning and the end of the enlargement phase (Gričar *et al.*, 2009).

Which statistical test to use for comparing critical dates?

The first study case showed that the tests on mean were more sensitive than the tests on median, while parametric and bootstrap tests gave very similar results. This first study case is a confirmation that, even if Student's t-test and Wilcoxon's rank sum test should be theoretically avoided – because of the problem of variance and normality for the first one, and because of the presence of tied values in the dataset for the second one – practically they yield sound results. The second study case showed that, reassuringly, none of the studied tests are mislead by variance differences when comparing equal means or medians. The third study case showed that when sample variances are not equal, only the bootstrap test on median is mislead, the others still being able to detect a difference in central tendency of the reference populations. This third study case is quite problematic because the results could be the perfect opposite if there was any "outlier" in the dataset (data not shown). So we suggest using the bootstrap test on median in routine because, even if it is less sensitive, it is the safer choice. If there is no outlier in the data (i.e. if means and medians are close together), then the bootstrap t-test is a more accurate alternative.

Wood formation phenology of firs and pines in a temperate forest

This study shows that cambial activity of pines and firs, in a temperate forest in northeast France during 2006, started between the middle of April and the beginning of May and stopped in September. Wood formation finished at the end of October for firs as well as for pines. This means that the period of cambial activity lasted around five months (146 and 162 days for firs and pines respectively), while the total wood formation duration exceeded six months (182 and 203 days for firs and pines respectively). These results contrast greatly with most of those found in the literature and which come from cold forests in mountain or boreal regions (Antonova and Stasova, 1997; Deslauriers *et al.*, 2003; Mäkinen *et al.*, 2003; Schmitt *et al.*, 2004; Rossi *et al.*, 2007; Seo *et al.*, 2008). A global analysis on conifers from cold forests (Rossi *et al.*, 2008) shows that cambial activity starts between the beginning of May and the middle of June, and stops between the middle of July and the end of August resulting in a period of cambial activity lasting less than 100 days. The end of wood formation occurs between the middle of August and the beginning of October, resulting in a period of wood formation lasting less than 150 days. Wodzicki (1971) however, finds, for Scots pine in a temperate forest of Poland, that cambial activity starts mid-April and stops mid-September and that wood formation stops in the very beginning of November. This shows that the intra-annual dynamics of cambial activity and wood formation is quite different for temperate forests than for cold boreal and mountain forests, exhibiting the need for more data from temperate forests.

In 2006, in our study site, cambial activity and wood formation started significantly earlier for pines than for firs, stopped significantly later (except for cambial activity) and lasted significantly longer. These results are in agreement with those from the literature showing that pine species start earlier, stop later and so grow longer than the other conifer species present in the same locations (Rossi *et al.*, 2007, 2009a).

Conclusion

This paper proposed objective definitions of the main phenological events of cambial activity and wood formation (beginning and ending of enlarging phase, beginning and ending of maturing phase and beginning of mature phase) based on sound anatomical observations (the presence/absence of cells in a given state) and translated them into efficient, ready to use, algorithms (used to compute the date at which there is a 50% probability that this phase has started or stopped). The duration of the enlarging phase (i.e. the duration of cambial activity), the duration of the maturing phase and the total duration of wood formation (i.e. the total duration of xylogenesis) are also defined on the same principles. CAVIAR, a dedicated R add-on package, implements these definitions in order to compute critical dates and durations from the observed anatomical raw data using logistic regressions, assorting each date with its standard deviation.

Critical dates and durations are then plotted in an original way using a CAVIAR function in order to draw a wood formation calendar for a group of trees. Calendars can be compared between tree groups representing different species, locations or years for visual insight of the phenological patterns at play.

In order to compare these phenological calendars in a more quantifiable way, we evaluated different statistical tests of significance: Student's t-test, the Wilcoxon rank sum test and the bootstrap tests on mean and median. Based on theoretical considerations and on the analysis of virtual-data study cases, it has been shown that the bootstrap test on median is the most appropriated for comparing wood formation critical dates. This test is implemented in a CAVIAR function, which allows taking into account individual critical date confidence intervals for more accurate comparison between two groups of trees.

A rigorous comparison between the critical dates and durations of the two studied conifers species (silver fir and Scots pine), growing in the same location was then conducted for illustrating the use of the proposed methods. From this application, we have concluded that cambial activity and wood formation starts significantly earlier in pines than in firs, stops later and lasts longer. These conclusions are in agreement with those of previous comparable studies on wood formation phenology when pines are compared to other conifer species.

We believe that the development of such objective definitions and data processing, visualisation and analysis tools will reinforce the discipline by contributing efficiently to the homogenisation of methodologies. CAVIAR development will continue in order to provide solutions for data standardization and growth curve fitting and plotting, which are also key-steps in wood formation studies.

Availability of the CAVIAR package

The CAVIAR package is available as an add-on package in R. Interested users can download and install R from the Comprehensive R Archive Network website: http://cran.r-project.org/.Within R, CAVIAR can be installed, loaded, and the help pages (with embedded examples) can be seen using the following commands:

> install.packages("CAVIAR") # Download CAVIAR package from the CRAN repository site and install it on the computer
> library(CAVIAR) # Load CAVIAR package for use in the current R session
> ?CAVIAR # Call CAVIAR help file for a description of the package and its functionalities

The package is also available for download and installation via the terminal (R CMD INSTALL CAIAR) on the first author's website: http://www.nancy.inra.fr/foret_bois_lerfob/personnels_de_l_umr/scientifiques/rathgeber_cyrille.

Acknowledgements

The French National Institute for Agricultural Research (INRA) and the regional council of Lorraine founded this work. The authors wish to thanks Sergio Rossi and Annie Deslauriers, who helped the author to start this work. The authors wish also to thanks Emmanuel Cornu, Etienne Farré, Maryline Harroué, Pauline Karcher, Alain Mercanti and Pierre Gelhaye (who drew Fig. 1) for technical support during field and laboratory work.

References

Abe, H., Funada, R., Ohtani, J., Fukazawa, K., 1997. Changes in the arrangement of cellulose microfibrils associated with the cessation of cell expansion in tracheids. *Trees* **11**, 328–332.

Antonova, G.F., Shebeko, V.V., 1981. Applying cresyl violet in studying wood formation. *Khimiya Drevesiny* **4**, 102–105.

Antonova, G.F., Stasova, V.V., 1997. Effects of environmental factors on wood formation in larch (*Larix sibirica* Ldb.) stems. *Trees* **11**, 462–468.

Brown, H.P., Panshin, A.J., Forsaith, C.C., 1949. *Textbook of Wood Technology*. McGraw-Hill, New York, 652 pp.

Crawley, M.J., 2005. *Statistics: An Introduction using R. John Wiley & Sons,* Chichester, England, 327 pp.

Crawley, M.J., 2007. *The R Book. John Wiley & Sons*, Chichester, England, 942 pp.

Deslauriers, A., Morin, H., Begin, Y., 2003. Cellular phenology of annual ring formation of *Abies balsamea* in the Quebec boreal forest (Canada). *Canadian Journal of Forest Research* **33**, 190–200.

Efron, B., Tibshirani, R.J., 1993. *An Introduction to the Bootstrap.* Chapman & Hall, New York, 436 pp.

Fengel, D., Wegener, G., 1989. *Wood: Chemistry, Ultrastructure, Reactions.* Walter de Gruyter, Berlin, 613 pp.

Good, P., 2004. *Permutation, Parametric, and Bootstrap Test of Hypothesis.* Springer, 376 pp.

Gričar, J., Čufar, K., Oven, P., Schmitt, U., 2005. Differentiation of terminal latewood tracheids in silver fir trees during autumn. *Annals of Botany* **95**, 959–965.

Gričar, J., Krze, L., Čufar, K., 2009. Number of cells in xylem, phloem and dormant cambium in silver fir (*Abies alba*), in trees of different vitality. *IAWA Journal* **30**, 121–133.

Kutscha, N.P., Hyland, F., Schwarzmann, J.M., 1975. *Certain seasonal changes in balsam fir cambium and its derivatives.* Wood Science and Technology 9, 175–188. Legendre, P., Legendre, L., 1998. Numerical Ecology. Elsevier, Amsterdam, 853 pp.

Mäkinen, H., Nojd, P., Saranpää, P., 2003. Seasonal changes in stem radius and production of new tracheids in Norway spruce. *Tree Physiology* **23**, 959–968.

Manly, B.F.J., 2007. *Randomization, Bootstrap and Monte Carlo Methods in Biology.* Chapman & Hall/CRC, Boca Raton, 455 pp.

Murrell, P., 2006. *R Graphics. Chapman & Hall/CRC*, London, 301 pp.

Panshin, A.J., de Zeeuw, C., 1980. *Textbook of Wood Technology*. McGraw-Hill, New York, 722 pp.

Plomion, C., Leprovost, G., Stokes, A., 2001. Woodformation in trees. *Plant Physiology* **127**, 1513–1523.

R Development Core Team, 2007. R: A Language and Environment for Statistical Computing. R Development Core Team, Vienna, Austria.

Rossi, S., Anfodillo, T., Menardi, R., 2006a. Trephor: A new tool for sampling microcores from tree stems. *IAWA Journal* **27**, 89–97.

Rossi, S., Deslauriers, A., Anfodillo, T., 2006b. Assessment of cambial activity and xylogenesis by microsampling tree species: an example at the alpine timberline. *IAWA Journal* **27**, 383–394.

Rossi, S., Deslauriers, A., Anfodillo, T., Carraro, V., 2007. Evidence of threshold temperatures for xylogenesis in conifers at high altitudes. *Oecologia* **152**, 1–12.

Rossi, S., Deslauriers, A., Gričar, J., Seo, J.W., Rathgeber, C.B.K., Anfodillo, T., Morin, H., Levanic, T., Oven, P., Jalkanen, R., 2008. Critical temperatures for xylogenesis in conifers of cold climates. *Global Ecology and Biogeography* **17**, 696–707.

Rossi, S., Rathgeber, C.B.K., Deslauriers, A., 2009a. Comparing needle and shoot phenology with xylem development on three conifer species in Italy. *Annals of Forest Science* **66**, 206.

Rossi, S., Simard, S., Deslauriers, A., Morin, H., 2009b. Wood formation in *Abies balsamea* seedlings subjected to artificial defoliation. Tree Physiology 29, 551–558.

Rossi, S., Simard, S., Rathgeber, C.B.K., Deslauriers, A., De Zan, C., 2009c. Effects of a 20- day-long dry period on cambial and apical meristem growth in *Abies balsamea* seedlings. *Trees* **23**, 85–93.

Schmitt, U., Jalkanen, R., Eckstein, D., 2004. Cambiumdynamics of *Pinus sylvestris* and Betula spp. in the northern boreal forest in Finland. *Silva Fennica* **38**, 167–178.

Seo, J.-W., Eckstein, D., Jalkanen, R., Rickebusch, S., Schmitt, U., 2008. Estimating the onset of cambial activity in Scots pine in northern Finland by means of the heat-sum approach. *Tree Physiology* **28**, 105–112.

Skene, D.S., 1969. The period of time taken by cambial derivatives to grow and differentiate into tracheids in *Pinus radiata* DDon. *Annals of Botany* **33**, 253–262.

Timel, T.E., 1980. Organization and ultrastructure of the dormant cambial zone in compression wood of *Picea abies*. *Wood Science and Technology* **14**, 161–179.

Venables, W.N., Ripley, B.D., 2002. *Modern Applied Statistics with S. Springer*, New York.

Wilson, B.F., 1970. *The Growing Tree*. The University of Massachusetts Press, Amherst, 152 pp.

Wilson, B.F., Wodzicki, T.J., Zahner, R., 1966. Differentiation of cambial derivatives: proposed terminology. *Forest Science* **12**, 438–440.

Wodzicki, T.J., 1971. Mechanism of xylem differentiation in Pinus sylvestris L. *Journal of Experimental Botany* **22**, 670–687.

Wodzicki, T.J., Zajaczkowski, S., 1970. Methodical problems in studies on seasonal production of cambial xylem derivatives. *Acta Societatis Botanicorum Poloniae* **39**, 509–520.

Appendix A. Variable list.

Name	Definition
DY	Day of the year
RF	Radial file identification number
nC	Number of cells in the cambial zone
nDC	Number of cells in the dormant cambial zone
nE	Number of cells in the enlargement zone
nL	Number of cells in the thickening and lignification zone
nM	Number of cells in the mature zone
t_iD	Beginning of the dividing phase
t_iE	Beginning of the enlarging phase
t_iL	Beginning of the maturing phase
t_iM	Beginning of the mature phase
t_fD	End of the dividing phase
t_fE	End of the enlarging phase
t_fL	End of the maturing phase
ΔtE	Duration of the enlarging phase
ΔtL	Duration of the maturing phase
ΔtX	Total duration of xylem development

Appendix B. Presentation of the input and output tables (see Appendix A for variable definitions)

Input table of raw data.

Tree	DY	RF	nC	nE	nL	nM
1	82	1	7	0	0	0
1	82	2	7	0	0	0
1	82	3	8	0	0	0
1	109	1	6	0	0	0
.						
.						
.						
10	312	3	8	0	1	79
10	319	1	8	0	0	78
10	319	2	8	0	0	79
10	319	3	8	0	0	80

Output table of critical dates and durations.

Tree	bE	±	bL	±	bM	±	cE	±	cL	±	dE	±	dL	±	dX	±
1	127	0.7	133	0.7	162	0.7	263	1.2	291	1.3	136	1.4	158	1.5	164	1.5
2	120	0.7	134	0.7	158	1.3	267	0.7	294	0.7	147	1.0	160	1.0	174	1.0
3	113	0.7	126	0.7	147	0.7	263	1.2	294	0.6	150	1.4	168	0.9	181	0.9
4	126	0.7	141	0.7	155	0.7	280	0.7	301	0.7	154	1.0	160	1.0	175	1.0
5	113	0.7	127	0.7	137	1.3	266	0.7	294	0.7	153	1.0	167	1.0	181	1.0
6	99	0.6	127	0.7	155	0.7	255	26.7	294	0.7	156	26.7	167	1.0	195	0.9
7	102	1.3	120	0.7	155	0.7	260	0.7	301	0.7	158	1.5	181	1.0	199	1.5
8	106	0.6	134	0.7	155	0.7	225	30.3	294	0.7	119	30.3	160	1.0	188	0.9
9	99	0.7	120	0.7	148	0.7	256	1.3	305	1.3	157	1.5	185	1.5	206	1.5
10	102	1.2	119	0.7	148	0.7	259	0.7	309	11	157	1.4	190	11.0	207	11.1

Appendix C. Plots of individual critical dates

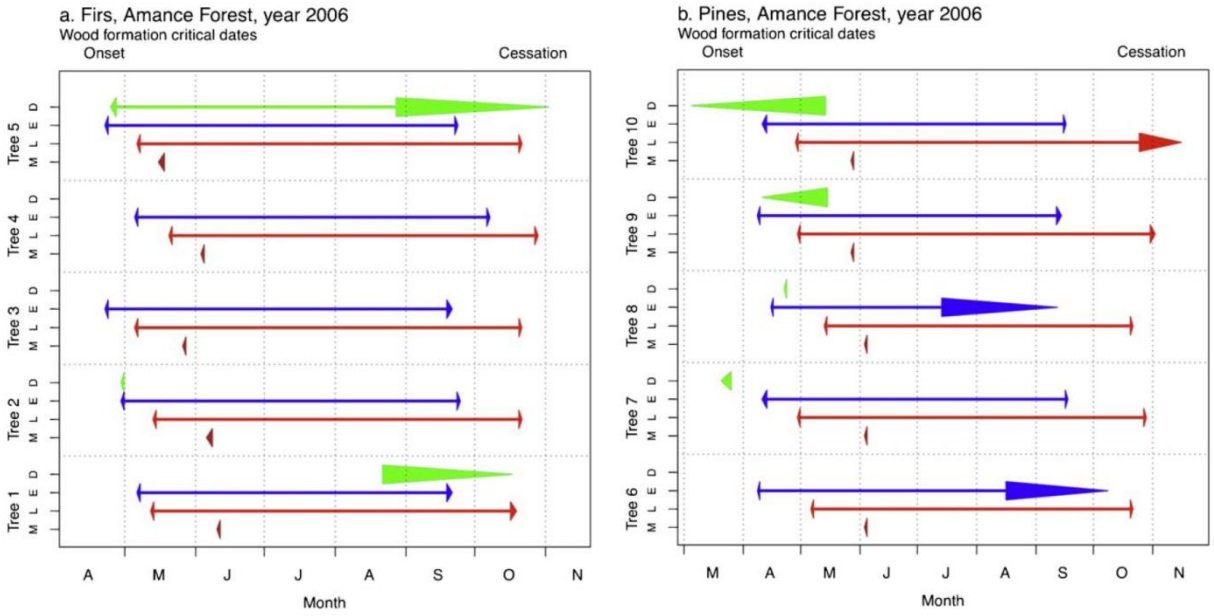

Résumé

La formation du bois (xylogénèse) produit une large partie de la biomasse de la planète et une ressource essentielle pour l'Homme. Les cellules du bois sont produites par division dans le cambium puis s'élargissent, forment une paroi épaisse lignifiée et meurent. Pendant l'année, ces processus sont définis par des dates, durées et vitesses qui caractérisent la dynamique intra-annuelle de la xylogénèse. Cette dynamique reste peu explorée alors que c'est un aspect clé, car c'est elle qui détermine la quantité et la qualité du bois produit et c'est sur elle que les facteurs de régulation agissent. Ce travail vise à améliorer nos connaissances sur la dynamique intra-annuelle de la xylogénèse.

Pendant trois ans (2007 – 2009), la xylogénèse a été suivie pour 45 arbres de trois espèces de conifères (sapin pectiné, épicéa commun et pin sylvestre) dans les Vosges. Pour ça, des petits échantillons de bois ont été prélevés chaque semaine sur le tronc des arbres sélectionnés. Les échantillons ont été préparés au laboratoire, puis des sections anatomiques ont été réalisées pour observer la xylogénèse au microscope.

Cette thèse a permis d'améliorer notre connaissance du fonctionnement de la xylogénèse, un système biologique d'une fascinante complexité. Nous avons caractérisé – grâce à l'innovation d'une méthode statistique performante – les aspects méconnus de la dynamique de différenciation des cellules du bois. Nous avons alors pu dévoiler les mécanismes par lesquels la dynamique de la xylogénèse donne forme à la structure du cerne, établir la dynamique intra-annuelle de l'accumulation du carbone dans le bois et évaluer les mécanismes de l'influence du climat sur la xylogénèse.

Mots-clés : Activité cambiale – Cerne de croissance – Climat – Conifères – Croissance de l'arbre – Forêt tempérée – Formation du bois – Xylogénèse

Summary

Wood formation (xylogenesis) produces a large part of the biomass of this planet and provides a crucial resource to Mankind. Wood cells are produced by division in the cambium, after what they enlarge, build a lignified thick wall and die. During a year, these processes take place at certain dates, last for certain durations and go at certain rates. These dates, durations and rates characterize the intra-annual dynamics of xylogenesis. This dynamics remains poorly explored whereas it is a key aspect as it determines the quantity and quality of the produced wood and conveys the influence of intrinsic (gene, hormone) and extrinsic (environment) regulatory factors. This work aims to improve our knowledge on the intra-annual dynamics of xylogenesis.

During three years (2007 – 2009), xylogenesis was monitored for 45 trees of three conifer species (silver fir, Norway spruce, and Scots pine) in northeast France. For that, small wood samples were collected weekly on tree stem. Samples were prepared at the laboratory, and anatomical sections were cut to observe xylogenesis under a light microscope.

This thesis has improved our knowledge on the functioning of xylogenesis, a biological system of a fascinating complexity. We characterized – thanks to the development of an efficient statistical method – the little known aspects of wood cell differentiation dynamics. Based on this characterization, we eluded the mechanisms by which xylogenesis dynamics shapes tree ring structure, we established the intra-annual dynamics of carbon accumulation in wood and we evaluated the mechanisms of the climate influence on xylogenesis.

Keywords: Cambial activity – Tree ring – Climate – Conifers – Tree growth – Temperate forests – Wood formation – Xylogenesis